New insights on the human and murine GnRH system through functionnal assays and 3D-imaging

Gaëtan Ternier

UNIVERSITÉ DE LILLE
École Doctorale Biologie-Santé

THÈSE

Pour l'obtention du grade de

DOCTEUR DE L'UNIVERSITÉ DE LILLE

Spécialité : Neurosciences

NEW INSIGHTS ON THE HUMAN AND MURINE GNRH SYSTEM THROUGH FUNCTIONAL ASSAYS AND 3D-IMAGING

GAËTAN TERNIER

Sous la supervision du Dr Paolo Giacobini

Thèse présentée et soutenue le 9 décembre 2021 à Lille

Composition du jury :

Pr Sophie Catteau-Jonard, MD, PhD	Présidente
Pr Ulrich Boehm, PhD	Rapporteur
Pr Erik Hrabovszky, MD, PhD	Rapporteur
Dr Andrea Messina, PhD	Examinateur
Pr Anne-Simone Parent, MD, PhD	Examinatrice
Dr Paolo Giacobini, PhD	Directeur de thèse

SHORT FRENCH ABSTRACT

Chez les mammifères, le contrôle central de la reproduction repose principalement sur une population hypothalamique de neurones à gonadolibérine (GnRH). Malgré la multitude d'études menées chez diverses espèces ces dernières décennies, les aspects physiologiques et pathologiques du système GnRH ne restent que partiellement décrits et requièrent d'être mieux documentés. Dans un premier temps, et par une technique moderne d'imagerie tridimensionnelle chez la souris, nous apportons de nouvelles données sur le développement et la distribution des neurones à GnRH et de leurs partenaires de l'embryon à l'adulte. De plus, grâce à des études fonctionnelles, nous décrivons comment des mutations de facteurs impliqués dans le développement du système GnRH contribuent aux pathologies des fonctions de reproduction chez l'humain. Ces travaux enrichissent les connaissances sur le contrôle central de la reproduction, et posent les bases de futures études reposant sur des approches tridimensionnelles.

SHORT ENGLISH ABSTRACT

In mammals, the central control of the reproductive functions relies on a hypothalamic population of gonadotropin-releasing hormone (GnRH) neurons. Despite extensive studies in numerous species over the last decades, the physiological and pathological aspects of the GnRH system remain only partially described and require further investigation. First, using a modern three-dimensional imaging technique in mice, we provide new insights on the development and distribution of GnRH neurons and their interactors from the embryo to the adult. Second, using functional assays, we investigate how mutations of factors involved in the development of the GnRH system can contribute to pathologies of the reproductive functions in humans. We thus bring novel data on the central regulation of reproduction in mice and humans, and set the basis for future studies relying on three-dimensional approaches.

FRENCH ABSTRACT

Chez les mammifères, la fonction de reproduction est assurée par l'axe hypothalamo-hypophyso-gonadique (HHG). Dans ce système, des neurones à gonadolibérine (GnRH) parsemés dans l'hypothalamus projettent vers l'éminence médiane pour sécréter la GnRH dans la circulation porte hypothalamo-hypophysaire. La GnRH stimule les cellules gonadotropes de l'hypophyse, qui en réponse produisent et sécrètent les l'hormone lutéinisante (LH) et l'hormone folliculostimulante (FSH) dans la circulation systémique. La LH et la FSH agissent en périphérie pour activer la gamétogénèse et la stéroïdogenèse dans les gonades, et les stéroïdes sexuels ferment la boucle en exerçant un rétrocontrôle au niveau central. Une particularité des neurones à GnRH tient dans leur origine, puisqu'ils naissent dans la région nasale avant de migrer vers leur lieu d'installation dans le cerveau durant le développement embryonnaire. De plus, les neurones à GnRH poursuivent leur maturation après la naissance en interagissant avec diverses populations neuronales et non-neuronales, formant ainsi un « réseau GnRH » qui permet l'intégration de signaux physiologiques et environnementaux pour réguler finement l'axe HHG. De fait, les défauts impactant la genèse, la migration, les interactions ou l'activité des neurones à GnRH sont associés à des pathologies de la reproduction et causent une absence de puberté et une infertilité. Ces pathologies incluent l'hypogonadisme hypogonadotrope (HH) et, si les patients présentent également une anosmie ou hyposmie, le syndrome de Kallmann (SK). Dû à la complexité des mécanismes moléculaires régissant le développement prénatal et postnatal du réseau GnRH, et puisque les mutations identifiées jusqu'ici n'expliquent qu'une fraction des cas de HH et SK, des études plus approfondies sont nécessaires pour comprendre la migration des neurones à GnRH depuis la région nasale et leur maturation dans le cerveau. En outre, de nouvelles approches doivent être adoptées pour décrire le développement prénatal et postnatal du réseau GnRH : les techniques histologiques conventionnelles ont notamment été limitantes, en partie car les neurones à GnRH et leurs partenaires sont éparpillés dans le cerveau et projettent parfois sur de longues distances. L'objectif des présents travaux est de compléter les connaissances sur le contrôle central de la reproduction, en recourant à des techniques complémentaires chez la souris

et chez l'humain. Dans un premier temps, nous avons étudié les mutations de gènes codant pour la molécule de guidance Semaphorine 3F et son récepteur la Plexine A3, retrouvées chez l'humain, et avons évalué leur contribution à la pathogenèse du HH. Nous suggérons que la signalisation par la Semaphorine 3F est impliquée dans la migration des neurones à GnRH dans le nez, et qu'un défaut dans ce processus participe à l'étiologie du HH et du SK. Dans un second temps, nous avons contourné les limites inhérentes aux coupes de tissus en implémentant chez la souris l'immunomarquage et la transparisation d'échantillons entiers, suivis d'une imagerie en microscopie à feuille de lumière, permettant la visualisation et l'analyse tridimensionnelles des neurones à GnRH depuis l'embryon jusqu'à l'adulte. Nous revisitons ainsi la migration des neurones à GnRH, et révélons l'étendue de leur distribution et de leurs projections – y compris dans des régions extra-hypothalamiques jusqu'ici peu considérées – suggérant par là même de potentiel nouveaux rôles pour la GnRH dans le cerveau des mammifères. En résumé, les travaux présentés ici apportent de nouvelles données sur le développement physiologique et pathologique des circuits neuraux contrôlant la reproduction chez la souris et l'humain.

ENGLISH ABSTRACT

In mammals, reproductive functions depend on the hypothalamus-pituitary-gonadal axis. In this system, a specialized population of gonadotropin-releasing hormone (GnRH) neurons scattered in the hypothalamus project to the median eminence to release GnRH in the hypothalamus-pituitary portal circulation. GnRH reaches the anterior pituitary and stimulates the gonadotropic cells, which in response produce and release the gonadotropins LH and FSH in the general circulation. LH and FSH in turn act at the periphery to promote gametogenesis and production of sexual steroids in the gonads, and the sexual steroids close the loop via feedback mechanisms taking place at the central level. A surprising characteristic of GnRH neurons lies in their origin, as they are born in the nose and then migrate towards their final location in the brain during embryonic development. Additionally, the GnRH neurons continue their maturation after birth by establishing interactions with several neuronal and non-neuronal populations in the brain, forming a GnRH network which enables them to integrate diverse physiological and environmental cues and finely regulate the downstream HPG axis. Accordingly, defects in the processes governing the birth, migration, interactions or activity of GnRH neurons are associated with pathologies of reproductive functions leading to absent puberty and infertility. Such pathologies include hypogonadotropic hypogonadism (HH) and, when patients also present with anosmia or hyposmia, Kallmann Syndrome (KS). Given the molecular complexity underlying the prenatal and postnatal development of the GnRH network, and because mutations identified so far only account for a fraction of reported HH/KS cases, further investigations are needed to dissect the mechanisms guiding the migration of GnRH neurons in the nasal compartment and their maturation in the brain. Moreover, new approaches are needed to better document the prenatal and postnatal maturation of the GnRH network: notably, conventional histological approaches have been a limiting factor in previous studies, due in part to GnRH neurons and their partners being scattered in the brain and sometimes projecting over long distances. In the present work, we set out to complete our current knowledge on the central control of reproduction through the use of different, complementary approaches in mice and human. First, we have investigated

human mutations of the genes coding for the guidance molecule Semaphorin 3F and and its receptor Plexin A3, and have assessed their contribution to the pathogenesis of hypogonadotropic hypogonadism. We propose that Semaphorin 3F signalling is involved in the migration of GnRH neurons in the nasal region in humans, and that defects in this process can participate to the etiology of HH and KS. Second, we overcame the limitations of classical sectioning techniques by implementing whole-mount immunolabelling, solvent-based tissue-clearing and light-sheet imaging to allow three-dimensional visualization and analysis of GnRH neurons from the embryo to the adult mouse. This sheds some new light on the migration and distribution of GnRH neurons and their projections in the murine model, and unexpectedly reveals their extent in previously overlooked extra-hypothalamic regions, thus setting the basis for future studies aimed at dissecting potential new roles for GnRH in mammals. Overall, the present work brings novel data on the physiological and pathological development of the neural circuits controlling reproduction in mice and humans.

TABLE OF CONTENTS

ABBREVIATIONS

3D	Three-dimension / Three-dimensional
3DISCO	Three-dimensional imaging of solvent-cleared organs
3V	Third ventricle
AChE	Acetylcholine esterase
ACTH	Adrenocorticotropic hormone
AgRP	Agouti-related peptide
a-GSU	Glycoprotein hormone alpha subunit
AMH	Anti-müllerian hormone
AMH-R2	Type 2 receptor for the anti-müllerian hormone
ANOS1	Anosmin-1
AOB	Accessory olfactory bulb
ARC	Arcuate nucleus
AVP	Arginin-vasopressin
AVPV	Anteroventral periventricular nucleus
BABB	Benzyl Alcohol Benzyl Benzoate
BrDU	5-bromo-2'-deoxyuridine
cDNA	Complementary deoxyribonucleic acid
ChAT	Choline acetyltransferase
CHD7	Chromodomain helicase DNA binding protein 7
CLARITY	Clear Lipid-exchanged Acrylamide-hybridized Rigid Imaging/Immunostaining/In situ hybridization-compatible Tissue-hYdrogel
CRF	Corticotropin-releasing factor/hormone
CRH-R1	Corticotropin-releasing hormone receptor type 1
CUBIC	Clear, unobstructed brain imaging cocktails and computational analysis
DAPI	4’,6-diamidino-2-phenylindole
DBE	Dibenzyl ether
DCX	Doublecortin
DMEM	Dulbecco's Modified Eagle Medium
DNA	Deoxyribonucleic acid
EDTA	Ethylenediaminetetraacetic acid
EdU	5-Ethynyl-2’-deoxyuridine
ER	Endoplasmic reticulum
ERK	Extracellular signal-regulated kinase
ERα	Estrogen receptor alpha

ERβ	Estrogen receptor beta
ES	Exome sequencing
FGF(R)	Fibroblast growth factor (receptor)
FSH	Follicle-stimulating hormone
FSHβ	Follicle-stimulating hormone subunit beta
GABA	Gamma-aminobutyric acid
GAP	GnRH-associated peptide
GAP-43	Growth Associated Protein 43
GAPDH	Glyceraldehyde-3-Phosphate Dehydrogenase
GFAP	Glial fibrillary acidic protein
GFP	Green Fluorescent Protein
GnRH	Gonadotropin-releasing hormone
GnRH-R	Gonadotropin-releasing hormone receptor
GPR54	G-protein-coupled receptor 54 (kisspeptin receptor)
GW	Gestation week
H2O2	Hydrogen Peroxide
HEK293T	Human embryonic kidney 293 cells
HH	Hypogonadotropic hypogonadism
HPA	Hypothalamic-pituitary-adrenal axis
HPG	hypothalamic-pituitary-gonadal
HRP	Horseradish peroxidase
ICV	Intracerebroventricular
iDISCO(+)	Immunolabeling-enabled three-dimensional imaging of solvent-cleared organs
IHH	Idiopathic hypogonadotropic hypogonadism
IL-1Racc	Interleukin 1 receptor accessory protein
KAL1	Kallmann Syndrome-1
KISS1	Kisspeptin
KISS1R	Kisspeptin receptor
KNDy	Kisspeptin-NeurokininB-Dynorphin
KS	Kallmann syndrome
LH	Luteinizing hormone
LHRH	Luteinizing-hormone releasing hormone
LHβ	Luteinizing hormone subunit beta
MAPK	Mitogen-activated protein kinase
ME	Median eminence

MRI	Magnetic resonance imaging
mRNA	Messenger ribonucleic acid
NCAM	Neural Cell Adhesion Molecule
NDNF	Neuron-derived neurotrophic factor
NDS	Normal donkey serum
NELF	Nasal embryonic LHRH factor
NKB	Neurokinin B
nNOS	Neuronal nitric oxide synthase
NO	Nitric oxide
NPY	Neuropeptide Y
OB	Olfactory bulb
OE	Olfactory epithelium
OEC	Olfactory ensheating cells
OMP	Olfactory Marker Protein
ON	Olfactory nerve
OP	Olfactory placode
OSN	Olfactory sensory neuron
OVLT	Organum vasculosum of the lamina terminalis
PACT	Passive clarity technique
PARS	Perfusion-assisted agent release *in situ*
PBS	Phosphate buffered saline
PGE2	Prostaglandin E2
PMV	Premammillary nucleus
POA	Preoptic area
POMC	Pro-opiomelanocortin
PSI	Plexin/Semaphorin/Integrin
PVN	Paraventricular nucleus
RAS-GAP	Ras GTPase-activating proteins
RFRP	RFamide-related peptide
RP3V	Rostral periventricular nucleus
rPOA	Rostral preoptic area
RT	Room temperature
SCN	Suprachiasmatic nucleus
sDISCO	Stabilized three-dimensional imaging of solvent-cleared organs
SDS	Sodium dodecyl sulfate

SeeDB	See Deep Brain
SNP	single-nucleotide polymorphism
SOX10	SRY-box transcription factor 10
TAC3	Tachykinin-3/Neurokinin B
TACR3	Tachykinin-3/Neurokinin B receptor
TBS	Tris buffered saline
TBS-T	TBS-TritonX100 / TBS-Tween20
TGG	Trigeminal ganglion
THF	Tetrahydrofuran
TN	Terminal nerve
TUJ1	Neuron-specific class III beta-tubulin
uDISCO	Ultimate three-dimensional imaging of solvent-cleared organs
vDISCO	VHH-boosted three-dimensional imaging of solvent-cleared organs
VNN	Vomeronasal nerve
VNO	Vomeronasal organ
VSN	Vomeronasal sensory neuron
WT	Wild-type
YFP	Yellow Fluorescent Protein

CHAPTER ONE: THE HYPOTHALAMIC-PITUITARY-GONADAL AXIS AND THE PHYSIOPATHOLOGY OF GNRH NEURONS

I. The hypothalamic-pituitary-gonadal axis and the control of reproduction

A. Overview of the mammalian HPG axis

In the animal reign, reproduction is an ultimate, innate goal encoded in all individuals to secure the survival of the species. Although reproduction has taken several forms during evolution, sexual reproduction is considered the most advanced and is represented in vertebrates and invertebrates alike: in mammals more particularly, the control of reproduction relies on a multi-level axis involving two central components, namely the hypothalamus and the pituitary, and a peripheral component constituted by the gonads (Figure I-1).

i. The hypothalamus

The hypothalamus is a small part of the brain located at the base of the organ, below the thalamus. It is a region of great importance in the survival of both the individual and the species, since this centre is involved in numerous biological processes such as metabolism, homeostasis, sleep/wake cycles, and reproduction. Anatomically, it consists of several nuclei with specialized functions, distributed on both sides of the third ventricle: these nuclei are highly connected both locally and with other parts of the brain. The hypothalamus is also comprised of two circumventricular organs – the organum vasculum of lamina terminalis (OVLT) and the median eminence (ME) – which are specialized structures with fenestrated blood capillaries allowing communication between the brain and the periphery, exceptions to the general blood-brain-barrier (Schröder et al. 2020). In the reproductive frame, the hypothalamus is host to the gonadotropin-releasing hormone (GnRH) neurons, which produce and release GnRH in a pulsatile manner in the median eminence to target the pituitary.

ii. The pituitary

Located below the hypothalamus, and connected to it by a portal capillary circulation, the pituitary is a two-part gland consisting of an anterior and posterior part. While the posterior pituitary

mainly consists in axons coming from the brain, the anterior pituitary contains different types of endocrine cells, which integrate signals from the portal circulation to regulate hormonal secretion. Among those signals, GnRH is brought *via* the portal circulation to the pituitary where it binds the specific GnRH receptor (GnRH-R) located at the membrane of gonadotropic cells. Upon GnRH stimulation, the gonadotropic cells then produce the follicle-stimulating hormone (FSH) and the luteinizing hormone (LH), both of which are released to the systemic blood circulation to reach the gonads (Cohen-Tannoudji et al. 2014, Stamatiades and Kaiser 2017).

iii. The gonads

If the central components of the reproductive axis are relatively similar in males and females, the gonads are instead highly dimorphic. In males, the testis is composed of seminiferous tubules organized in lobules and surrounded by a parenchyma. The seminiferous tubules join the rete testis and efferent ducts, to then open on the epididymis. The testicular parenchyma is host to the Leydig cells, which upon LH stimulation produce the sexual steroid hormone Testosterone from blood cholesterol. Sertoli cells, on the other hand, are found along the seminiferous tubules and will mainly activate gametogenesis upon FSH stimulation. In summary, the coordinated action of LH and FSH on the male gonads will promote steroidogenesis and the continuous gametogenesis (Jégou et al. 2014). In females, the ovaries contain follicles at different stages, ranging from early primordial follicles to luteal follicles. Folliculogenesis, or maturation of the follicles, starts *in utero* and continues after birth, with the final folliculogenesis processes only happening after puberty onset. During their maturation, sensibility of the follicles to LH and FSH does not remain constant: while FSH and LH are involved in the basal development of follicles up to the pre-ovulatory stage, it is to a lesser extent than the terminal maturation when gonadotrophins are essential to the selection and maintenance of the ovulatory follicle. After puberty, gonadotrophins are responsible for triggering ovulation and, by acting on theca and granulosa cells of the follicles, they also promote the production of progesterone, testosterone, and estradiol. In summary, LH

and FSH act on the ovary to promote gametal maturation, steroidogenesis and ovulation (Monniaux et al. 2014).

iv. The final link: a feedback between the components of the HPG axis

A feedback mechanism establishes the final link between the components of the reproductive axis: sexual steroids (testosterone, progesterone, estradiol) not only act locally in the gonads, but are also released in the systemic circulation to exert a retro-control on the hypothalamus and the pituitary. This retro-control can be positive or negative depending on the hormone at play and the timeframe of action, i.e. depending on the phase of the menstrual cycle.

During the menstrual cycle, estradiol first exerts a negative feedback at the central level, associated mostly to an inhibition of FSH secretion, and then switches to a positive feedback leading to an increase in LH levels in preparation of ovulation. The role of progesterone in the luteal phase of the cycle is mainly a negative retro-control suppressive of gonadotropin secretion, and it seems to require synergy with estradiol, since estradiol deficiency reduces the progesterone-mediated feedback. Similarly, testosterone has been shown to possess an inhibiting effect on gonadotropin secretion, and thus exerts a negative feedback on the HPG axis (Herbison 2015).

Interestingly, the positive and/or negative feedbacks of sexual steroids are not mediated by a single cell type nor in a single location. Instead, they can act at the hypothalamic and/or the pituitary levels, not necessarily through the same mechanisms (Pitteloud et al. 2008), and several populations have been involved including the GnRH neurons, their hypothalamic partners, and the gonadotropic cells, depending on specific receptor expression (Marques et al. 2000).

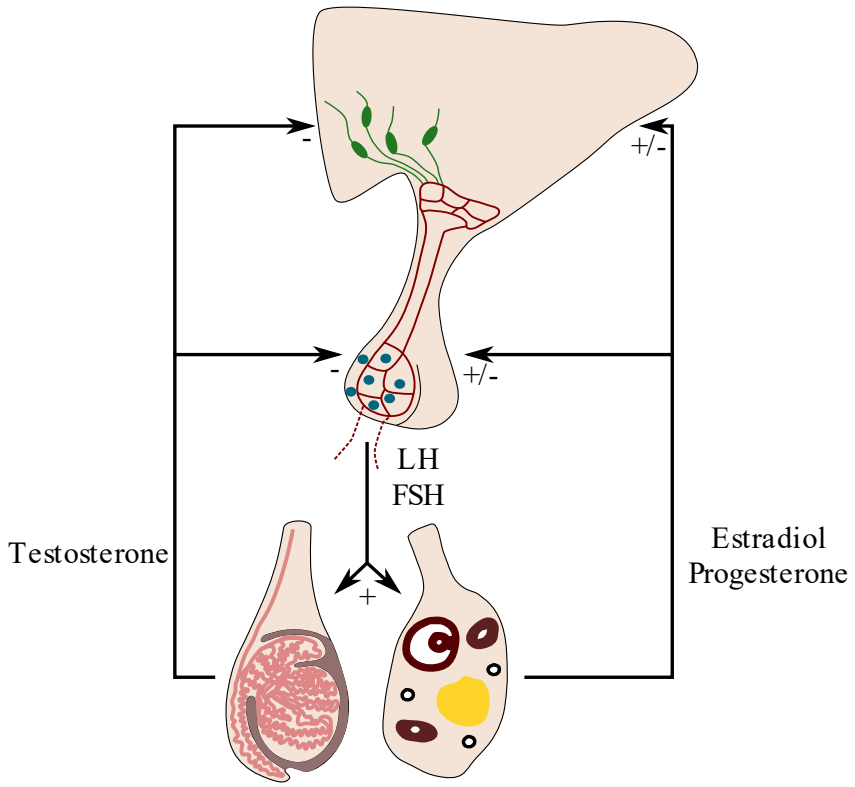

Figure I-1. Overview of the hypothalamic-pituitary-gonadal axis*. Hypothalamic GnRH neurons (in green) project to the median eminence and release GnRH in the hypothalamus-pituitary portal circulation (red lines) to target the gonadotropic cells of the anterior pituitary (blue). Gonadotropic cells then secrete the gonadotropins LH and FSH in the systemic circulation (dashed red lines). In the gonads, LH and FSH promote gametogenesis and steroidogenesis. The sexual steroids testosterone, estradiol and progesterone finally exert a feedback at the central levels.*

B. Timeline of development of the HPG axis in rodents and humans

i. Intrauterine development

The mammalian reproductive axis starts developing *in utero*: starting from the third week of human embryonic development, the expression of sex-specific genes triggers the differentiation of the so-far bipotential gonads derived from the mesonephros. Development of the testes will promote regression of the presumptive female sexual ducts, and growth of the male sexual organs – namely the epididymis, vas deferens and the prostate – while development of ovaries will be

accompanied by growth of the fallopian tube, uterus and vagina (Eggers et al. 2014, Biason-Lauber and Chaboissier 2015). Similarly in the murine model, the undifferentiated gonads appear at embryonic day E10.5, and the differentiation starts 24 hours later driven by sex-specific gene expression, leading to the development of the female or male reproductive tract (Yildirim et al. 2020). Also during the embryonic development, the GnRH neurons migrate from their birth location in the nasal compartment, starting at the 5th gestational week in human and around E10 in mice, to reach notably the preoptic and hypothalamic regions and send projections to the median eminence (Wray et al. 1989, Schwanzel-Fukuda et al. 1989, Casoni, Malone et al. 2016).

A transient intrauterine activation of the HPG axis occurs during the human fetal development (Figure I-2), with a measurable rise in LH and FSH around the 12th gestational weeks and to mid-gestation, before placental hormones exert a progressive silencing effect on the axis. It is proposed that this activation plays a role in gonadal development, and notably in testicular descent. At birth, the main sexual structures and reproductive circuits are in place, but they still require maturation.

ii. Minipuberty

Shortly after birth, between postnatal day 10 (PN10) and PN15 in mice and within the first months of life in human infants, a new transient activation of the HPG axis happens which is termed minipuberty (Figure I-2). Minipuberty is associated with a rise in circulating gonadotropins and sexual steroids, and is believed to promote the first postnatal events of sexual maturation: activation of the testis occurs in males with an increase in size and production of Sertoli cells, Leydig cells and germ cells; and an increase in follicular development is observed in female ovaries. Minipuberty appears to play a key role in brain sexual differentiation as well, with impacts on language skills and potentially on behaviour. The HPG axis is once again silenced after minipuberty, and remains quiescent until puberty (Kuiri-Hänninen et al. 2014, Becker and Hesse 2020).

iii. Puberty

The timing of puberty onset in human varies depending on several factors including genetic background, environment or socio-economical status. However, it usually occurs between 9 and 14 years of age, and more precociously in females than males (Figure I-2). Puberty is characterized by body as well as psychosocial changes. The main body changes include testicular enlargement, penile growth and development of public hair in males, breast development and apparition of pubic hair in females, later followed by production of sperm and first ejaculations in males, and start of menstrual cycles in females (Spaziani et al. 2021). In mice also, the timing of puberty varies between strains and several changes are observed: depending on which manifestation is used to date pubertal onset, it is thus estimated to occur between PN21 and PN40 (Pinter et al. 2007).

Puberty is synonym to the re-activation of the HPG axis, and this event depends upon several factors among which the potent kisspeptin, a neuropeptide produced notably by specialized populations of the hypothalamus. Mutations studies have indeed concluded that kisspeptin, and kisspeptin receptor (GPR54) were necessary for pubertal activation of the GnRH neurons, and that a failure of this system was associated with absent puberty and subsequent infertility (De Roux et al. 2003, Seminara et al. 2003). Other actors include neurokinin B (NKB), Dynorphin, Glutamate and γ-aminobutyric acid (GABA), Leptin and ghrelin (reviewed in Spaziani et al. 2021) each with their own permissive or suppressive effect, and together they impose a pulsatile rhythm of GnRH secretion that will in turn trigger the release of gonadotropins from the pituitary gonadotropic cells. In addition to gonadal maturation, the subsequent production of sexual steroids will participate to brain development and explain psychosocial and behavioural changes (Özdemir et al. 2016, Wood et al. 2019, Spaziani et al. 2021). Together, these changes mark the acquisition of the reproductive functions, which are normally conserved throughout life in males, and until menopause occurs in women when depletion of the follicular reserve leads to a decrease in estrogen production. Of note, a progressive decrease of testosterone production with age in

males exists, that is associated with impaired reproductive functions and termed andropause. (Davis et al. 2015, Jakiel et al. 2015)

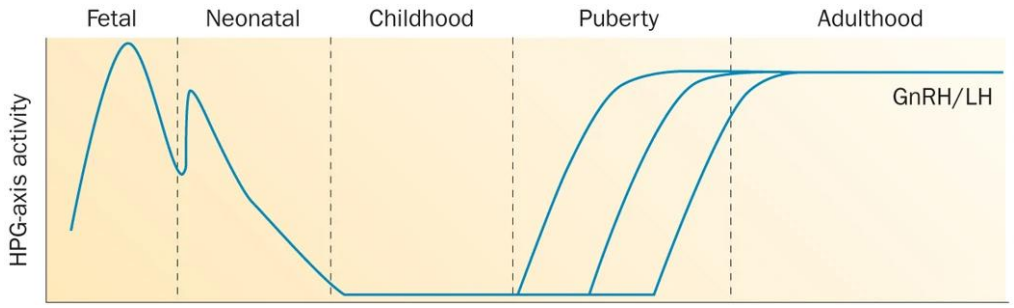

Figure I-2. Timeline of activation of the HPG axis*. The blue line represents variations in the secretion of GnRH/LH in life. The HPG axis undergoes a first activation* in utero*, then peaks again shortly after birth during minipuberty. Quiescent throughout childhood, the axis is activated again at puberty, a time that marks the acquisition of reproductive functions, and remains active during adulthood. Adapted from Boehm et al. 2015*

iv. The postpubertal GnRH system: a story of surges and pulses

Conservation of the reproductive functions after pubertal activation of the HPG axis necessitates a highly specific GnRH neuronal activity consisting of two patterns: GnRH neurons indeed show a pulsatile secretion of GnRH in both sexes, involved in gametogenesis and steroidogenesis, with additional surges in females associated with ovulatory events. It is noteworthy that a partial population of GnRH neurons is sufficient to maintain the pulsatility of GnRH and subsequent gonadotropin production and secretion, with less than a hundred neurons being able to ensure LH pulsatility in mice (Kokoris et al. 1988, Campos and Herbison 2014).

Clarke and Cummins (1982), through collection of blood in the hypothalamus-pituitary portal circulation of the ewe, were able to demonstrate that pulses of LH were synchronized with pulses of GnRH, almost four decades after the concept of pituitary stimulation by hypothalamus factors was proposed by Harris (1948), and a few years only after pulsatility of GnRH release was shown in rhesus monkeys (Carmel et al. 1976).

> *"The significant feature of our data is the exact temporal relationship between GnRH secretion and LH secretion. It is clear that each LH pulse was synchronous with a GnRH pulse. Peak values of GnRH and LH always occurred within the same sampling interval. No LH pulses were observed without concomitant GnRH pulses."* Clarke and Cummins (1982)

Around this time, pulsatility of GnRH was also evidenced in several other species including rodents and humans, and several groups set out to elucidate its physiological relevance on gonadotropin profiles, notably by abolishing and/or restoring this pulsatility. Use of GnRH antisera in ewes, for instance, was correlated with the abolition of LH pulses (Caraty et al. 1984), and they were retrieved with injection of a GnRH agonist. In rhesus monkeys with lesions of the hypothalamus, the continuous administration of GnRH failed to restore normal gonadotropin levels, whereas intermittent administration succeeded in doing so (Figure I-3, Belchetz et al. 1978).

This GnRH-driven LH pulsatility is essential for the maintenance of the reproductive capacities: in the menstrual cycle, a low-frequency GnRH pulsatility progressively speeds up during the follicular phase, imprinting a gradual rise of LH levels. This is quickly followed by a strong elevation of LH secretion resulting in the mid-cycle LH surge – the trigger for ovulation. The frequency of GnRH pulses then decreases over the luteal phase of the cycle, to increase again as the next follicular phase is starting. Constant low GnRH and LH pulsatility during the menstrual cycle are associated with reproductive disorders such as hypothalamic amenorrhea, while maintained high pulsatility is found in polycystic ovary syndrome; and anovulation is a feature of both of these pathologies (Marques et al. 2000). In men and women alike, GnRH deficiency is a cause of hypogonadotropic hypogonadism, a condition in which reproductive functions are diminished or abolished.

While the importance of the specific secretion pattern for GnRH has been established, the factors at play remain only partially understood. The current model proposes the existence of a pulse generator, responsible for pulsatile secretion, and a surge generator involved in the triggering of

the pre-ovulatory surge of LH. These generators are not limited to the GnRH neurons but instead require the cooperation of a multitude of actors, including specialized neuronal populations and glial cells, that together form the "GnRH network" and will be discussed later (Herbison 2016).

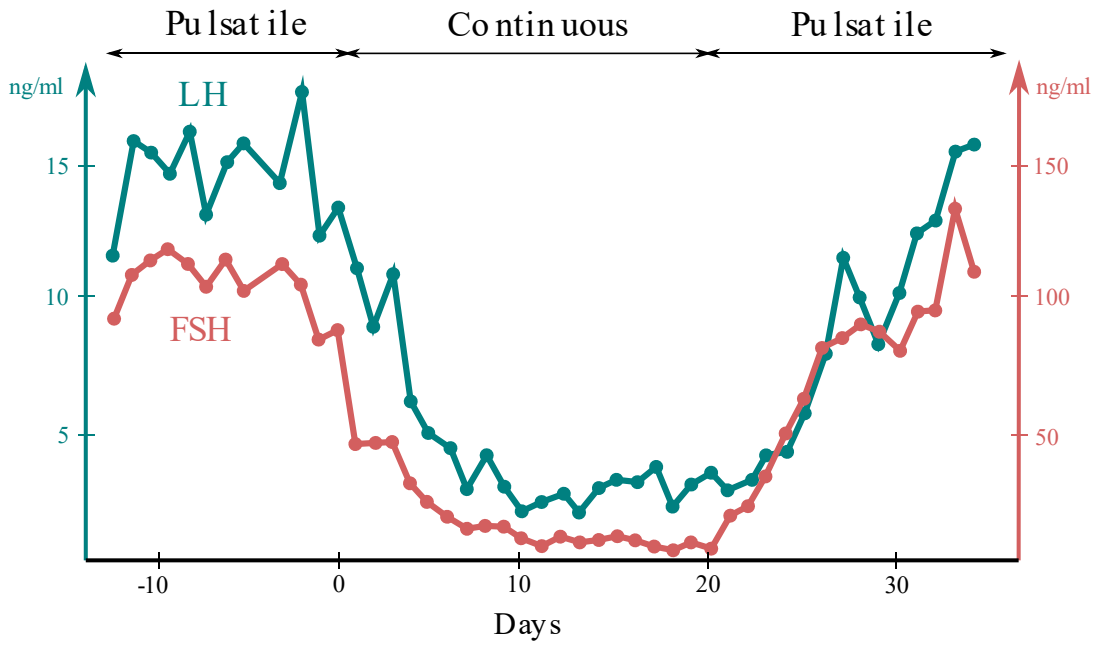

Figure I-3. Gonadotropin profiles in relation to GnRH in an ovariectomized rhesus monkey*. LH and FSH exhibit normal, pulsatile secretion driven by pulsatile GnRH administration. Continuous infusion of GnRH inhibits gonadotropin release, an effect rescued by the return to a pulsatile administration of GnRH. Adapted from Belchetz et al. 1978*

In the current frame, the hypothalamic GnRH system is considered the master regulator of the reproductive functions. To understand how this specific circuitry develops and achieves such a central role in the HPG axis, it is necessary to dive into the specificities of the GnRH neurons in several aspects, ranging from their birth origin to their final distribution, and their interactions with diverse partners to finely regulate the downstream axis.

II. The development and distribution of GnRH neurons

A. GnRH: from gene to action

i. GnRH production and secretion

There are to date three known forms of GnRH in vertebrates, respectively termed GnRH-1, GnRH-2 and GnRH-3. In mammals, GnRH-3 is absent and GnRH-2 functionality has been lost is numerous species (Stewart et al. 2009) and only GnRH-1, referred to as GnRH in the present work, is involved in the control of the reproductive functions. While it was initially called LHRH (luteinizing hormone-releasing hormone), this acronym was progressively replaced by GnRH due to the ability of the hormone to control the release of both LH and FSH. GnRH was first described in 1971 when it was isolated and sequenced from porcine hypothalamic, as a decapeptide of sequence Glu-His-Trp-Ser-Tyr-Gly-Leu-Arg-Pro-Gly-NH2 (Schally et al. 1971). Studies have shown that the GnRH sequence is highly conserved throughout evolution, an expected feature considering the key role of reproduction in species preservation (Roch et al. 2011). The hormone actually derives from a prepropeptide containing the sequence of GnRH as well as the sequence of a 56 amino-acids long GnRH-associated peptide or GAP (Seeburg and Adelamn 1984). Studies conducted around in the late 1980s showed that GnRH-producing cells are indeed immmunoreactive for GnRH and GAP in several species, and that the two peptides are found together in secretion vesicles, being even co-secreted in the hypothalamic-pituitary portal circulation (Clarke et al. 1987, Song et al. 1987, Sarkar & Mitsugi 1990). GAP has been mainly described as an inhibitor of prolactin secretion, which was first evidenced in cultured pituitary from rats and then confirmed *in vivo* (Nikolics et al. 1985, Yu et al. 1988). The latter group has also shown a stimulatory effect of GAP on gonadotrophins release *in vivo* in rats, although it was less potent than GnRH (Yu et al. 1989). In human, two studies on cultured pituitary cells have concluded to opposite results regarding the inhibitory effect of GAP on prolactin secretion (Ishibashi et al. 1987, Wormald et al. 1989). Overall, it is proposed that the coordinated processing and release of GnRH and GAP from the same initial prepropeptide establish a crosslink between the gonadotropic and lactatotropic pituitary components.

ii. GnRH signalling and decoding

After its release in the hypothalamic-pituitary portal circulation, the GnRH peptide has a short half-life of approximately 2 to 4 minutes (Handelsman and Swerdloff 1986), compatible with its fast delivery to the pituitary gonadotropic cells expressing the GnRH receptor. The GnRH-R is a 7-domains transmembrane G protein-coupled receptor, which like GnRH shows high conservation between several mammalian species including mouse, rat, sheep or human. It is interesting to note that GnRH-R expression in the gonadotropic cells is regulated by several factors including the sexual steroid hormones. Notably, estradiol has a positive effect on GnRH-R expression and availability in the pituitary, while progesterone has been shown to have an opposite effect, decreasing GnRH-R availability (Rispoli and Nett 2005). In a similar fashion, stimulation of the gonadotropic cells by activin leads to an increase in the gene expression and the number of GnRH-R, while inhibin shows opposite effects in rodents (Gregory & Kaiser 2004). Importantly, GnRH itself is also a key player in this regulation: studies have shown that GnRH pulses stimulate GnRH-R expression, while continuous exposure to GnRH leads to a decrease in GnRH-R availability in gonadotropic cells (Rispoli and Nett 2005). The regulation of the expression and availability of the GnRH-R in the gonadotropic cell undoubtedly participates in decoding GnRH inputs and regulating gonadotropin expression and secretion, but acts in synergy with other mechanisms. Indeed, the gonadotropins LH and FSH are composed of a common alpha subunit (α-GSU) and a differential beta subunit (LHβ or FSHβ) and the genes coding for these subunits are regulated by GnRH pulsatility. A high pulsatility triggers preferentially LHβ expression, while a low pulsatility increases FSHβ expression. The common subunit however does not seem subjected to the same regulation, since it is expressed in a similar manner in both cases, and even under continuous GnRH exposure (Stamatiades et Kaiser 2018). Several signalling pathways have been proposed downstream of the GnRH-R upon GnRH binding, among which the MAPK/ERK has notably been involved in regulation of gonadotropin expression (Roberson et al. 1995, Sundaresan et al. 1996, White et al. 1999, Kanasaki 2005). Moreover, the effect of GnRH on the gonadotropins is not limited to the regulation of their expression: as binding of GnRH to the GnRH-R also induces a rise in intracellular calcium levels, this leads to the rapid

exocytosis of gonadotropins by the cells, linking GnRH rhythmicity with gonadotropin secretion (Naor, 2009). Despite numerous studies in different models, the signalling pathways downstream of the GnRH receptor are not fully elucidated. Importantly, most of the studies conducted so far have been performed on primary cultures or immortalized and transgenic cell lines, sometimes not best representative of the physiological truth. They have however made it clearer that several pathways are contributing to the decoding of GnRH pulsatility, through modulation of gene expression and receptor availability, to differentially regulate LH and FSH production and secretion by gonadotropic cells (Stamatiades et Kaiser 2018). Lastly, transgenic approaches have recently been proposed that constitute a valuable tool for future studies aimed at dissecting the cellular and intracellular mechanisms occurring in gonadotropic cells (Wen et al. 2008, Alim et al. 2012, Tran et al. 2013, Fortin et al. 2014, Beck et al. 2017), and since GnRH-R expression is not restricted to the pituitary, they will be crucial in uncovering the extent and roles of GnRH signalling during development and in the adult brain (Wen et al. 2010, Wen et al. 2011, Schauer et al. 2015).

B. Embryonic origin of GnRH neurons

i. A journey from the nose to the brain

Unlike other neurons, the GnRH neurons originate outside the brain and are born in the nasal region during the embryonic development. In 1980, Schwanzel-Fukuda and Silverman demonstrated the presence of cell bodies and fibers immunoreactive for several antisera directed against GnRH in the nasal region of the guinea pig at several stages between embryonic days 28-45. They were able to follow a scattered population of GnRH neurons in the path of the nervus terminalis – later recognized as cranial nerve 0 – from the ventromedial side of the brain to the nose through the cribriform plate. In the nasal region, some cell bodies and their axons were described as intertwined with the olfactory nerves, and axons were seen in close proximity to blood vessels, prompting the idea that these neurons could exert a sensory function. However, at later stages of development and in the postnatal guinea pig, the authors did not report data on the

nasal region because extraction of the brain from the skull disrupted the nervus terminalis (Schwanzel-Fukuda and Silverman, 1980). The same year, another group released a mapping of the GnRH neurons and fibers in the golden hamster brain, in which they were able to decalcify skull bones and observe GnRH immunoreactivity in the nasal region close to the olfactory and vomeronasal nerves (Jennes and Stumpf 1980). Complementary observations were made some years later in the gray opossum, with GnRH-immunoreactive neurons detected in the nose along the olfactory/vomeronasal/terminal nerves even at early postnatal stages (Schwanzel-Fukuda et al. 1988). Interestingly, there was no formal conclusion regarding the developmental origin of the GnRH neurons themselves, a fact which the authors explained by a lack of immunoreactivity for GnRH in very early embryonic specimen – preventing the identification of their original birth region. However, they hinted at a peripheral origin because of the greater number of GnRH-immunoreactive cells in the nasal region compared to the brain at early stages.

> "*The fact that more LHRH-immunoreactive cells were seen in the peripheral ganglia of the nervus terminalis than in the central nervous system early in development is suggestive of an origin from the neural crest or olfactory placode*" Schwanzel-Fukuda et al. 1988

In 1989, a study demonstrated the extra-cerebral origin of the GnRH neurons using mouse embryos from embryonic days 9 to 20 (Schwanzel-Fukuda and Pfaff, 1989). Immunoreactivity for GnRH was detected as early as the 11th embryonic day in the olfactory placodes of the nasal region, in the area of the future vomeronasal organ. GnRH neurons were described associated to the vomeronasal and terminal nerves throughout the nose, reaching the ventromedial forebrain and engaging towards the preoptic area and the hypothalamus by day 14. The authors notably remarked that the increase in brain GnRH neurons was correlated with a decrease in peripheral GnRH neurons, compatible with a migration from the nose to the brain. Concomitantly, a second group combined immunohistochemistry with *in situ* hybridization and resulted in the same conclusion: GnRH mRNA and immunoreactivity were found in the olfactory placodes but not in the brain around the 11th embryonic day, and some positive neurons had reached the brain at E12.5

by migrating along vomeronasal and terminal nerve projections. Interestingly, the study reported that virtually all GnRH neurons had migrated out of the nasal region at E16.5, and that all GnRH neurons detected at E12.5 – approximately 800 – were accounted for in the adult brain. Moreover, this study provided insights pertaining to the birth of these GnRH neurons, which does not necessarily reflect the time at which the peptide itself is expressed: the authors relied on tritiated thymidine injections to determine that the GnRH neurons entered a post-mitotic stage around E10-E11, shortly before the peptide is expressed. They also estimated from these results that around 100 progenitor cells could give birth to the whole GnRH neuronal population (Wray et al. 1989).

In a study relying on the neural cell adhesion molecule (NCAM) immunostaining to stain the sensory projection of the olfactory, vomeronasal and terminal nerves, Schwanzel-Fukuda et al. (1992) noted that migrating GnRH neurons were always in close association with vomeronasal and terminal projections, but not OMP-expressing olfactory projections, and that the crossing of the cribriform plate by the projections precedes that of the GnRH neurons. They thus concluded to a dependency of the neurons on the scaffolding formed by the sensory projections. Interestingly, some GnRH neurons were still observed by the authors in the nose of postnatal and adult animals.

Long debated, the precise nature of the GnRH neurons progenitors remains uncertain decades later. Indeed, the olfactory placodes where GnRH neurons are first detected do not have a unique embryonic origin: while some cells derive from the neural crest, others have been shown to derive from non-neural ectodermal progenitors (reviewed in Forni and Wray 2012) and the cell composition of this specific structure, as well as the extent to which both of its origins contribute to the embryonic derivatives, is thus unclear. In 2011, Forni and collaborators released their work on the use of transgenic mouse lines to investigate the origin of GnRH neurons. Mice expressing the Cre recombinase either under the control of the *Wnt1* promoter (expressed in neural crest cells) or the AP-2α cis-regulatory element (*Crect*, expressed in ectodermal cells) were crossed with Rosa26-LacZ or YFP reporter mice. The resulting *Wnt1Cre/RLacZ* or *Wnt1Cre/RYFP*

animals expressed the tracers in neural crest derivatives, while the *Crect/RLacZ* and *Crect/RYFP* animals expressed the tracers in ectodermal derivatives. As could be expected from the double origin of the olfactory placode, the GnRH cells did not appear as a homogenous population. GnRH Immunostainings and cell counting at PN0 on these reporter lines instead enabled the authors to determine that around 37% of the total GnRH population derives from the neural crests progenitors, while a complementary 73% of the population is of ectodermal origin. In summary, neural crest progenitor cells and ectodermal progenitor cells contribute in the olfactory placode to form the whole GnRH population (Forni et al. 2011). More recently, Shan et al. (2020) investigated the expression of the Islet-1/2 transcription factors in the developing and migrating GnRH neurons in the nose of mouse embryos. They found that a majority of – but not all – GnRH neurons were immunoreactive for Islet-1/2, with approximately 25% showing no staining. Interestingly, using the transgenic *Wnt1Cre/RYFP* reporter line, the Islet-1/2 negative GnRH cells were also shown to be YFP positive, that is to say neural crest derivative, an observation coherent with the dual origin of this specific population.

While the evidence for intermixed origin of GnRH neurons is compelling in these studies, one needs to keep in mind that a controversy exists in the literature. Notably, a study in zebrafish from 2018 lead to the conclusion that GnRH-3 neurons – the hypophysiotropic population, equivalent to the mammalian GnRH-1 neurons – derived exclusively from ectodermal progenitors (Aguillon et al. 2018). This is in contrast with previous work showing a neural crest contribution to the GnRH population (Whitlock et al. 2003). Challenging conclusions have also been reached through graft studies conducted in chicken: grafts of presumptive neural crests from GFP-expressing transgenic embryos to wild-type embryos demonstrated that the neural crests were not contributing to the generation of GnRH neurons, which showed no GFP expression contrarily to the expected neural crest derivatives (Sabado et al. 2012).

The different results obtained over the last decades regarding the neural crest and/or ectodermal origin of GnRH neurons could be explained in several ways. First, we cannot rule out inter-species differences in the ontogeny of the GnRH population: one could hypothesize that, during

evolution, some species have lost a contributing subpopulation, resulting in a specific ectodermal or neural crest origin, while in other species both lineages would be involved. The controversy could also have arisen from the experimental methods themselves. For example, while transgenic reporter mice proved to be a useful tool for lineage tracing, the argumentation would benefit from an increased number of reporter genes to confirm the nature of the putative progenitors. In live-imaging and software-assisted backtracking studies on zebrafishes injected with synthetic mRNAs encoding for fluorescent histones (Aguillon et al. 2018), one needs to pay attention to several pitfalls such as off-target/incomplete delivery and video undersampling inherent to the technique, as well as a lack of contextual markers to determine the precise original location of the cells.

In summary, while differences may exist in vertebrates, to date the results are strongly in favour of a dual contribution to the GnRH population at least in mammals. Future studies combining the techniques used so far in a single more integrative work, and/or new approaches overcoming their limitations, might put an end to the controversy in a near future. After their birth around E10.5 in mice, GnRH neurons migrate along sensory projections constitutive of the vomeronasal and terminal nerves in the medial part of the nose (Wray et al. 1989, Schwanzel-Fukuda et al. 1989, Schwanzel-Fukuda et al.1992) to reach and cross the cribriform plate and enter the brain. They are not, however, alone on their path to the brain.

ii. The olfactory epithelium and the olfactory nerve

On the rostral part of the developing mouse embryo, around E9, the olfactory placode forms from a thickening of the ectoderm and progressively invaginates to give rise to the olfactory pit, future olfactory epithelium and vomeronasal organ (Figure I-4). In the same time window, the olfactory bulbs start to form from the telencephalon, and by E11.5 to E13 the olfactory epithelium, the presumptive vomeronasal organ (VNO) and the developing olfactory bulbs (OB) are identifiable in the medial part of the head, on both sides of the midline (reviewed in Treloar et al. 2010, Miller et al. 2010).

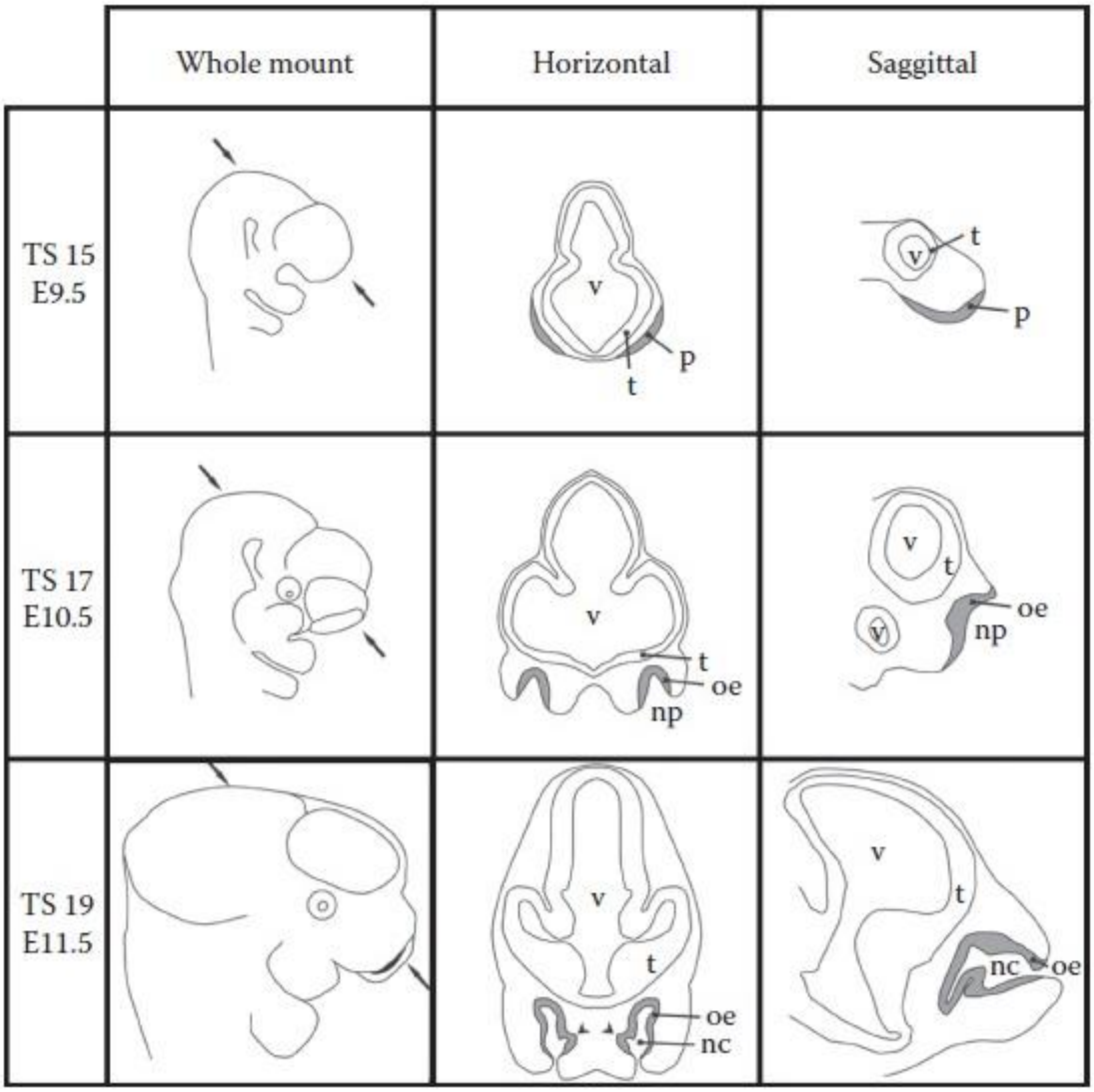

Figure I-4. Schematic of the developing nasal cavity from E9.5 to E11.5*. A thickening of the ectoderm forms the nasal/olfactory placode (p), which invaginates to give rise to the nasal/olfactory pit (np). The olfactory epithelium (oe) develops as the pit deepens to form the nasal cavity (nc). V: ventricle, t: telencephalon. Adapted from Treloar et al. 2010*

If neuronal staining is detected around E9.5 in the olfactory placode, at that time the axons from the olfactory sensory neurons (OSNs) that will later project to the olfactory bulbs are not yet visible. 24 hours later however, peripherin-positive axons emanating from the olfactory epithelium are detectable in the medial region, together building the presumptive olfactory nerve. The nerve will subsequently increase in density and organize in fascicles with the joining of new axons. Of note, a heterogeneous population of cells precedes the axons in crossing the basal

lamina of the olfactory epithelium towards the nasal mesenchyme, suggesting a guiding role for these cells forming a "migratory mass" (Valverde et al. 1992). By E12, axons from the olfactory epithelium have reached the developing olfactory bulb and in the following 24 hours, 80% of the migratory mass cellular population disappears, consistent with the putative role of this transient population in guidance of the olfactory axons and scaffolding of the nerves. At the level of the olfactory bulbs the remaining cells participate, together with the olfactory axons, to the constitution of the nerve layer of the olfactory bulbs after crossing the presumptive cribriform plate. As the projections that have reached the olfactory bulbs start establishing synapses locally around E15, more olfactory axons grow from the olfactory epithelium towards the telencephalon, and continue to join the olfactory nerve bundle.

In the postnatal rodent, the olfactory system consists in a large cavity encapsulated in tubinates on both sides of the medial nasal septum. These turbinates present with the respiratory epithelium, as the first component of the respiratory tract, and the olfactory epithelium responsible for detection of the odorant cues. OSNs projections from the olfactory epithelium join into the olfactory nerves in the nasal mesenchyme, cross the cribriform plate through its perforation, and reach the glomerular layer of the olfactory bulbs (reviewed in Treloar et al. 2010, Miller et al. 2010).

iii. The vomeronasal organ and the vomeronasal nerve

Similarly to the olfactory epithelium, the vomeronasal epithelium develops during embryogenesis from an invagination of the ectoderm-derived olfactory placode, and becomes distinctly identifiable around E11. Shortly after, and around the same time when the olfactory sensory axons emanate from the olfactory epithelium, axons from the vomeronasal sensory neurons (VSNs) emerge from the vomeronasal epithelium medially and on each side of the midline to travel through the nasal mesenchyme towards the telencephalon. Fascicles of VSNs axons together with cells of the "migratory mass" progressively constitute a vomeronasal nerve that densifies with the addition of new VSNs axons, and while the olfactory nerves projects to the developing main

olfactory bulbs, the vomeronasal nerves instead innervate and establish synapses in the accessory olfactory bulb (AOB) located in the medio-caudal part of the OB. By birth, the structure of the vomeronasal nerve is similar to that of the adult, but the system still requires maturation to achieve functionality. In the adult mouse, the VNO is an oblong-shaped organ encapsulated in cartilage and located on both side of the midline, at the floor of the nasal cavity, and it remains anatomically linked with the rest of the nasal cavity through a vomeronasal duct. In the vomeronasal epithelium, which is a pseudo-stratified structure, are VSNs presenting microvilli towards the VNO lumen, and sending axons towards the mesenchyme. The axons emanating from the VSNs bundle into the vomeronasal nerves which travel along the nasal septum, cross the cribriform plate and engage into the brain in-between the bulbs to take a lateral turn and join the accessory olfactory bulb (Dulac and Torello 2003, Zancarano 2014).

Although the VNO has been primarily associated to the detection of pheromonal cues (Dulac and Torello 2003), studies have also shown that VSNs of the vomeronasal epithelium can respond to olfactory cues, while OSNs of the olfactory epithelium can respond to pheromone-like compounds. Challenging the idea that the olfactory epithelium and VNO exert two functionally distinct roles, this suggest a complementary function in the detection of odors and pheromones (Brennan 2010). Despite the common origin of the VNO and olfactory epithelium, the similar organization and projections of the two systems, and their concurrent developmental time-window, it must be noted that the projections emanating from the VNO and olfactory epithelium do not intermix in the two structures they form: indeed, the olfactory and vomeronasal nerves remain anatomically distinct and innervate differently the olfactory bulbs (Wagner et al. 2006).

iv. The terminal nerve

Although the terminal nerve, also termed “cranial nerve 0” or “cranial nerve N”, has been discovered more than a century ago, it has been mostly overlooked in the scientific literature (Sonne et al. 2021). This nerve has been described as a diffuse and non-homogeneous structure, in that it is composed of different types of neurons scattered along its extension from the nasal

region to the brain. First identified in sharks, where this nerve is anatomically well discriminated from the olfactory nerves, it has subsequently been described in a number of vertebrates including rodents and humans. The projections and cells constituting the terminal nerve emanate from the region of the vomeronasal organ and travel intermixed with the vomeronasal nerves and olfactory nerves in the nasal compartment, before engaging through the cribriform plate into the forebrain. There, the terminal nerve separates from the vomeronasal and olfactory nerves and lies ventral to the olfactory bulbs, progressing caudally to reach the brain where it projects to several areas including olfactory and hypothalamic areas, as well as the amygdala (Wirsig-Wiechmann et al. 2002). Immunocytochemical and electron microscopy studies have shown that the fibers of the terminal nerves are unmyelinated, and that its neuronal projections are bordered by glial processes (Jennes 1987). The origin of the terminal nerve is linked, like for its olfactory and vomeronasal counterparts, to the olfactory placode of which the ablation is associated with an absence of olfactory/vomeronasal/terminal structures. In addition, it has been proposed that neurons from the neural plate reach the olfactory placode, and from there migrate to form the terminal nerve (Wirsig-Wiechmann et al. 2002).

In 1980, GnRH cells were for the first time characterized as a subpopulation of the terminal nerve neurons (Schwanzel-Fukuda and Silverman 1980), while neuropeptide-Y (NPY)-like / FMRF-amide neurons and cholineacetyltransferase (ChAT) neurons were also described along the terminal nerve of several vertebrate species. However, strong differences may exist: for example, if NPY immunoreactivity was found together with GnRH immunoreactivity in the same neurons in fishes, no such colocalization was observed in mammals where the two populations seem to be distinct from one another; additionally the amount of GnRH-immunoreactive neurons in the terminal nerve greatly varies across species (Wirsig-Wiechmann et al. 2002). Retrograde transport studies in mice, based on intracerebral True Blue injections and intravascular horseradish peroxidase (HRP) injections, demonstrated that GnRH-immunoreactive as well as immunonegative neurons of the terminal nerve project to the amygdala and to the nasal epithelium, but also come in contact with fenestrated blood vessels (Jennes 1987).

The roles of the terminal nerve and its constituting populations remain unclear, and could differ between species. However the presence of GnRH-immunoreactive neurons and fibers, together with the projections from the vomeronasal epithelium to different areas of the brain, are suggestive of its participation to sex-related behaviours dependant for example on pheromonal detection.

v. The olfactory system from rodents to humans

Although the rodent model is used in all types of study to mirror human physiopathology, it should be obvious that not all observations and results can be transposed to humans. As the development of the olfactory systems and migratory mass are not an exception to the general rule, similarities and differences exist between species and are worth mentioning to fully understand how far parallels can be drawn.

While the general organization is comparable between the rodent and human nasal cavity, the latter is often considered less developed: the relative olfactory epithelium surface is less important in the human nose, being restricted to the region just below the cribriform plate, and respiratory epithelium covers the most part of the turbinates. Similar to rodents, human olfactory sensory axons emanating from the olfactory epithelium expand through the mesenchyme, associated with olfactory ensheating cells, to reach and cross the cribriform plate. Perhaps the biggest anatomical difference in the peripheral olfactory system between the species considered here lies in the vomeronasal system: while it has been observed in a number of mammals, the vomeronasal organ is believed to be absent or vestigial in human adults – and so is the accessory olfactory bulb; moreover even when a vomeronasal structure is found, no vomeronasal sensory nerves can be identified in the nasal mesenchyme (Trotier et al. 2000). The system was not completely lost in evolution though, since a normal-appearing VNO is transiently observable in the developing foetus and presents characteristics similar to that of other species, including the establishment of sensory projections that will guide the migration of the GnRH neurons, before the organ starts to regress (Trotier 2011, Smith and Bhatnagar 2019). From there, it is tempting to speculate that the

only remaining role of the human vomeronasal organ is to give rise to the structures allowing the emergence and the guidance of the GnRH neurons on their journey from the nose to the brain, the lack of functionality at later stages thus explaining its subsequent regression.

vi. The migratory mass

During the investigation of the embryonic distribution of the GnRH system (Schwanzel-Fukuda and Silverman, 1980) and when the nasal origin of GnRH neurons was first established (Wray et al. 1989, Schwanzel-Fukuda and Pfaff 1989), other non-GnRH immunoreactive cells of seemingly different natures were described on the same migratory tracts. Together with the GnRH neurons, they form an ensemble called the migratory mass that was described by Valverde et al. (1992) in a morphological study of the developing olfactory system in rat. The authors observed that the olfactory axons projecting towards the brain were accompanied by groups of cells and, based on the shapes of their cytoplasms and nuclei, they believed these cells were heterogeneous in type. They identified some of them as olfactory ensheating cells (OECs), and other as migratory cells and neurons. In addition to being of heterogenous composition, the migratory mass is not formed from a defined number of cells that originate at a specific time point and then scatter throughout the nasal compartment, but instead is also a niche that generates new cells during embryonic development. Indeed, using 5-bromo-2'-deoxyuridine (BrDU) injections to identify mitotic and newborn cells in the mouse embryo between E10 and E12, Blanchart et al. (2011) have revealed that the migratory mass acts as a niche giving birth to new cells during the development of the main and accessory olfactory system.

Olfactory ensheating cells. The olfactory ensheating cells were previously discovered as glial fibrillary acidic protein (GFAP)-positive cells, found in association with the axons of the olfactory/vomeronasal sensory neurons, together constituting the olfactory/vomeronasal nerves. First identified as an equivalent of the peripheral nerve Schwann cells, light and electron microscopy later revealed that the OECs had more of an astrocyte-like phenotype, and these cells are now considered to have a mixed phenotype between peripheral and central glial cells (Fraher

1982, Barber et al. 1982, Fairless and Barnett 2005). During embryonic development, and in the context of the migratory mass, OECs and their projections encapsulate the sensory axons as well as other cells in the continuum reaching from the nasal sensory epithelia to the telencephalon, and are necessary for the proper scaffolding of the olfactory system.

Barraud et al. (2013) have used *in situ* hybridization and immunohistochemistry in mouse embryos to demonstrate that OECs express SOX10 in the nasal compartment during the establishment of the olfactory/vomeronasal/terminal scaffold in the time window of the GnRH neuronal migration. Interestingly, SOX10 disruption was associated with defasciculation of the olfactory nerve and a decreased number of mature olfactory sensory neurons in the olfactory epithelium, as well as impaired neuronal migration towards the olfactory bulbs: fewer GnRH neurons were found entering the brain of SOX10-disrupted animals compared to controls of the same stage. These results highlight the capital role of OECs in the development of the nasal migratory scaffold and subsequent GnRH neuronal migration. This is consistent with other reports of a guidepost role of OECs in this region during embryonic development, and in accordance with them expressing cell-adhesion and guidance molecules (Huilgol and Tole 2016, Perera et al. 2020).

Additionally, a subpart of the OECs population that associates with the axons crossing the nasal mesenchyme reach the telencephalon at the level of the developing olfactory bulbs. There, they facilitate the integration of the olfactory sensory axons in the olfactory bulbs, and they are incorporated into the olfactory nerve layer and glomerular layer of the olfactory bulbs (Ramón-Cueto and Avila 1998, Fairless and Barnett 2005, Blanchart et al. 2011).

If the original dogma stated that OECs were derivatives of the ectodermal olfactory placode, this idea was challenged by more recent works. Graft studies in chicken suggested that they in fact originated from the neural crest, and the same group found this to be true also in mouse using lineage tracing (Barraud et al. 2010). Soon after, another group working with transgenic mice models supported these results: using reporter lines, where Cre-mediated recombination triggers

permanent expression of a reporter specifically in cells of neural crest or ectodermal lineages, Forni et al. (2011) have shown that OECs were derived from neural crest progenitors.

During development, OECs thus originate from neural crest progenitor cells, and join the olfactory placode formation to migrate through the nasal mesenchyme and act as guideposts for sensory axons and migrating cells targeting the olfactory bulbs and the brain.

Neurons. If the first descriptions of neurons in the migratory mass were mainly based on morphological attributes, the use of specific markers later helped in the identification of their nature. Thus GAP-43, a protein involved in neuronal development and in mechanisms such as axonal growth and neurotransmitter release, can be used to determine the neuronal nature of cells in the embryonic nasal region. In rats, GAP-43 is expressed in the sensory neurons of the developing olfactory system, but also in a subpopulation of the migrating cells accompanying the sensory axons of the olfactory and vomeronasal epithelia, confirming previous reports of their neuronal nature (Pellier et al. 1994). Similarly, GAP-43 was later found in the migratory mass of mice in the time window corresponding to the formation of the olfactory/vomeronasal scaffold (Miller et al, 2010). In fact, staining of immature neurons with β-tubulin III, a protein constitutive of the neuronal microtubules, enables identification of neuronal populations in the olfactory pit as early as E9.5 in mice. While some of these neurons are olfactory sensory neurons that will project to the olfactory bulb, other show a migratory phenotype and migrate to the mesenchyme to then engage caudally towards the brain. This neuronal population is not unique and homogenous, but instead is comprised of several types of neurons different in their morphologies and markers (Miller et al. 2010). Among these cells of course are the previously described GnRH-expressing neurons.

Valverde et al. (1993) noticed the presence of olfactory marker protein (OMP) immunoreactive cells located along the sensory projections of the olfactory epithelia during the rat embryonic development. These OMP+ cells were later shown to express olfactory receptors in mouse, and to specifically associate with projections expressing the same olfactory receptors: this prompted the idea that the OMP+ cells of the migratory mass might be involved in the guidance and

selection of the olfactory sensory axons during their growth towards the olfactory bulbs (Conzelmann et al. 2002).

Additionally, a subpart of the neuronal population in the migratory mass has been shown to express acetylcholine esterase (AChE) in rats. AChE immunoreactivity is found in the olfactory placode and in a number of cells migrating from it along olfactory sensory projections, but different from GnRH+ and OMP+ cells. These AChE+ cells, of which the neuronal nature was confirmed by TUJ1 (a β-tubulin III clone) labelling, were seen to exit the olfactory placode before the other cells of the migratory mass, and to sometimes migrate independent from sensory projections. After they invade the telencephalon, both ventrally and dorsally, the AChE immunoreactivity fades away as the embryo progresses towards the end of its intrauterine development (De Carlos et al. 1995).

In 1996, Hilal and collaborators detected the neuropeptide Y (NPY), a known modulator of GnRH neurons, in the nasal region of the developing chick (Hilal et al. 1996). NPY neurons were similar in morphology to GnRH neurons, and were intermixed with them along sensory projections reaching towards the brain. It was noted though that there were fewer NPY neurons than GnRH neurons at all developmental stages observed, both in the nasal compartment and in the brain.

Overall, different neuronal populations emerge from the olfactory placode to contribute to the migratory mass. While specific populations are well characterized, such as GnRH+ and OMP+ neurons, the fate of other migrating neurons remains unclear and it was for instance proposed that they could be involved in the development of the olfactory bulbs and telencephalon (De Carlos et al. 1995) or the olfactory nerve (Miller et al. 2010). Moreover, using Doublecortin (DCX)-GFP transgenic mice to detect migrating neurons, Miller et al. (2010) made it clear that the so-far identified neurons of the migratory mass do not account for the whole neuronal component of the migratory mass, thus motivating further studies.

C. Regulation of the GnRH neuronal migration

i. Diversity of molecules involved the migration of GnRH neurons

Early work on the migrating GnRH neurons have concluded, based on the timing of emergence and on local interactions, to their dependency upon the scaffolding of the olfactory/vomeronasal/terminal projections for proper migration (Schwanzel-Fukuda et al. 1992). In addition, cases of defective axonal targeting of these sensory projections to the brain were associated with a failure in GnRH neuron migration (Schwanzel-Fukuda et al. 1989). The ensemble of mechanisms involved in the interactions between the GnRH neurons, the nerves and other cells of the migratory mass remained however to elucidate. Since then, numerous guidance molecules have been identified, and mutation and disruption studies have largely contributed to the current knowledge (Figure I-5).

Neural cell-adhesion molecule (NCAM) was among the first molecule suggested as a cue for proper GnRH migration. The work of Schwanzel-Fukuda et al. (1992) revealed strong NCAM immunoreactivity on the migratory path of the GnRH neurons, including in the sensory axons of the olfactory, vomeronasal and terminal nerves, but also in cells of the migratory mass. Moreover, when NCAM antibodies were injected in the developing olfactory pit, a delay was observed in the extraction of migrating cells from the olfactory pit epithelium, although this did not prevent proper targeting of the sensory projection and subsequent migration. In addition to showing NCAM's role in the development of the migratory mass, these results also demonstrate the multifactorial, compensatory nature of guidance mechanisms involved in this complex process.

Several cell surface molecules, as well as secreted molecules, and their downstream signalling pathways play a role in the regulation of GnRH neuronal migration through direct or indirect effects. Anosmin is a secreted guidance protein which has been involved in the proper development and targeting of the olfactory axons to the olfactory bulbs, and its disruption is associated with anomalies in the migration of GnRH neurons (Legouis et al. 1991, Wierman et al. 2011). Ephrins are cell-surface molecules with roles in axon guidance, and a mutation of the Ephrin receptor EphA5 is responsible for abnormal accumulation of GnRH neurons in the nasal

region (Gamble et al. 2005). Similarly, inhibition of NELF (nasal embryonic LHRH factor), a membrane protein found in migrating GnRH neurons and in olfactory sensory neurons, is deleterious for both olfactory axons scaffolding and GnRH neuronal migration (Kramer and Wray 2000). These are just a few examples out of many molecules regulating the early events of GnRH development (Wierman et al. 2011, Oleari et al. 2021), and it is undoubtable that numerous other molecules remain to discover. Among them and of particular interest in the context of the present work are specific guidance proteins and their interactors, namely the semaphorins, neuropilins, plexins and integrins.

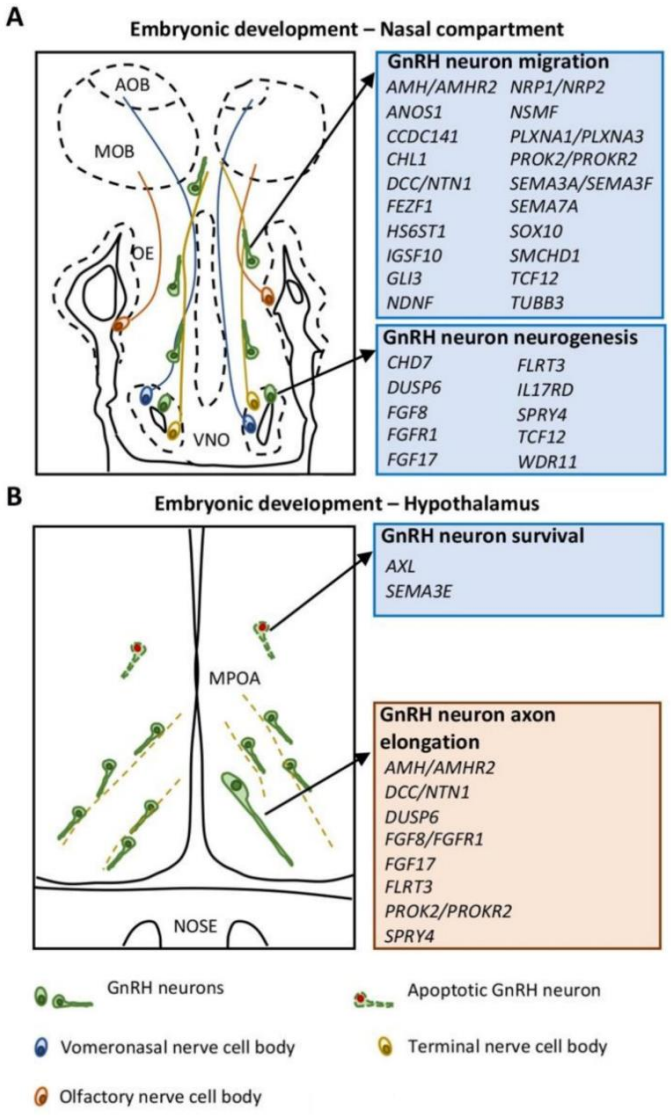

Figure I-5. Genes contributing to the development of the GnRH system*. This schematic illustrates the great diversity of genes involved in the regulation of the GnRH neuronogenesis and migration (A) and*

maturation (B). VNO: vomeronasal organ: OE: olfactory epithelium; MOB: main olfactory bulb; AOB: accessory olfactory bulb; MPOA: medial preoptic area. Modified from Oleari et al. 2021

ii. The particular case of semaphorin signalling

Over the recent years, it has become increasingly obvious that semaphorins, proteins known to be involved in guidance mechanisms, play a central role in the development of the GnRH system. Semaphorins are a family of membrane-bound or secreted proteins found in vertebrates and invertebrates alike, and divided in specific subclasses with classes 3 to 7 being specific of vertebrates (Figure I-6). All semaphorins notably possess *sema* and PSI (Plexins/Semaphorins/Integrins) domains, these regions being necessary for interaction with other semaphorins and with their receptors. The membrane-bound receptors for semaphorins include plexins, the main actors and transducers of semaphorin signalling, which can require additional cooperation from neuropilins and integrins. Like semaphorins, vertebrate plexins are divided in classes (PlexinA-D) and possess *sema* as well as PSI domains for interactions, while neuropilin-1/2 (Nrp1 and Nrp2) lack those (Messina and Giacobini 2013). Of note, neuropilins are thought not to be directly involved in the signalling but rather in its facilitation through stabilization of semaphorin/plexin interaction. Integrins on the other hand are cell-adhesion transmembrane receptors which are more directly involved in semaphorin signalling, as they have been shown to possess *sema* domains and/or domains homologous to the PSI domain. Finally, semaphorin binding and signalling is not limited to plexins/neuropilins/integrins system, but can also rely on other contributors such as proteoglycans, tyrosine kinase receptors or diverse cell-adhesion molecules (Alto and Terman 2017).

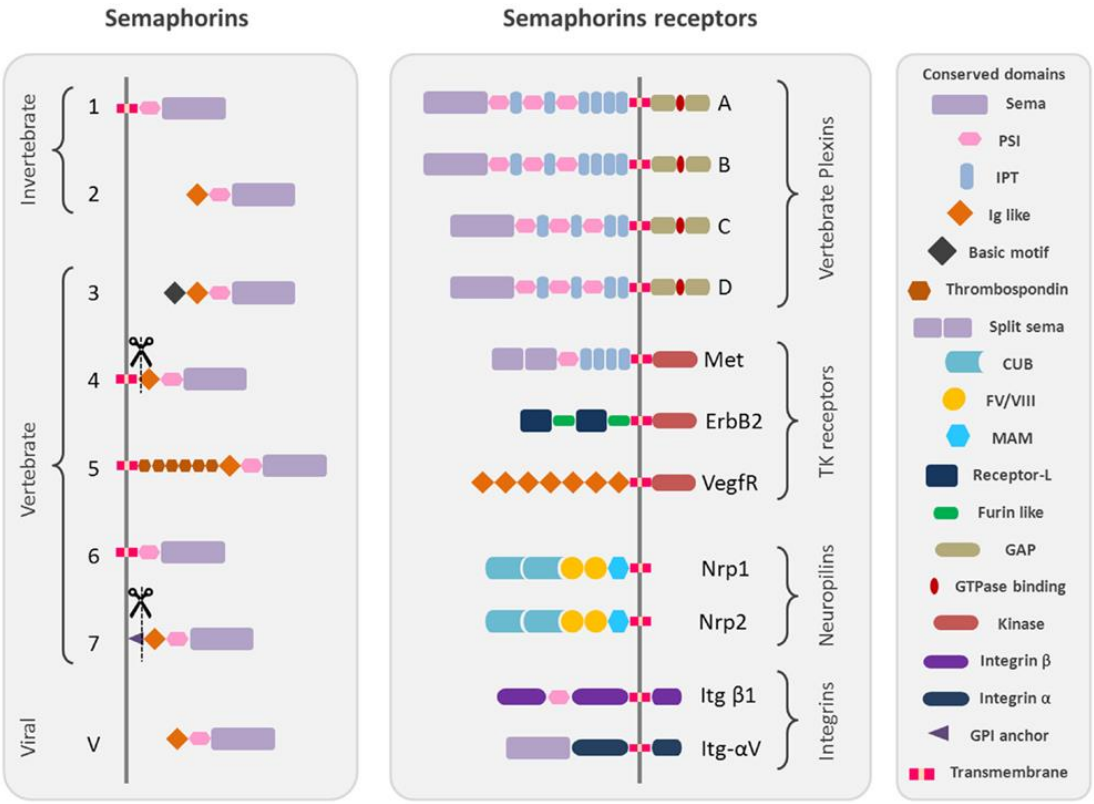

Figure I-6. Diversity of semaphorins and their receptors*. PSI: plexin semaphorin integrin; IPT: Ig-like Plexin Transcription factors; Ig-like: immunoglobulin like; CUB: complement C1r/C1s: Uegf: Bmp1; FV/VIII: coagulation factor V/VIII homology like; MAM: meprin like; GPI: glycosylphosphatidylinositol. From Messina and Giacobini 2013.*

Several semaphorins and associated receptors have been directly or indirectly involved in the development of the GnRH system, mainly through guidance mechanisms necessary for neuronal migration or axonal outgrowth. Indeed, semaphorins are expressed along the migratory path of GnRH neurons from the nose to their settling location and are necessary for proper establishment of the scaffold as well as cell migration. In the 1990s, Kawakami et al. (1996) demonstrated the expression of neuropilin in the rodent olfactory system and notably in the olfactory epithelium, the olfactory nerves and the olfactory bulbs, around the same time as the expression of semaphorin 3 and 4 were also reported in these regions (Giger et al. 1996, de Castro et al. 1999).

In 2000 the role of semaphorin 3A in the development of the olfactory axonal scaffolding was put forward, as semaphorin 3A was found in cells associated with olfactory axons and namely in olfactory ensheating cells, and the olfactory axons themselves were expressing the receptor neuropilin-1. In mice lacking functional semaphorin 3A, mistargeting of olfactory axons to the olfactory bulbs was observed although no defasciculation of the nerve was seen (Schwarting et al. 2000). Cariboni et al. (2011) later demonstrated that proper fasciculation of the vomeronasal nerves relied on semaphorin 3A signalling: in mice deficient for semaphorin 3A, improper targeting of vomeronasal nerves was further associated with a defective migration of GnRH neurons. Abnormal migration was also seen in mice lacking functional neuropilin-1 or neuropilin-2, both being expressed in the vomeronasal axons, but severe defects were only observed in mice lacking both neuropilins with only a handful GnRH neurons then reaching the brain – thus revealing a partial compensatory mechanisms. Semaphorin 3A was also involved in the regulation of hypothalamic GnRH plasticity: semaphorin 3A, expressed by endothelial cells of the median eminence, was indeed able to trigger the extension of GnRH terminals towards the capillaries in *ex vivo* experiments, an effect that appeared to be mediated by neuropilin-1 signalling and was crucial to the reproductive cycle (Giacobini et al. 2014).

Semaphorin 4D is another semaphorin expressed in the developing nasal region, with immunoreactivity detected in the nasal mesenchyme and at the nose-forebrain junction notably, while its receptor Plexin B1 was found in GnRH, olfactory and vomeronasal epithelia cells. Accordingly in mice lacking Plexin B1, migratory defects are observed in the GnRH population with an accumulation of cells in the nose during development, and a reduction of the number of cells and projections to the median eminence was also noted in postnatal animals, confirming the importance of semaphorin 4D/Plexin B1 signalling in these events (Giacobini et al. 2008).

Messina et al. (2011) later revealed in developing mice immunoreactivity for semaphorin 7A and Plexin C1 on the migratory route of GnRH neurons, and notably in the vomeronasal/olfactory epithelia and their projections to the forebrain. Additionally, they showed that migratory GnRH neurons express β1-integrin, and post-migratory GnRH neurons found in the forebrain express

Plexin C1. Interestingly, mice deficient for semaphorin 7A showed a defective migration and an altered distribution of GnRH neurons in the brain compared to control animals, associated with reduced fertility but without impairments of the olfactory/vomeronasal scaffold, while Plexin C1 deficient mice did not show any alteration in the distribution of GnRH neurons. Lastly, functional assays demonstrated that semaphorin 7A acts through β1-integrin to promote GnRH neuronal migration in the nasal compartment, and through Plexin C1 to inhibit cell motility. These results led to the conclusion that semaphorin 7A and its interactors play different spatio-temporally regulated roles on the regulation of the GnRH neuron migration and projections. Consistent with this idea, further studies showed that β1-integrin deletion in GnRH neurons also caused an alteration of GnRH projections to the median eminence and reduced fertility in mice, and that Semaphorin7A/PlexinC1/β1-integrin signalling was involved in the plasticity of these GnRH projections during the reproductive cycle (Parkash et al. 2012, Parkash et al. 2015).

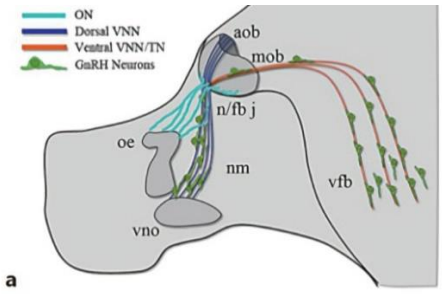

SEMAs	type	OE/VNO	NM	OB
SEMA3A	secreted	✓	✓	✓
SEMA3B	secreted	✓	✗	✓
SEMA3C	secreted	✓	✗	✓
SEMA3F	secreted	✓	✗	✓
SEMA4A	transmembrane	✓	✗	N.D.
SEMA4B	transmembrane	✓	✓	N.D.
SEMA4C	transmembrane	✓	✗	N.D.
SEMA4D	transmembrane/secreted	✗	✓	✓
SEMA7A	GPI-anchored/secreted	✓	✗	✓

b

Figure I-7. Semaphorins in the developing olfactory and vomeronasal system. *(a) Schematic of the embryonic GnRH neuron migration along the sensory projections. (b) Expression of diverse semaphorins on the migratory route of GnRH neurons. aob/mob: accessory/main olfactory bulb; n/fb j: nose/forebrain junction; nm: nasal mesenchyme; ob: olfactory bulb; oe: olfactory epithelium; on: olfactory nerve; TN: terminal nerve; vfb: ventral forebrain; VNN: vomeronasal nerve; vno: vomeronasal organ; From Giacobini (2015)*

The above-mentioned semaphorins and receptors only represent a fraction of the whole picture and other class 3 and 4 semaphorins, as well as neuropilin-2 or Plexin A1 for example, are expressed in the developing olfactory system and on the migratory route of GnRH neurons (Figure I-7, Giacobini 2015). In summary and whether the mechanisms involved are direct (on the

chemotaxis and axonophilic interactions of the migratory GnRH neurons) or indirect (on the projections of the guiding olfactory/vomeronasal/terminal nerves), semaphorins play a key role in the development and maturation of the GnRH system, and several members of this large family have already been implicated in these processes. Even after the nose-to-forebrain migration, proper distribution of the GnRH neurons in the brain and subsequent projections to the median eminence rely on cell motility, chemotaxis and axon targeting: in this context, semaphorins and their interactors – among other guidance cues – are promising candidates for further studies elucidating the establishment of the central control of reproduction.

D. Distribution of GnRH neurons in the adult murine and human brains

i. The adult mouse brain

After their migration during embryonic development, GnRH neurons reach the brain and settle in their final location. This location is not unique, however, as GnRH neurons do not form a single well-defined population of cells grouped in a specific area: instead, they are found scattered in the murine brain. Cartography of immunoreactivity for GnRH was made possible with the generation of antibodies against the peptide in the 1970s (Barry et al. 1973) before other groups contributed to this mapping over the years. The majority of GnRH neurons cell bodies, and evidently the most described to date, form an inverted Y-shaped distribution spreading from the septal region of the anterior brain all the way to the posterior hypothalamus in mice. Even in this pseudo-continuum the distribution of cells is not even, with a higher density of cell bodies being found in the preoptic area, notably close to the OVLT, the circumventricular organ of the anterior hypothalamus which receives GnRH neuronal projections (Figure I-8). Also strongly immunoreactive is of course the median eminence where a great number of GnRH neurons terminals project to reach the portal circulation (Zimmerman et al. 1974, Gross 1976). When focusing on the control of reproduction, it is interesting to mention that not all of the reported GnRH neurons project to the median eminence and are actually hypophysiotropic: aiming to identify GnRH neurons with access to fenestrated capillaries, Jennes and Stumpf performed

horseradish peroxidase uptake assays combined with GnRH immunolabeling and demonstrated that, in the different regions where GnRH cell bodies are found, both HRP-positive and negative neurons are present with a maximum of 65% GnRH neurons uptaking HRP from the capillaries (Jennes and Stumpf 1986). This approach, however, is not selective of access to the median eminence exclusively, as GnRH neurons in contact with capillaries in other regions could have uptaken HRP.

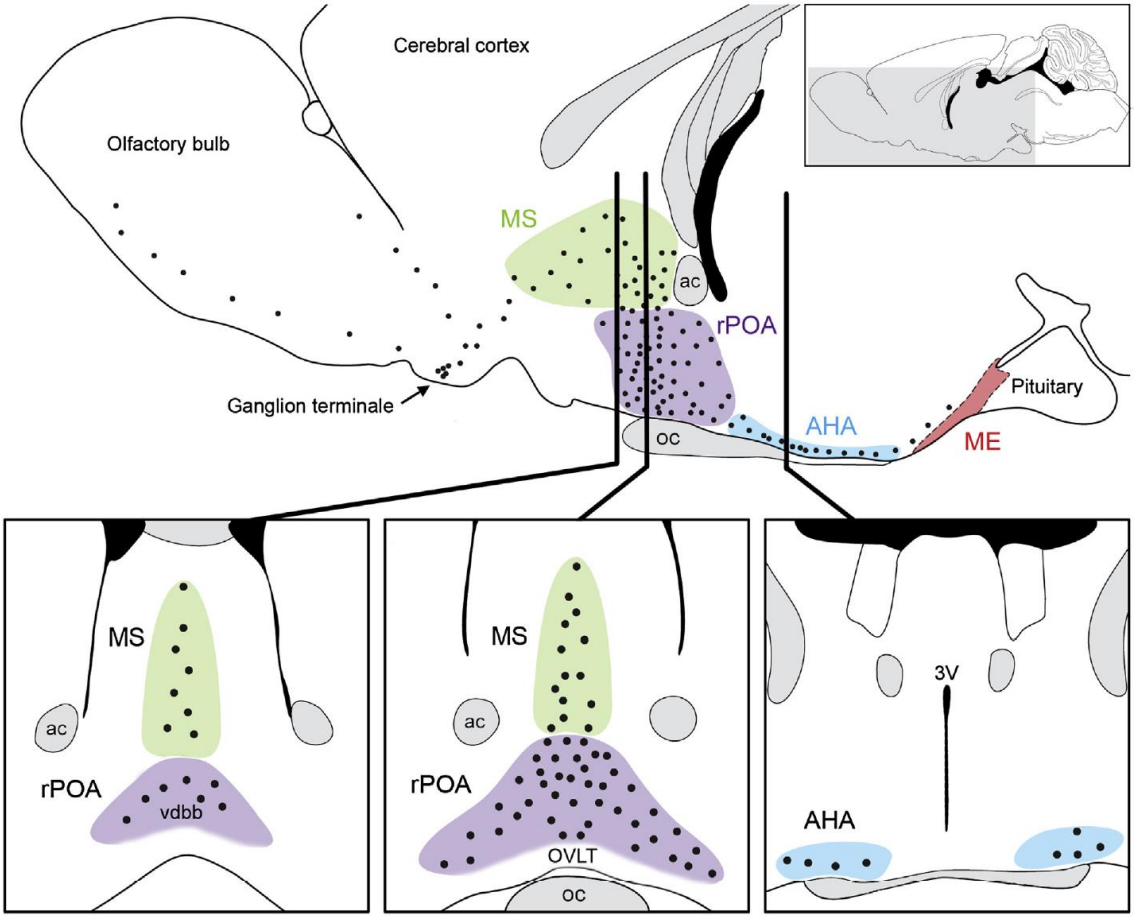

Figure I-8. Distribution of GnRH cell bodies in the mouse brain. *Black dots represent GnRH neurons cell bodies in sagittal (top) and coronal (bottom) sections. While the whole population extends from the olfactory bulbs to the posterior hypothalamus, a high number of GnRH neurons is found in a region defined by the medial septal nucleus and the preoptic area. Close to the OVLT, the population divides in two branches forming an inverted Y shape (bottom center panel). 3V: third ventricle; ac: anterior commissure; AHA: anterior hypothalamic area; ME: median eminence; MS: medial septal region; oc: optic chiasma;*

OVLT: organum vasculorum of lamina terminalis; rPOA: rostral preoptic area. Taken from Herbison (2015)

Probably the second major location of GnRH neurons is in the olfactory areas, notably in the region of the olfactory bulbs where numerous GnRH immunoreactive cell bodies and fibers are observed. Cells bodies are indeed present as a band reaching from the medial septum to the region anteroventral to the OB, but also dispersed more anterior to the OB and associated with projections of the olfactory/vomeronasal/terminal systems from the nasal compartment. Some cell bodies are also found in the accessory olfactory bulb and in close proximity, associated to the vomeronasal nerve (Figure I-9, Jennes 1986). These observations were corroborated by more recent work in rodents relying on three-dimensional imaging and also illustrating this so-called "olfactory GnRH system", notably with projections from GnRH neurons forming a ring around the olfactory bulbs, and cell bodies distributed in the OB and olfactory nerve layer (Casoni et al. 2016). The precise roles of the olfactory GnRH system, including those located in the nasal cavity, still need to be thoroughly investigated: functional connections between the olfactory/vomeronasal sensory systems and GnRH have been proposed, and lesions of the terminal nerve have been shown to impair sex-related behaviours, strongly suggesting that GnRH in this region acts as a neuromodulator in olfaction and pheromonal detection (Wirsig-Wiechmann and Wiechmann 2001, Wirsig-Wiechmann 2001).

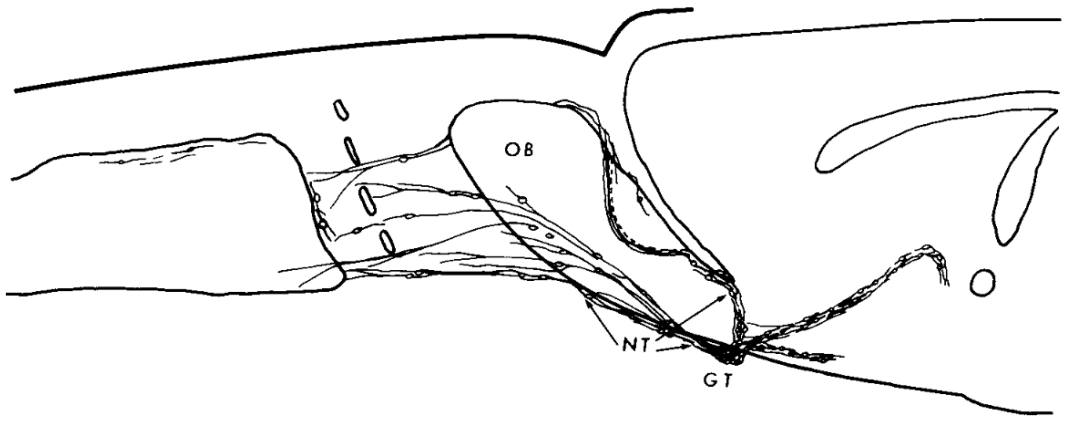

Figure I-9. Schematic representation of the olfactory GnRH system. *GnRH cell bodies (circles) and projections are shown scattered from the medial septal region of the brain to the nasal compartment. GnRH immunoreactive fibers form a ring around the caudal part of the olfactory bulbs, while projections and cell bodies form a continuum extending in-between the bulbs and through the cribriform plate. GT: ganglion terminale; NT: terminal nerve; OB: olfactory bulb. From Jennes (1986)*

Apart from this two major hypothalamic and olfactory regions, several other areas of the brain also host GnRH neurons, as cell bodies have been observed to reach the cingulate cortex, the subfornical organ, or the corpus callosum, although it is not known whether they were just lost in migration or if they are actually integrated in specific networks (Herbison 2015). Additionally, GnRH immunoreactive projections have been described in numerous regions including the epithalamus, the amygdala and the mesencephalon (Barry et al. 1973, King and Anthony 1984).

In all regions and species, characteristics of the GnRH neurons remain similar: they were described as being for the vast majority bipolar, around 20 µm in diameter, and usually present with a thickening of the projections in their most proximal part. These projections can cover several hundreds of micrometers, and both these fibers and the cell bodies can be covered with numerous plastic dendritic spines. Finally, an interesting feature of the projections consists in them being a hybrid dendrite/axon neurite, able to receive synaptics inputs, propagate axon potentials and exert a secretory function in the terminals. This notably has implications in the distal regulation of GnRH secretion (King and Anthony 1984, Herbison 2015, Campbell 2018).

Overall, GnRH neurons are distributed in several regions of the mouse brain, forming a pseudo-continuum from the olfactory regions to the hypothalamus inherited from their nose-to-brain migration during embryonic development. It is worth noting however that other areas of the brain contain GnRH cell bodies, and while it is not yet clear what their role is or where they project to, it is tempting to hypothesize that this distribution plays a role in the integration of diverse inputs important for the regulation of reproduction.

ii. The adult human brain

The study of the GnRH system in humans has been impaired by the availability of tissues and the limited amount of applicable techniques compared to animal models. Several groups have however investigated GnRH neurons and their distribution in the human brain.

The migration of GnRH from the nose to the brain, reviewed in details before, follows a similar pattern in humans: GnRH neurons are first seen in the olfactory placodes around the 5th week of gestation, and migrate along vomeronasal and terminal nerves branches towards the telencephalon over the next days. However, and in addition to the common ventral migratory pathway towards the hypothalamus, a subset of migrating GnRH neurons engages more dorsally into the developing brain in humans, towards the neocortex and developing hippocampus. Of note, the number of migrating GnRH neurons is also significantly higher than in rodents reaching approximately 10,000 during human development, with around 2,000 neurons engaging ventrally and 8,000 dorsally in the brain (Casoni et al. 2016, Skrapits and Hrabovszky 2018).

In situ hybridization and immunohistochemistry experiments were used to map the GnRH system on postmortem human brain sections. GnRH neurons also form a scattered population in the human brain, although their distribution differs from that of the rodent GnRH system: they are even more dispersed, with the highest concentration of cell bodies found in the ventral and basal hypothalamus, and less in the rostral hypothalamic areas. In summary, GnRH cell bodies were identified in the preoptic and hypothalamic areas, the septal region, the amygdala, the pallidum,

the putamen, the nucleus accumbens notably, for a total of approximately 7,000 hypothalamic and 6,000 extra-hypothalamic reported cells (Figure I-10, King and Anthony 1984, Rance et al. 1994, reviewed in Skrapits and Hrabovszky 2018). The presence of GnRH neurons and projections in the nasal compartment of the adult, as observed in several rodent species, remains however undescribed so far.

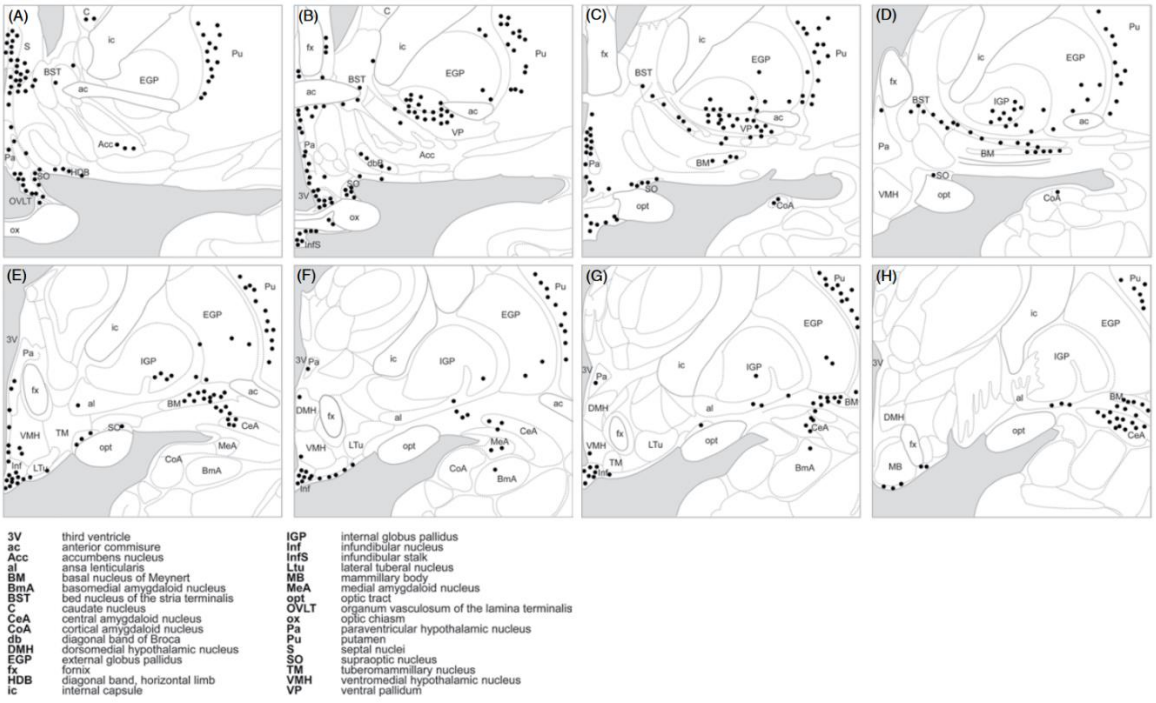

Figure I-10. Distribution of GnRH neurons in the human brain. *Black dots represent GnRH neurons identified by* in situ *hybridization or immunohistochemistry on human brain sections, and reveal the dispersion of the GnRH system in hypothalamic and extra-hypothalamic regions. Taken from Skrapits and Hrabovszky 2018*

More recently, a new study shed light on a previously overlooked population of GnRH cells in the adult human basal ganglia and forebrain, revealing an unexpectedly high number of extrahypothalamic cell bodies (150,000 to 200,000) scattered in these regions and verified to express the GnRH mRNA as well as the decapeptide (Skrapitz et al. 2021). Given the significant difference between the 10,000 migrating neurons observed in human foetuses (Casoni et al. 2016) and the estimated >150,000 cells in the adult, it can be hypothesized that a large portion of the human GnRH population does not in fact originate from the olfactory placode, but instead is born

in the brain itself. Interestingly, most of the extrahypothalamic GnRH cell bodies and projections in the human brain are contrasting with the well-known GnRH neuron morphology, as they exhibit a multipolar aspect and a low spine density. Additionally, the study revealed that a majority of extrahypothalamic human GnRH cells are cholinergic, a characteristic shared by approximately one third of hypothalamic GnRH neurons and visibly acquired after GnRH neurons migration from the nose reach the brain, and thus that these newly identified GnRH cells are certainly involved in functions other than the sole regulation of reproduction (Skrapitz et al. 2021).

iii. Heterogeneity of GnRH neurons

During the embryonic development, GnRH neurons derive from mixed progenitors of the neural crest and ectodermal lineages in the nasal compartment before they migrate into the brain (Wray et al. 1989, Schwanzel-Fukuda et al. 1989, Forni et al. 2011) and, in humans notably, additional on-site origins are highly probable for a large portion of the GnRH immunoreactive cells. This is consistent with several studies showing heterogeneity in the GnRH neuronal population, either regarding the morphological aspect, projection patterns, or gene and protein expression in these neurons in different species.

GnRH neurons were described as possessing different morphologies, sometimes intermixed in the same regions of the murine and human brain. Rance et al. (1994) thus characterized 3 types of GnRH neurons in the human brain: type 1 neurons were described as exhibiting a small and fusiform soma with extensive labelling of both the cell body and the processes (by *in situ* hybridization) and were primarily found in the mediobasal hypothalamus; type 2 neurons were depicted as small, roundish soma with low labelling; type 3 neurons were bigger with an area double of that of type 1 and 2 neurons, intermediate labelling intensity, and were numerous in the basal forebrain. All three types were found in different regions in varying proportions. The authors suggested that these differences and distributions were probably reflecting the existence of subgroups of GnRH neurons in the human. Similarly in mice, filling the neurons with a

fluorescent tracer revealed different morphologies, from unipolar to bipolar and more ramified all mixed in the preoptic area, in addition to changes in proportions of these subtypes triggered after the onset puberty (Cottrell et al. 2006).

As an example of differences in gene expression, in a study from 2005 on isolated cytoplasm of GnRH neurons from different regions including the medial septum and the preoptic area, the authors verified the expression of selected stress-related receptors and revealed that their expression in not homogeneous in the population. Indeed, 27% of the GnRH neurons studied showed expression of the corticotropin-releasing hormone receptor type 1 (CRH-R1) and 23% showed expression of interleukin 1 receptor accessory protein (IL-1Racc), but both expressions did not overlap, illustrating the existence of subpopulations of GnRH neurons (Jasoni et al. 2005). Similarly, a more recent study demonstrated that a subset (>50%) of GnRH neurons express the type 2 receptor for the anti-mullerian hormone (AMH-R2) in mice and humans, and that 50 to 70% of GnRH neurons are activated by AMH *ex vivo* (Cimino et al. 2016), another evidence for subgroups of neurons with specific phenotypes and functions.

Apart from morphology and expression, the large distribution of GnRH neurons is also a source of heterogeneity. Interestingly and in relation with the particular origin of GnRH neurons, it seems that the fate regarding their final location is dependent upon their time of birth. Jasoni et al. (2009) used a pulsatile 5-bromo-2-deoxyuridine (BrdU, which is incorporated in DNA during replication) approach in mice to show that early-born GnRH neurons were preferentially settling in the more rostral regions of the brain, while late-born GnRH neurons were ceasing their migration more caudally. The authors hypothesized that this phenomenon could be explained by changes in the progenitors of GnRH neurons and/or in the migrating environment over time. The mixed origin of GnRH neurons, together with changes in the progenitors during development, would explain differences in morphology and protein expression such as those mentioned before. While a good candidate for the determination of the stopping point of GnRH neuronal migration, a change in the migrating environment alone would not however justify the co-existence of

subtypes of neurons in close proximity, suggesting that a combination of factors is at play in this population's heterogeneity.

Accordingly, GnRH neurons do not seem to all exert the same function, and in all the species studied, only a part of the population is actually hypophysiotropic and responsible for the release of GnRH in the median eminence. While this does not exclude the rest of the population from the regulation of reproductive functions, through more indirect mechanisms, it reinforces the idea of specialized groups in the GnRH system as evidenced both in rodents (Silverman et al. 1987) and primates (Goldsmith et al. 1990). In these studies, and depending on the brain region, a maximum of ~60% GnRH neurons were projecting to the median eminence.

In summary, we would be mistaken to consider the GnRH neurons as a homogeneous population in the mammalian brain: there are evidently several subpopulations each with their own specificities and, to fully understand the organization of the GnRH network and dissect its multiple roles, further investigations are needed. Recent works, building on the observations of previous studies, have started to characterize in more details the heterogeneity of the GnRH neurons and surely pave the way for future works relying on trending techniques such as single-cell approaches and spatial transcriptomics, well-suited to differentiate functional subpopulations.

III. How interactions and integration shape the production and secretion of GnRH

A. The GnRH neuron as a central integrator

Proper functioning of the reproductive axis requires a fine regulation of hormonal secretions at all levels – hypothalamus, pituitary and gonads. Over the decades an accumulation of studies demonstrated that the reproductive axis is sensitive to internal cues, such as the metabolic status of the organism or its stress level, as well as environmental variables such as the photoperiod and circadian rhythms, olfactory and/or pheromonal cues, that regulate the production and secretion of the hormones. The mechanisms at play are not limited to the adult functioning of the

hypothalamic-pituitary-gonadal axis, but are also important during development (establishment of connections, fetal and minipubertal activations, etc.) and the GnRH neurons appear as the final integrators in this complex system.

Before discussing some of the signals integrated in the GnRH network, it is useful to remember that a double profile exists in GnRH secretion: a pulsatile release responsible and necessary for production and secretion of the gonadotropins LH and FSH, and a surge triggering the pre-ovulatory LH peak mid-cycle in spontaneously ovulating females. Both can be affected, either together or separately, in the regulation of the GnRH network.

i. The feedback loop: integration of sexual steroids

As covered previously, the peripheral organs of the HPG axis, namely the gonads, produce and secrete sexual steroids in response to gonadotropin stimulation – estradiol, progesterone, testosterone – which exert a positive and/or negative feedback at the central level.

Estradiol has been shown to possess mixed effects on GnRH-driven gonadotropin levels. Direct action of estradiol on GnRH neurons has been proposed, mediated by the estrogen receptor β (ERβ) – its alpha variant (ERα) being absent in GnRH neurons, but remains controversial and instead, indirect action through other cell populations is the preferred theory. As an example of direct mechanism, ERβ has been involved in the direct facilitation of glutamatergic and GABA-ergic stimulation of GnRH neurons (Farkas et al. 2018). Regarding partner populations able to mediate estrogenic effects, tracing studies revealed that several populations expressing ERα (which mediates the vast majority of estradiol's actions) were located in preoptic and hypothalamic regions, host to numerous GABA-, glutamate- and kisspeptin-producing neurons with connections to GnRH neurons. Estradiol's positive feedback plays an important role in the LH surge, when elevated and sustained levels of the hormone are required hours prior to the surge for it to happen. In rodents, lesion studies have demonstrated that populations essential to the induction of the LH surge by estradiol were located in the rostral periventricular region (RP3V).

There, GABA, glutamate and kisspeptin neurons have all been linked to the surge, as around this time GABA and glutamate are increased, and kisspeptin neurons are activated. Estradiol's negative feedback is more obscure, as some investigators concluded to an effect mediated by neurons in the preoptic area or the mediobasal hypothalamus, but this was not consistent with results from lesions studies. Candidate for the relay of the negative feedback are the preoptic GABAergic neurons and arcuate kisspeptin neurons. The latter have been shown to express ERα and show an increased expression of kisspeptin with ovariectomy, restored by estradiol (Herbison 2015).

Progesterone's feedback is mainly negative and effective after ovulation, during the luteal phase of the cycle. Because mature GnRH neurons of several species do not seem to express progesterone receptors, indirect effects are again most probably involved in its negative feedback. Opioid peptides and dynorphin-expressing population of the arcuate nucleus have been involved in this action, while the mediation of the positive progesterone effects probably relies on the same actors that permit the positive estrogen feedback (Herbison 2015).

Finally, testosterone has been shown to modulate LH and FSH release from the pituitary, and proposed to inhibit the GnRH pulse generator (Matsumoto and Bremner 1984). However, for a lack of androgen receptor in GnRH neurons, this effect is not direct, but requires upstream partners (such as kisspeptin neurons) and has been established to act either via androgenic pathways or estrogenic pathways after aromatisation of testosterone (Marques et al. 2000, Navarro et al. 2011, Moore et al. 2018).

ii. Integration of circadian rhythms

The evidence for the integration of circadian rhythm, and notably photoperiod, in the control of reproductive functions has been long established. In their natural habitat, most mammals have adapted their breeding strategies to the moment of the year which is most favourable for survival of both the mother and offspring, and this adaptation can take several forms such as periods of

impotency or very long pregnancies. Additionally, artificial maintenance of animals under controlled conditions in laboratories, thus suppressing natural photoperiod changes, have been shown to impact the reproductive functions (Reiter 1980).

The biology of circadian rhythms is complex and its centre lies in a specialized region of the hypothalamus, namely the suprachiasmatic nuclei (SCN) which receive inputs from the visual system. Isolated SCN show an intrinsic cyclic activity *in vitro*, involving a number of "clock" genes that form retro-controlled loops to maintain this cyclicity (Migaud 2014). Ablation of the suprachiasmatic nuclei, or mutations and deletions in genes involved in circadian rhythmicity lead to infertility in rodents. As an example in mice, a deletion in the *Clock* gene altering the CLOCK protein caused irregular cycles, alteration of the levels of LH and sexual steroids, and increased pregnancy failures (Miller et al. 2004). The authors notably concluded that the abnormal cyclicity was not linked to the levels of sexual steroids, as supplementation did not rescue the phenotype, nor to pituitary defects as cultured gonadotropic cells presenting with the mutation were responding normally to GnRH. Instead, they proposed that a lack of synchronization between circadian signals from the suprachiasmatic nuclei and GnRH neurons was responsible for the alterations observed in mutant mice.

Other than the intrinsic activity, the evidence for extrinsic cues is strong in seasonal breeders, where the influence of the photoperiod has been long demonstrated and the duration of daylight influences the reproductive capacities of the animal. In the syrian hamster, artificial exposure to short daylight supresses the reproductive functions, thus mimicking the natural breeding rhythms of the species which does not reproduce during winter. This integration of daylight involves the pineal gland, downstream of the SCN, and secretion of melatonin (Migaud 2014). While GnRH neurons themselves do not express the melatonin receptors, other populations expressing those receptors can relay the signals, such as RFamide-related peptide (RFRP) and kisspeptin neurons of the hypothalamus which are upstream of GnRH neurons (Revel et al. 2006, Ancel et al. 2012).

Recently, a melatonin-proficient mouse (the MSM mouse strain) was proposed as a model for the study of photoperiod integration by neuroendocrine circuits. In this mouse, indices of

reproductive functions (testicular mass, hormone levels) decreased with the transition from long to short photoperiods, consistent with differences in melatonin expression, while no change was observed in control melatonin-deficient C57 mice. This alternative laboratory model can help elucidate some of the mechanisms which we cannot observe in common mouse strains used in reproductive studies (Sàenz de Miera et al. 2020).

iii. Integration of the metabolic status

The integration of metabolic cues in the control of reproductive functions is once again a logical adaptation for the preservation of the species, restricting breeding to the only individuals able to survive and care for the offspring. As a result, undernutrition is associated to diminished reproductive functions and/or alterations in the offspring (litter size, body mass). This requires the ability for the circuits controlling reproduction to sense peripheral cues reflecting the metabolic status of the organism. One such cue is a well-studied adipokine, namely leptin, of which the circulating levels are proportional to the adipose tissue in the animal.

Leptin's role in the control of the hypothalamic-pituitary-gonadal axis was first evidenced by the defective maturation of the axis in obese mice with mutations in the gene encoding for leptin (*ob/ob* mice), rendering them infertile (Swerdloff et al. 1976). Two decades later, intraperitoneal administration of recombinant leptin in these same mice was shown to restore fertility and permit ovulation and successful pregnancy (Chehab et al. 1996). Interestingly, a rise in circulating levels of leptin occurs during prenatal (humans) or postnatal (rodents) development with no link to adipocity or the control of food intake, but rather involved in the development of metabolic and neuroendocrine circuits. In a leptin receptor-deficient mouse, where this perinatal rise in leptin cannot exert its effects, a number of metabolic alterations, but also reproductive defects are observed which cannot be rescued with subsequent leptin-receptor reactivation (Ramos-Lobo et al. 2019).

As GnRH neurons do not express the leptin receptor, it was first uncertain how the effects of leptin were mediated. Studies conducted around 2010 pointed to neurons of the ventral premammillary nucleus (PMV) as relays of the leptin signalling, since lesions in this nucleus abolish leptin-mediated restoration of fertility in *ob/ob* mice. Neurons in the PMV that responded to leptin were shown to send projections towards kisspeptin neurons in the preoptic region and GnRH terminals in the median eminence, two possible ways for the stimulation of GnRH neurons. (Donato et al. 2011) The precise mechanisms are still elusive, and several candidates have been proposed in the transduction of leptin signalling from PMV neurons to either kisspeptin or GnRH neurons, including glutamate and nitric oxide. Additionally, sensing of leptin by orexigenic neuropeptide Y/Agouti-related peptide (NPY/AgRP) neurons of the arcuate nucleus could also be involved (reviewed in Childs et al. 2021).

Another potential player at the crossroad of energy balance and reproduction is ghrelin, a hormone mainly secreted by the stomach, which acts as an orexigenic signal. Ghrelin has been shown to decrease LH levels in rats, inhibit GnRH secretion *in vitro*, and affect the timing of puberty in male but not female rats (Fernandez-Fernandez et al. 2006). Of note, a lack of ghrelin receptor in the GnRH neurons points to a relay of ghrelin signalling *via* upstream populations with connections to the GnRH neurons. Kisspeptin neurons are again candidates for this relay, as a subset of arcuate kisspeptin neurons expresses the ghrelin receptor and is activated by ghrelin *ex vivo* (Frazao et al. 2014). Anorexigenic and orexigenic neurons of the arcuate nucleus, the pro-opiomelanocortin (POMC) and NPY/AgRP neurons well-known for their controlling of food intake, also possess the ghrelin receptor, are connected with kisspeptin neurons and could potentially directly and indirectly affect GnRH neuronal activity (reviewed in Navarro and Kaiser 2013).

If only leptin and ghrelin where mentioned here, other factors such as insulin are also investigated in the link between the sensing of metabolic cues and the central control of the HPG axis (Navarro and Kaiser 2013, Roa and Tena-Sempere 2014). Overall, the coupling of metabolism and reproduction does not rely on a single mechanism, but instead seems to involve the integration of

a multitude of signals reflecting different aspects of the energetic status (adiposity, hunger, etc.), and these signals are using more than one route to fine-tune GnRH production and secretion. Finally, if undernutrition or obesity can lead to a reduction or loss of fertility, they are also inducers of immune stress which can participate to their negative impact on reproductive functions.

iv. Integration of stress

Physiological and psychosocial stressors are known to alter reproductive functions, and include a plethora of metabolic, immune, emotional or environmental perturbations for example. As stress is a coping mechanism for the organism facing changes or distress, and is resource-demanding, it often leads to the inhibition of functions that are not capital for its survival, including reproduction. Stressors act via the activation of the hypothalamic-pituitary-adrenal axis: corticotropin-releasing factor (CRF) and arginine vasopressin (AVP) are released from the hypothalamus into the portal circulation to stimulate the production of adrenocorticotrophic hormone (ACTH), which reaches the adrenal gland to increase glucocorticoids (cortisol/corticosterone) release. This activation is responsible for a number of physiological changes increasing survival chances (accelerated heart rate and respiration, increased glucose levels) and inhibiting dispensable processes (immune response, memory). Routes for the activation of the HPA axis are diverse, with the endpoint being in the paraventricular nucleus of the hypothalamus (PVN) where CRF and AVP-expressing neurons are located (Li and O'Byrne 2015).

The effect of the HPA on reproductive function in the context of an immune stress can be mimicked by injections of lipopolysaccharide, a constituent of bacteria membranes, or cytokins such as interleukins. The most observed result is a suppression of LH pulsatility in several species including rodents and monkeys, and in ewes a loss of GnRH pulsatility was also observed.

Psychosocial stressors have been studied in rodents using mainly changes in environment and restraint, and was investigated in monkeys using restraint chairs, showing again a loss of LH pulsatility that was recovered with habituation. Primates studies also revealed alterations of GnRH secretion and LH pulsatility under social stressors such as low social status or aggression (reviewed in Li and O'Byrne 2015).

In their search for the mechanisms causing a defect in GnRH and thus LH release and pulsatility under stress conditions, investigators have proposed a role for kisspeptin-expressing neurons. Expressions of kisspeptin and its receptor are reduced under the influence of various stressors, and administration of glucocorticoids to mimic levels found in stress-induced conditions provokes a similar decrease in expression. Whether the effects of glucocorticoids on kisspeptin neurons are direct or indirect is not certain, as glucorticoids receptor expression seems to vary with location and species. Alternatively, CRF release by hypothalamic populations could also act, either directly or *via* a proxy, on kisspeptin neurons to in turn modulate GnRH neurons. Possible relays of the stress-induced suppression of reproductive functions also include the well-known GnRH neuron regulator GABA, since GABA-ergic signalling is affected by a number of stressors and by administration of CRF, as well as RFRP which is upregulated under stress conditions (reviewed in Li and O'Byrne 2015, Sominsky et al. 2017).

If the link between stress and silencing of reproductive functions is clear in all species, the circuits involved remain to be further elucidated. Induction of stress in animal models, through environmental, physical, or even genetic modifications are providing new leads on the interactions between the HPA and the HPG axes. However, it appears from current knowledge that they rely on synergistic mechanisms that are both central and peripheral, with probable variation between species, and with the precise circuitry of the GnRH system still being investigated, dissection of these mechanisms will require time and extensive work.

v. Interactions of GnRH neurons and non-neuronal cells

If non-neuronal contribution to the GnRH system development has been covered previously, so far only neuronal interactions were mentioned in the present section. However, several studies have hinted at and then confirmed the fundamental contribution of glial cells to the control of reproductive functions, since association of GnRH neurons and their terminals with glial cells prompted the idea of a role for glial cells in the regulation of GnRH physiology in the 1990s.

One of these glial cells interacting with GnRH neurons is the astrocyte. Astrocytes processes and cell bodies are found associated with GnRH neurons, they produce and release prostaglandin E2 (PGE2), and PGE2 triggers depolarization and generation of action potentials in GnRH neurons, as well as the release of GnRH through a post-synaptic excitatory effect. In addition, chemical blockade of PGE2 synthesis, as well as a deficiency in PGE2 production by astrocytes, both cause impaired GnRH neuron firing, strongly suggesting a role for astrocytes in the regulation of GnRH neuronal excitability (Clasadonte et al. 2011, reviewed in Prévot and Sharif 2018).

The second glial cell type with a strong role in the neuroendocrine control of reproduction is the tanycyte. Tanycytes are specialized ependymal cells lining the wall of the third ventricle, shown to send their projections towards the vessels of the median eminence notably, and their endfeet also encapsulate GnRH terminals while showing structural plasticity during the estrous cycle (Prévot et al. 1999), thus providing a regulation of GnRH terminals access to the portal circulation (reviewed in Prévot and Sharif 2018). Such plasticity appears to depend upon the guidance molecule semaphorin 7A, expressed by tanycytes, that promotes both retraction of GnRH terminals and extension of tanycytic endfeets (Parkash et al. 2015).

Finally, endothelial cells have also been investigated in neuroendocrine-related structural changes in the median eminence. First reports of the structural plasticity included apparent cycle-dependant evaginations of the basal lamina in rats, and the aforementioned sprouting of GnRH terminals, a phenomenon which was then proposed to involve the contribution of endothelial cells (Prévot et al. 1999). It was later revealed that endothelial cells of the portal system in the median eminence express and release semaphorin 3A, with varying levels across the estrous cycle, and

via semaphorin 3A signalling they can attract neuropilin-1-expressing GnRH terminals. Of note, neutralization of semaphorin 3A or neuropilin-1 *in vivo* in the median eminence of rats disrupts the estrous cycle (Giacobini et al. 2014).

In summary, non-neuronal contribution to the control of GnRH neurons is well-established, both at the level of neuronal activity and excitability with the role of astrocytes, or in the control of the GnRH release in the median eminence through regulation of axonal accessibility to the portal circulation by tanycytes and endothelial cells (Figure I-11). Interestingly, several of these mechanisms have been linked to specific phases of the estrous cycle and correlated with the levels of sexual steroids, pointing to their importance in the regulation of the pre-ovulatory GnRH/LH surge (Prévot and Sharif 2018).

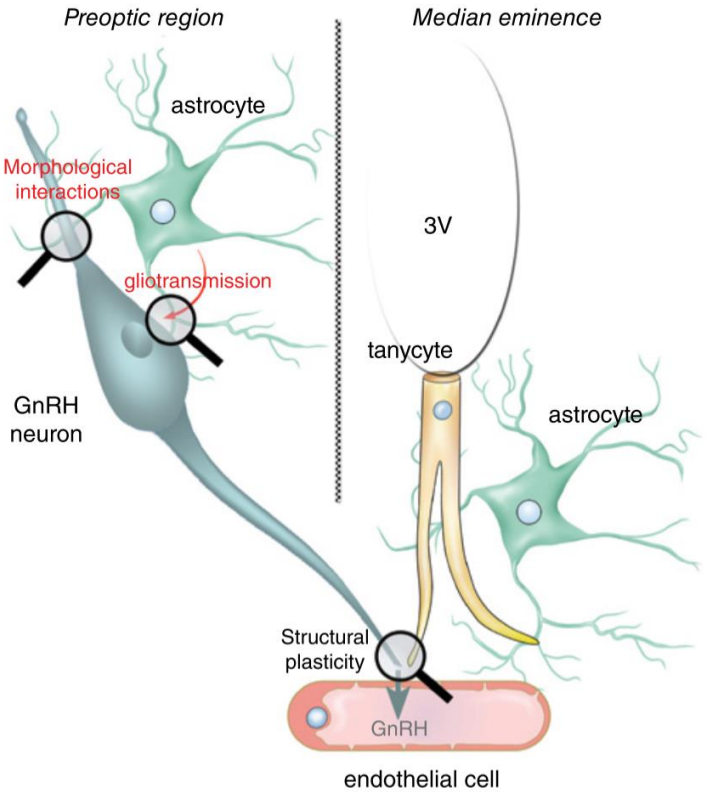

Figure I-11. Non-neuronal cells in the central control of reproduction. *The schematic illustrates the roles of glial cells such as astrocytes and tanycytes, and endothelial cells in the regulation of GnRH neurons via morphological, molecular and structural interactions. Taken from Prévot and Sharif 2018*

vi. Modular control of the GnRH neurons

Based on the different internal and environmental cues impacting the reproductive functions via their regulation of GnRH neurons across species, Herbison (2016) has proposed a modular design of the GnRH network (Figure I-12). In this design, the GnRH system is organized in core components with optional species-specific modules. Among the core components are the migration, distribution and morphology of GnRH neurons which are relatively conserved in mammals, and the GnRH pulse generator driving pulsatile LH. Functional modules include the ones related to the surge generator, which would differ greatly between spontaneous and reflex ovulators for example, steroid feedback mechanisms, and sensing of internal/external influencers such as those mentioned before (rhythms, metabolic cues, stressors…).

Interestingly, specific populations of kisspeptin-expressing neurons are a key part of several of the components in this design, as they are connected to both the GnRH pulse generator and surge generator, and those same kisspeptin neurons have been mentioned before in the integration of internal and external cues to regulate GnRH neurons. The importance of kisspeptin neurons and kisspeptin signalling in the GnRH network and in reproduction warrants going into more details about these neurons.

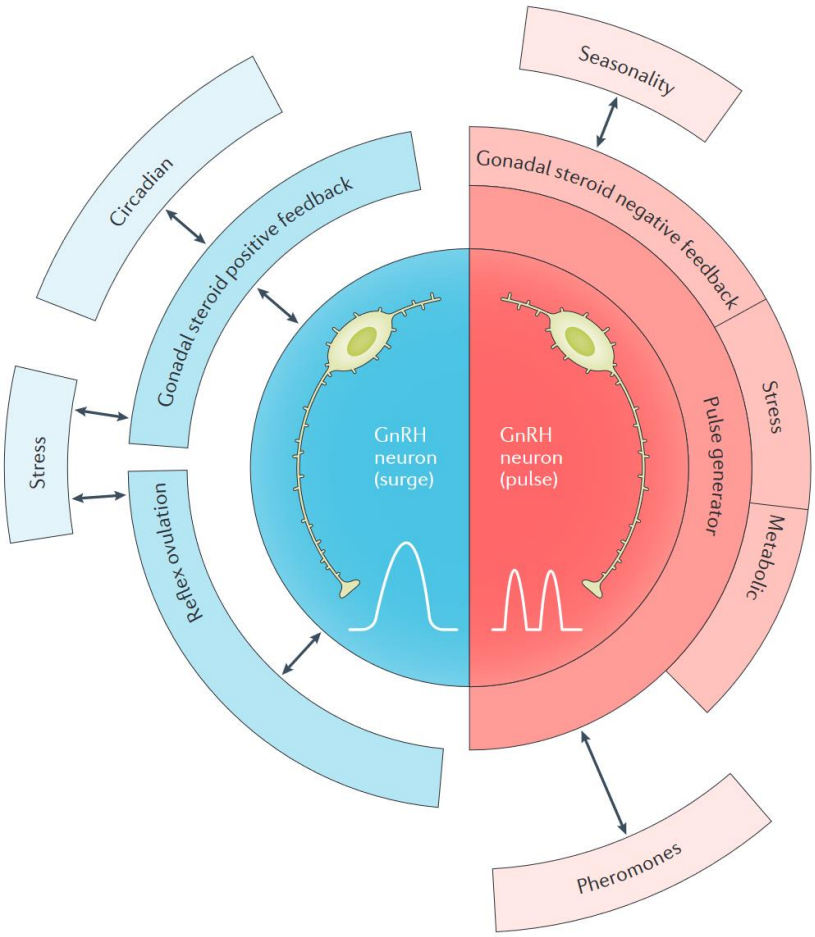

Figure I-12. Herbison's proposed model of the GnRH network regulation. *The two profiles of GnRH neurons, responsible for surges and pulses of GnRH release, are represented in the centre of the design. Modules common to all species, such as pulse generation, influenced by integration of gonadal steroid/stress/metabolic hormones are attached directly to the core components, while species-specific and non-obligatory modules are distant. Taken from Herbison (2016)*

B. Kisspeptin and GnRH neurons, a special relationship

i. Kisspeptin in the brain

Although kisspeptin has a fundamental role in the control of reproduction, as will be discussed later in the text, this is not its only role in the mammalian brain. The kisspeptin cDNA was discovered in 1996 from non-metastatic melanoma cells, and identified in several organs including heart, liver, lungs, muscles and brain (Lee et al. 1996). In the next years, several peptides derived from the kisspeptin (KISS1) protein were discovered, namely kisspeptin-54, kisspeptin-14, kisspeptin-13 and kisspeptin-10, of respectively 54, 14, 13 and 10 amino acids, and all were able to bind the orphan receptor GPR54 later renamed KISS1R.

In the brain, most of kisspeptin immunoreactivity is found in cell bodies and fibers distributed throughout the preoptic area and the hypothalamus in rodents, but fibers are also present in other brain regions such as the thalamus, the amygdala, the septum or the brainstem. Accordingly, KISS1R expression seems to be present in all regions were KISS was found, and to possess an even larger distribution, based on *in situ* hybridization assays. This large distribution, while variable between species, is suggestive of numerous roles for the kisspeptin system in the brain. Although these roles are still being investigated, kisspeptin's stimulation of oxytocin and vasopressin neurons, presumably *via* both central and peripheral actions, have been described (Scott and Brown 2011), as well as a role in the arcuate nucleus through stimulation of POMC neurons and inhibition of NPY neurons (Fu and van den Pol 2010). Additionally, kisspeptin has been suggested to act as a neuromodulator in the hippocampus and in memory processes (reviewed in Liu and Herbison 2016).

However, most of the effects of kisspeptin described above are not as potent as those it exerts on GnRH neurons, suggesting the control of reproduction as the most relevant physiological function of kisspeptin.

ii. Kisspeptin and reproduction

The major role of kisspeptin in puberty and thus reproductive functions was demonstrated in the early 2000s, when two studies pointed at mutations of the kisspeptin receptor GPR54/KISS1R in the etiology of hypogonadotropic hypogonadism, with manifestations such as impuberism, partial breast development, low circulating gonadotropins and sexual steroids in affected families. In addition, $GPR54^{-/-}$ mice exhibited alterations of the HPG axis including a lack of sexual maturation and disrupted estrous cycles. While it was not yet clear at which level of the axis kisspeptin and its receptor were acting, the ability of peripheral organs to react to gonadotropins in patients and mutant mice were suggesting a central mechanism of action (de Roux et al. 2003, Seminara et al. 2003).

Mapping of kisspeptin and its receptor in the brain revealed their expression in regions were GnRH neurons and projections are also found, compatible with a direct action on GnRH neurons: kisspeptin mRNA was thus detected in the preoptic area, the anteroventral periventricular nucleus (AVPV) and the arcuate nucleus in rodents (Gottsch et al. 2004), while GPR54 mRNA was detected in GnRH neurons themselves (Herbison et al. 2010). Notably, low doses of kisspeptin are able to stimulate GnRH release *in vitro* (Novaira et al. 2009), as well as *in vivo*, and intracerebroventricular (ICV) administration of kisspeptin elicits LH release in a GnRH-dependant manner (Gottsch et al. 2004).

An interesting feature is the dimorphism in the number of kisspeptin-expressing neurons observed in the AVPV, but not the arcuate nucleus of rodents, with 10 times more neurons in females than males. Also, AVPV kisspeptin neurons show a progressive increase in number during postnatal development and until puberty, which is not the case of the arcuate nucleus population, and together with close appositions between kisspeptin fibers and GnRH neurons, this prompted the idea that the AVPV population was the one responsible for pubertal reactivation of the HPG axis (Clarkson and Herbison 2006).

From there it became clear that kisspeptin, as a central player in puberty onset and potent stimulator of GnRH neurons, was a good candidate in the integration of internal and external cues

for the regulation of GnRH production and release, which generated a great interest in the neuroendocrine community. Numerous studies soon focused on their role in the integration of photoperiod, steroid feedback, metabolic status or stress in the control of reproduction (mentioned before and reviewed in Clarke et al. 2015).

In parallel, studies aiming to better understand the connections between GnRH and kisspeptin neurons were undertaken and great progress was made using transgenic mouse lines. In mice expressing a microtubule-associated τGFP after Cre recombinase-mediated recombination driven by kisspeptin expression, kisspeptin neurons were observed as early as E13.5 in the arcuate nucleus of females, and increased in number to reach approximately 1000 by E16.5, with projections to the preoptic area also detected. Interestingly, a similar reporter model for GPR54 revealed that expression of the kisspeptin receptor in GnRH neurons starts at E13.5 and progressively increases during development, and 50% of GnRH neurons express GPR54 at E16.5. Moreover, trans-synaptic tracing further demonstrated that kisspeptin neurons of the arcuate nucleus were connected to and upstream of a subset of GnRH neurons already at E16.5 (Kumar et al. 2014). Of note, almost identical data were obtained on the prenatal development of the arcuate kisspeptin population in male embryos using these approaches (Kumar et al. 2015). Genetically engineered trans-synaptic tracing also established that kisspeptin neurons of both the AVPV and arcuate nucleus are synaptically connected to GnRH neurons in adult mice, but subpopulations exist since not all kisspeptin neurons show this connection. Noteworthy, all kisspeptin neurons in contact with GnRH neurons express ERα, consistent with a relay of estradiol signalling (Kumar et al. 2015). Finally, viral-based conditional tract tracing demonstrated that kisspeptin neurons of the AVPV contact mainly GnRH cell bodies and their proximal projections, while arcuate kisspeptin neurons do not, and conversely are seen contacting the distal part of GnRH projections and their terminals near the median eminence (Yip et al. 2015).

Given the differential development of the AVPV and arcuate nucleus kisspeptin populations and their projections to GnRH neurons and terminals, their proposed roles in integration of diverse internal and external cues, and the general timeline of development of the kisspeptin/GnRH

system, a model of kisspeptin-GnRH interactions in the regulation of the HPG axis was recently proposed (Herbison 2016). During prenatal and postnatal development, GnRH neurons receive stimulatory inputs from the arcuate nucleus kisspeptin neurons, which are silenced during the juvenile period, and return in the prepubertal period. At puberty, the stimulation from both the AVPV and ARC kisspeptin neurons (among other partners) allows acquisition of proper reproductive functions. In this model, arcuate kisspeptin neurons are believed to be involved in pulse generation, while AVPV neurons are responsible for the surge mechanism (Figure I-13).

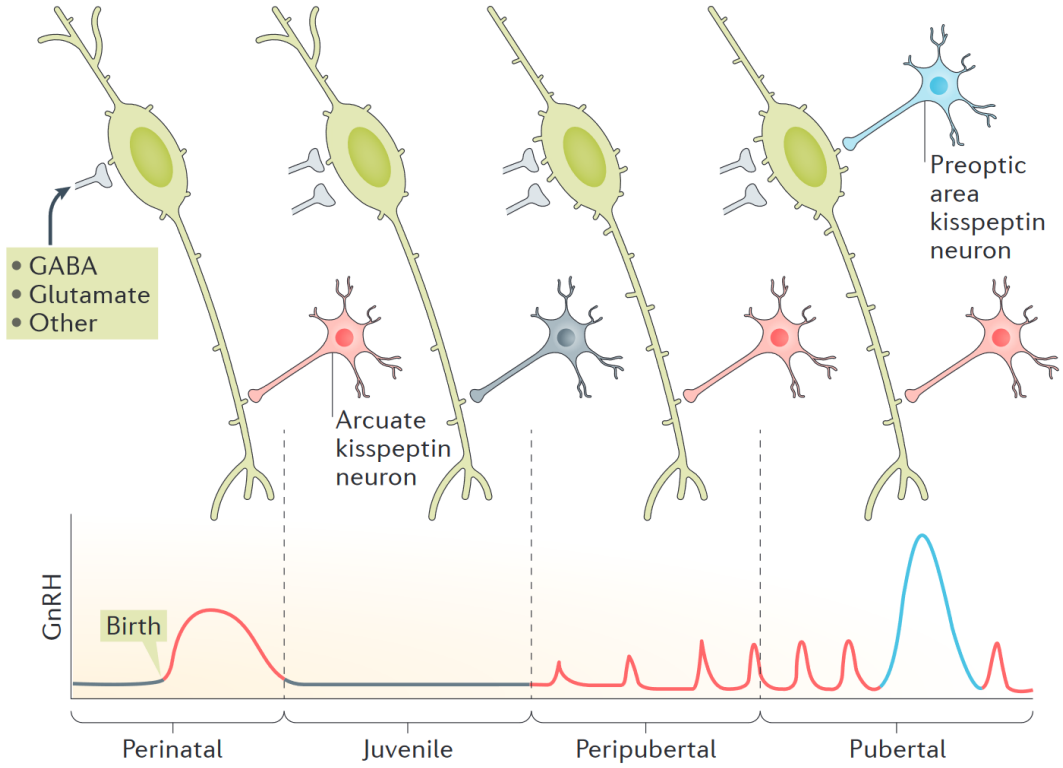

Figure I-13. Timeline of development of the GnRH/Kisspeptin system. *Arcuate kisspeptin neurons (red) contact distal GnRH (green) projections* in utero *and are involved in perinatal activations of the HPG axis. The system is silenced during the juvenile period (gray). As puberty approaches, arcuate kisspeptin inputs return, suggested to be involved in pulsatile GnRH secretion, and AVPV kisspeptin neurons interactions develop (blue) to allow surge generation. Taken from Herbison (2016)*

iii. The KNDy neurons in the GnRH network

Despite the crucial roles for kisspeptin discussed above, kisspeptin neurons also express other peptides involved in the stimulation or modulation of GnRH neurons. Indeed, neurokinin B and dynorphin are also found in a subset of arcuate kisspeptin-expressing neurons as first described in the ewes before extension to other species (Goodman et al. 2007, Lehman et al. 2013), and mutations in neurokinin B and its receptor were associated with altered reproductive functions in humans (Topaloglu et al. 2009). This led to these specific sets of neurons being nicknamed KNDy (Kisspeptin-NeurokininB-Dynorphin) neurons.

The modes of action of kisspeptin, neurokinin and dynorphin are believed to be multiple in the control of GnRH neurons. KNDy neurons emit projections towards GnRH cell bodies and terminals in the hypothalamus, but also establish contacts between themselves forming an interconnected network able to fine-tune GnRH release. While kisspeptin and neurokinin B have been shown to be stimulators of GnRH and LH release, the kisspeptin receptor is not found in KNDy neurons, but the receptor for neurokinin B is expressed in those cells and points to neurokinin B as the candidate synchronizer for the KNDy population. A different case is made for dynorphin which is considered as the mediator of the negative feedback of sexual steroids (reviewed in Lehman et al. 2010, Uenoyama et al. 2021) and thus a final modulator of GnRH neurons. Overall, it is currently proposed that arcuate KNDy neurons form an interconnected population that integrates a number of physiological cues and synchronizes its activity through stimulatory neurokinin B and modulatory dynorphin inputs, to finely regulate GnRH pulses *via* kisspeptin, GABA and glutamate signalling (Uenoyama et al. 2021). Finally, and while most studies used ovine or rodent models, less data is currently available on the KNDy neurons in human and primate physiology. So far however, immunohistochemistry demonstrated colocalization of kisspeptin, neurokinin B and dynorphin in arcuate nucleus neurons, mutations in the kisspeptin and neurokinin B signalling pathways are associated with altered reproductive functions, and endogenous opioids such as dynorphin have been linked with inhibition of

GnRH/LH secretion; all suggesting at least a partial applicability of the proposed model to the human control of reproduction (reviewed in Lehman et al. 2019).

Perhaps a more integrative view of the control of GnRH neurons by partner neuronal populations in the hypothalamus is better recapitulated in the recently proposed KiNG (kisspeptin, nNOS, GnRH) system which also takes into account the nitric oxide (NO) synthetizing neurons of the hypothalamus. These neurons are found in several nuclei of the hypothalamus, including the preoptic area and the arcuate nucleus, and possess the neuronal nitric oxide synthase (nNOS). Moreover, NO production and release is under the influence of sexual steroids, is involved in the control of GnRH neurons, and a subset of nNOS neurons are close to kisspeptin-expressing neurons/fibers and express the kisspeptin receptor. As a result, NO has been proposed as an actor in the control of pulse generation, by modulating the refractory response of GnRH neurons after stimulation by kisspeptin, and promoting their return to excitability. Additionally, nNOS neurons could play a role in the surge of GnRH/LH by restraining GnRH neuron activity to promote their synchronization at the time of the surge. While it is supported by several recent studies, the validity of this model requires further investigation to be confirmed (reviewed in Delli et al. 2021).

IV. Central defects in the HPG axis and alteration of fertility

A. Hypogonadotropic hypogonadism and Kallmann Syndrome

The previous sections emphasized the importance of the development and maturation of the neuroendocrine and peripheral systems comprising the HPG axis for the acquisition and maintenance of reproductive functions. At the central level, the ontogeny, migration and interactions of GnRH neurons, and the integration of diverse parameters by the GnRH network, are complex processes relying on a broad range of molecules. Accordingly, anomalies in these processes can lead to defects in the HPG axis and cause reproductive disorders.

Notably and when considering the GnRH network, a deficiency in the production, secretion or activity of GnRH, and thus gonadotropin control, manifests by incomplete/absent puberty and

infertility, a condition termed Hypogonadotropic Hypogonadism (HH). HH is a heterogenous disease, as it can sometimes present with other anomalies of the facial or skeletal development. Of note, in approximately 60% of cases it can be associated to an impaired sense of smell and when a patient presents with anosmia/hyposmia, HH is then termed Kallmann Syndrome (KS) after Kallmann's description of this co-segregation in 1944. These are rare diseases with an estimated incidence of 1:10,000 to 1:100,000, and with a male predominance of 3-5 to 1 (Kallmann et al. 1944, Bianco and Kaiser 2009, Boehm et al. 2015).

Clinically, HH can be detected as soon as the neonatal period in some patients. Indeed, in males a deficiency of the HPG axis during perinatal development can be the cause of cryptorchidism or micropenis, but the condition is harder to detect in females at that stage. The condition is more easily detected during adolescence and in the adult: in both sexes, absent puberty after the age of normal puberty onset can reveal HH, with undervirilization, cryptorchidism and micropenis in males, while females generally exhibit no breast development and absent menstruation. Additionally, poor or absent sense of smell points to Kallmann Syndrome. As a side effect, psychosocial manifestations can be encountered (low libido and self-esteem, depression). In general, confirmation of the diagnostic relies on the exclusion of other pathologies presenting with similar manifestations, and on hormonal profiling to assess levels of circulating gonadotropins or sexual steroids. In cases of KS, MRI can reveal defective olfactory bulb development. Finally, and because the conditions have a hereditary component, genetic testing and counselling are warranted for HH/KS patients. After initial diagnostic and confirmation, treatments are available to correct the manifestations of HH: several approaches exist to rectify cryptorchidism/micropenis (surgery, testosterone or gonadotropin injections), develop sexual characteristics and fertility in males (pulsatile GnRH administration, gonadotropin or testosterone injections), and in females (administration of estradiol, gonadotropin or GnRH therapy), and such treatment occasionally trigger HH reversal (Boehm et al. 2015).

As for its clinical aspects, HH is heterogenous in its genetic origins, with sporadic and familial cases, and monogenic as well as oligogenic forms reported. Franco et al. (1991) were the first to

identify a gene associated with Kallmann Syndrome, and named it *KAL1*. The investigators noted at the time that the predicted product of this gene showed similarities with molecules involved in cell adhesion and axonal pathfinding (Franco et al. 1991). The nature of the protein was confirmed later when discovery was made that the gene codes for anosmin-1, a secreted glycoprotein, which prompted renaming *KAL1* as *ANOS1* (Hardelin et al. 1999). Since then, the list of genes involved in HH and KS has incremented gradually, and today counts more than 50 genes (Oleari et al. 2021), but approximately half of reported HH/KS cases remain of unidentified cause (Table I-1).

The deficiency in GnRH secretion, production or activity in HH and KS can result from a number of alterations in the neuroendocrine circuitry of reproduction: abnormal development or migration of GnRH neurons in the nose, defect in neuronal projections and interactions, altered hormone synthesis or release, and defective hormone signalling (Forni and Wray 2015). Interestingly, genes identified from patients and families presenting with HH and KS are involved in all of these processes (Figure I-14, Table I-1). For instance, pertaining to GnRH production, secretion and action, mutations have been found in the genes coding for GnRH (*GNRH1*, Chan et al. 2009) or its receptor (*GNRHR*, de Roux et al. 1997), kisspeptin (*KISS1*, Chan et al. 2011) and its receptor (*GPR54*, Nimri et al. 2011), neurokinin B and its receptor (*TAC3*/*TACR3*, Topaloglu et al. 2009), among others (Marino et al. 2014, Boehm et al. 2015, Forni and Wray 2015).

Because of their particular interest in the context of the present work, the next section will focus on mutations of genes involved in the origin and migration of GnRH neurons, and their contribution to the etiology of HH/KS.

GENE	PROTEIN	ROLE IN GNRH SYSTEM	PHENOTYPE
AMH	*anti-Müllerian hormone*	Migration and axon elongation	nHH/KS
AMHR2	*Type 2 receptor for the anti-Müllerian hormone*	Migration and axon elongation	nHH/KS
ANOS1	*anosmin-1*	Migration	KS
CHD7	*chromodomain helicase DNA binding protein 7*	Neurogenesis	nHH/KS
FGF8	*fibroblast growth factor 8*	Neurogenesis and axon elongation	nHH/KS
FGF17	*fibroblast growth factor 17*	Neurogenesis and axon elongation (hypothesized)	HH
FGFR1	*fibroblast growth factor receptor 1*	Neurogenesis and axon elongation	nHH/KS
GNRH1	*gonadotropin-releasing hormone*	Signalling and secretion	nHH
KISS1	*kisspeptin*	Signalling and secretion	nHH
KISS1R	*kisspeptin receptor / GPR54*	Signalling and secretion	nHH
NDNF	*neuron-derived neurotrophic factor*	Migration	KS
NRP1	*neuropilin-1*	Migration	KS
NRP2	*neuropilin-2*	Migration	KS
PLXNA1	*plexin A1*	Migration	KS
PLXNA3	*plexin A3*	Migration	nHH/KS
SEMA3A	*semaphorin 3A*	Migration	nHH/KS
SEMA3E	*semaphorin 3E*	Survival	KS
SEMA3F	*semaphorin 3F*	Migration	nHH/KS
SEMA7A	*semaphorin 7A*	Migration	nHH/KS
TAC3	*tachykinin-3 / neurokinin B*	Signalling and secretion	nHH
TACR3	*tachykinin receptor 3 / neurokinin B receptor*	Signalling and secretion	nCHH

Table I-1. Selected hypogonadotropic hypogonadism-associated genes*. The table illustrates the diversity of genes with known mutations in hypogonadotropic hypogonadism and Kallmann Syndrome, with a selection of genes relevant to the present section. 23 out of more than 50 genes reported so far are listed,*

together with the corresponding proteins and associated roles in GnRH neuron development, and the phenotype of affected patients. (n)HH: normosmic hypogonadotropic hypogonadism; KS: Kallmann Syndrome. Adapted from Oleari et al. 2021.

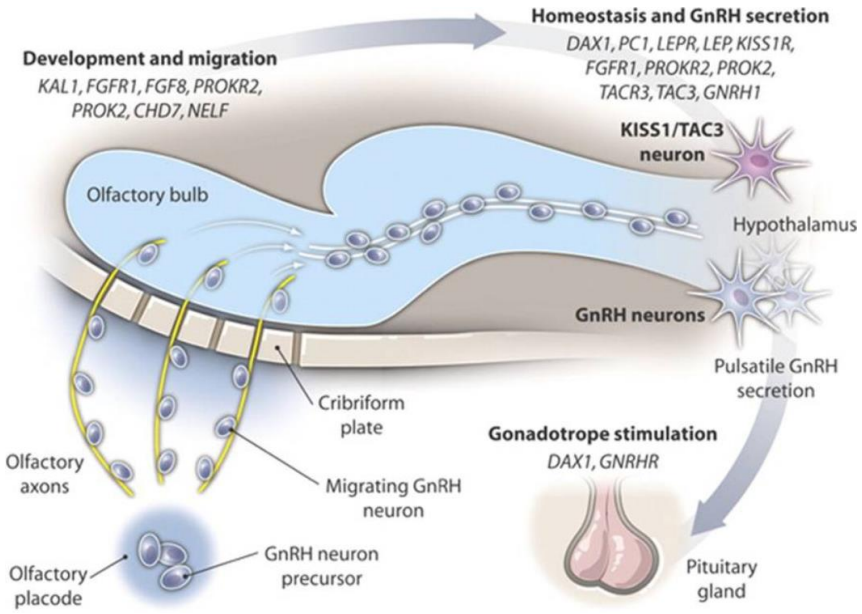

Figure I-14. Numerous genes are involved in the development of the GnRH network*. The ontogeny and migration of GnRH neurons, and the maturation of the GnRH network, rely on a wide range of mechanisms and a diversity of genes, many of which are known to be mutated in patients with hypogonadotropic hypogonadism and Kallmann Syndrome. Taken from Balasubramanian and Crowley (2011)*

B. Guidance molecules and HH/KS: a long and incomplete story

Already in 1989, soon after the nasal origin of GnRH neurons was uncovered in rodents (Wray et al. 1989, Schwanzel-Fukuda and Pfaff 1989), Schwanzel-Fukuda and colleagues reported the absence of GnRH neurons in the brain of a Kallmann fetus, but accumulation of these neurons in the nose (Schwanzel-Fukuda et al. 1989). It was then postulated than cases of KS could derive from a failure of migration of GnRH neurons to their final location in the brain. Over the years, studies from different groups have unveiled a number of mutations of genes involved in the birth and migration of GnRH neurons from the nose to the preoptic/hypothalamic regions.

i. Defects in the origin of GnRH neurons

Defects in the origin of GnRH neurons usually result from abnormal development of the nasal region during embryogenesis, or defective GnRH neurogenesis itself (Forni and Wray 2015). This is nicely illustrated by mutations affecting fibroblast growth factor 8 (FGF8) signalling.

Nonsense mutations of the *FGF8* gene were identified in families presenting with HH, KS, and associated developmental defects such as cleft lip and palate, or deafness (Falardeau et al. 2008, Trarbach et al. 2010). FGF8 was later proven to play a crucial role in the development of the face, and notably the formation of the nose (Griffin et al. 2013) and, as a result, mutations of the gene coding for FGF8 resulted in abnormal craniofacial development and disruption of GnRH neurogenesis in both rodents and humans (Forni and Wray 2015). In addition, mutations of the gene coding for the receptor for FGF8, namely *FGFR1*, were also found in HH/KS families, further demonstrating the role of FGF signalling in the ontogeny of GnRH neurons (Dodé et al. 2003, Pitteloud et al. 2006, Villanueva and de Roux 2010). Of note, it was recently reported that deletion of FGFR1 in GnRH neurons themselves did not prevent acquisition of reproductive functions in mice, with normal GnRH migration to the brain, supporting the indirect role of altered FGF8/FGFR1 signalling in GnRH deficiency (Dela Cruz et al. 2020).

Another example is the *CHD7* (chromodomain helicase DNA binding protein 7) gene, which was found mutated in KS patients (Ogata et al. 2006, Gonçalves et al. 2019, Xu et al. 2021). After CHD7 was shown to play a role in cell proliferation and protein synthesis (Zentner et al. 2010), further investigation demonstrated its involvement in cellular proliferation at the level of the olfactory placode (Layman et al. 2011), and in the migration of cells from the neural crests (Schulz et al. 2014), the structures upon which development of the olfactory and GnRH systems depends (Forni et al. 2011). Defects in CHD7 could thus impair olfactory and GnRH neurogenesis.

ii. Defects in the migration of GnRH neurons

As discussed in previous sections, guidance mechanisms are central to the migration of GnRH neurons, either by directly influencing GnRH neurons, or indirectly by affecting the olfactory/vomeronasal/terminal scaffold they use to migrate. Accordingly, mutations in a number of genes coding for molecules involved in cell adhesion, motility, chemoattraction/repulsion, have been identified in patients suffering from HH/KS, such as the *KAL1*/*ANOS1* gene mentioned before (Franco et al. 1991, Hardelin et al. 1999).

Semaphorin signalling has been introduced previously, together with its major role in GnRH neuron migration and regulation. It is then not surprising that genes coding for several semaphorins and their receptors have been found mutated in patients exhibiting HH/KS phenotypes.

Cariboni et al. (2011) demonstrated that proper semaphorin 3A signalling through neuropilin-1/2 is important for the patterning of vomeronasal projections and migration of GnRH neurons: in *Sema3a*-null mutant mouse embryos, desfasciculation of vomeronasal axons and accumulation of GnRH neurons in the nose were observed, reminiscent of the KS phenotype. Consistently, shortly after, several *SEMA3A* mutations were identified in cohorts of HH and KS patients (Hanchate et al. 2012, Young et al. 2012, Känsäkoski et al. 2014). Of note, in one of these studies, functional cell assays were performed to further characterize the effects of the identified mutations, and

revealed impaired secretion or action of semaphorin 3A for these variants (Hanchate et al. 2012). Since then, novel *SEMA3A* variants have been identified through the screening of HH/KS patients (Marcos et al. 2017, Dai et al. 2020).

Other class 3 semaphorins were also implicated in the etiology of HH/KS. A mutation in *SEMA3E*, coding for semaphorin 3E, was found in brothers presenting with a KS phenotype, and subsequent investigations in rodents revealed that disruption of semaphorin 3E and its receptor plexin D1 impaired GnRH neuron survival *in vitro* and *in vivo* (Cariboni et al. 2015). Similarly, Oleari et al. (2021) uncovered a mutation of *SEMA3G* in two HH brothers presenting also with developmental defects. In trying to dissect the potential roles of its product semaphorin 3G on GnRH neuron development, they found that the identified mutation of semaphorin 3G increased its affinity for plexins and diminished semaphorin 3A-induced response *in vitro*, and they described a reduced number of GnRH neurons in the forebrain of *Sema3g*-null embryos, although an overall normal HPG axis was observed in the adults.

Another class of semaphorin has also been involved in HH/KS. Semaphorin 7A signalling through Plexin C1 and β1-integrin is involved in GnRH neuron migration, as evidenced from their altered migration and distribution in *Sema7a*-null mice, and these mice also exhibit altered fertility, a feature of HH (Messina et al. 2011). Interestingly, two *SEMA7A* missense variants were identified in patients presenting with HH and KS (Känsäkoski et al. 2014), and more recently, a point mutation in an intron of *SEMA7A* was reported in a female case of KS (Zhao et al. 2020).

Finally, mutations in the plexin and neuropilin families, known receptors of semaphorins, can also contribute to hypogonadotropic hypogonadism. Thus, in a study from 2017, Marcos and colleagues identified several missense mutations of *PLXNA1*, coding for plexin A1, in a cohort of KS patients. They further demonstrated that genetic deletion of plexin A1 in mice triggered failure of the olfactory/vomeronasal/terminal axons to reach the brain, and restriction of GnRH neurons to the nasal compartment in some embryos, together with decreased fertility in adult male mice, all consistent with a KS phenotype. Functional cell assays associated seven of the identified *PLXNA1* mutations with defective production or localization of the receptor (Marcos et al. 2017).

In the same study, missense mutations of *NRP1* and *NRP2*, coding for neuropilin-1 and neuropilin-2 respectively, were also detected in KS patients (Marcos et al. 2017).

Noteworthy, many of the mutations mentioned above were found in a heterozygous state in patients, while studies of semaphorin signalling in animals (*Sema7a*-, *Sema3a*-, *Sema3e*-null mice for instance) usually relied on homozygous deletion to investigate their effect on GnRH neuron development (Messina et al. 2011, Cariboni et al. 2011, Cariboni et al. 2015). Observations in patients are however consistent with an oligogenic inheritance pattern in HH/KS, as several mutations are often found in patients and can together contribute to the phenotype (Pitteloud et al. 2007, Boehm et al. 2015). Accordingly in a mice model of double heterozygous deletion of *Plxnd1* and *Chd7* (*Plxnd1*$^{+/-}$ *Chd7*$^{+/-}$ animals), Cariboni and colleagues demonstrated that the compound heterozygous animals exhibited a stronger alteration in GnRH innervation, and smaller testes, than their *Plxnd1*$^{+/-}$ or *Chd7*$^{+/-}$ counterparts harbouring only one of the two heterozygous mutations (Cariboni et al. 2015).

In summary, numerous mutations causing HH/KS have been identified so far in genes that directly or indirectly impact GnRH neuron development (ontogeny, migration, survival) and function (GnRH production, secretion and signalling). However, given the wide range of mechanisms governing the migration and maturation of the GnRH system, and the fact that ~50% of HH/KS cases are still to elucidate (Marino et al. 2014, Boehm et al. 2015), there remains a great need for investigations aimed at dissecting the genetic complexity of HH/KS, and subsequently provide adequate treatment and counselling to the patients.

The next chapter presents our participation in this effort, as we have investigated mutations of the genes coding for semaphorin 3F and plexin A3, respectively *SEMA3F* and *PLXNA3*, found in patients presenting with HH/KS, to assess their contribution to the etiology of these pathologies.

V. References for chapter one

1.Adelman, J. P., Mason, A. J., Hayflick, J. S. & Seeburg, P. H. Isolation of the gene and hypothalamic cDNA for the common precursor of gonadotropin-releasing hormone and prolactin release-inhibiting factor in human and rat. Proc Natl Acad Sci U S A 83, 179–183 (1986).

2.Aguillon, R. et al. Cell-type heterogeneity in the early zebrafish olfactory epithelium is generated from progenitors within preplacodal ectoderm. Elife 7, e32041 (2018).

3.Alim, Z. et al. Gonadotrope plasticity at cellular and population levels. Endocrinology 153, 4729–4739 (2012).

4.Alto, L. T. & Terman, J. R. Semaphorins and their Signaling Mechanisms. Methods Mol Biol 1493, 1–25 (2017).

5.Ancel, C. et al. Stimulatory Effect of RFRP-3 on the Gonadotrophic Axis in the Male Syrian Hamster: The Exception Proves the Rule. Endocrinology 153, 1352–1363 (2012).

6.Barber, P. C. & Lindsay, R. M. Schwann cells of the olfactory nerves contain glial fibrillary acidic protein and resemble astrocytes. Neuroscience 7, 3077–3090 (1982).

7.Barraud, P., John, J. A. S., Stolt, C. C., Wegner, M. & Baker, C. V. H. Olfactory ensheathing glia are required for embryonic olfactory axon targeting and the migration of gonadotropin-releasing hormone neurons. Biology Open 2, 750–759 (2013).

8.Barraud, P. et al. Neural crest origin of olfactory ensheathing glia. Proc Natl Acad Sci U S A 107, 21040–21045 (2010).

9.Barry, J., Dubois, M. P. & Poulain, P. LRF producing cells of the mammalian hypothalamus. A fluorescent antibody study. Z Zellforsch Mikrosk Anat 146, 351–366 (1973).

10.Beck, A. et al. Functional Characterization of Transient Receptor Potential (TRP) Channel C5 in Female Murine Gonadotropes. Endocrinology 158, 887–902 (2017).

11.Becker, M. & Hesse, V. Minipuberty: Why Does it Happen? HRP 93, 76–84 (2020).

12.Belchetz, P. E., Plant, T. M., Nakai, Y., Keogh, E. J. & Knobil, E. Hypophysial responses to continuous and intermittent delivery of hypopthalamic gonadotropin-releasing hormone. Science 202, 631–633 (1978).

13.Biason-Lauber, A. & Chaboissier, M.-C. Ovarian development and disease: The known and the unexpected. Seminars in Cell & Developmental Biology 45, 59–67 (2015).

14.Blanchart, A., Martín-López, E., Carlos, J. A. D. & López-Mascaraque, L. Peripheral contributions to olfactory bulb cell populations (migrations towards the olfactory bulb). Glia 59, 278–292 (2011).

15.Boehm, U. et al. Expert consensus document: European Consensus Statement on congenital hypogonadotropic hypogonadism--pathogenesis, diagnosis and treatment. Nat Rev Endocrinol 11, 547–564 (2015).

16.Brennan, P. A. Pheromones and Mammalian Behavior. in The Neurobiology of Olfaction (ed. Menini, A.) (CRC Press/Taylor & Francis, 2010).

17.Campbell, R. E. Morphology of the Adult GnRH Neuron. in The GnRH Neuron and its Control 121–148 (John Wiley & Sons, Ltd, 2018). doi:10.1002/9781119233275.ch6.

18.Campos, P. & Herbison, A. E. Optogenetic activation of GnRH neurons reveals minimal requirements for pulsatile luteinizing hormone secretion. Proc Natl Acad Sci U S A 111, 18387–18392 (2014).

19.Caraty, A., Martin, G. B. & Montgomery, G. A new method for studying pituitary responsiveness in vivo using pulses of LH-RH analogue in ewes passively immunized against native LH-RH. Reprod Nutr Dev 24, 439–448 (1984).

20.Cariboni, A. et al. Defective gonadotropin-releasing hormone neuron migration in mice lacking SEMA3A signalling through NRP1 and NRP2: implications for the aetiology of hypogonadotropic hypogonadism. Hum. Mol. Genet. 20, 336–344 (2011).

21.Carmel, P. W., Araki, S. & Ferin, M. Pituitary stalk portal blood collection in rhesus monkeys: evidence for pulsatile release of gonadotropin-releasing hormone (GnRH). Endocrinology 99, 243–248 (1976).

22.Casoni, F. et al. Development of the neurons controlling fertility in humans: new insights from 3D imaging and transparent fetal brains. Development 143, 3969–3981 (2016).

23.Chehab, F. F., Lim, M. E. & Lu, R. Correction of the sterility defect in homozygous obese female mice by treatment with the human recombinant leptin. Nat Genet 12, 318–320 (1996).

24.Childs, G. V., Odle, A. K., MacNicol, M. C. & MacNicol, A. M. The Importance of Leptin to Reproduction. Endocrinology 162, (2021).

25.Cimino, I. et al. Novel role for anti-Müllerian hormone in the regulation of GnRH neuron excitability and hormone secretion. Nat Commun 7, 10055 (2016).

26.Clarke, H., Dhillo, W. S. & Jayasena, C. N. Comprehensive Review on Kisspeptin and Its Role in Reproductive Disorders. Endocrinol Metab (Seoul) 30, 124–141 (2015).

27.Clarke, I. J. & Cummins, J. T. The temporal relationship between gonadotropin releasing hormone (GnRH) and luteinizing hormone (LH) secretion in ovariectomized ewes. Endocrinology 111, 1737–1739 (1982).

28.Clarke, I. J., Cummins, J. T., Karsch, F. J., Seeburg, P. H. & Nikolics, K. GnRH-associated peptide (GAP) is cosecreted with GnRH into the hypophyseal portal blood of ovariectomized sheep. Biochem Biophys Res Commun 143, 665–671 (1987).

29.Clarkson, J. & Herbison, A. E. Postnatal development of kisspeptin neurons in mouse hypothalamus; sexual dimorphism and projections to gonadotropin-releasing hormone neurons. Endocrinology 147, 5817–5825 (2006).

30.Clasadonte, J. et al. Prostaglandin E2 release from astrocytes triggers gonadotropin-releasing hormone (GnRH) neuron firing via EP2 receptor activation. Proc Natl Acad Sci U S A 108, 16104–16109 (2011).

31.Cohen-Tannoudji, Combarnous & Counis. La sécrétion des hormones gonadotropes hypophysaires et sa régulation. in 185–203 (2014).

32.Conzelmann, S., Levai, O., Breer, H. & Strotmann, J. Extraepithelial cells expressing distinct olfactory receptors are associated with axons of sensory cells with the same receptor type. Cell Tissue Res 307, 293–301 (2002).

33.Cottrell, E. C., Campbell, R. E., Han, S.-K. & Herbison, A. E. Postnatal Remodeling of Dendritic Structure and Spine Density in Gonadotropin-Releasing Hormone Neurons. Endocrinology 147, 3652–3661 (2006).

34.Davis, S. R. et al. Menopause. Nat Rev Dis Primers 1, 1–19 (2015).

35.De Carlos, J. A., López-Mascaraque, L. & Valverde, F. The telencephalic vesicles are innervated by olfactory placode-derived cells: a possible mechanism to induce neocortical development. Neuroscience 68, 1167–1178 (1995).

36.de Castro, F., Hu, L., Drabkin, H., Sotelo, C. & Chédotal, A. Chemoattraction and chemorepulsion of olfactory bulb axons by different secreted semaphorins. J Neurosci 19, 4428–4436 (1999).

37.de Roux, N. et al. Hypogonadotropic hypogonadism due to loss of function of the KiSS1-derived peptide receptor GPR54. Proc Natl Acad Sci U S A 100, 10972–10976 (2003).

38.Delli, V., Silva, M. S. B., Prévot, V. & Chachlaki, K. The KiNG of reproduction: Kisspeptin/ nNOS interactions shaping hypothalamic GnRH release. Molecular and Cellular Endocrinology 532, 111302 (2021).

39.Donato, J. et al. Leptin's effect on puberty in mice is relayed by the ventral premammillary nucleus and does not require signaling in Kiss1 neurons. J Clin Invest 121, 355–368 (2011).

40.Dulac, C. & Torello, A. T. Molecular detection of pheromone signals in mammals: from genes to behaviour. Nat Rev Neurosci 4, 551–562 (2003).

41.Eggers, S., Ohnesorg, T. & Sinclair, A. Genetic regulation of mammalian gonad development. Nat Rev Endocrinol 10, 673–683 (2014).

42.Fairless, R. & Barnett, S. C. Olfactory ensheathing cells: their role in central nervous system repair. The International Journal of Biochemistry & Cell Biology 37, 693–699 (2005).

43.Farkas, I. et al. Estradiol Increases Glutamate and GABA Neurotransmission into GnRH Neurons via Retrograde NO-Signaling in Proestrous Mice during the Positive Estradiol Feedback Period. eNeuro 5, ENEURO.0057-18.2018 (2018).

44.Fernandez-Fernandez, R. et al. Novel signals for the integration of energy balance and reproduction. Mol Cell Endocrinol 254–255, 127–132 (2006).

45.Forni, P. E. & Wray, S. Neural crest and olfactory system: new prospective. Mol Neurobiol 46, 349–360 (2012).

46.Forni, P. E. & Wray, S. GnRH, anosmia and hypogonadotropic hypogonadism - where are we? Front Neuroendocrinol 36, 165–177 (2015).

47.Forni, P., Taylor-Burds, C., Senkus Melvin, V., Williams, T. & Wray, S. Neural crest and Ectodermal cells intermix in the nasal placode to give rise to GnRH-1 Neurons, Sensory Neurons and Olfactory Ensheathing Cells. J Neurosci 31, 6915–6927 (2011).

48.Fortin, J., Boehm, U., Weinstein, M. B., Graff, J. M. & Bernard, D. J. Follicle-stimulating hormone synthesis and fertility are intact in mice lacking SMAD3 DNA binding activity and SMAD2 in gonadotrope cells. FASEB J 28, 1474–1485 (2014).

49.Fraher, J. P. The ultrastructure of sheath cells in developing rat vomeronasal nerve. J Anat 134, 149–168 (1982).

50.Frazao, R. et al. Estradiol modulates Kiss1 neuronal response to ghrelin. American Journal of Physiology-Endocrinology and Metabolism 306, E606–E614 (2014).

51.Fu, L.-Y. & van den Pol, A. N. Kisspeptin directly excites anorexigenic proopiomelanocortin neurons but inhibits orexigenic neuropeptide Y cells by an indirect synaptic mechanism. J Neurosci 30, 10205–10219 (2010).

52.Gamble, J. A. et al. Disruption of ephrin signaling associates with disordered axophilic migration of the gonadotropin-releasing hormone neurons. J Neurosci 25, 3142–3150 (2005).

53.Giacobini, P. Shaping the Reproductive System: Role of Semaphorins in Gonadotropin-Releasing Hormone Development and Function. NEN 102, 200–215 (2015).

54.Giacobini, P. et al. Semaphorin 4D regulates gonadotropin hormone–releasing hormone-1 neuronal migration through PlexinB1–Met complex. Journal of Cell Biology 183, 555–566 (2008).

55.Giacobini, P. et al. Brain Endothelial Cells Control Fertility through Ovarian-Steroid–Dependent Release of Semaphorin 3A. PLOS Biology 12, e1001808 (2014).

56.Giger, R. J., Wolfer, D. P., De Wit, G. M. & Verhaagen, J. Anatomy of rat semaphorin III/collapsin-1 mRNA expression and relationship to developing nerve tracts during neuroembryogenesis. J Comp Neurol 375, 378–392 (1996).

57.Goldsmith, P. C., Thind, K. K., Song, T., Kim, E. J. & Boggant, J. E. Location of the Neuroendocrine Gonadotropin-Releasing Hormone Neurons in the Monkey Hypothalamus by Retrograde Tracing and Immunostaining*,**. Journal of Neuroendocrinology 2, 157–168 (1990).

58.Goodman, R. L. et al. Kisspeptin neurons in the arcuate nucleus of the ewe express both dynorphin A and neurokinin B. Endocrinology 148, 5752–5760 (2007).

59.Gottsch, M. L. et al. A Role for Kisspeptins in the Regulation of Gonadotropin Secretion in the Mouse. Endocrinology 145, 4073–4077 (2004).

60.Gregory, S. J. & Kaiser, U. B. Regulation of gonadotropins by inhibin and activin. Semin Reprod Med 22, 253–267 (2004).

61.Gross, D. S. Distribution of gonadotropin-releasing hormone in the mouse brain as revealed by immunohistochemistry. Endocrinology 98, 1408–1417 (1976).

62.Handelsman, D. J. & Swerdloff, R. S. Pharmacokinetics of gonadotropin-releasing hormone and its analogs. Endocr Rev 7, 95–105 (1986).

63.Harris, G. W. Neural control of the pituitary gland. Physiol Rev 28, 139–179 (1948).

64.Herbison, A. E. Chapter 11 - Physiology of the Adult Gonadotropin-Releasing Hormone Neuronal Network. in Knobil and Neill's Physiology of Reproduction (Fourth Edition) (eds. Plant, T. M. & Zeleznik, A. J.) 399–467 (Academic Press, 2015). doi:10.1016/B978-0-12-397175-3.00011-9.

65.Herbison, A. E. Control of puberty onset and fertility by gonadotropin-releasing hormone neurons. Nat Rev Endocrinol 12, 452–466 (2016).

66.Herbison, A. E., d'Anglemont de Tassigny, X., Doran, J. & Colledge, W. H. Distribution and Postnatal Development of Gpr54 Gene Expression in Mouse Brain and Gonadotropin-Releasing Hormone Neurons. Endocrinology 151, 312–321 (2010).

67.Hilal, E. M., Chen, J. H. & Silverman, A. J. Joint migration of gonadotropin-releasing hormone (GnRH) and neuropeptide Y (NPY) neurons from olfactory placode to central nervous system. J Neurobiol 31, 487–502 (1996).

68.Huilgol, D. & Tole, S. Cell migration in the developing rodent olfactory system. Cell Mol Life Sci 73, 2467–2490 (2016).

69.Ishibashi, M. et al. Effect of GnRH-associated peptide on prolactin secretion from human lactotrope adenoma cells in culture. Acta Endocrinol (Copenh) 116, 81–84 (1987).

70.Jakiel, G., Makara-Studzińska, M., Ciebiera, M. & Słabuszewska-Jóźwiak, A. Andropause – state of the art 2015 and review of selected aspects. Prz Menopauzalny 14, 1–6 (2015).

71.Jasoni, C. L., Porteous, R. W. & Herbison, A. E. Anatomical location of mature GnRH neurons corresponds with their birthdate in the developing mouse. Developmental Dynamics 238, 524–531 (2009).

72.Jasoni, C. L., Todman, M. G., Han, S.-K. & Herbison, A. E. Expression of mRNAs Encoding Receptors That Mediate Stress Signals in Gonadotropin-Releasing Hormone Neurons of the Mouse. NEN 82, 320–328 (2005).

73.Jégou, Rolland & Albert. Le testicule. in La reproduction animale et humaine 87–113 (2014).

74.Jennes, L. The nervus terminalis in the mouse: light and electron microscopic immunocytochemical studies. Ann N Y Acad Sci 519, 165–173 (1987).

75.Jennes, L. & Stumpf, W. E. LHRH-systems in the brain of the golden hamster. Cell Tissue Res 209, 239–256 (1980).

76.Jennes, L. & Stumpf, W. E. Gonadotropin-releasing hormone immunoreactive neurons with access to fenestrated capillaries in mouse brain. Neuroscience 18, 403–416 (1986).

77.Jennes, L. The olfactory gonadotropin-releasing hormone immunoreactive system in mouse. Brain Research 386, 351–363 (1986).

78.Kanasaki, H., Bedecarrats, G. Y., Kam, K.-Y., Xu, S. & Kaiser, U. B. Gonadotropin-releasing hormone pulse frequency-dependent activation of extracellular signal-regulated kinase pathways in perifused LbetaT2 cells. Endocrinology 146, 5503–5513 (2005).

79.Kawakami, A., Kitsukawa, T., Takagi, S. & Fujisawa, H. Developmentally regulated expression of a cell surface protein, neuropilin, in the mouse nervous system. J Neurobiol 29, 1–17 (1996).

80.King, J. C. & Anthony, E. L. P. LHRH neurons and their projections in humans and other mammals: Species comparisons. Peptides 5, 195–207 (1984).

81.Kokoris, G. J., Lam, N. Y., Ferin, M., Silverman, A. J. & Gibson, M. J. Transplanted gonadotropin-releasing hormone neurons promote pulsatile luteinizing hormone secretion in congenitally hypogonadal (hpg) male mice. Neuroendocrinology 48, 45–52 (1988).

82.Kramer, P. R. & Wray, S. Novel gene expressed in nasal region influences outgrowth of olfactory axons and migration of luteinizing hormone-releasing hormone (LHRH) neurons. Genes Dev. 14, 1824–1834 (2000).

83.Kuiri-Hänninen, T., Sankilampi, U. & Dunkel, L. Activation of the Hypothalamic-Pituitary-Gonadal Axis in Infancy: Minipuberty. HRP 82, 73–80 (2014).

84.Kumar, D. et al. Specialized Subpopulations of Kisspeptin Neurons Communicate With GnRH Neurons in Female Mice. Endocrinology 156, 32–38 (2015).

85.Kumar, D. et al. Murine arcuate nucleus kisspeptin neurons communicate with GnRH neurons in utero. J. Neurosci. 34, 3756–3766 (2014).

86.Kumar, D., Periasamy, V., Freese, M., Voigt, A. & Boehm, U. In Utero Development of Kisspeptin/GnRH Neural Circuitry in Male Mice. Endocrinology 156, 3084–3090 (2015).

87.Lee, J. H. et al. KiSS-1, a novel human malignant melanoma metastasis-suppressor gene. J Natl Cancer Inst 88, 1731–1737 (1996).

88.Legouis, R. et al. The candidate gene for the X-linked Kallmann syndrome encodes a protein related to adhesion molecules. Cell 67, 423–435 (1991).

89.Lehman, M. N., Coolen, L. M. & Goodman, R. L. Minireview: Kisspeptin/Neurokinin B/Dynorphin (KNDy) Cells of the Arcuate Nucleus: A Central Node in the Control of Gonadotropin-Releasing Hormone Secretion. Endocrinology 151, 3479–3489 (2010).

90.Lehman, M. N., He, W., Coolen, L. M., Levine, J. E. & Goodman, R. L. Does the KNDy Model for the Control of Gonadotropin-Releasing Hormone Pulses Apply to Monkeys and Humans? Semin Reprod Med 37, 71–83 (2019).

91.Lehman, M. N., Hileman, S. M. & Goodman, R. L. Neuroanatomy of the kisspeptin signaling system in mammals: comparative and developmental aspects. Adv Exp Med Biol 784, 27–62 (2013).

92.Li, X.-F. & O'Byrne, K. T. Chapter 36 - Stress and the Reproductive System. in Knobil and Neill's Physiology of Reproduction (Fourth Edition) (eds. Plant, T. M. & Zeleznik, A. J.) 1637–1660 (Academic Press, 2015). doi:10.1016/B978-0-12-397175-3.00036-3.

93.Liu, X. & Herbison, A. E. Kisspeptin Regulation of Neuronal Activity throughout the Central Nervous System. Endocrinol Metab (Seoul) 31, 193–205 (2016).

94.Marques, P., Skorupskaite, K., Rozario, K. S., Anderson, R. A. & George, J. T. Physiology of GnRH and Gonadotropin Secretion. in Endotext (eds. De Groot, L. J. et al.) (MDText.com, Inc., 2000).

95.Matsumoto, A. M. & Bremner, W. J. Modulation of pulsatile gonadotropin secretion by testosterone in man. J Clin Endocrinol Metab 58, 609–614 (1984).

96.Messina, A. et al. Dysregulation of Semaphorin7A/β1-integrin signaling leads to defective GnRH-1 cell migration, abnormal gonadal development and altered fertility. Hum. Mol. Genet. 20, 4759–4774 (2011).

97.Migaud, M. Rythmes biologiques et reproduction. 751 p. (Editions Quae, 2014).

98.Miller, A. M., Treloar, H. B. & Greer, C. A. Composition of the migratory mass during development of the olfactory nerve. Journal of Comparative Neurology 518, 4825–4841 (2010).

99.Miller, B. H. et al. Circadian Clock Mutation Disrupts Estrous Cyclicity and Maintenance of Pregnancy. Current Biology 14, 1367–1373 (2004).

100.Monniaux et al. Le développement folliculaire ovarien et l'ovulation. in La reproduction animale et humaine 41–55 (2014).

101.Moore, A. M., Coolen, L. M., Porter, D. T., Goodman, R. L. & Lehman, M. N. KNDy Cells Revisited. Endocrinology 159, 3219–3234 (2018).

102.Naor, Z. Signaling by G-protein-coupled receptor (GPCR): Studies on the GnRH receptor. Frontiers in Neuroendocrinology 30, 10–29 (2009).

103.Navarro, V. M. et al. Regulation of NKB Pathways and Their Roles in the Control of Kiss1 Neurons in the Arcuate Nucleus of the Male Mouse. Endocrinology 152, 4265–4275 (2011).

104.Navarro, V. M. & Kaiser, U. B. Metabolic influences on neuroendocrine regulation of reproduction. Curr Opin Endocrinol Diabetes Obes 20, 335–341 (2013).

105.Nikolics, K., Mason, A. J., Szönyi, E., Ramachandran, J. & Seeburg, P. H. A prolactin-inhibiting factor within the precursor for human gonadotropin-releasing hormone. Nature 316, 511–517 (1985).

106.Novaira, H. J., Ng, Y., Wolfe, A. & Radovick, S. Kisspeptin increases GnRH mRNA expression and secretion in GnRH secreting neuronal cell lines. Mol Cell Endocrinol 311, 126–134 (2009).

107.Oleari, R., Massa, V., Cariboni, A. & Lettieri, A. The Differential Roles for Neurodevelopmental and Neuroendocrine Genes in Shaping GnRH Neuron Physiology and Deficiency. Int J Mol Sci 22, 9425 (2021).

108.Özdemir, A., Rn, Utkualp, N. & Palloş, A. Special Article Physical and Psychosocial Effects of the Changes in Adolescence Period. 9, (2016).

109.Parkash, J. et al. Suppression of β1-Integrin in Gonadotropin-Releasing Hormone Cells Disrupts Migration and Axonal Extension Resulting in Severe Reproductive Alterations. J. Neurosci. 32, 16992–17002 (2012).

110.Parkash, J. et al. Semaphorin7A regulates neuroglial plasticity in the adult hypothalamic median eminence. Nat Commun 6, 6385 (2015).

111.Pellier, V., Astic, L., Oestreicher, A. B. & Saucier, D. B-50/GAP-43 expression by the olfactory receptor cells and the neurons migrating from the olfactory placode in embryonic rats. Developmental Brain Research 80, 63–72 (1994).

112.Perera, S. N. et al. Insights into olfactory ensheathing cell development from a laser-microdissection and transcriptome-profiling approach. Glia 68, 2550–2584 (2020).

113.Pinter, O., Beda, Z., Csaba, Z. & Gerendai, I. Differences in the onset of puberty in selected inbred mouse strains. Endocrine Abstracts 14, (2007).

114.Pitteloud, N. et al. Inhibition of luteinizing hormone secretion by testosterone in men requires aromatization for its pituitary but not its hypothalamic effects: evidence from the tandem study of normal and gonadotropin-releasing hormone-deficient men. J Clin Endocrinol Metab 93, 784–791 (2008).

115.Prevot, V. et al. Definitive evidence for the existence of morphological plasticity in the external zone of the median eminence during the rat estrous cycle: implication of neuro-glio-endothelial interactions in gonadotropin-releasing hormone release. Neuroscience 94, 809–819 (1999).

116.Prevot, V. & Sharif, A. Unveiling the Importance of Glia and Vascular Endothelial Cells in the Control of GnRH Neuronal Function. in The GnRH Neuron and its Control 225–258 (John Wiley & Sons, Ltd, 2018). doi:10.1002/9781119233275.ch10.

117.Ramón-Cueto, A. & Avila, J. Olfactory ensheathing glia: properties and function. Brain Research Bulletin 46, 175–187 (1998).

118.Ramos-Lobo, A. M. et al. Long-term consequences of the absence of leptin signaling in early life. eLife 8, e40970 (2019).

119.Rance, N. E., Young, W. S. & McMullen, N. T. Topography of neurons expressing luteinizing hormone-releasing hormone gene transcripts in the human hypothalamus and basal forebrain. J Comp Neurol 339, 573–586 (1994).

120.Reiter, R. J. The Pineal and Its Hormones in the Control of Reproduction in Mammals*. Endocrine Reviews 1, 109–131 (1980).

121.Revel, F. G. et al. Kisspeptin Mediates the Photoperiodic Control of Reproduction in Hamsters. Current Biology 16, 1730–1735 (2006).

122.Rispoli, L. A. & Nett, T. M. Pituitary gonadotropin-releasing hormone (GnRH) receptor: structure, distribution and regulation of expression. Anim Reprod Sci 88, 57–74 (2005).

123.Roa, J. & Tena-Sempere, M. Connecting metabolism and reproduction: Roles of central energy sensors and key molecular mediators. Molecular and Cellular Endocrinology 397, 4–14 (2014).

124.Roberson, M. S., Misra-Press, A., Laurance, M. E., Stork, P. J. & Maurer, R. A. A role for mitogen-activated protein kinase in mediating activation of the glycoprotein hormone alpha-subunit promoter by gonadotropin-releasing hormone. Mol Cell Biol 15, 3531–3539 (1995).

125.Roch, G. J., Busby, E. R. & Sherwood, N. M. Evolution of GnRH: Diving deeper. General and Comparative Endocrinology 171, 1–16 (2011).

126.Sabado, V., Barraud, P., Baker, C. V. H. & Streit, A. Specification of GnRH-1 neurons by antagonistic FGF and retinoic acid signaling. Dev Biol 362, 254–262 (2012).

127.Sáenz de Miera, C. et al. Photoperiodic regulation in a wild-derived mouse strain. Journal of Experimental Biology 223, (2020).

128.Sarkar, D. K. & Mitsugi, N. Correlative changes of the gonadotropin-releasing hormone and gonadotropin-releasing-hormone-associated peptide immunoreactivities in the pituitary portal plasma in female rats. Neuroendocrinology 52, 15–21 (1990).

129.Schally, A. V. et al. Gonadotropin-releasing hormone: one polypeptide regulates secretion of luteinizing and follicle-stimulating hormones. Science 173, 1036–1038 (1971).

130.Schauer, C. et al. Hypothalamic gonadotropin-releasing hormone (GnRH) receptor neurons fire in synchrony with the female reproductive cycle. J Neurophysiol 114, 1008–1021 (2015).

131.Schröder, H., Moser, N. & Huggenberger, S. The Mouse Hypothalamus. in Neuroanatomy of the Mouse: An Introduction (eds. Schröder, H., Moser, N. & Huggenberger, S.) 205–230 (Springer International Publishing, 2020). doi:10.1007/978-3-030-19898-5_9.

132.Schwanzel-Fukuda, M., Abraham, S., Crossin, K. L., Edelman, G. M. & Pfaff, D. W. Immunocytochemical demonstration of neural cell adhesion molecule (NCAM) along the migration route of luteinizing hormone-releasing hormone (LHRH) neurons in mice. J Comp Neurol 321, 1–18 (1992).

133.Schwanzel-Fukuda, M., Fadem, B. H., Garcia, M. S. & Pfaff, D. W. Immunocytochemical localization of luteinizing hormone-releasing hormone (LHRH) in the brain and nervus terminalis of the adult and early neonatal gray short-tailed opossum (Monodelphis domestica). J Comp Neurol 276, 44–60 (1988).

134.Schwanzel-Fukuda, M. & Pfaff, D. W. Origin of luteinizing hormone-releasing hormone neurons. Nature 338, 161–164 (1989).

135.Schwanzel-Fukuda, M. & Silverman, A. J. The nervus terminalis of the guinea pig: a new luteinizing hormone-releasing hormone (LHRH) neuronal system. J Comp Neurol 191, 213–225 (1980).

136.Schwarting, G. A. et al. Semaphorin 3A Is Required for Guidance of Olfactory Axons in Mice. J Neurosci 20, 7691–7697 (2000).

137.Scott, V. & Brown, C. H. Kisspeptin activation of supraoptic nucleus neurons in vivo. Endocrinology 152, 3862–3870 (2011).

138.Seeburg, P. H. & Adelman, J. P. Characterization of cDNA for precursor of human luteinizing hormone releasing hormone. Nature 311, 666–668 (1984).

139.Seminara, S. B. et al. The GPR54 gene as a regulator of puberty. N. Engl. J. Med. 349, 1614–1627 (2003).

140.Shan, Y., Saadi, H. & Wray, S. Heterogeneous Origin of Gonadotropin Releasing Hormone-1 Neurons in Mouse Embryos Detected by Islet-1/2 Expression. Front Cell Dev Biol 8, 35 (2020).

141.Silverman, A. J., Jhamandas, J. & Renaud, L. P. Localization of luteinizing hormone-releasing hormone (LHRH) neurons that project to the median eminence. J. Neurosci. 7, 2312–2319 (1987).

142.Skrapits, K. & Hrabovszky, E. The Anatomy of the GnRH Neuron Network in the Human. in The GnRH Neuron and its Control (ed. Herbison, A. E.) 149–175 (John Wiley & Sons, Ltd, 2018). doi:10.1002/9781119233275.ch7.

143.Skrapits, K. et al. The cryptic gonadotropin-releasing hormone neuronal system of human basal ganglia. eLife 10, e67714 (2021).

144.Smith, T. D. & Bhatnagar, K. P. Chapter 2 - Anatomy of the olfactory system. in Handbook of Clinical Neurology (ed. Doty, R. L.) vol. 164 17–28 (Elsevier, 2019).

145.Sominsky, L. et al. Linking Stress and Infertility: A Novel Role for Ghrelin. Endocr Rev 38, 432–467 (2017).

146.Song, T., Nikolics, K., Seeburg, P. H. & Goldsmith, P. C. GnRH-prohormone-containing neurons in the primate brain: immunostaining for the GnRH-associated peptide. Peptides 8, 335–346 (1987).

147.Sonne, J., Reddy, V. & Lopez-Ojeda, W. Neuroanatomy, Cranial Nerve 0 (Terminal Nerve). in StatPearls (StatPearls Publishing, 2021).

148.Spaziani, M. et al. Hypothalamo-Pituitary axis and puberty. Molecular and Cellular Endocrinology 520, 111094 (2021).

149.Stamatiades, G. A. & Kaiser, U. B. Gonadotropin regulation by pulsatile GnRH: Signaling and gene expression. Mol. Cell. Endocrinol. (2017) doi:10.1016/j.mce.2017.10.015.

150.Stewart, A. J., Katz, A. A., Millar, R. P. & Morgan, K. Retention and silencing of prepro-GnRH-II and type II GnRH receptor genes in mammals. Neuroendocrinology 90, 416–432 (2009).

151.Sundaresan, S., Colin, I. M., Pestell, R. G. & Jameson, J. L. Stimulation of mitogen-activated protein kinase by gonadotropin-releasing hormone: evidence for the involvement of protein kinase C. Endocrinology 137, 304–311 (1996).

152.Swerdloff, R. S., Batt, R. A. & Bray, G. A. Reproductive hormonal function in the genetically obese (ob/ob) mouse. Endocrinology 98, 1359–1364 (1976).

153.Taroc, E. Z. M., Prasad, A., Lin, J. M. & Forni, P. E. The terminal nerve plays a prominent role in GnRH-1 neuronal migration independent from proper olfactory and vomeronasal connections to the olfactory bulbs. Biology Open 6, 1552–1568 (2017).

154.Topaloglu, A. K. et al. TAC3 and TACR3 mutations in familial hypogonadotropic hypogonadism reveal a key role for Neurokinin B in the central control of reproduction. Nat Genet 41, 354–358 (2009).

155.Tran, S. et al. Impaired fertility and FSH synthesis in gonadotrope-specific Foxl2 knockout mice. Mol Endocrinol 27, 407–421 (2013).

156.Treloar, H. B., Miller, A. M., Ray, A. & Greer, C. A. Development of the Olfactory System. in The Neurobiology of Olfaction (ed. Menini, A.) (CRC Press/Taylor & Francis, 2010).

157.Trotier, D. Vomeronasal organ and human pheromones. European Annals of Otorhinolaryngology, Head and Neck Diseases 128, 184–190 (2011).

158.Trotier, D. et al. The Vomeronasal Cavity in Adult Humans. Chemical Senses 25, 369–380 (2000).

159.Uenoyama, Y., Nagae, M., Tsuchida, H., Inoue, N. & Tsukamura, H. Role of KNDy Neurons Expressing Kisspeptin, Neurokinin B, and Dynorphin A as a GnRH Pulse Generator Controlling Mammalian Reproduction. Frontiers in Endocrinology 12, 1128 (2021).

160.Valverde, F., Heredia, M. & Santacana, M. Characterization of neuronal cell varieties migrating from the olfactory epithelium during prenatal development in the rat. Immunocytochemical study using antibodies against olfactory marker protein (OMP) and luteinizing hormone-releasing hormone (LH-RH). Brain Res Dev Brain Res 71, 209–220 (1993).

161.Valverde, F., Santacana, M. & Heredia, M. Formation of an olfactory glomerulus: morphological aspects of development and organization. Neuroscience 49, 255–275 (1992).

162.Wagner, S., Gresser, A. L., Torello, A. T. & Dulac, C. A multireceptor genetic approach uncovers an ordered integration of VNO sensory inputs in the accessory olfactory bulb. Neuron 50, 697–709 (2006).

163.Wańkowska, M. & Polkowska, J. Gonadotrophin-releasing hormone and GnRH-associated peptide neurobiology from the rearing period until puberty in the female sheep. J Chem Neuroanat 38, 9–19 (2009).

164.Wen, S., Ai, W., Alim, Z. & Boehm, U. Embryonic gonadotropin-releasing hormone signaling is necessary for maturation of the male reproductive axis. Proc Natl Acad Sci U S A 107, 16372–16377 (2010).

165.Wen, S. et al. Genetic identification of GnRH receptor neurons: a new model for studying neural circuits underlying reproductive physiology in the mouse brain. Endocrinology 152, 1515–1526 (2011).

166.Wen, S. et al. Functional characterization of genetically labeled gonadotropes. Endocrinology 149, 2701–2711 (2008).

167.White, B. R., Duval, D. L., Mulvaney, J. M., Roberson, M. S. & Clay, C. M. Homologous regulation of the gonadotropin-releasing hormone receptor gene is partially mediated by protein kinase C activation of an activator protein-1 element. Mol Endocrinol 13, 566–577 (1999).

168.Whitlock, K. E., Wolf, C. D. & Boyce, M. L. Gonadotropin-releasing hormone (GnRH) cells arise from cranial neural crest and adenohypophyseal regions of the neural plate in the zebrafish, Danio rerio. Dev Biol 257, 140–152 (2003).

169.Wierman, M. E., Kiseljak-Vassiliades, K. & Tobet, S. Gonadotropin-releasing hormone (GnRH) neuron migration: Initiation, maintenance and cessation as critical steps to ensure normal reproductive function. Frontiers in Neuroendocrinology 32, 43–52 (2011).

170.Wirsig-Wiechmann, C. R. Function of gonadotropin-releasing hormone in olfaction. Keio J Med 50, 81–85 (2001).

171.Wirsig-Wiechmann, C. R. & Wiechmann, A. F. The Prairie Vole Vomeronasal Organ is a Target for Gonadotropin-releasing Hormone. Chemical Senses 26, 1193–1202 (2001).

172.Wirsig-Wiechmann, C. R., Wiechmann, A. F. & Eisthen, H. L. What defines the nervus terminalis? Neurochemical, developmental, and anatomical criteria. in Progress in Brain Research vol. 141 45–58 (Elsevier, 2002).

173.Wood, C. L., Lane, L. C. & Cheetham, T. Puberty: Normal physiology (brief overview). Best Practice & Research Clinical Endocrinology & Metabolism 33, 101265 (2019).

174.Wormald, P. J., Abrahamson, M. J., Seeburg, P. H., Nikolics, K. & Millar, R. P. Prolactin-inhibiting activity of GnRH associated peptide in cultured human pituitary cells. Clin Endocrinol (Oxf) 30, 149–155 (1989).

175.Wray, S., Grant, P. & Gainer, H. Evidence that cells expressing luteinizing hormone-releasing hormone mRNA in the mouse are derived from progenitor cells in the olfactory placode. Proc. Natl. Acad. Sci. U.S.A. 86, 8132–8136 (1989).

176.Yildirim, E., Aksoy, S., Onel, T. & Yaba, A. Gonadal development and sex determination in mouse. Reproductive Biology 20, 115–126 (2020).

177.Yip, S. H., Boehm, U., Herbison, A. E. & Campbell, R. E. Conditional Viral Tract Tracing Delineates the Projections of the Distinct Kisspeptin Neuron Populations to Gonadotropin-Releasing Hormone (GnRH) Neurons in the Mouse. Endocrinology 156, 2582–2594 (2015).

178.Yu, W. H., Arisawa, M., Millar, R. P. & McCann, S. M. Effects of the gonadotropin-releasing hormone associated peptides (GAP) on the release of luteinizing hormone (LH), follicle stimulating hormone (FSH) and prolactin (PRL) in vivo. Peptides 10, 1133–1138 (1989).

179.Yu, W. H., Seeburg, P. H., Nikolics, K. & McCann, S. M. Gonadotropin-releasing hormone-associated peptide exerts a prolactin-inhibiting and weak gonadotropin-releasing activity in vivo. Endocrinology 123, 390–395 (1988).

180.Zancanaro, C. Vomeronasal Organ: A Short History of Discovery and an Account of Development and Morphology in the Mouse. in Neurobiology of Chemical Communication (ed. Mucignat-Caretta, C.) (CRC Press/Taylor & Francis, 2014).

181.Zimmerman, E. A., Hsu, K. C., Ferin, M. & Kozlowski, G. P. Localization of gonadotropin-releasing hormone (Gn-RH) in the hypothalamus of the mouse by immunoperoxidase technique. Endocrinology 95, 1–8 (1974).

CHAPTER TWO: LOSS-OF-FUNCTION VARIANTS IN *SEMA3F* AND *PLXNA3* ENCODING SEMAPHORIN-3F AND ITS RECEPTOR PLEXIN-A3 RESPECTIVELY CAUSE IDIOPATHIC HYPOGONADOTROPIC HYPOGONADISM

The content of this chapter was published as a research article in Genetics in Medecine

Kotan, Ternier et al. 2021 - PMID: 33495532 - DOI: 10.1038/s41436-020-01087-5

LOSS-OF-FUNCTION VARIANTS IN *SEMA3F* AND *PLXNA3* ENCODING SEMAPHORIN-3F AND ITS RECEPTOR PLEXIN-A3 RESPECTIVELY CAUSE IDIOPATHIC HYPOGONADOTROPIC HYPOGONADISM

Leman Damla Kotan[1, 15], Gaetan Ternier[2, 15], Aydilek Dagdeviren Cakir[3], Hamdi Cihan Emeksiz[4], Ihsan Turan[1], Gaspard Delpouve[2], Asli Derya Kardelen[5], Bahar Ozcabi[6], Emregul Isik[7], Eda Mengen[8], Esra Deniz P. Cakir[9], Aysegul Yuksel[10], Sebahat Yilmaz Agladioglu[11], Semine Ozdemir Dilek[1], Olcay Evliyaoglu[3], Feyza Darendeliler[5], Fatih Gurbuz[1], Gamze Akkus[12], Bilgin Yuksel[1], Paolo Giacobini [2, 16, *], A. Kemal Topaloglu [13, 14, 16,]

[1] Division of Pediatric Endocrinology, Cukurova University, Faculty of Medicine, Adana, 01330 Turkey
[2] Univ. Lille, Inserm, CHU Lille, U1172 - LilNCog - Lille Neuroscience & Cognition, Lille, 59045 France
[3] Division of Pediatric Endocrinology, Istanbul University, Cerrahpasa Faculty of Medicine, Istanbul, 34098 Turkey
[4] Division of Pediatric Endocrinology, Istanbul Medeniyet University, Faculty of Medicine, Istanbul, 34700 Turkey
[5] Division of Pediatric Endocrinology, Istanbul University, Istanbul Medical Faculty, Istanbul, 34093 Turkey
[6] Division of Pediatric Endocrinology, Health Science University, Zeynep Kamil Maternity and Children's Training and Research Hospital, İstanbul, 34668 Turkey
[7] Clinic of Pediatric Endocrinology, Afyonkarahisar State Hospital, Afyonkarahisar, 03030 Turkey
[8] Clinic of Pediatric Endocrinology, Ankara City Hospital, Children's Hospital, Ankara, 06800 Turkey
[9] Division of Pediatric Endocrinology, Health Sciences University, Istanbul Bakırkoy Dr. Sadi Konuk Research and Training Hospital, İstanbul, 34147 Turkey
[10] Clinic of Pediatric Endocrinology, Derince Training and Research Hospital, Kocaeli, 41900 Turkey
[11] Clinic of Pediatric Endocrinology, Memorial Hospital, Istanbul, 34728 Turkey
[12] Division of Endocrinology, Cukurova University, Faculty of Medicine, Adana, 01330 Turkey
[13] Department of Pediatrics, Division of Pediatric Endocrinology, University of Mississippi Medical Center, Jackson, Mississippi
[14] Department of Neurobiology and Anatomical Sciences, University of Mississippi Medical Center, Jackson, Mississippi
[15] These authors contributed equally to this work.
[16] These authors contributed equally to this work.

ABSTRACT

Purpose

Idiopathic hypogonadotropic hypogonadism (IHH) is characterized by absent puberty and subsequent infertility due to gonadotropin-releasing hormone (GnRH) deficiency. IHH can be accompanied by normal or compromised olfaction (Kallmann syndrome). Several semaphorins are known potent modulators of GnRH, olfactory, and vomeronasal system development. In this study, we investigated the role of Semaphorin-3F signaling in the etiology of IHH.

Methods

We screened 216 IHH patients by exome sequencing. We transiently transfected HEK293T cells with plasmids encoding wild type (WT) or corresponding variants to investigate the functional consequences. We performed fluorescent IHC to assess SEMA3F and PLXNA3 expression both in the nasal region and at the nasal/forebrain junction during the early human fetal development.

Results

We identified ten rare missense variants in SEMA3F and PLXNA3 in 15 patients from 11 independent families. Most of these variants were predicted to be deleterious by functional assays. SEMA3F and PLXNA3 are both expressed along the olfactory nerve and intracranial projection of the vomeronasal nerve/terminal nerve. PLXNA1-A3 are expressed in the early migratory GnRH neurons.

Conclusion

SEMA3F signaling through PLXNA1-A3 is involved in the guidance of GnRH neurons and of olfactory and vomeronasal nerve fibers in humans. Overall, our findings suggest that Semaphorin-3F signaling insufficiency contributes to the pathogenesis of IHH.

I. Introduction

Idiopathic hypogonadotropic hypogonadism (IHH) is a rare genetic disorder characterized by complete or partial pubertal failure caused by gonadotropin-releasing hormone (GnRH) deficiency. According to olfactory function, IHH is divided into two major forms: normal sense of smell (normosmic IHH, nIHH) and inability to smell, anosmia, defined as Kallmann syndrome (KS). However, this distinction is often blurred, probably reflecting the wealth of pathophysiological mechanisms and their variety of combinations in individual cases. Up to the present, nearly 50 genes have been reported to be associated with IHH (Topaloglu 2017); these account for nearly 50% of all cases thus suggesting that other associated genes remain to be discovered. To date, the genes implicated in IHH impact GnRH neuron ontogenesis, GnRH neuron migration and/or axon growth, GnRH secretion, and/or gonadotrope function. GnRH-secreting neurons are unique neuroendocrine cells as they originate in the nasal placode, outside the central nervous system, during embryonic development, and migrate to the hypothalamus along the vomeronasal and terminal nerves (VNN, TN) (Wray et al. 1989). This process is evolutionarily conserved and follows a similar spatiotemporal pattern in all mammals (Wray et al. 1989), including humans (Casoni et al. 2016, Schwanzel-Fukuda and Pfaff 1989). Maldevelopment of this neuroendocrine system results in hypothalamic hypogonadotropic hypogonadism. Unraveling new genetic pathways involved in the development or function of GnRH neurons is relevant for understanding the basis of pathogenesis leading to IHH in humans.

Proper navigation of growing axons and neurons during embryonic development depend on the action of guidance cues, which include semaphorins, a large and diverse family of secreted and membrane-associated proteins (Pasterkamp 2012). Correct targeting of GnRH neurons and olfactory/vomeronasal projections have been shown to depend on the orchestrated action of this family of guidance cues (Giacobini 2015). Mutations in members of class-3 semaphorins, *SEMA3A*, *SEMA3E* and *SEMA3G*, have been associated with IHH (Oleari et al. 2020, Cariboni et al. 2015, Hanchate et al. 2012). To exert its functions, SEMA3s bind to Neuropilin co-receptors (NRP1 and NRP2) in hetero-complexes with PlexinA1-4 (PLXNA1-4) receptors to activate plexin signal-

transduction (Janssen et al. 2012). Loss of function of Plxna1, Nrp1 and Nrp2 have been linked to defective GnRH neuron development in mice (Hanchate et al. 2012, Cariboni et al. 2007, Marcos et al. 2017, Oleari et al. 2019), and nonsynonymous heterozygous variants in PLXNA1 and NRP2 have been identified in KS individuals (Marcos et al. 2017).

Among SEMA3s, there is semaphorin-3F (SEMA3F), a secreted protein that serves as a guidance cue to repel late-arriving olfactory axons that express neuropilin-2 (Nrp2) receptor to the olfactory bulbs (Takeuchi et al. 2010). SEMA3F, PLXNA3, and NRP2 have a spatio-temporal expression consistent with a possible role on the regulation of the GnRH system, olfactory, and vomeronasal development (Casoni et al. 2016, Oleari et al. 2019, Takeuchi et al. 2010).

II. Materials and methods

Patients

A total of 216 IHH patients (nIHH, n = 181 and KS, n = 35) from 178 independent families recruited in Turkey were included in the study. IHH patients had absent pubertal development by age 13 and 14 in girls and boys respectively and low or normal basal gonadotropin levels in the face of low estradiol/testosterone levels. The KS patients additionally had anosmia/hyposmia. The levels of olfactory function were determined based on self-reporting and physical examination by administering a culturally appropriate 10-item (mint, lemon, soap etc.) smell test.

All individuals and/or their legal guardians provided written informed consent, and the study was approved by the Ethics Committee of the Cukurova University Faculty of Medicine and by the institutional review board of the University of Mississippi Medical Center.

DNA Sequencing and Rare Variant Analyses

The genomic DNA samples for exome sequencing (ES) were prepared as an Illumina sequencing library, and in the second step, the sequencing libraries were enriched for the desired target using the

Illumina Exome Enrichment protocol. The captured libraries were sequenced using Illumina HiSeq 2000 Sequencer (Macrogen, Seoul, Korea). The reads were mapped against UCSC (https://genome.ucsc.edu/cgi-bin/hgGateway) hg19. The presence of significant variants was verified by Sanger sequencing on an Applied Biosystems PRISM 3130 auto sequencer. The details of DNA sequencing and rare variant analyses including burden testing are found in Supplementary Information.

Cell-Based Functional assays

In order to test the functionality of the variants identified in KS and nIHH probands, we transiently transfected HEK293T cells with plasmids encoding the human wild-type proteins (SEMA3F and PLXNA3) or the corresponding variants and investigated whether the *SEMA3F* secretory capacity or *PLXNA3* protein maturation and trafficking of transfected cells was affected. The details of Cell-Based Functional assays are provided in Supplementary Information.

Collection and Processing of Human Fetuses

Human fetal tissues were made available in accordance with French bylaws (Good Practice Concerning the Conservation, Transformation, and Transportation of Human Tissue to Be Used Therapeutically, published on December 29, 1998). The studies on human fetal tissue were approved by the French agency for biomedical research (Agence de la Biomédecine, Saint-Denis la Plaine, France, protocol n: PFS16–002). Non-pathological fetuses (7.5 and 10.5 gestational weeks (GW), n = 2 per each developmental stage) were obtained from voluntarily terminated pregnancies after written informed consent was obtained from the parents (Gynaecology Department, Jeanne de Flandre Hospital, Lille, France) and were fixed by immersion in 4% PFA at 4°C for 5 days. The tissues were then cryoprotected in PBS containing 30% sucrose at 4°C overnight, embedded in Tissue-Tek OCT compound (Sakura Finetek), frozen in dry ice, and stored at -80°C until sectioning. Frozen samples were cut serially at 20 μm with a Leica CM 3050S cryostat (Leica Biosystems Nussloch GmbH) and immunolabeled, as described below and as previously described (Casoni et al. 2016, Malone et al. 2019).

Immunohistochemistry

Immunohistochemistry for GnRH was performed as previously reported (Casoni et al. 2016, Malone et al. 2019) using the following antibodies: Guinea pig anti-GnRH (EH#1018; 1:10000), produced by Dr. Erik Hrabovszky (Laboratory of Endocrine Neurobiology, Institute of Experimental Medicine of the Hungarian Academy of Sciences, Budapest, Hungary) ; Rabbit anti-peripherin (Millipore AB1530, 1:2000) ; Goat anti-Plexin A1 (R&D AF4309, 1:50) ; Rat anti-Plexin A2 (R&D Systems MAB5486, 1:100) ; Goat anti-Plexin A3 (R&D AF4075, 1:200) ; Rabbit anti-Plexin A4 (Abcam ab39350, 1:250) ; Goat anti-Neuropilin2 (R&D AF2215, 1:50) ; Sheep anti-Semaphorin 3F (R&D AF3237, 1:500) ; Goat anti-TAG1 1:500 (R&D AF4439, 1:500).

Sections were first subjected to antigen retrieval in homemade citrate buffer for 20 minutes at 90°C, then rinsed in PBS and blocked for 2 h at room temperature in blocking solution: PBS, 0.3% Triton X-100 (T8787, Sigma), 0.25% Bovine Serum Albumin (Euromedex), 10% normal donkey serum (D9663; Sigma). Sections were incubated in a cocktail of primary antibodies diluted in blocking solution for 48 h at 4°C. Sections were then rinsed in PBS and incubated in a cocktail of fluorochrome-conjugated secondary antibodies (all raised in donkey; Alexa-Fluor 488-, 568-, 647-conjugated secondary antibodies; Molecular Probes, Invitrogen) diluted at 1:400 in blocking solution for 2 h at room temperature. Sections were then rinsed in PBS, coverslipped with Mowiol, and imaged using an inverted laser scanning Axio observer confocal microscope (LSM 710, Zeiss; BICeL Imaging Core Facility of the University of Lille 2, France).

III. Results

We identified heterozygous or hemizygous missense variants in *SEMA3F* (HGNC:10728) and *PLXNA3* (HGNC:9101) genes respectively in 15 patients from 11 unrelated families. Clinical and molecular genetic characteristics of the patients and their alterations are shown in Table II-1 and Supplementary Table II-1, respectively. The location of the variants on *SEMA3F* and *PLXNA3* gene diagrams and the pedigrees are depicted in Figures II-1 and II-2. We found six rare *SEMA3F* variants

located in critical regions for the proper protein function or its dimerization (Figure II-1A). We identified one variant (T29M) located close to the signal sequence (SS) of the protein, one (P452T) located within the SEMA domain, one (A652S) in the Ig domain and three (R699W, P722L, T724M) located in the basic motif of the protein (Figure II-1A). Seven IHH patients carried variants in *PLXNA3* respectively in the SEMA binding domain (R108C), in the Plexin-Semaphorin-Integrin (PSI2) domain (S646P) and in the Ig domain (IPT3 region) (L1086V), and RAS-GAP domain (R1359C), which suggest that these mutants are likely to affect ligand and co-receptor interactions (Figure II-2A).

In order to avoid harmless polymorphisms, in addition to quality and read depth filtering, we filtered the protein altering heterozygous/hemizygous variants by setting a threshold occurrence of 1:10.000. These 10 variants were either not seen or extremely rare with a minor allele frequency <0.0001 in the two largest reference population databases, TOPMed and gnomAD. Similarly, these variants were not reported in a much smaller but regional database, the Greater Middle East Variome (GME) (except for the *SEMA3F* R699W variant appearing once in 163 Turkish alleles). Sanger sequencing confirmed the presence of these variants. No variant was seen in ClinVar. These variants were all classified as variants of uncertain significance (VUS) by ACMG/AMP classification (Richards et al. 2015). Detailed information regarding these variants is given in Supplementary Table II-1.

In the etiology of IHH, almost all causative gene alterations show phenotypic variability and segregations in families are often irregular as in some of the pedigrees in this study. Oligogenic etiology (Sykiotis et al. 2017) and clinical reversibility (Sidhoum et al. 2014), among others, are well recognized in this condition to explain these complex pedigrees.

In six of the 11 kindreds (54%), there was at least one more gene known to be associated with IHH (oligogenecity) (Topaloglu 2017, Sykiotis et al. 2010). This high rate is consistent with our recent observation of the increased detection of oligogenecity in the etiology of IHH (Bouilly et al. 2018), which was earlier reported to be 10-20% (Sykiotis et al. 2010). This probably reflects increased number of recognized genes for IHH as well as recent diagnostic popularity of exome sequencing.

In Family C and F, the other variants (a homozygous TACR3 and a heterozygous FGFR1, respectively) were already classified in the ClinVar database as pathogenic and likely pathogenic for IHH, respectively. We believe that these additional variants were the main driving force of the IHH phenotypes. The effects of the SEMA3F variants on the phenotypes were predicted to be minor. Overall, the pattern of inheritance among the *SEMA3F* pedigrees is consistent with an autosomal dominant inheritance of each variant with variable penetrance and expressivity, irrespective of the inheritance whether it is familial or sporadic, which was repeatedly observed in recent IHH gene discoveries (Bouilly et al. 2018). The inheritance of *PLXNA3* variants are consistent with X-linked recessive pattern. With the exception of one *SEMA3F* (p.Pro452Thr) and one *PLXNA3* (p.Arg108Cys) variants, all other variants were encountered once. Notably, two sisters in family G had variants in both *SEMA3F* and *PLXNA3*, which were both inherited from their apparently unaffected mother, but their phenotypes were not more severe, in fact, these sisters had a lighter phenotype, one of the sisters having only delayed menarche. Yet, a third sister (G-II-3), even though she has the same genotype as the affected two sisters, did not display any abnormal pubertal or reproductive phenotype. We cannot readily explain the inconsistencies of the phenotypes among these three sisters who have the same genotype. However, it is increasingly well appreciated in the genetic of IHH that oligogenic contribution with variably reduced penetrance complicates pedigrees (Xu et al. 2017). Overall, six of 15 (40%) patients (five of them with *SEMA3F* variants) had compromised olfaction. In two of them, brain MRIs were obtained, which showed hypoplastic/aplastic olfactory bulbs. Figure 1C depicts the absent olfactory bulbs in Case D-II-2 due to p.Thr29Met in *SEMA3F*. These data are consistent with previous rodent studies showing the role of *SEMA3F* in the proper projections and fasciculations of the olfactory nerve and thus in the development of the olfactory bulb (Takeuchi et al. 2010). Interestingly, the same *SEMA3F* variant (Pro452Thr) was associated with normosmia or anosmia in two different families (Family A and B respectively). On the other hand, male patients in both families had cryptorchidism, indicating the presence of severe congenital hypogonadism. In congenital IHH, fetal pituitary gonadotropin secretion is low, leading to inadequate testosterone levels in fetal serum. As the testicular descent and growth of phallus are androgen-dependent, consequently, boys with severe IHH present with

micropenis, cryptorchidism, and hypospadias at birth (Pitteloud et al. 2002). Again, there was a discrepancy in olfactory function in patients carrying the same *PLXNA3* variant (p.Arg108Cys) in two different kindreds (Family H and I, Figure II-2A, B). These observations suggest that there is a complex input to the olfactory phenotype. To date, all Semaphorin signaling gene variant discoveries were carried out solely in the KS patients cohorts (Hanchate et al. 2012, Marcos et al. 2017, Young et al. 2012). This may have obscured the breadth of the phenotypic spectrum associated with these versatile family of molecules. Our population, on the contrary, is made up of all-inclusive IHH patients regardless of their olfactory functions. Therefore, our study has an unrestricted ability to observe all possible phenotypes. Case in point, in a previous screening study of PLXNA1 mutant cases in the same cohort as in this study, we found nine cases, among which only one third had compromised olfaction (Kotan et al. 2019). In contrast, the seminal publication on this gene was from an all anosmic (KS) cohort (Marcos et al. 2017).

Western blot analysis revealed normal protein content of *SEMA3F* variants in whole cell lysates (Supplementary Figure II-1A, B). By contrast, *SEMA3F*s harboring the P452T, T29M, and T724M missense variants showed impaired SEMA3F secretion, as shown by western blot analysis of the conditioned media (Supplementary Figure II-1A, C). The P722L variant on the other hand had secreted levels of protein similar to the wild type. Since the Family E proband has SEMA3F P722L only, it is curious if this variant is responsible for the IHH phenotype. Even though SEMA3F P722L is an extremely rare variant, the functional studies did not support its potential deleterious ramifications. Therefore, it is unlikely that this variant is solely responsible for the IHH phenotype in the family E proband. Interestingly this proband also has a variant in *QRFP* (NM_198180:c.G277A:p.E93K), which is heavily expressed in the hypothalamic arcuate nucleus and is known to regulate food intake (Chartrel et al. 2016). Its product, Pyroglutamylated RFamide peptide 43, has been shown to stimulate the hypothalamic-pituitary-gonadal axis via gonadotropin-releasing hormone in rats (Patel et al. 2008). Given the extreme obesity and IHH of this patient, it's tempting to think that variants in these two genes together contributed to the IHH phenotype of this patient. Since SEMA3F is a bifunctional guidance molecule that can exert both axon-repulsive and

-attractive effects depending on its gradient and on receptors' composition on target cells (Kolk et al. 2009), future studies will be aimed at understanding how different SEMA3F concentrations and different receptors' complexes may affect GnRH neuronal migration and/or olfactory and vomeronasal axon orientation. We also tested the effect of the *PLXNA3* variants (with the exception of R1359C and L1086V) on receptor synthesis by western-blot analyses on transfected HEK293T cells producing *PLXNA3* WT, *PLXNA3* S646P and *PLXNA3* R108C (Supplementary Figure II-2). The fact the two untested variants (L1086V and R1359C) are located, respectively, in the Ig domain (IPT3 region) and in the RAS-GAP domain (R1359C), suggests that these mutants are likely to affect ligand and co-receptor interactions, based on the structural model of the protein (van der Klaauw et al. 2019).

Immunoblots on cell lysates from HEK293T cells transfected with *PLXNA3* WT or with the mutant proteins revealed the expression of a band for PLXNA3 at the expected molecular weight (220 kDa), which was absent in mock-transfected cells (Supplementary Figure II-2A). However, cells expressing the mutant *PLXNA3*s presented two isoforms (Supplementary Figure II-2A), which suggests glycosylation modifications at the level of the ER ("immature forms of proteins").

We next immunostained transfected HEK293 cells for PLXNA3 and Calnexin, a marker of the endoplasmic reticulum (ER). WT PLXNA3 was predominantly localized on the plasma membrane (Supplementary Figure II-2B). In contrast, S646P, but not R108C, variant showed PLXNA3 localization exclusively in the ER (Supplementary Figure II-2B, II-2C), indicating that the variant S646P disrupts cell-surface localization of PLXNA3. Overall, these data revealed the existence of two PLXNA3 isoforms, which raises two functional hypotheses: 1) these variants could affect the processing and/or maturation of the glycosylation of the receptor with a subsequent accumulation of PLXNA3 in endoplasmic reticulum (ER); and/or 2) these mutations could affect the protein trafficking of the receptor from the ER to the cell surface. The observation that PLXNA3 S646P variant was predominantly found within the endoplasmic reticulum rather than at the cell surface, supports those hypotheses. Interestingly, all probands carrying mutations in PLXNA3 were males (Table II-1). These data together with the fact that PLXNA3 lies on the X chromosome suggest that

these individuals have likely minimal signaling through PLXNA3 and argue in favor of the pathogenic effect of PLXNA3 mutants in IHH.

With the exception of NRP2 (Casoni et al. 2016), expression of SEMA3F signaling pathway has never been investigated in the developing human GnRH and olfactory system. We, thus, evaluated the expression pattern of *SEMA3F* and PLXNA1-A4 receptors in sagittal and coronal sections of human fetal heads (gestational weeks post amenorrhea: GW, GW7.5 and GW10.5), together with the expression of GnRH and peripherin, a marker of the developing olfactory and vomeronasal fibers (Casoni et al. 2016, Fueshko ans Wray 1994) (Figures II-3, II-4). At GW7.5, the great majority of GnRH neurons migrate in chains across the nasal septum along vomeronasal/terminal peripherin-positive fibers directed toward the forebrain (Figure II-3 B, C, E, H), in agreement with our previous immunohistochemical study (Casoni et al. 2016). *PLXNA3* expression was found along the vomeronasal and terminal nerves (Figure II-3 D-H), as well as in migratory GnRH neurons (see arrows in Figure II-3 F, G). At GW11, about 80% of GnRH neurons have been reported to enter the brain and migrate toward their final target areas (Casoni et al. 2016). Our immunofluorescence analysis of a GW10.5 fetus indeed revealed robust GnRH-immunoreactivity in migratory cells invading the developing forebrain (Figure II-3 I, J, M). Similarly to the mouse olfactory system, where *SEMA3F* is secreted by early-arriving olfactory axons and deposited at the anterodorsal olfactory bulb (OB) (Takeuchi et al. 2010), in GW10.5 human fetuses, *SEMA3F* is expressed along the olfactory nerve (on), by the developing olfactory epithelium (oe) and by the vomeronasal and terminal nerves (VNN and TN) entering the brain (Figure II-3 K, N). *SEMA3F* expression was absent in human migratory GnRH neurons (Figure II-3 M, N). At this fetal stage, like at GW7.5, *PLXNA3* is expressed along the vomeronasal and terminal nerves, which also express its ligand (Figure II-3 L-P). However, at GW10.5 GnRH neurons are PLXNA3-negative (Figure II-3 M, O, P), thus suggesting that PLXNA3 could be downregulated in GnRH neurons that entered the brain compartment.

In order to assess the expression pattern of the other PLXN receptors through which *SEMA3F* can possibly signal, we next performed double-immunofluorescence staining of sagittal sections of

GW7.5 fetuses using antibodies raised against GnRH and PLXNA1, PLXNA2 and PLXN4. This analysis revealed that GnRH neurons migrating in the nasal compartment express PLXNA1 and PLXNA2 (Figure II-4 A-F; arrows) but not PLXNA4 (Figure II-4 G, H). Also, PLXNA1 was found to be expressed by the vomeronasal/terminal nerves that form the migratory scaffold for GnRH neurons (Figure II-4 D). GnRH neurons migrate together with a heterogeneous coalescence of placode-derived and neural crest-derived migratory cells and olfactory axons, collectively called the 'migratory mass' (MM) (Valverde et al. 1992). At this stage, we observed a mixed mass of GnRH neurons and other cells migrating across the nasal mesenchyme towards the telencephalon expressing PLXNA2 (Figure II-4 E, F). Overall, these results show that SEMA3F and PLXNA3 are both expressed along the olfactory nerve (on) and along the intracranial projection of the vomeronasal nerve/terminal nerve (vnn/tn). Our immohistochemical data also indicated that the signal-transducing receptors PLXNA1-A3 are expressed in early migratory GnRH neurons, therefore suggesting that SEMA3F signaling through PLXNA1-A3 could be involved in the guidance of GnRH neurons and of olfactory and vomeronasal nerve fibers in humans.

IV. Discussion

Our findings suggest that SEMA3F signaling is necessary for correct human puberty onset and reproduction. To substantiate this point, we present clinical, molecular, genetic, and *in vitro* functional data from 15 patients who belonged to 11 independent families. These patients all presented with pubertal failure and were clinically diagnosed with IHH or KS. Our study reveals that 6.9% of probands with nIHH/KS harbor variants in *SEMA3F* and/or *PLXNA3*. This indicates that genes in the SEMA3F signaling pathway are among the most frequently mutated ones in congenital GnRH deficiency, together with *FGFR1* and *CHD7* (Topaloglu 2017).

With regards to any previous implication of SEMA3F in human puberty/reproduction, in a large genome-wide association study, an SNP near *SEMA3F* was found to be strongly correlated with "age at first birth," which indicates earlier puberty timing and reproductive success (Day et al. 2016), suggesting the relevance of *SEMA3F* to reproductive function in humans.

To support further our message, we provide unequivocal human embryonic data showing the expression of SEMA3F along the developing human GnRH migratory pathway. Moreover, our data provide compelling evidence that all the receptors required for the SEMA3F signaling, including PLXNA3, a key component of the SEMA3F holoreceptor complex (Sharma et al. 2012), are expressed by the human GnRH and olfactory/vomeronasal systems. Based on the expression of SEMA3F signaling pathway in the nasal compartment of early human fetuses, and on the chemotactic role of this semaphorin reported in other species (Sharma et al. 2012), our data raise the hypotheses that SEMA3F/PLXNA3 could regulate GnRH neuronal migration and olfactory/vomeronasal axonal elongation in humans. Notably, our data indicated that the signal-transducing receptors PLXNA1-A3 are expressed in early migratory GnRH neurons. This is consistent with a recent investigation highlighting cooperation of Plxna1 and Plxna3 in the formation of the GnRH migratory scaffold in mice, based on which the human orthologue of Plxna3 (i.e., *PLXNA3*), like PLXNA1, was proposed to be a candidate gene for mutation screening in patient with KS (Oleari et al. 2019). Indeed, in that study the authors have shown that, while mice lacking plxna1 or plxna3 present only mild or absent defects in the development of the GnRH neuron and olfactory systems, double-mutant *Plxna1* $^{-/-}$*; Plxna3* $^{-/-}$ animals phenocopied the full spectrum of nasal axon and GnRH neuron defects typical of KS (Oleari et al. 2019). In line with the oligogenic nature of KS, these data suggest that *Plxna1* synergises with *Plxna3* during nasal axon guidance required for proper GnRH neuron migration.

The existing literature indicates that the SEMA3F signals through Nrp2/Plxna3 holoreceptor complex, while Sema3a signaling occurs mainly via Nrp1/Plxna1 (Giacobini 2015, Sharma et al. 2012). Importantly, Nrp2 and its ligand, SEMA3F, are expressed by olfactory sensory neurons in rodents in a complementary manner that is important for establishing olfactory map topography (Takeuchi et al. 2010). Despite these evidences, based on typical GnRH migration patterns and expected numbers of GnRH neurons in the Sema3f deficient mice, this guidance molecule was reported to be dispensable for GnRH neuron migration (Cariboni et al. 2011). However, similarly to the recently described cooperation of *Plxna1* with *Plxna* (Oleari et al. 2019), it is possible that *Sema3f* may synergize with other Semaphorins to regulate the proper GnRH migratory process and/or

olfactory axonal elongation. Moreover, pubertal and adult reproductive phenotypes of *Sema3f* $^{-/-}$ mice, such as the timing of puberty onset, first estrus, fertility index, litter size, etc. have not been investigated. Besides, species-specific differences in Sema3s functions between mice and humans may exist. In fact, significant species differences, even with well-established reproductive genes including *TAC3/TACR3* and *KISS1/KISS1R*, have been previously documented. Specifically, patients bearing mutations in *TAC3* and *TACR3* (Topaloglu et al. 2009) have sexual infantilism and infertility due to GnRH deficiency. In contrast, a recent transgenic Tacr3(-/-) mouse model demonstrated that normal sexual maturation occurs in these mice, albeit some significant reproductive defects are evident in adulthood (Yang et al. 2012). Likewise, while humans with *KISS1* (Topaloglu et al. 2012) and *KISS1R* (Seminara et al. 2003) mutations typically suffer from pubertal failure and infertility, a considerable proportion of female Kiss1 and Kiss1r knockout mice exhibit normal estrous cyclicity, and some male Kiss1- and Kiss1r-null mice exhibit spermatogenesis (Lapatto et al. 2007). These species differences underscore the importance of human studies in puberty/reproduction research.

Finally, a recent work provided compelling evidence that SEMA3s-mediated signalling drives the development of hypothalamic melanocortin circuits and that mutations in these pathways cause obesity (van der Klaauw et al. 2019). Interestingly, the hypothalamic pro-opiomelanocortin (POMC)-expressing neurons have been repeatedly observed to send projections to and be in close contact with kisspeptin/neurokinin B/dynorphin (KNDy) cells (Manfredi-Lozano et al. 2018, Moore et al. 2019). A plethora of investigations have recently identified the role of the hypothalamic KNDy neuronal population as the GnRH pulse generator (Topaloglu 2017, Moore et al. 2019). Importantly, in the study of van der Klaauw and colleagues, one of the patients harboring a *PLXNA3* variant (D1710N) had hypogonadotropic hypogonadism in addition to obesity (van der Klaauw et al. 2019). However, since the majority of the probands in that study were pre-pubertal age children, the true prevalence of hypogonadotropic hypogonadism among variant carriers may be underestimated (van der Klaauw et al. 2019). Although we noted in this study that a significant proportion of the patients (40%) was obese, *SEMA3F/PLXNA3* variants were not statistically more enriched in the subset of obese IHH patients than in our general IHH cohort, where 56 patients (26.0%) featured overweight or obesity

($p = 0.24$). It would be interesting in the future to carefully look at larger and multiple IHH cohorts and determine whether statistical significance in the frequency of obesity or metabolic disorders could emerge when analysing larger populations and probands carrying variants in SEMA3F signalling pathway.

In summary, we provide clinical, genetic, molecular/cellular, and developmental evidence to implicate variants in SEMA3F signalling in the etiology of IHH. We propose that this phenotype could be exerted via a direct deleterious effect of these mutants on the GnRH neuronal migration and potentially a harmful impact of *SEMA3F*/*PLXNA3* mutants on the development of hypothalamic melanocortin circuits involved in the regulation of energy homeostasis, which are also known to influence GnRH secretion and reproduction. Each of these events or a combination could hence negatively affect the development and function of the HPG axis. Further studies aimed at addressing the contribution of SEMA3F and PLXNA3 in each one of the above-mentioned developmental processes may uncover new mechanisms underlying human disorders characterized by central hypothalamic dysfunction and infertility.

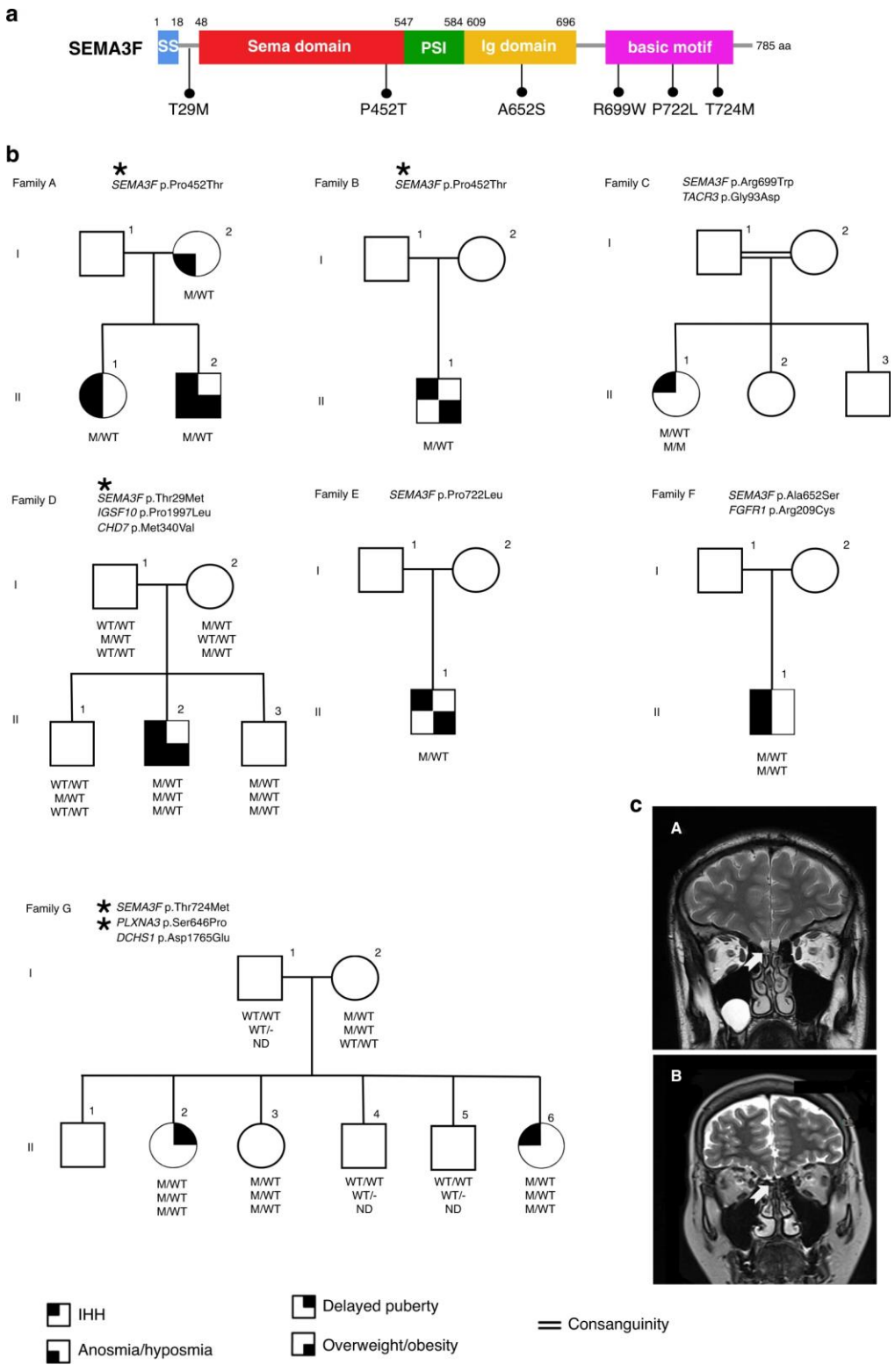

Figure II-1. SEMA3F Mutations in the etiology of idiopathic hypogonadotropic hypogonadism.

A*. The mutations are depicted on the functional gene diagram of SEMA3F.* ***B****. The pedigrees of seven families with SEMA3F mutations are shown. Affected males and females are represented by black squares and black circles respectively. White square symbols indicate unaffected male family members, white circle*

symbols represent unaffected female family members, and the double line indicates consanguinity. Under each symbol are the genotypes in the same order as the gene and variant descriptions, with WT and M denoting wild type and mutant, respectively. ND: Not determined. Since PLXNA3 is on the X chromosome male individuals are expected to have only one allele. – means allele absent. ***C****. The T2-weighted magnetic resonance imaging (MRI) from a healthy control (a) and from patient DII-2 (b). The arrows point to normal (a) and aplastic olfactory bulbs (b).*

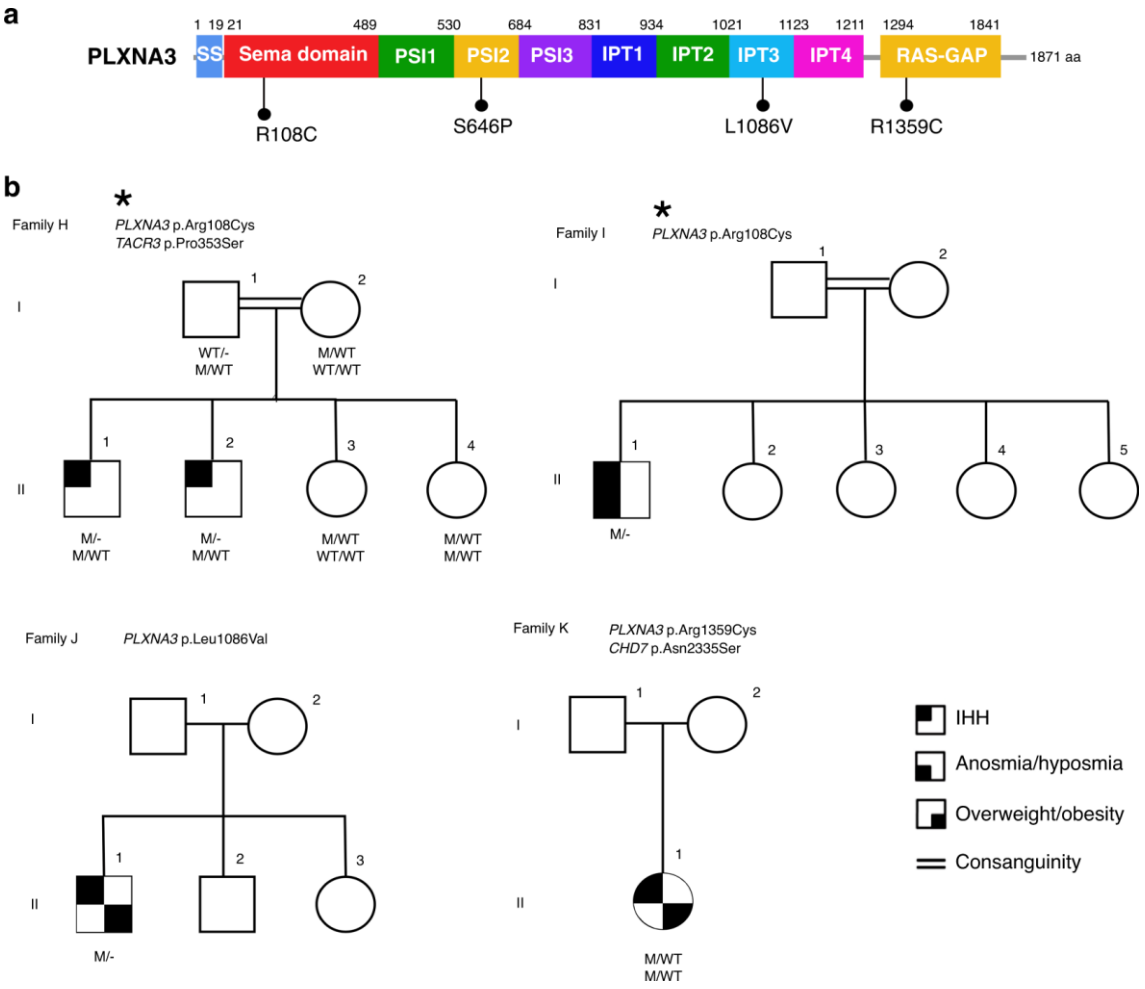

Figure II-2. PLXNA3 mutations in patients with idiopathic hypogonadotropic hypogonadism. ***A****. The diagram of PLXNA3 showing the positions of the missense mutations found in patients.* ***B****. The pedigrees of the three families with PLXNA3 mutations are shown. Note that patients in Family G in Figure 1 also have PLXNA3 mutations in addition to SEMA3F mutations. Affected males and females are represented by black squares and black circles respectively. White square symbols indicate unaffected male family members, white circle symbols represent unaffected female family members, and the double line indicates*

consanguinity. Under each symbol are the genotypes in the same order as the gene and variant descriptions, with WT and M denoting wild type and mutant, respectively. Since PLXNA3 is on the X chromosome male individuals are expected to have only one allele. – means allele absent.

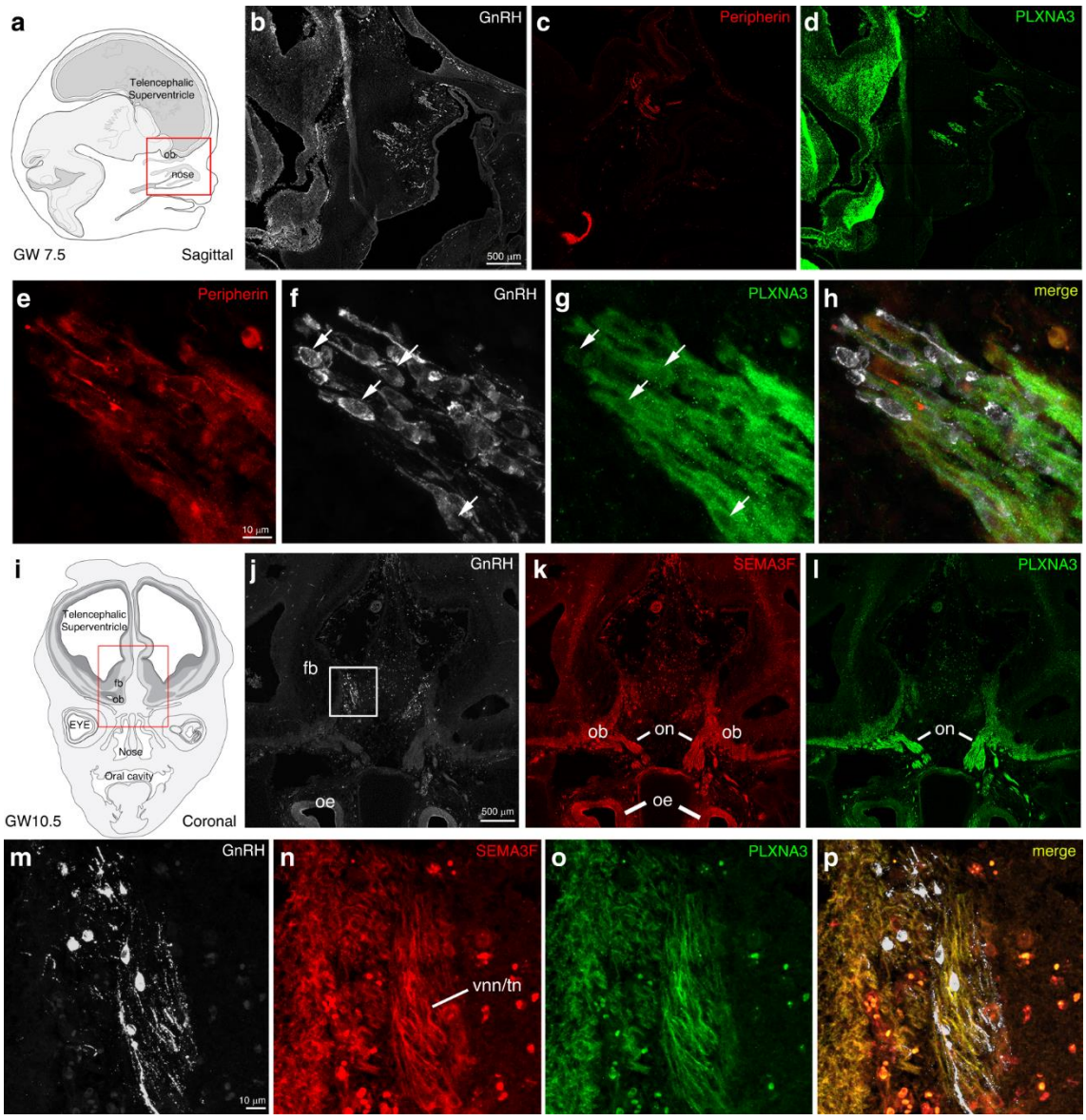

Figure II-3. Semaphorin 3F and Plexin A3 are expressed along the migratory route of GnRH neurons in human fetuses. *Fluorescent IHC was performed to assess SEMA3F and PLXNA3 expression both in the nasal region (**A**) and at the nasal/forebrain junction (**I**) during the early fetal development. (**B-D**) Representative immunostaining for GnRH, Peripherin and Plexin A3 on sagittal sections of a GW7.5 human fetus. (**E-H**) Magnification of the boxed area in B, revealing that PLXNA3 is found in the peripherin-positive olfactory/vomeronasal scaffold, as well as in GnRH neurons (arrows) during their migration*

*through the nasal compartment. (**J-L**) Representative pictures of immunolabelings for GnRH, PLXNA3 and SEMA3F on coronal sections of a GW10.5 human fetus. (**M-P**) Magnification of the boxed area in **J**. The olfactory and vomeronasal/terminal nerves still show immunoreactivity for PLXNA3 at the nose/forebrain junction. SEMA3F is strongly expressed in this region and detected along the PLXNA3-positive nerves. GnRH neurons migrating inside the forebrain do not longer express PLXNA3. fb, forebrain; ob, olfactory bulbs; oe, olfactory epithelium; on, olfactory nerves; vnn/tn, vomeronasal/terminal nerves. Scale bars: **B**, **J** = 500 µm; **E**, **M** = 10 µm.*

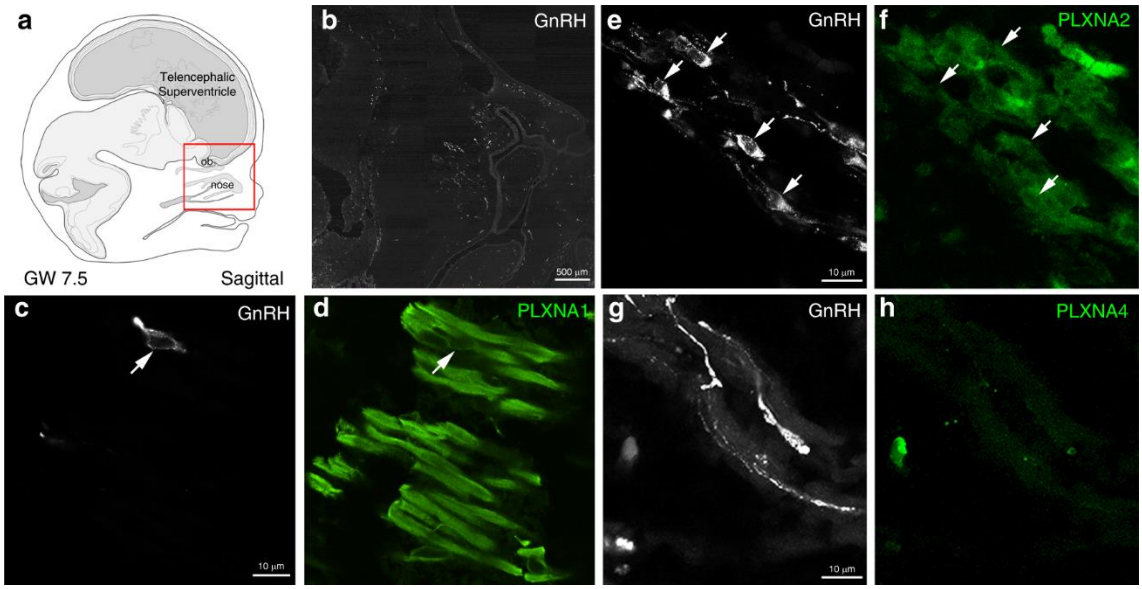

Figure II-4. PLXNA1 and PLXNA2 could also contribute to SEMA3F signalling in the human fetal nose. *Since SEMA3F can signal not only through PLXNA3, but through the PLXNA1-A4 family, additional stainings were performed to check for PLXNA1-A4 expression in the nasal compartment of a GW7.5 human fetus. In addition to PLXNA3, migrating GnRH neurons and the olfactory/vomeronasal scaffold also express PLXNA1 (**C-D**) while PLXNA2 was detected in GnRH neurons and other cells of the migratory mass, but not in the olfactory/vomeronasal projections (**E-F**). However, PLXNA4 immunoreactivity was only found in scattered cells, distant from the migratory route of GNRH neurons (**G-H**). ob, olfactory bulbs. Scale bars: **B** = 500 µm; **E,C,G** = 10 µm.*

Family/individual number	Gene/variant	Age at diagnosis	Sex	Obesity	Olfaction	Reproductive phenotype
A I-2	*SEMA3F* p.Pro452Thr	28	F	No	Anosmic	No delayed puberty or infertility reported
A II-1	*SEMA3F* p.Pro452Thr	20	F	No	Anosmic	Absent puberty, primary amenorrhea
A II-2	*SEMA3F* p.Pro452Thr	12	M	Obese	Anosmic	Absent puberty, cryptorchidism
B II-1	*SEMA3F* p.Pro452Thr	10.5	M	Overweight	Normosmic	Cryptorchidism
C II-1	*SEMA3F* p.Arg699Trp	16	F	No	Normosmic	Absent puberty, primary amenorrhea
D II-2	*SEMA3F* p.Thr29Met	17	M	Obese	Hyposmic	Absent puberty, cryptorchidism
E II-1	*SEMA3F* p.Pro722Leu	14	M	Obese	Normosmic	Absent puberty
F II-1	*SEMA3F* p.Ala652Ser	35	M	No	Hyposmic	Absent puberty, micropenis, infertility
G II-2	*SEMA3F* p.Thr724Met *PLXNA3* p.Ser646Pro	20	F	No	Normosmic	Primary amenorrhea, delayed menarche at age 16
G II-6	*SEMA3F* p.Thr724Met *PLXNA3* p.Ser646Pro	14	F	No	Normosmic	Absent puberty
H II-1	*PLXNA3* p.Arg108Cys	19	M	No	Normosmic	Absent puberty
H II-2	*PLXNA3* p.Arg108Cys	17	M	No	Normosmic	Absent puberty
I II-1	*PLXNA3* p.Arg108Cys	21	M	No	Hyposmic	Absent puberty, cryptorchidism
J II-1	*PLXNA3* p.Leu1086Val	14	M	Overweight	Normosmic	Absent puberty, micropenis
K II-1	*PLXNA3* p.Arg1359Cys	18	F	Obese	Normosmic	Absent puberty, primary amenorrhea

Table II- 1. Clinical characteristics of individuals with SEMA3F and PLXNA3 variants.

V. Supplementary data

DNA sequencing and rare variant analyses

The ES data from the 216 IHH cohort patients were screened for rare sequence variants (RSVs) in the *SEMA3F* (NM_004186) and *PLXNA3* (NM_017514). A total of 53 genes (*AMH*, *AMHR*, *ANOS1*, *AXL*, *CCDC141*, *CHD7*, *DMXL2*, *DUSP6*, *FEZF1*, *FGF17*, *FGFR1*, *FGFR8*, *FLRT3*, *FSHB*, *GNRH1*, *GNRHR*, *HESX1*, *HS6ST1*, *IGSF10*, *IL17RD*, *KISS1*, *KISS1R*, *KLB*, *LEP*, *LEPR*, *LHB*, *NDNF*, *NR0B1*, *NSMF*, *OTUD4*, *PCSK1*, *PLXNA1*, *PNPLA6*, *POLR3A*, *POLR3B*, *PROK2*, *PROKR2*, *RAB18*, *RAB3GAP1*, *RAB3GAP2*, *RNF216*, *SEMA3A*, *SEMA3E*, *SMCHD1*, *SOX10*, *SPRY4*, *SRA1*, *STUB1*, *TAC3*, *TACR3*, *TBC1D20*, *TUBB3*, and *WDR11*) known to be associated with nIHH/KS were also screened with added scrutiny for additional variants. Moreover, these data were also analyzed for new candidate gene detection in the etiology of IHH. The presence of significant variants was verified by Sanger sequencing on an Applied Biosystems PRISM 3130 auto sequencer.

The NHLBI Trans-Omics for Precision Medicine Whole Genome Sequencing Program, TOPMed (https://bravo.sph.umich.edu/freeze5/hg38/), the Genome Aggregation Consortium, gnomAD (http://gnomad.broadinstitute.org/), and the Greater Middle East Variom Project, GME (http://igm.ucsd.edu/gme/data-browser.php) were used to determine the allelic frequencies. Variants with minor allele frequency (MAF) <0.01% in each of these database were considered rare.

The Combined Annotation Dependent Depletion, CADD (https://cadd.gs.washington.edu/snv) scores were used for *in silico* prediction. Additionally, variants were evaluated by four different *in silico* pathogenicity prediction methods: MutationTaster; SIFT, Sorting Intolerant From Tolerant; LRT, Likelihood Ratio Test; PolyPhen-2, Polymorphism Phenotyping v2. The pathogenicity prediction scores 0-4 out of 4 were obtained for each variant. InterVar (http://wintervar.wglab.org/) was used to determine variant classification based on the 2015 American College of Medical Genetics and Genomics and Association for Molecular Pathology guidelines (ACMG/AMP) (Richards et al. 2015).

Cell-Based Functional Assays

SEMA3F and PLXNA3 protein expression

A cDNA containing the entire coding region of the human SEMA3F transcript variant 1 (GenBank: NM_004186.5) was inserted into a modified pcDNA3.1+ expression vector containing a his-tag at the 5'end (GeneCust). Similarly, plasmid encoding *SEMA3F* mutants were obtained using modified pcDNA3.1+ expression vector containing a myc-tag at the 5'end of the coding region (GeneCust). A cDNA containing the entire coding region of the human *PLXNA3* (GenBank: NM_017514.5) was inserted into a modified pcDNA3.1+ expression vector containing a his-tag at the 5'end (GeneCust). Similarly, plasmid encoding PLNXA3 mutants were obtained using modified pcDNA3.1+ expression vector containing a myc-tag at the 5'end of the coding region (GeneCust).

To assess the impact of the variants on *SEMA3F* expression and secretion, and on PLNXA3 signaling, we performed western-blot assays as previously described (Hanchate et al. 2014, Malone et al. 2019).

Cell cultures

Kidney cells (HEK 293T) from human embryo were cultured under standard conditions in a DMEM-based medium containing 5% fetal bovine serum and appropriate selection antibiotics; they were re-plated before reaching 80% confluency and were passaged < 20 times. HEK 293T were authenticated based on morphology, and DNA staining revealed no mycoplasma contamination.

Transfection was performed in 6- or 12-well plates using Fugene6 (Promega) according to the manufacturer's protocol, in a transfection rate of 3:1 (Fugene6:DNA) and for 48 h at 37°C. Conditioned media were collected for secretion assays, and the plates were quickly rinsed with PBS and frozen on dry ice for subsequent expression assays. Proteins from conditioned media and cells were subjected to western blot analysis as described below.

Western blots

Homemade Tris-Triton lysis buffer was used for cell lysis and protein extraction, and the protein concentration was determined for each sample using the Pierce BCA protein assay kit (Thermofisher). For SEMA3F and PLXNA3 assays, 10 µg or 20 µg of proteins were loaded in each well of 6% or 8% hand-casted acrylamide gels, respectively. Migration was carried out in Tris/Glycine/SDS buffer and proteins were subsequently transferred to a 0.45 µm nitrocellulose membrane in Tris/Glycine/Methanol. The membranes were cut into strips and blocked in TBS-T (TBS, 0.05% Tween 20) + 5% milk for 1h at RT, followed by incubation with primary antibodies in TBS-T + 5% Bovine Serum Albumin overnight at 4°C. The next day, membranes were incubated with HRP-conjugated secondary antibodies in TBS-T + 5% milk for 1h at RT. Finally, the strips were incubated in SuperSignal West Pico PLUS (ThermoFisher) and revelation was performed in a dark room using X-ray films. Quantification was performed in FIJI, and GAPDH was used for normalization. Primary antibodies: Sheep anti-Semaphorin 3F (R&D AB3237, 1:1000), Goat anti-Plexin A3 (R&D AB4075, 1:500), Rabbit anti-GAPDH (Sigma G9545, 1:5000). Secondary antibodies: Anti-rabbit HRP-conjugated (Cell Signaling 7074S, 1:10000), Anti-Sheep HRP-conjugated (R&D HAF016, 1:5000), Anti-Goat HRP-conjugated (Vector Labs PI-9500 , 1:5000).

Immunocytochemistry on transfected HEK293 cells

HEK293T cells were seeded on poly-L-lysin coated coverslips in a 24 wells-plate, and were transfected for 48h with *PLXNA3* variants using Fugene 6 (Promega) and following manufacturer's recommendations. Cells were fixed with paraformaldehyde 4% in PBS for 10 minutes, and rinsed three times before immunocytochemistry to assess the cellular distribution of PLEXIN A3 (PLXNA3). Immunocytochemistry was performed as follows: cells were first blocked and permeabilized for 1h in blocking buffer (PBS, 0.1% Triton, 5% Normal Donkey Serum) then incubated overnight in blocking buffer with primary antibodies (goat anti-PlexinA3 1:500, AF4275 R&D Systems, rabbit anti-Calnexin 1:1000, ab92573 Abcam), rinsed in PBS, and incubated for 2 hours in blocking buffer with secondary antibodies (donkey anti Goat/Rabbit, Alexa Fluor 488/568 conjugated, 1:500, Invitrogen). Cells were rinsed again in PBS, and nuclei were stained with DAPI

1:5000 in PBS for 2 minutes before mounting with Mowiol. Slides were imaged on an inverted laser scanning Axio observer confocal microscope (LSM 710, Zeiss; BICeL Imaging Core Facility of the University of Lille, France) using a 63x/1.40 oil-immersion objective, and 15 to 20 single-plane pictures were taken for each condition.

PLEXIN A3 cellular localization analysis

Signal analysis was performed using Fiji: Plexin A3 and endoplasmic reticulum stainings from single-plane acquisitions were thresholded with constant parameters. Plexin A3 signal was used as a mask to segment the ER staining and subsequently quantify the proportion of Plexin A3 in the ER. Statistical analysis was performed in Graphpad Prism 7: data was first subjected to D'Agostino & Pearson normality test, and analyzed using a one-way ANOVA with Dunnett's multiple comparisons test.

Statistical analysis

Statistical analyses were performed using Prism 5 (GraphPad Software). Data sets were assessed for normality (Shapiro-Wilk test) and variance. Where appropriate a one-way or two-way ANOVA followed by post hoc testing (specified in the figure legends) was performed and for non-Gaussian distributions, a Kruskal-Wallis test followed by Dunn's multiple comparison test was used – indicated in figure legends.

Family/individual no	Gene	Variant at cDNA level	Variant at protein level	CADD score	TOPMed	gnomAD	InterVar	*In silico** pathogenicity	Other IHH gene mutation/ zygosity
A I-2, II-1, II-2	*SEMA3F*	c.1354C>A	p.Pro452Thr	26.9	absent	0.00001	VUS: PM1, PM2, PP3	4/4	None
B II-1	*SEMA3F*	c.1354C>A	p.Pro452Thr	26.9	absent	0.00001	VUS: PM1, PM2, PP3	4/4	None
C II-1	*SEMA3F*	c.2095C>T	p.Arg699Trp	26.2	<0.00001	0.00003	VUS: PM1	2/4	*TACR3* p.Gly93Asp Hom
D II-2	*SEMA3F*	c.86C>T	p.Thr29Met	3.2	0.00001	0.00003	VUS: PM1, BP4	0/4	*IGSF10* p.Pro1997Leu Het, *CHD7* p.Met340Val Het
E II-1	*SEMA3F*	c.2165C>T	p.Pro722Leu	16.5	absent	0.00001	VUS: PM1, PM2	1/4	None
F I-1	*SEMA3F*	c.1954G>T	p.Ala652Ser	15.8	absent	absent	VUS: PM1, PM2	0/4	*FGFR1* p.Arg209Cys Het
G II-3, II-6	*SEMA3F* *PLXNA3*	c.2171C>T c.1936T>C	p.Thr724Met p.Ser646Pro	14.4 24.6	0.00001 absent	0.00002 absent		1/4 4/4	*DCHS1* p.Asp1765Glu Het
H II-1, II-2	*PLXNA3*	c.322C>T	p.Arg108Cys	31.0	absent	0.00001	VUS: PM1, PM2	4/4	*TACR3* p.Pro353Ser Het
I II-1	*PLXNA3*	c.322C>T	p.Arg108Cys	31.0	absent	0.00001	VUS: PM1, PM2	4/4	None
J II-1	*PLXNA3*	c.3256C>G	p.Leu1086Val	14.7	absent	absent	VUS: PM1, PM2	0/4	None

K II-2	*PLXNA3*	c.4075C>T	p.Arg1359Cys	29.3	absent	0.00005	VUS: PM1	4/4	*CHD7* p.Asn2335Ser

Supplementary Table II-1. The molecular genetic characteristics of the SEMA3F and PLXNA3 variants. *Hom, homozygous; Het, heterozygous; gnomAD, The Genome Aggregation Consortium; TOPMed, The NHLBI Trans-Omics for Precision Medicine Whole Genome Sequencing Program; InterVar, interpretation of genetic variants by the ACMG/AMP 2015; VUS, variant uncertain significance; PM, pathogenic moderate; PP, pathogenic supporting; BP, benign supporting. Variants are described according to the RefSeq numbers following the gene names: SEMA3F, NM_004186; PLXNA3, NM_017514; TACR3, NM_001059; IGSF10, NM_178822; CHD7, NM_017780; FGFR1, NM_023110; and DCHS, NM_003737. In silico pathogenicity prediction tests are Mutation Taster; SIFT, Sorting Intolerant From Tolerant; LRT, Likelihood Ratio Test; PolyPhen-2, Polymorphism Phenotyping v2. The column depicts number of harmful predictions out of 4 tests.*

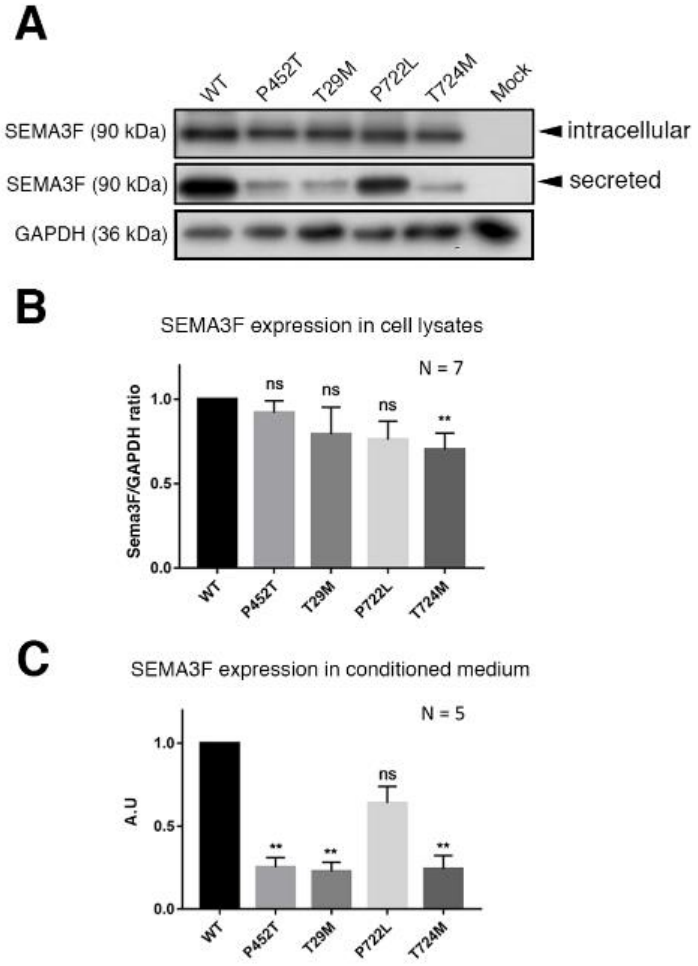

Supplementary Figure II-1. Variants of SEMA3F are loss of function. *The expression and secretion profiles of several SEMA3F variants, and the signaling of PLXNA3 variants were assessed using HEK293T cells transfected for 48h. (**A**) Representative western blot for intracellular and secreted SEMA3F. (**B, C**) While only the T724M SEMA3F variant was associated with a significant decrease in expression, the variants strongly affected SEMA3F secretion with an approximate threefold decrease in three out of four variants (P452T, T29M, T724M) relative to the WT. Each experiment was performed three times independently. ** P < 0.01 (Kruskal-Wallis test followed by Dunn's multiple comparisons test).*

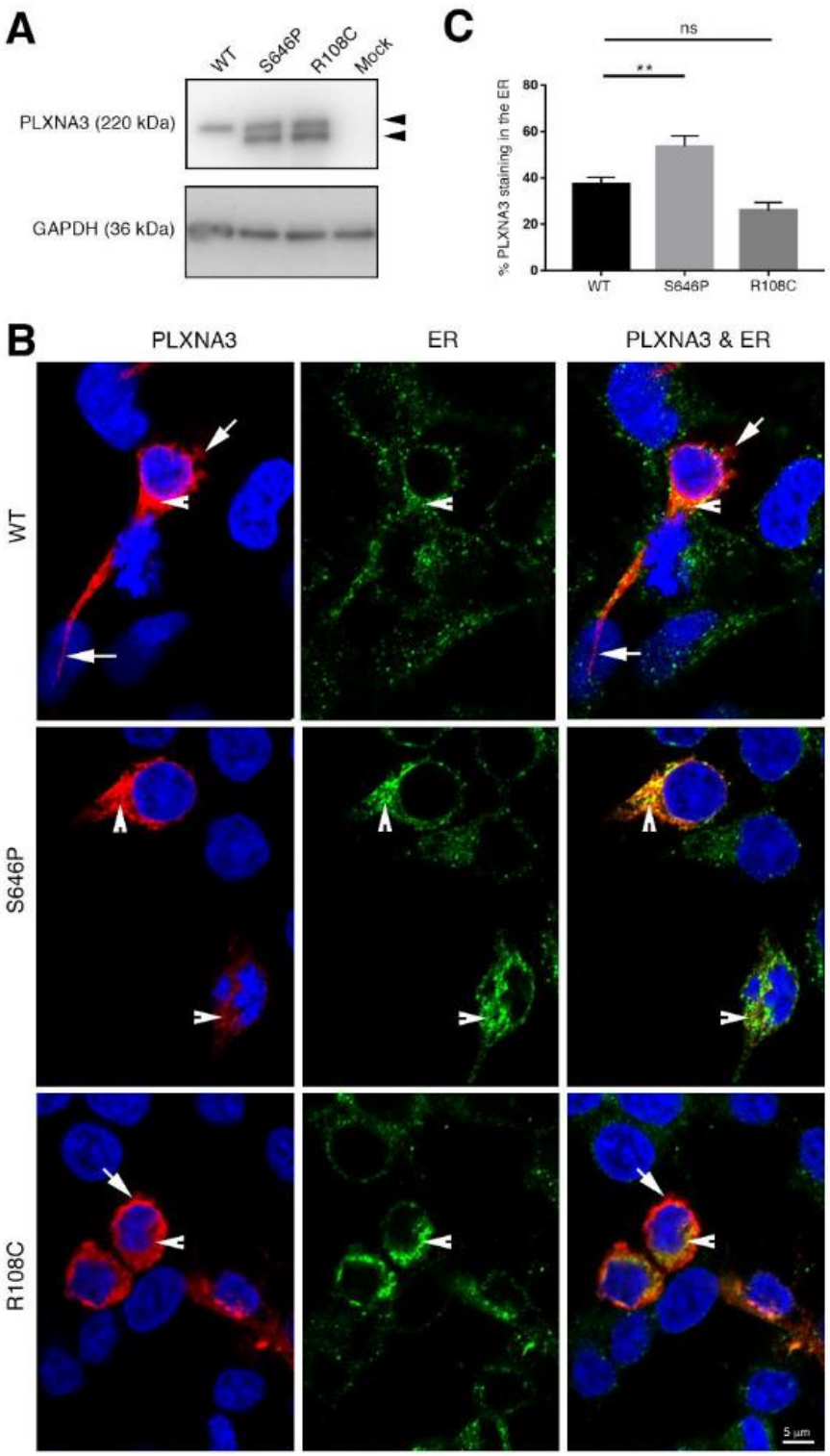

Supplementary Figure II-2. Functional validation of PLXNA3 variants. (A) *Representative western blot for PLXNA3 in HEK293T transfected or not with PLXNA3 WT and variants (S646P and R108C). Detection of two isoforms for the S646P and R108C variants (arrowheads), but not the WT variant of PLXNA3, suggests post-translational modifications affecting only or more strongly the mutant variants. Each experiment was performed three times independently. ** P < 0.01 (Kruskal-Wallis test followed by Dunn's*

multiple comparisons test). ***(B)*** *Representative fluorescent immunocytochemistry for PLXNA3 and Calnexin, a marker of the endoplasmic reticulum (ER), in transfected HEK293 cells. PLXNA3 WT and R108C variant are localized mainly at the plasma membrane (arrows), even though some signal is also detectable in the ER (arrowheads). S646P variant is only visible in the ER (arrowheads) but not in the membrane. (**C**) Quantitative analysis showing the relative proportion of PLXNA3 staining in the ER in HEK293T cells transfected with PLXNA3 WT and PLXNA3 variants. ** P < 0.01 (One-way ANOVA with Dunnett's multiple comparisons test, data is shown as mean ± SEM). ER, endoplasmic reticulum. Scale bar: 5 µm.*

Accessions: The following variants with associated clinical information were submitted to Clin Var: *SEMA3F* p.Pro452Thr, p.Arg699Trp, p.Thr29Met, p.Pro722Leu, p.Ala652Ser, p.Thr724Met. *PLXNA3* p.Ser646Pro, p.Arg108Cys, p.Leu1086Val, p.Arg1359Cys.

Acknowledgments We thank the midwives of the Gynecology Department, Jeanne de Flandre Hospital of Lille (Centre d'Orthogénie), France, for their kind assistance and support; M Tardivel and A Bongiovanni (BICeL core microscopy facility of the Lille University School of Medicine) for expert technical assistance. The authors acknowledge support of the Inserm Cross-Cutting Scientific Program (HuDeCA). This work was supported by the Institut National de la Santé et de la Recherche Médicale (INSERM), France [grant number U1172], by the European Research Council (ERC) under the European Union's Horizon 2020 research and innovation program (ERC-2016-CoG to P.G. grant agreement n° 725149/REPRODAMH), Agence Nationale de la Recherche (ANR), France (grant number ANR-18-CE14-0017-02 to P.G.). This study was supported by a start-up grant (DN00305) by UMMC to AKT. This work was supported by the Cukurova University scientific research project number 11364.

Description of supplemental data Supplemental data include text on subjects, methods and supplemental references.

Declaration of interests The authors declare no competing interests.

Web Resources: HGNC, https://www.genenames.org/
GenBank, https://www.ncbi.nlm.nih.gov/genbank/
TOPMed, https://bravo.sph.umich.edu/freeze5/hg38/
gnomAD Browser, https://gnomad.broadinstitute.org/
Greater Middle East Variom Project (GME), http://igm.ucsd.edu/gme/data-browser.php
InterVar http://wintervar.wglab.org/
ClinVar https://www.ncbi.nlm.nih.gov/clinvar/
Combined Annotation Dependent Depletion (CADD), https://cadd.gs.washington.edu
MutationTaster, http://www.mutationtaster.org
PolyPhen-2, http://genetics.bwh.harvard.edu/pph2/
SIFT, http://sift.bii.a-star.edu.sg/
LRT, http://www.genetics.wustl.edu/jflab/lrt_query.html

VI. References for chapter two

1.Bouilly, J. et al. DCC/NTN1 complex mutations in patients with congenital hypogonadotropic hypogonadism impair GnRH neuron development. Human Molecular Genetics 27, 359–372 (2018).

2.Cariboni, A. et al. Dysfunctional SEMA3E signaling underlies gonadotropin-releasing hormone neuron deficiency in Kallmann syndrome. J Clin Invest 125, 2413–2428 (2015).

3.Cariboni, A. et al. Defective gonadotropin-releasing hormone neuron migration in mice lacking SEMA3A signalling through NRP1 and NRP2: implications for the aetiology of hypogonadotropic hypogonadism. Human Molecular Genetics 20, 336–344 (2011).

4.Cariboni, A. et al. Neuropilins and Their Ligands Are Important in the Migration of Gonadotropin-Releasing Hormone Neurons. J. Neurosci. 27, 2387–2395 (2007).

5.Casoni, F. et al. Development of the neurons controlling fertility in humans: new insights from 3D imaging and transparent fetal brains. Development 143, 3969–3981 (2016).

6.Chartrel, N. et al. The Neuropeptide 26RFa (QRFP) and Its Role in the Regulation of Energy Homeostasis: A Mini-Review. Frontiers in Neuroscience 10, 549 (2016).

7.Day, F. R. et al. Physical and neurobehavioral determinants of reproductive onset and success. Nat Genet 48, 617–623 (2016).

8.Fueshko, S. & Wray, S. LHRH Cells Migrate on Peripherin Fibers in Embryonic Olfactory Explant Cultures: An in Vitro Model for Neurophilic Neuronal Migration. Developmental Biology 166, 331–348 (1994).

9.Giacobini, P. Shaping the Reproductive System: Role of Semaphorins in Gonadotropin-Releasing Hormone Development and Function. NEN 102, 200–215 (2015).

10.Hanchate, N. K. et al. SEMA3A, a Gene Involved in Axonal Pathfinding, Is Mutated in Patients with Kallmann Syndrome. PLOS Genetics 8, e1002896 (2012).

11.Harvey, A. Receptor complexes for each of the Class 3 Semaphorins. Frontiers in Cellular Neuroscience 6, 28 (2012).

12.Janssen, B. J. C. et al. Neuropilins lock secreted semaphorins onto plexins in a ternary signaling complex. Nat Struct Mol Biol 19, 1293–1299 (2012).

13.Kolk, S. M. et al. Semaphorin 3F Is a Bifunctional Guidance Cue for Dopaminergic Axons and Controls Their Fasciculation, Channeling, Rostral Growth, and Intracortical Targeting. J. Neurosci. 29, 12542–12557 (2009).

14.Kotan, L. D. et al. Prevalence and associated phenotypes of PLXNA1 variants in normosmic and anosmic idiopathic hypogonadotropic hypogonadism. Clinical Genetics 95, 320–324 (2019).

15.Lapatto, R. et al. Kiss1−/− Mice Exhibit More Variable Hypogonadism than Gpr54−/− Mice. Endocrinology 148, 4927–4936 (2007).

16.Malone, S. A. et al. Defective AMH signaling disrupts GnRH neuron development and function and contributes to hypogonadotropic hypogonadism. Elife 8, e47198 (2019).

17.Manfredi-Lozano, M., Roa, J. & Tena-Sempere, M. Connecting metabolism and gonadal function: Novel central neuropeptide pathways involved in the metabolic control of puberty and fertility. Frontiers in Neuroendocrinology 48, 37–49 (2018).

18.Marcos, S. et al. Defective signaling through plexin-A1 compromises the development of the peripheral olfactory system and neuroendocrine reproductive axis in mice. Human Molecular Genetics 26, 2006–2017 (2017).

19.Moore, A. M., Coolen, L. M. & Lehman, M. N. Kisspeptin/Neurokinin B/Dynorphin (KNDy) cells as integrators of diverse internal and external cues: evidence from viral-based monosynaptic tract-tracing in mice. Sci Rep 9, 14768 (2019).

20.Oleari, R. et al. A Novel SEMA3G Mutation in Two Siblings Affected by Syndromic GnRH Deficiency. NEN 111, 421–441 (2021).

21.Oleari, R. et al. PLXNA1 and PLXNA3 cooperate to pattern the nasal axons that guide gonadotropin-releasing hormone neurons. Development 146, (2019).

22.Pasterkamp, R. J. Getting neural circuits into shape with semaphorins. Nat Rev Neurosci 13, 605–618 (2012).

23.Patel, S. R. et al. Pyroglutamylated RFamide Peptide 43 Stimulates the Hypothalamic-Pituitary-Gonadal Axis via Gonadotropin-Releasing Hormone in Rats. Endocrinology 149, 4747–4754 (2008).

24.Pitteloud, N. et al. Predictors of Outcome of Long-Term GnRH Therapy in Men with Idiopathic Hypogonadotropic Hypogonadism. The Journal of Clinical Endocrinology & Metabolism 87, 4128–4136 (2002).

25.Richards, S. et al. Standards and guidelines for the interpretation of sequence variants: a joint consensus recommendation of the American College of Medical Genetics and Genomics and the Association for Molecular Pathology. Genet Med 17, 405–423 (2015).

26.Schwanzel-Fukuda, M. & Pfaff, D. W. Origin of luteinizing hormone-releasing hormone neurons. Nature 338, 161–164 (1989).

27.Seminara, S. B. et al. The GPR54 Gene as a Regulator of Puberty. New England Journal of Medicine 349, 1614–1627 (2003).

28.Sidhoum, V. F. et al. Reversal and Relapse of Hypogonadotropic Hypogonadism: Resilience and Fragility of the Reproductive Neuroendocrine System. The Journal of Clinical Endocrinology & Metabolism 99, 861–870 (2014).

29.Sykiotis, G. P. et al. Oligogenic basis of isolated gonadotropin-releasing hormone deficiency. PNAS 107, 15140–15144 (2010).

30.Takeuchi, H. et al. Sequential Arrival and Graded Secretion of Sema3F by Olfactory Neuron Axons Specify Map Topography at the Bulb. Cell 141, 1056–1067 (2010).

31.Topaloğlu, A. K. Update on the Genetics of Idiopathic Hypogonadotropic Hypogonadism. J Clin Res Pediatr Endocrinol 9, 113–122 (2017).

32.Topaloglu, A. K. et al. TAC3 and TACR3 mutations in familial hypogonadotropic hypogonadism reveal a key role for Neurokinin B in the central control of reproduction. Nat Genet 41, 354–358 (2009).

33.Topaloglu, A. K. et al. Inactivating KISS1 Mutation and Hypogonadotropic Hypogonadism. New England Journal of Medicine 366, 629–635 (2012).

34.Valverde, F., Santacana, M. & Heredia, M. Formation of an olfactory glomerulus: Morphological aspects of development and organization. Neuroscience 49, 255–275 (1992).

35.van der Klaauw, A. A. et al. Human Semaphorin 3 Variants Link Melanocortin Circuit Development and Energy Balance. Cell 176, 729-742.e18 (2019).

36.Wray, S., Grant, P. & Gainer, H. Evidence that cells expressing luteinizing hormone-releasing hormone mRNA in the mouse are derived from progenitor cells in the olfactory placode. PNAS 86, 8132–8136 (1989).

37.Yang, J. J., Caligioni, C. S., Chan, Y.-M. & Seminara, S. B. Uncovering Novel Reproductive Defects in Neurokinin B Receptor Null Mice: Closing the Gap Between Mice and Men. Endocrinology 153, 1498–1508 (2012).

38.Young, J. et al. SEMA3A deletion in a family with Kallmann syndrome validates the role of semaphorin 3A in human puberty and olfactory system development. Human Reproduction 27, 1460–1465 (2012).

39.KLB, encoding β-Klotho, is mutated in patients with congenital hypogonadotropic hypogonadism. EMBO Molecular Medicine 9, 1379–1397 (2017).

CHAPTER THREE: METHODS IN PHYSIOPATHOLOGICAL STUDIES OF THE GNRH SYSTEM - PRINCIPLES, LIMITATIONS AND DEVELOPMENTS

I. Then and now: from classical histological approaches to tissue-clearing

Working on a complex and multiplayer network, such as the one controlling the reproductive functions, poses technical difficulties. First, the GnRH network involves several key players, not all of them being located in a small well-defined region, and GnRH neurons themselves are scattered in the brain and do not form a homogeneous population; second, they exhibit hundreds-micrometres-long projections that are hard to trace from origin to endpoint; third, their peculiar birth and subsequent migration in the embryo dampens the understanding of their physiological development (all developed in the previous sections). Until recently, studies on GnRH neurons were exclusively using classical sectioning methods and histological approaches to detect and describe the GnRH neurons in several species – from fishes to birds, rodents or primates and even humans. This fact is not surprising given the lack of reliable three-dimensional approaches, the inadaptability of standard microscopes to image large tissues, and the difficulty in processing large imaging data in the previous decades. In the best cases, it was possible to perform reconstruction after serial sectioning, immunolabeling and acquisition (Berlanga et al. 2011); but this was resource demanding and still provided incomplete information because of potential loss of sections, and the absence of overlapping regions.

In recent years, a new trend developed and was adopted in numerous of fields of biology: with a combination of tissue clearing and light-sheet microscopy, it is now possible to render biological samples transparent and image them in a three-dimensional approach. While not a new technology, light-sheet imaging had been mainly applied to naturally-transparent biological samples or models in the past, before tissue clearing broadened its use in the last decade, and both will undoubtedly benefit greatly to neuroendocrinology.

II. Principles and benefits of tissue clearing

A. Tissue clearing and 3D-imaging: different techniques, a common idea

i. Light-sheet microscopy: getting the full picture

Light-sheet microscopy is a specific imaging modality in which usually one or several aligned sheet(s) of light of a few micrometres in thickness, are used to selectively illuminate a thin plane of a transparent sample, virtually slicing said sample. The (auto)fluorescence coming for the virtual slice can then be acquired through the detection pathway, usually perpendicular to the illumination pathway. Thus, moving the sample along the axis perpendicular to that of the light sheets (the Z axis) then allows sequential imaging of several tens or hundreds of planes, while moving it in the X and Y axes changes the field of view and allows for mosaic or multiposition acquisitions (Figure III-1). Because the light sheet(s) illuminate the different planes sequentially, and entire planes are acquired at once, light-sheet imaging performs faster than scanning microscopy and results in reduced photobleaching, rendering it particularly interesting for imaging large samples, and effectively enabling democratization of volume imaging (Jährling et al. 2017). Noteworthy, where epifluorescence and confocal microscopes can reach the nanometre-scale and are ideal for subcellular imaging, most current light-sheet microscopes are still limited in resolution and usually provide micrometre-scale resolution: thus, they were primarily designed for investigations at the level of cellular networks or organs, and up to organisms in naturally transparent samples. This is subject to change, however, as great progress has been made over the years in light-sheet microscopy, notably by the development of new illumination and detection strategies (Saghafi et al. 2014, Voigt et al. 2019), and since several ways of achieving optical clearing of biological samples were introduced, accompanied by a new need for fast and reliable 3D imaging with high resolution (Figure III-1).

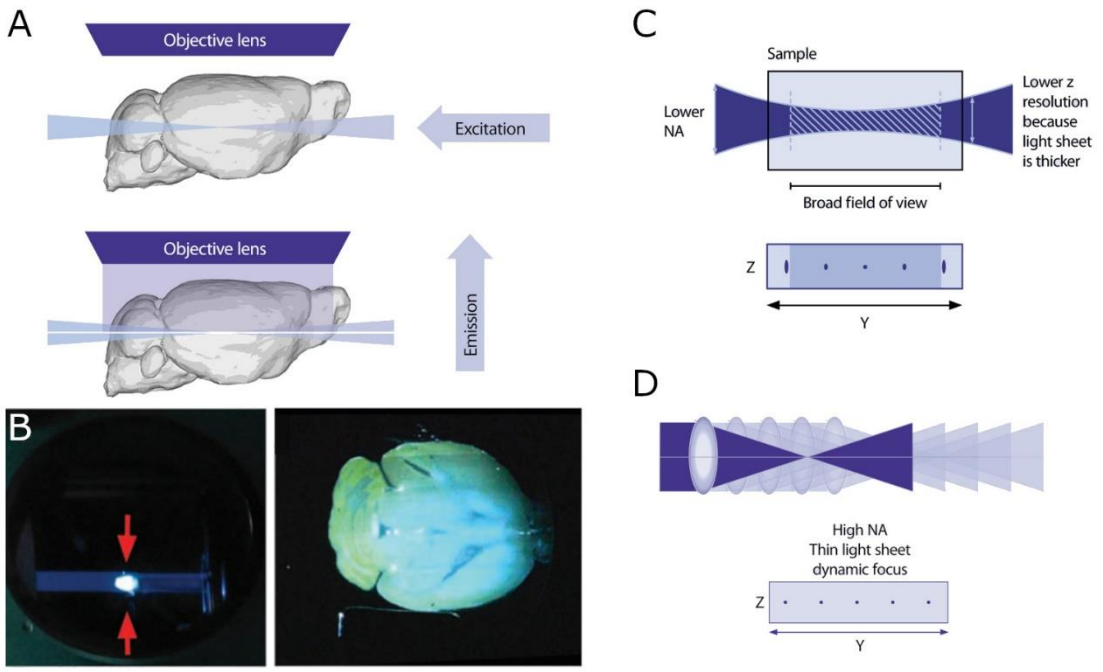

Figure III-1. Principle of light-sheet imaging applied to a large sample. ***A****: Illustration of a dual-sided laser sheet selectively illuminating a single plane of a cleared mouse brain. The resulting fluorescence from the whole plane is collected through the objective lens.* ***B****: Application of the principle described in A. Single plane illumination enables optical slicing of the sample.* ***C****: Example of limitation in the illumination strategy of a light-sheet microscope. The thickness of the laser sheet is not constant, resulting in a better axial resolution in the centre of the field of view, which degrades from the centre out along the Y axis.* ***D****: Recent optimizations in the illumination strategies compensate this issue by horizontally moving the narrowest portion of the laser sheet across the sample, thus achieving best resolution all along the Y axis. Adapted from Erturk et al. 2012, with illustrations from the Miltenyi Biotec website (www.miltenyibiotec.com)*

ii. The basics of tissue clearing

Tissue clearing is not *per se* a recent technique, as the first occurrence of biological tissue rendered transparent appeared in the beginning of the 20th century, when the German anatomist Werner Spalteholz set up a protocol using organic solvents (benzyl alcohol and methyl salicylate) to clear initially opaque biological samples (Spalteholz 1914). However, the method was labor-intensive as it required various dehydration, tissue bleaching, and clearing steps, which eventually led to clearing few millimeters of tissue after several months of preparation. This method was rapidly

forgotten because of the above-mentioned reasons and due to the lack of appropriate imaging modalities at that time. However, during the last decade, with the advent of new microscopy setups (light-sheet) Spalteholz method was rejuvenated, as new increasing interest in the scientific community emerged. Over the last decade notably, numerous protocols have been proposed and modified, each time giving birth to a new technique: while some of them have been designed to be applicable to a wide variety of tissues and uses, others are instead restricted to specific organs and applications. Going through the entire catalogue of tissue-clearing techniques would make little sense, since their applicability is highly variable and because the list is ever-growing. In the next paragraphs however, we will discuss some of the most commonly used techniques, their classification as well as pros and cons.

If tissue clearing protocols can greatly differ from one to another, their initial aim remains the same: a biological sample, through which light cannot pass because of the physical principles of absorption, diffraction and refraction, is chemically altered to alleviate or eliminate these disturbances. Absorption is the extinction of light by the sample as a function of distance/depth: in imaging of biological samples, absorption is mainly due to pigmentation stopping the photons on their way to the detection path of the microscope. Diffraction, on the other hand, is a scattering of the photons that has been strongly associated to the lipidic content of the tissue. Finally, refraction is a modification of the speed and path of the light as a result of a change in the refractive indices between two media, i.e. when passing from air to water (Ryan et al. 2017).

Tissue clearing techniques tackle these three limitations in volume imaging through 1) depigmentation or decolorization to reduce absorption of light, 2) delipidation to reduce diffraction and scattering of light and 3) equilibration of the refractive indices both inside and around the sample to reduce deviation of light. In doing so, tissue clearing renders the tissues transparent to the eye and enables light to pass through a biological sample in a more homogeneous way, thus opening new imaging possibilities on samples previously impossible to explore because of their size and opacity.

iii. An overview of tissue clearing approaches

The initial protocols for tissue clearing all used a different approach to achieve transparency, and they underwent a series of optimizations over time to maximize their compatibility with immunostaining procedures, specific types of tissues, or imaging and analysis modalities. To date, basically all clearing protocols and their adaptations can be divided in three groups (Figure III-2) based on their refractive index-matching approach: hydrophobic or solvent-based, hydrogel-based, and hydrophilic or aqueous-based tissue clearing (Ueda et al. 2020, Molbay et al. 2021).

The pioneer investigators of modern tissue clearing applied to neurosciences relied on Spalteholz's work, and proposed to overcome the limitations in ultramicroscopy by rendering biological tissue transparent through a solvent-based treatment (Dodt et al. 2007). Insects, embryos, pieces of brains or even intact brains of young mice were cleared by ethanol dehydration followed by immersion in a refractive-index matching solution comprised of benzyl alcohol and benzyl benzoate (BABB). In older animals (more than 3 weeks of age) however, the authors reported increased scattering of the light and difficulties to obtain complete clearing, which they attributed to the heavy myelinization in some regions of the brain. Overall, their work provided the template for all solvent-based tissue clearing protocols, which form the first group of tissue-clearing techniques. From there, other groups overcame the limitations of the first method by delipidating tissue before clearing: Erturk and colleagues used tetrahydrofuran (THF) to both delipidate and dehydrate tissues, and replaced BABB with dibenzyl ether (DBE) in the refractive index matching step, thus obtaining better preservation of endogenous GFP fluorescence (Erturk et al. 2012a, Erturk et al. 2012b).

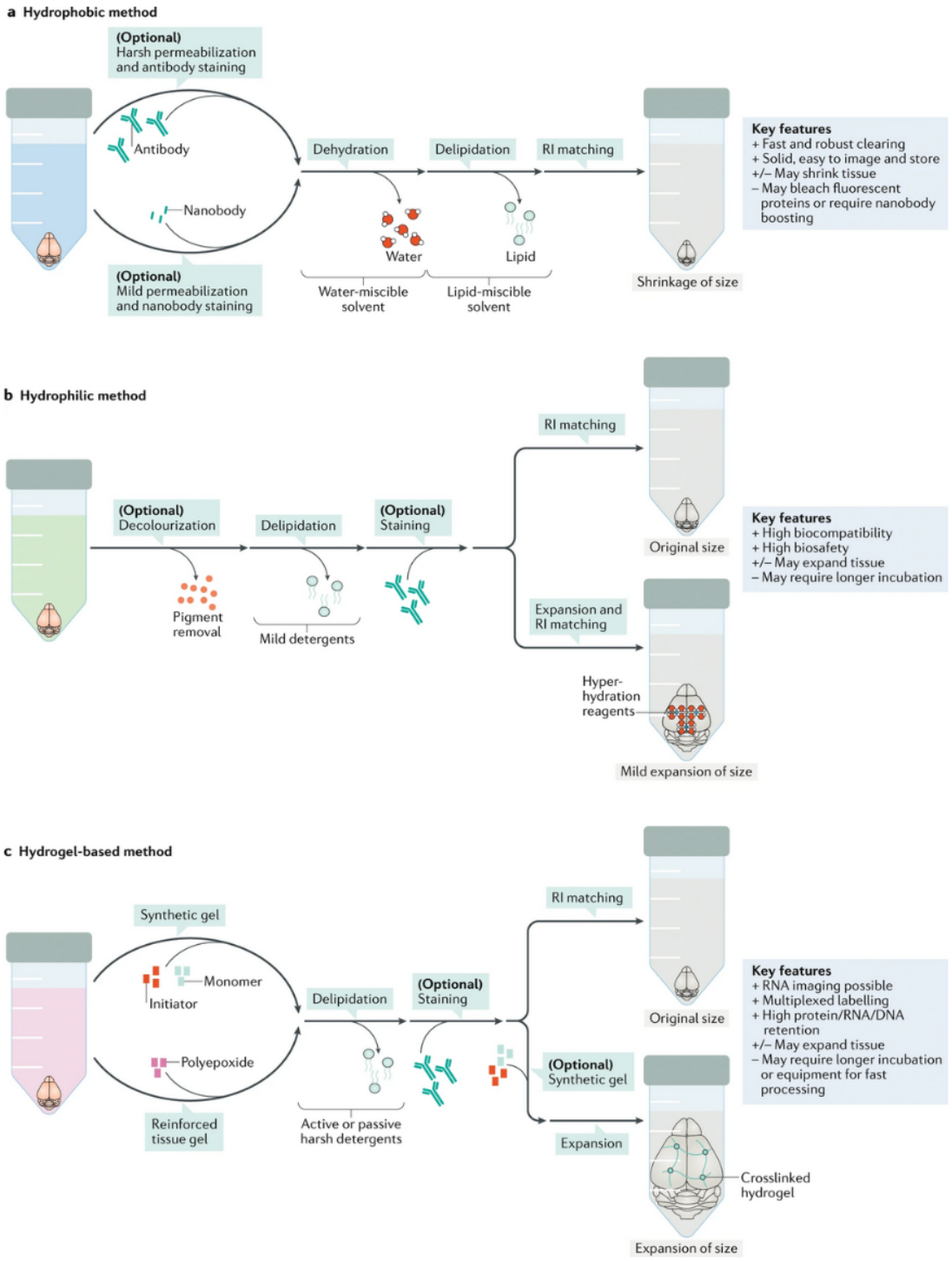

Figure III-2. Simplified workflows for the main tissue clearing techniques. *Hydrophobic (a), hydrophilic (b) and hydrogel-based (c) strategies for delipidation/decolorization, staining, and refractive-index matching are presented. Secondary effects or applications, such as tissue shrinkage or expansion are also illustrated, together with notable features for the different techniques. Taken from Ueda et al. 2020*

Their protocol, termed “3-Dimensional imaging of solvent cleared organs” (3DISCO), was later revisited by several groups to apply the technique to a broader range of tissues and fluorophores, and variants of 3DISCO quickly multiplied: uDISCO opened ways to image larger specimen up to the whole mouse (Pan et al. 2016), sDISCO introduced stabilization of media to decrease oxidization and increase fluorescence preservation (Hahn et al. 2019), FDISCO maximized compatibility with diverse fluorophores (Qi et al. 2019), while vDISCO brought perfusion-based nanobody delivery in the whole mouse body (Cai et al. 2019). Particularly, the work from Renier and colleagues has greatly facilitated the combination of *in toto* immunostaining approaches with solvent-based tissue clearing: building on 3DISCO, the group implemented a pretreatment of the samples with methanol and hydrogen peroxide to depigment and delipidate tissues, followed by immunolabeling and 3DISCO tissue-clearing. In reference to the original work form Erturk et al., they named their optimizations “immunolabeling-enabled three-dimensional imaging of solvent-cleared organs” (iDISCO, Renier et al. 2014). The main advantage of iDISCO is its compatibility with a broad range of tissues (brain, kidneys, embryos among others were successfully processed) and, because it is open to antibody labelling, the ability to transpose immunohistochemistry procedures instead of relying on transgenic models which are sometimes inaccessible or even unavailable. Soon after, the technique was further enhanced with iDISCO+ when the final dehydration step was modified by substituting THF for methanol, thus better preserving tissue morphology, and allowing program-based registration of datasets to a reference atlas and subsequent automated analysis of the signal (Renier et al. 2016). If solvent-based clearing is usually cheap, fast (transparency itself is achieved in 2-3 days) and efficient on a number of tissues, its downsides to date mostly reside in the toxicity of the chemicals used and in the damages they can cause to non-resistant materials, including microscopes and objective lenses, which can be a major obstacle to their broad adoption, as well as tissue shrinkage due to the strong dehydration.

Parallel to hydrophobic approaches, hydrophilic techniques were also developed with a similar goal to image sample at the network- or even organ-scale. These techniques involve either

substitution of water in the tissue with an aqueous-based refractive index-matching solution, or partial denaturation and hyperhydration of the sample, with or without prior delipidation and depigmentation. While the former works only for small samples, the latter has been successfully applied to larger and more heterogeneous tissues (Richardson and Litchman 2015). Among the first hydrophilic techniques was Sca*l*e, in which incubation of the sample in a solution of urea, glycerol and the detergent Triton X-100 (Sca*l*eA2) resulted in its controlled hyperhydration and tissue transparency, but required several days of weeks of clearing process (Hama et al. 2011). The initial Sca*l*eA2 solution was thus successfully used to clear mouse embryos and even whole brains, but slight expansion and increased fragility of the samples were noticed, which could then be overcome by small adaptations to the constituents of the clearing solution (Hama et al. 2011, Hama et al. 2015). The SeeDB (See Deep Brain) protocol was proposed soon after, this time relying on a gradual infusion of the tissues with a saturated fructose solution to increase and homogenize refractive indices in the sample: although the technique allowed clearing of mouse embryos and brains in just a few days, its clearing efficiency remained somewhat limited on adult and large tissues (Ke et al. 2013, Ke et al. 2016). While Sca*l*e did not tackle pigmentation issues, and SeeDB included neither delipidation or depigmentation steps, this was better addressed in another hydrophilic-based clearing protocol, "clear, unobstructed brain imaging cocktails and computational analysis" (CUBIC): by screening for chemicals similar to those of Sca*l*e, Susaki et al. (2014) developed solutions able to clear large specimens such as whole mouse and even marmoset brains, and they included delipidation with detergents and decolorization *via* heme elution by aminoalcohols. While CUBIC achieved transparency of samples faster than Sca*l*e, it sometimes induced tissue deformation and fragility. The protocol was later modified for application to different types of tissues and uses, which gave birth to optimizations for clearing of bones (Tainaka et al. 2014), fragile samples (CUBIC-f, Pinheiro et al. 2021), or to take advantage of sample expansion (CUBIC-X, Murakami et al. 2018) and whole-body perfusion (Tainaka et al. 2014). In general, hydrophilic methods appear to be particularly well-suited to small samples or thick sections, because of the usually long incubation times required to achieve transparency and their relatively low performance at clearing large organs compared to

hydrophobic methods. Their main advantage however is customizability, since the composition of the aqueous-based solutions can be modified to fine-tune refractive indices or tissue expansion, for instance (Tainaka et al. 2018).

The third class of tissue clearing techniques is that of hydrogel-based methods, which differ in their angle to achieve transparency. Here, the sample is infused with monomers that are then polymerized, thus creating a mesh inside the sample onto which the molecules of interest (proteins, fluorophores) are crosslinked. In CLARITY ("Clear Lipid-exchanged Acrylamide-hybridized Rigid Imaging/Immunostaining/In situ hybridization-compatible Tissue-hYdrogel", Chung et al. 2013), an acrylamide/bisacrylamide gel is formed in and around the tissue, and constituents of the samples (including proteins and nucleic acids) are bound to the gel by a fixative, before lipid extraction through detergent and electrophoresis. Only a hybrid structure of the hydrogel and attached sample molecules then remains, which is highly transparent, permeable to probes such as antibodies, and enables multiple rounds of labelling. However, the initial protocol required specific materials for electrophoretic delipidation, and a proprietary refractive index matching solution for imaging. Much like the hydrophilic methods mentioned above, hydrogel-based protocols have then multiplied and are now scalable to a plethora of samples like bones (BoneCLARITY, Greenbaum et al. 2017), small tissues or whole bodies (PACT/PARS, Yang et al. 2014) or applications such as *in situ* hybridization or expansion (Sylwestrak et al. 2016, Treweek et al. 2015). Noteworthy, specific devices were developed to shorten incubation and clearing times in CLARITY derivatives, but they are either not readily available, or their cost remains prohibitive (Lee et al. 2016). Additional drawbacks of hydrogel-based techniques include the long clearing times when adopting a passive immersion protocol, the partial destruction of the sample, and the toxicity of some compounds (acrylamide).

Overall, tissue clearing techniques are best considered as a set of modules that are somewhat interchangeable. Given that chemicals differ between protocols but serve a similar purpose, for example delipidation or depigmentation, one can assemble modules from the different techniques to constitute an optimal protocol based on several criteria: nature of the tissue, size of the sample,

type of staining, available equipment, or imaging modalities for instance. A modular view of clearing techniques with extended list of chemicals has recently been proposed in the context of developmental biology (Vieites-Prado and Renier 2021) and combinations of techniques have already been published (Lee et al. 2016, Cai et al. 2019, Xu et al. 2021). With the continued interest for tissue clearing, the multiplicity of protocols available (Figure III-3), and the development of newer, large-specimen compatible microscopes, investigations are now conducted at the organ and even organism scale to revolutionize neuroscience and systems biology (Susaki and Ueda 2016, Vigouroux et al. 2017, Ueda et al. 2020).

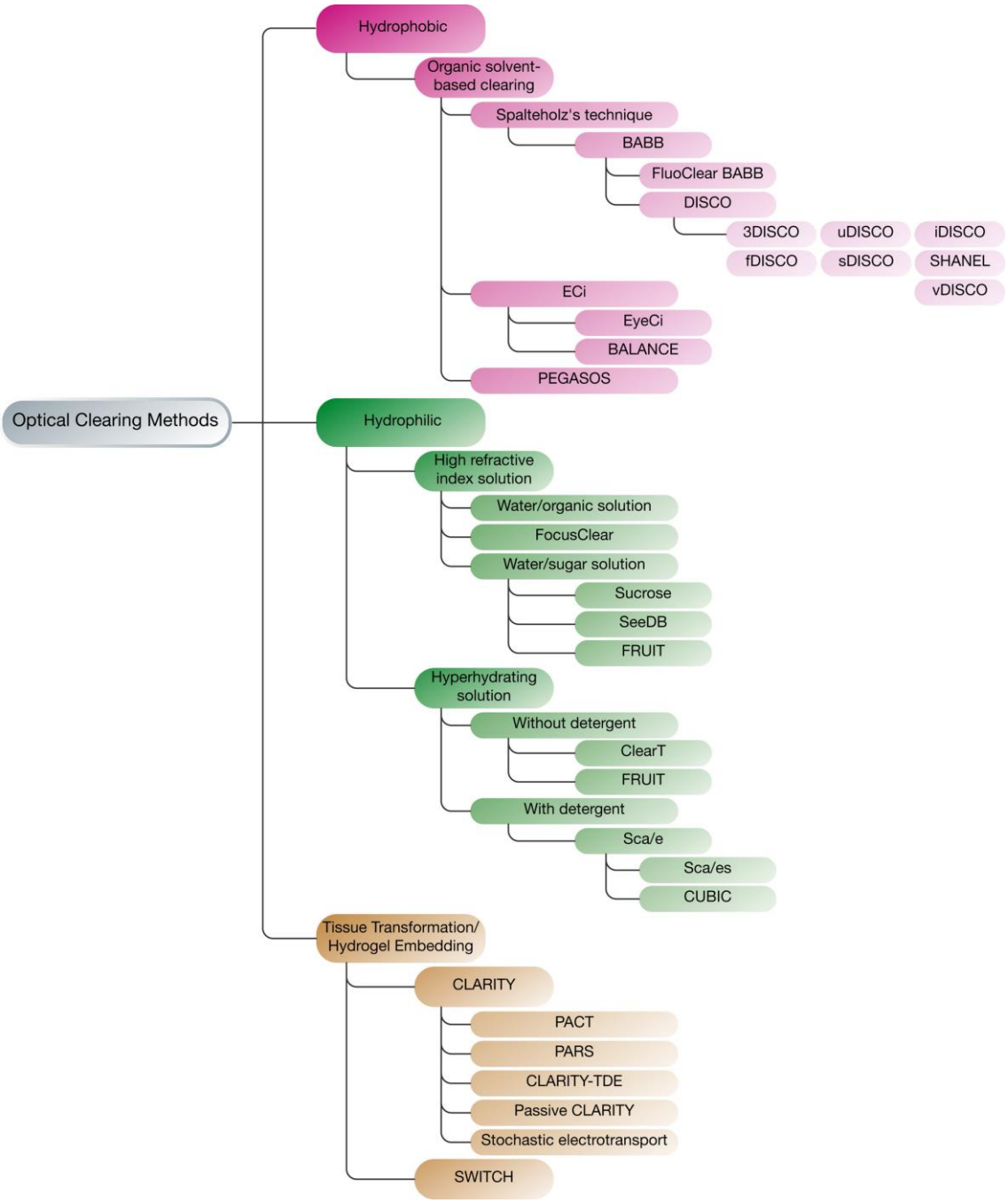

Figure III-3. An overview of tissue clearing techniques. *The schematic illustrates the great diversity of available tissue clearing protocols, and their repartition in three main groups: hydrophobic or solvent-based methods (pink) including 3DISCO and its derivatives, hydrophilic or aqueous methods (green) with notably Scale, CUBIC or SeeDB, and hydrogel-based methods (brown) such as CLARITY. Taken from Molbay et al. (2021)*

iv. Optimization and troubleshooting of solvent-based tissue-clearing protocols

Because solvent-based protocols are fast and efficient at clearing a broad range of samples, are compatible with both endogenous fluorescence and immunolabeling, and do not necessitate specific equipment, they are easy to adopt by groups interested in implementing tissue clearing. They do however possess some cons, among which we can cite the variable fluorescence preservation and the chemical toxicity. Some optimizations about the former were discussed above, such as boosting of fluorescence and stabilization of media (Cai et al. 2019, Hahn et al. 2019). When it comes to toxicity, the development of alternative ethyl cinnamate-based clearing techniques are worth mentioning: ethyl cinnamate is a non-toxic organic solvent, used in food industry, with a refractive index similar to that of dibenzyl ether (RI~1.54) and thus can be used as an alternative to its toxic counterpart (Klingberg et al. 2017, Masselink et al. 2019). Additionally, dehydration of the samples can be performed similarly to well-known and routine histological approaches, with ethanol or propanol, both of which are less toxic than methanol or tetrahydrofuran and show limited alteration of tissue morphology (Klingberg et al. 2017, Masselink et al. 2019). As a result of these recent chemical substitutions, one of the most promising protocol is probably BALANCE, which uses non-toxic ethanol dehydration and ethyl cinnamate clearing, together with tissue bleaching, to find a balance between efficient clearing and low toxicity. This protocol is however too recent to discuss its applicability to a wide range of tissues, and the lack of strong delipidation may impose some limitations and/or require adjustments to be made (Merz et al. 2019).

In summary, protocol optimizations and substitution of toxic compounds with safer alternatives enable the development of more efficient and user-friendly techniques, which will progressively become of easier access to the whole scientific community. This is even more true with the availability of new objectives calibrated for the refractive indices of solvents, and the democratization of custom-built light-sheet microscopes (Voigt et al. 2019) that offer new imaging modalities.

v. Considerations on three-dimensional imaging of cleared samples

Even if transparency of the sample, either natural or through tissue clearing, allows imaging thick and large tissues, there are still important considerations to keep in mind. First are considerations linked to the immunostaining and clearing methods: incomplete penetration of the probes, partial and insufficient clearing, fragility induced by a deterioration of integrity, or severe morphological changes during dehydration or electrophoresis steps, are among the most common problems. They can result in partial to complete loss of relevant information. In addition come the limitations of the imaging setup: those include the size of the imaging chamber, sometimes not adapted to whole organs and organisms, the resolution and working distance of the objectives which will impact the imaging depth and quality, and the illumination and acquisition strategies which greatly influence imaging speed and photobleaching of the samples.

Some of these limitations compensate for each other: shrinkage of dehydrated samples in solvent-based techniques can overcome the physical limit of the microscope pertaining to the size of the chamber or the working distance of the objective, for instance. Others add up and make it difficult to obtain valuable information, for example when poor clearing associates with suboptimal refractive index matching between the solution and the objective, resulting in aberrations. Of note, a review recapitulating limitations and potential solutions in tissue clearing and 3D imaging has recently been published (Weiss et al. 2021).

A last point to consider is the handling of data from 3D imaging: whether they come from confocal, two-photon or light-sheet microscopy, 3D acquisitions represent sequences of files of gigabytes, terabytes and even sometimes petabytes in size. In addition to the increased local storage space needed on-site, investigators thus also need powerful workstations and softwares allowing visualization and interaction of large datasets, but also network and storage infrastructures enabling sharing data with collaborators off-site, all of which come at a substantial cost. This is becoming a limiting factor as new techniques and microscopes permit deeper imaging at higher resolution, and generate an ever-growing amount of data (Molbay et al. 2021, Weiss et al. 2021).

B. Tissue clearing and the neuroendocrinology of reproduction

Interestingly, a number of tissue-clearing protocols mentioned before have been first developed specifically with the mouse brain in mind, revealing the particular interest for tissue clearing in the type of imaging analysis applied in neurosciences (Ueda et al. 2020). Considering first the mouse embryo and the mouse brain, counting and tracing of cells are among the types of analyses that benefit the most from a three-dimensional approach in neurosciences. Notably, counting in 3D provides results faster and closer to reality (although false positives and false negatives can still occur both from manual and automated detection) than estimates on sections which are generally based on partial counting and extrapolation (von Bartheld 2002, Renier et al. 2016). Tracing over long distances is rendered difficult and sometimes near-impossible from sectioning, while volume imaging associated with 3D analysis have made it straightforward, provided that the staining is of good quality (Ueda et al. 2020).

When it comes to the neuroendocrine circuits controlling reproduction, almost all studies so far have used sectioning of samples to 1) count the number of GnRH-immunoreactive neurons 2) evaluate the brain distribution of the GnRH neuronal population or 3) follow their projections over several hundreds of microns. Only very recent works have relied on a tissue-clearing approach to answer questions about the population of GnRH neurons or their partners, and already they have greatly enriched our understanding on these populations and unveiled new mechanisms in the elaboration of the central circuitry of reproduction in mice and humans.

Casoni et al. (2016) have thus uncovered a dorsal migratory pathway towards the neocortex for GnRH neurons, and demonstrated the ring-like distribution of GnRH-immunoreactive cells and fibres around the olfactory bulbs, in both mice and developing human foetuses and by using *in toto* immunolabelling and 3D-imaging. Malone et al. (2019) used this same technique in a mouse model of invalidation of gene coding for the type 2 receptor for the anti-Müllerian hormone (AMHR2), and observed that invalidation of this gene led to defective innervation of the olfactory bulb by the olfactory nerve and accumulation of GnRH neurons in the nose at E13.5, demonstrating the involvement of AMHR2 in the regulation of GnRH neuron migration.

Similarly, in Messina et al. (2020) I have used tissue clearing and light-sheet imaging when investigating mutations of the gene coding for the neuron-derived neurotrophic factor (NDNF) and their contribution to hypogonadotropic hypogonadism (for more details on this publication that I co-authored, see annexes). In a model of *Ndnf*-knockout mouse, we indeed observed perturbations of both olfactory innervation to the olfactory bulbs and GnRH neuron migration during development (Figure III-4), which with other results nicely demonstrated a role for NDNF in the development of the olfactory system and subsequent GnRH neuron migration. In another recent article of our lab (Vanacker et al. 2020), leveraging on these new imaging techniques, I documented the distribution of GnRH neurons and projections in mice exhibiting a selective deletion of neuropilin-1 in GnRH neurons. Using whole-brain immunolabeling combined with 3D-imaging, we revealed an abnormal accumulation of GnRH cells and fibres in the accessory olfactory bulb, as well as a higher number of GnRH neurons in the preoptic area and hypothalamus of mutant mice (for more details on this publication that I co-authored, see annexes). These differences were attributed to defective semaphorin 3A signalling through neuropilin-1, which increased cell survival and migration, as corroborated by functional assays on immortalized cells and nasal explants, and which resulted also in a peculiar phenotype of precocious puberty and weight gain.

Other than GnRH neurons, KNDy neurons were also studied through the use of tissue clearing and 3D imaging. Moore et al. (2018) thus applied the iDISCO protocol on dissected brains from ovariectomized rats to visualize kisspeptin- and neurokinin B-immunoreactive neurons and projections. They reported approximately 2,000 double-labelled cells (out of 2,400 kisspeptin-immunoreactive cells) located in the arcuate nucleus of rats and projecting to other hypothalamic nuclei notably, and observed an estradiol-induced decrease in kisspeptin and neurokinin B double-immunoreactivity in supplemented animals. They were also able to clear and image ovine hypothalamic blocks, revealing GnRH fibres passing through the kisspeptin neuronal population of the arcuate nucleus, on their way to the median eminence.

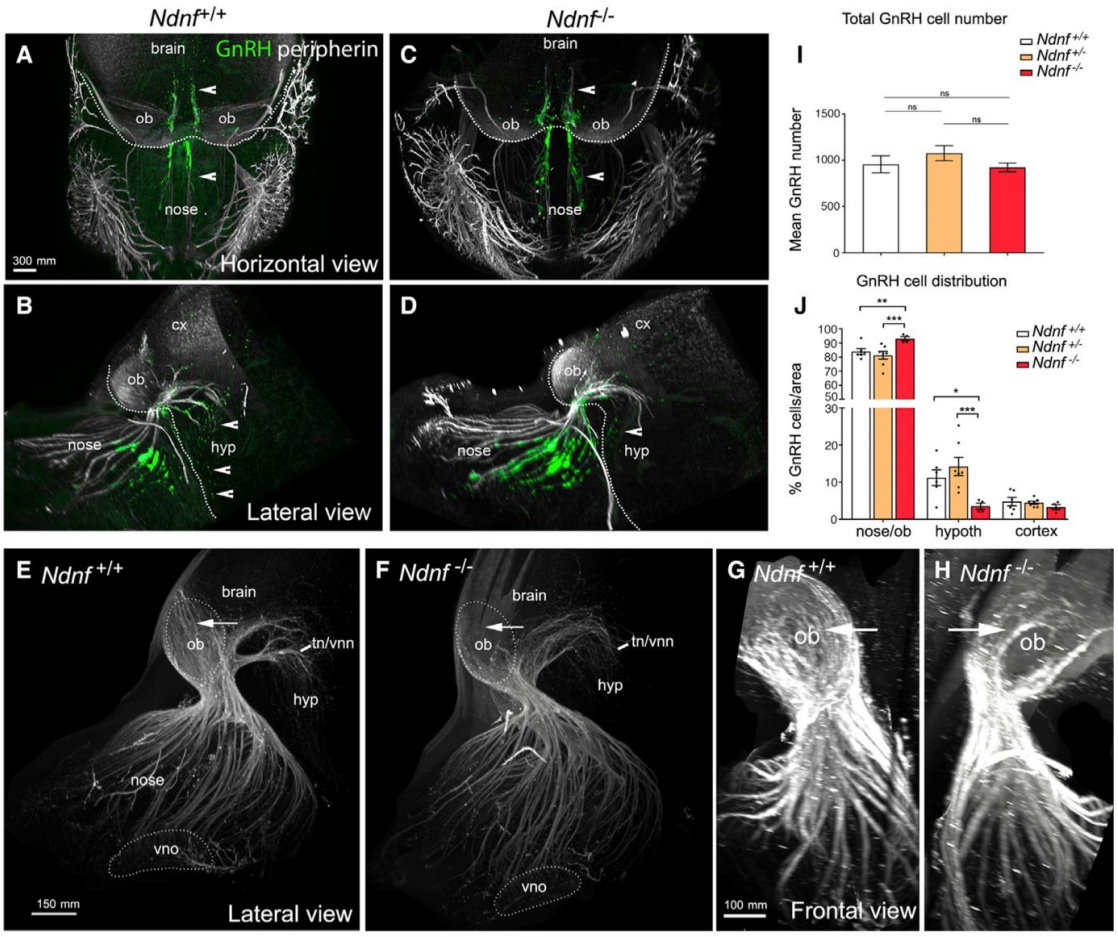

Figure III-4. Altered olfactory bulb innervation and GnRH neuron migration in a mouse model of Ndnf invalidation. *Whole-mount immunostaining and tissue clearing in Ndnf-knockout ($Ndnf^{-/-}$) and control ($Ndnf^{+/+}$) mouse embryos at E13.5 reveals an accumulation of GnRH neurons in the nasal region, with fewer cells reaching the forebrain (A-D, I-J), and a reduced innervation of the olfactory bulb by the olfactory and vomeronasal axons (E-H). Taken from Messina et al. (2020)*

These studies are, however, only the first applications of many to follow, and for sure much more information can be gathered from tissue-clearing and 3D imaging in the neuroendocrine control of reproduction, especially when they are combined with complementary approaches such as transgenic-based reporter expression, transsynaptic tracing, or automated atlas registration in mice. Additionally, and with the optimizations to tissue clearing protocols and imaging setups discussed above, application to larger animal or human samples will soon become more accessible. Given its relatively limited size, imaging of the human hypothalamus could be considered feasible in current conditions, and the ultimate goal of imaging the whole human brain

may soon be realized, maybe first through a combination of sectioning and clearing similar to that used on a rhesus macaque brain recently (Xu et al. 2021) or new combinations of permeabilizing and clearing reagents (Zhao et al. 2020).

III. References for chapter three

1.Belle, M. et al. Tridimensional Visualization and Analysis of Early Human Development. Cell 169, 161-173.e12 (2017).

2.Berlanga, M. et al. Three-Dimensional Reconstruction of Serial Mouse Brain Sections: Solution for Flattening High-Resolution Large-Scale Mosaics. Frontiers in Neuroanatomy 5, 17 (2011).

3.Cai, R. et al. Panoptic imaging of transparent mice reveals whole-body neuronal projections and skull-meninges connections. Nat Neurosci 22, 317–327 (2019).

4.Casoni, F. et al. Development of the neurons controlling fertility in humans: new insights from 3D imaging and transparent fetal brains. Development 143, 3969–3981 (2016).

5.Chung, K. et al. Structural and molecular interrogation of intact biological systems. Nature 497, 332–337 (2013).

6.Dodt, H.-U. et al. Ultramicroscopy: three-dimensional visualization of neuronal networks in the whole mouse brain. Nat Methods 4, 331–336 (2007).

7.Ertürk, A. et al. Three-dimensional imaging of solvent-cleared organs using 3DISCO. Nat Protoc 7, 1983–1995 (2012).

8.Ertürk, A. et al. Three-dimensional imaging of the unsectioned adult spinal cord to assess axon regeneration and glial responses after injury. Nat Med 18, 166–171 (2012).

9.Greenbaum, A. et al. Bone CLARITY: Clearing, imaging, and computational analysis of osteoprogenitors within intact bone marrow. Science Translational Medicine 9, eaah6518 (2017).

10.Hahn, C. et al. High-resolution imaging of fluorescent whole mouse brains using stabilised organic media (sDISCO). J Biophotonics 12, e201800368 (2019).

11.Hama, H. et al. ScaleS: an optical clearing palette for biological imaging. Nat Neurosci 18, 1518–1529 (2015).

12.Hama, H. et al. Scale: a chemical approach for fluorescence imaging and reconstruction of transparent mouse brain. Nat Neurosci 14, 1481–1488 (2011).

13.Inoue, M., Saito, R., Kakita, A. & Tainaka, K. Rapid chemical clearing of white matter in the post-mortem human brain by 1,2-hexanediol delipidation. Bioorg Med Chem Lett 29, 1886–1890 (2019).

14.Jährling, N., Becker, K., Saghafi, S. & Dodt, H.-U. Light-Sheet Fluorescence Microscopy: Chemical Clearing and Labeling Protocols for Ultramicroscopy. Methods Mol Biol 1563, 33–49 (2017).

15.Ke, M.-T., Fujimoto, S. & Imai, T. SeeDB: a simple and morphology-preserving optical clearing agent for neuronal circuit reconstruction. Nat Neurosci 16, 1154–1161 (2013).

16.Ke, M.-T. et al. Super-Resolution Mapping of Neuronal Circuitry With an Index-Optimized Clearing Agent. Cell Reports 14, 2718–2732 (2016).

17.Klingberg, A. et al. Fully Automated Evaluation of Total Glomerular Number and Capillary Tuft Size in Nephritic Kidneys Using Lightsheet Microscopy. J Am Soc Nephrol 28, 452–459 (2017).

18.Lee, E. et al. ACT-PRESTO: Rapid and consistent tissue clearing and labeling method for 3-dimensional (3D) imaging. Sci Rep 6, 18631 (2016).

19.Malone, S. A. et al. Defective AMH signaling disrupts GnRH neuron development and function and contributes to hypogonadotropic hypogonadism. Elife 8, e47198 (2019).

20.Masselink, W. et al. Broad applicability of a streamlined ethyl cinnamate-based clearing procedure. Development 146, dev166884 (2019).

21.Merz, S. F. et al. Contemporaneous 3D characterization of acute and chronic myocardial I/R injury and response. Nat Commun 10, 2312 (2019).

22.Messina, A. et al. Neuron-Derived Neurotrophic Factor Is Mutated in Congenital Hypogonadotropic Hypogonadism. Am J Hum Genet 106, 58–70 (2020).

23.Molbay, M., Kolabas, Z. I., Todorov, M. I., Ohn, T. & Ertürk, A. A guidebook for DISCO tissue clearing. Mol Syst Biol 17, e9807 (2021).

24.Moore, A. M., Lucas, K. A., Goodman, R. L., Coolen, L. M. & Lehman, M. N. Three-dimensional imaging of KNDy neurons in the mammalian brain using optical tissue clearing and multiple-label immunocytochemistry. Sci Rep 8, 2242 (2018).

25.Murakami, T. C. et al. A three-dimensional single-cell-resolution whole-brain atlas using CUBIC-X expansion microscopy and tissue clearing. Nat Neurosci 21, 625–637 (2018).

26.Pan, C. et al. Shrinkage-mediated imaging of entire organs and organisms using uDISCO. Nat Methods 13, 859–867 (2016).

27.Pinheiro, T. et al. CUBIC-f: An optimized clearing method for cell tracing and evaluation of neurite density in the salamander brain. Journal of Neuroscience Methods 348, 109002 (2021).

28.Qi, Y. et al. FDISCO: Advanced solvent-based clearing method for imaging whole organs. Sci Adv 5, eaau8355 (2019).

29.Renier, N. et al. Mapping of Brain Activity by Automated Volume Analysis of Immediate Early Genes. Cell 165, 1789–1802 (2016).

30.Renier, N. et al. iDISCO: a simple, rapid method to immunolabel large tissue samples for volume imaging. Cell 159, 896–910 (2014).

31.Richardson, D. S. & Lichtman, J. W. Clarifying Tissue Clearing. Cell 162, 246–257 (2015).

32.Ryan, J., Gerhold, A. R., Boudreau, V., Smith, L. & Maddox, P. S. Introduction to Modern Methods in Light Microscopy. Methods Mol Biol 1563, 1–15 (2017).

33.Saghafi, S., Becker, K., Hahn, C. & Dodt, H.-U. 3D-ultramicroscopy utilizing aspheric optics. J Biophotonics 7, 117–125 (2014).

34.Spalteholz, W. Über das Durchsichtigmachen von menschlichen und tierischen Präparaten und seine theoretischen Bedingungen, nebst Anhang: Über Knochenfärbung. (S. Hirzel, 1914).

35.Susaki, E. A. et al. Whole-Brain Imaging with Single-Cell Resolution Using Chemical Cocktails and Computational Analysis. Cell 157, 726–739 (2014).

36.Susaki, E. A. & Ueda, H. R. Whole-body and Whole-Organ Clearing and Imaging Techniques with Single-Cell Resolution: Toward Organism-Level Systems Biology in Mammals. Cell Chemical Biology 23, 137–157 (2016).

37.Sylwestrak, E. L., Rajasethupathy, P., Wright, M. A., Jaffe, A. & Deisseroth, K. Multiplexed Intact-Tissue Transcriptional Analysis at Cellular Resolution. Cell 164, 792–804 (2016).

38.Tainaka, K. et al. Whole-Body Imaging with Single-Cell Resolution by Tissue Decolorization. Cell 159, 911–924 (2014).

39.Tainaka, K. et al. Chemical Landscape for Tissue Clearing Based on Hydrophilic Reagents. Cell Rep 24, 2196-2210.e9 (2018).

40.Treweek, J. B. et al. Whole-body tissue stabilization and selective extractions via tissue-hydrogel hybrids for high-resolution intact circuit mapping and phenotyping. Nat Protoc 10, 1860–1896 (2015).

41.Ueda, H. R. et al. Tissue clearing and its applications in neuroscience. Nat Rev Neurosci 21, 61–79 (2020).

42.Vanacker, C. et al. Neuropilin-1 expression in GnRH neurons regulates prepubertal weight gain and sexual attraction. EMBO J 39, e104633 (2020).

43.Vieites-Prado, A. & Renier, N. Tissue clearing and 3D imaging in developmental biology. Development 148, dev199369 (2021).

44.Vigouroux, R. J., Belle, M. & Chédotal, A. Neuroscience in the third dimension: shedding new light on the brain with tissue clearing. Molecular Brain 10, 33 (2017).

45.Voigt, F. F. et al. The mesoSPIM initiative: open-source light-sheet microscopes for imaging cleared tissue. Nat Methods 16, 1105–1108 (2019).

46.von Bartheld, C. Counting particles in tissue sections: choices of methods and importance of calibration to minimize biases. Histol Histopathol 17, 639–648 (2002).

47.Weiss, K. R., Voigt, F. F., Shepherd, D. P. & Huisken, J. Tutorial: practical considerations for tissue clearing and imaging. Nat Protoc 16, 2732–2748 (2021).

48.Xu, F. et al. High-throughput mapping of a whole rhesus monkey brain at micrometer resolution. Nat Biotechnol 1–8 (2021) doi:10.1038/s41587-021-00986-5.

49.Yang, B. et al. Single-Cell Phenotyping within Transparent Intact Tissue through Whole-Body Clearing. Cell 158, 945–958 (2014).

50.Zhao, S. et al. Cellular and Molecular Probing of Intact Human Organs. Cell 180, 796-812.e19 (2020).

51.Benefits of light sheet microscopy | Light sheet microscopy | MACS Imaging and Microscopy | Products | Miltenyi Biotec | Österreich. https://www.miltenyibiotec.com/AT-en/products/macs-imaging-and-microscopy/light-sheet-microscopy/benefits-of-light-sheet-microscopy.html.

CHAPTER FOUR: MAKING THINGS CLEAR - A THREE-DIMENSIONAL ANALYSIS OF THE GNRH SYSTEM IN MICE

The content of this chapter recapitulates a research article currently in preparation

MAKING THINGS CLEAR - A THREE-DIMENSIONAL ANALYSIS OF THE GNRH SYSTEM IN MICE

Gaëtan Ternier[1], Samuel A. Malone[1], Laurine Decoster[1], Mauro B. Silva[1], Erik Hrabovszky[3], Ulrich Boehm[4], Paolo Giacobini[1,2]

[1]Univ. Lille, Inserm, CHU Lille, U1172 – LilNCog – Lille Neurosciences & Cognition, Laboratory of Development and Plasticity of the Neuroendocrine Brain, F-59000 Lille, France

[2]FHU 1,000 Days for Health, University of Lille, School of Medicine, F-59000 Lille, France

[3]Laboratory of Reproductive Neurobiology, Institute of Experimental Medicine, Budapest, Hungary

[4]Department of Pharmacology and Toxicology, University of Saarland School of Medicine, 66421 Homburg, Germany

I. Introduction

In mammals, the reproductive function is controlled by the hypothalamus-pituitary-gonadal (HPG) axis: at the hypothalamic level, a network of gonadotropin releasing hormone (GnRH) neurons integrates several biological cues to release GnRH in the hypothalamus-pituitary portal circulation at the level of the median eminence (ME), and GnRH in turn stimulates the release of the gonadotropins luteinizing hormone (LH) and follicle-stimulating hormone (FSH) from the gonadotropic cells of the pituitary. LH and FSH act in the periphery to promote steroidogenesis and gametogenesis in the gonads, and sexual steroids close the loop by exerting a feedback on the central components of the HPG axis. In this context, GnRH neurons are often described as the master regulators of reproduction. These neurons are very particular in their origin, as they are born during embryonic development in the olfactory placodes, a region of the nasal compartment which gives rise to the peripheral olfactory structures. GnRH neurons then migrate from the nose to the brain along intertwined sensory projections constitutive of the olfactory, vomeronasal and terminal nerves (ON/VNN/TN) (Wray et al. 1989, Schwanzel-Fukuda and Pfaff 1989). After crossing the cribriform plate, GnRH neurons mainly engage ventrally into the brain along branches of the TN to reach and settle in the hypothalamus where they establish interactions with neighbouring populations and send projections to the ME.

The current dogma relies on a multitude of observations performed in several mammalian species (all using immunohistochemistry or *in situ* hybridization realized on tissue sections) suggesting that GnRH neurons complete their migration before birth. Apart from a neonatal/perinatal activation, the GnRH system remains quiescent until puberty onset. Consistent with the particular journey of GnRH neurons during development and their fundamental role in the control of reproductive functions, numerous defects in the birth, migration or physiology of GnRH neurons have been described and associated to reproductive pathologies such as delayed puberty, hypogonadotropic hypogonadism (HH) or Kallmann Syndrome (KS) (Boehm et al. 2015). However, mutations identified so far in the etiology of these pathologies only accounts for a fraction of reported cases (Boehm et al. 2015), and more investigation is required to understand the processes at play in the development and physiology of the GnRH neuronal population. Additionally, both neuronal and non-neuronal interactors have emerged over the years as potent regulators of GnRH neurons – the GnRH network (Herbison 2016) – and while several groups set out to dissect the mechanisms through which they forward physiological cues to fine-tune GnRH release, these complex relationships still need to be further explored.

Because GnRH neurons are scattered in the brain, exhibit long projections and are part of an integrative network involving a multitude of partners over several brain regions (Herbison 2016), the conventional immunohistochemical approaches in 2D used so far to study their distribution and anatomical relationships with other populations resulted in a detrimental loss of information and a partial understanding of the network. Thus, adoption of new volumetric investigations to more precisely document these aspects are long overdue to complete our understanding of the development of the GnRH network.

Histology has been a golden tool for biological research for decades. Nevertheless, whole organ histology is extremely time and resource consuming and most of the time impossible due to the distortions and lack of algorithms to correctly align thousands of sections (Berlanga et al. 2011).

Light-sheet-based microscopy is an important, innovative tool that offers nondestructive optical sectioning of selectively stained thick tissues at a spatial resolution between that of micro MRI

and confocal microscopy and high-speed scanning capability (Reynaud et al. 2008, Ueda et al. 2020). Recently developed tissue clearing methods coupled with light-sheet microscopy made it possible to explore intact organs and to accurately acquire complete histological information about labeled cells/molecules in large tissues, including their spatial density and distribution (Ueda et al. 2020).

Among those techniques, the process called 3D imaging of solvent-cleared organs (3DISCO), and its immunolabeling-enabled derivative iDISCO, have been proved to be simple and inexpensive methods for 3D analysis of immunolabelled transparent organs in embryonic and postnatal animals (Erturk et al. 2012, Renier et al. 2014, Renier et al. 2016, Belle et al. 2017). Notably, recent works from our team combining whole-mount immunolabeling and tissue clearing in mice and on human samples, started to shed light on the development of the GnRH system in both species (Casoni et al. 2016).

Here, capitalizing on 3DISCO/iDISCO methods with modern three-dimensional imaging methods and on novel approaches that we developed to improve multiplex immunolabeling and imaging through the bones, we set out to thoroughly document the prenatal and postnatal development of the GnRH system in mice. We provide novel robust evidences about the nature of the scaffold used by GnRH neurons during their migratory process and we shed light on intriguing extra-hypothalamic and extra-cerebral populations of GnRH-expressing cells.

Our work offers a new perspective on the investigation of GnRH neurons and its cellular interactors in the mammalian brain, and opens a novel route for high-resolution studies of brain architecture in mammals in physiological and pathological conditions.

II. Methods

Animals

Animal studies were approved by the Institutional Ethics Committee for the Care and Use of Experimental Animals of the University of Lille 2 (France). All experiments were performed in accordance with the guidelines for animal use specified by the European Union Council Directive of September 22, 2010 (2010/63/EU) and with the guidelines established by the animal welfare committee of the University of Hamburg and the University of Saarland. Wild-type (C57/BL6J) and transgenic mice were kept in a regular light/day cycle with food and water *ad libitum*. Kisspeptin-IRES-Cre (KissIC; Mayer et al., 2010), GPR54-IRES-Cre (GPIC; Mayer and Boehm, 2011), R26-CAGS-τGFP (eR26-τGFP; Wen et al., 2011) and TH-GFP (Sawamoto et al. 2001, Matsushita et al. 2002) mice were described previously.

Whole-mount immunolabeling and tissue clearing

Mouse embryos at several embryonic stages were immersed in fixative (PFA 4% in PBS) for 1 night at 4°C. For whole-head processing at early postnatal stages, mice were anaesthetized and the whole head was collected in fixative and immersion-fixed for 24-96h depending on the age. Adult mice were perfused with ice-cold fixative, and the brain or head was post-fixed for 4 or 24 hours respectively. All samples were rinsed after fixation and kept in PBS at 4°C until further processing. Before iDISCO+ processing, postnatal and adult mouse heads were decalcified by immersion in 20% EDTA for 3 and 6 days respectively.

Samples were processed using an adapted version of the iDISCO+ protocol described previously (Belle et al. 2017). Briefly, samples were dehydrated with methanol, bleached with 5% H2O2, delipidated in a solution of 66% dichloromethane / 33% methanol, and rehydrated to PBS. They were then permeabilized and blocked in incubation solution (PBS, 0.2% gelatin, 0.5-1% Triton X100, 0.05% sodium azide) for 2 – 4 days. Samples were incubated with primary antibodies in incubation solution for 5-14 days, rinsed several times in incubation solution, and incubated further with secondary antibodies for 3 – 7 days. Samples were rinsed again several times in PBS

with 1% Triton X-100 to wash out the secondary antibodies. They were dehydrated in a gradient of methanol, then incubated overnight in 66% dichloromethane / 33% methanol, before a final wash for 1h in 100% dichloromethane. Finally, the samples were cleared by immersion in dibenzylether for at least 2 hours in rotation. After transparency was achieved, a fresh solution of dibenzylether was used for storage, and the samples were kept protected from light at room temperature until imaging.

Reprocessing of cleared samples for cryosectioning

Dibenzyl ether was removed from the samples by two washes in methanol (90 minutes each), before rehydration in a decreasing gradient of methanol/PBS. The samples were further rinsed in PBS and cryoprotected in sucrose 30% overnight. After embedding in Tissue-Tek® O.C.T. Compound, the samples were frozen in isopentane over dry ice. The blocks were kept at -80°C until cryosectioning on a Leica CM3050S cryostat, and free-floating serial sections of 30 µm were collected in PBS and kept at 4°C until further processing.

Immunolabeling of mouse brain sections

Sections were blocked in an incubation solution of Tris-buffered saline (TBS 0.05M, pH 7.6), 0.25% bovine serum albumin (BSA; Sigma, A9418), 0.3% Triton X-100 (TBS-T; Sigma, T8787) with 10% normal donkey serum (NDS; D9663; Sigma) for 2h at room temperature before incubation with the primary antibodies over 1-2 nights. After TBS rinses, the sections were further incubated with secondary antibodies for 2h, then rinsed in TBS several times. Finally, nuclear staining was performed (DAPI, 1:5000 in TBS; D1306; Fisher). The sections were coverslipped with a homemade mowiol mounting medium, and allowed to dry overnight before imaging.

Light-sheet and confocal imaging

Imaging of cleared tissues was performed in dibenzylether on the Ultramicroscope 1 (Lavision BioTec, available at the BioImaging Center of Lille) and using several objectives and magnifications: LVMI-Fluor 4x/0.3 objective with optional 2x zoom, MI PLAN 12x/0.53 with optional 2x zoom, Olympus MVPLAPO 2x/0.5 with optional 0.63-6.3x zoom. Sequences were

acquired with ImspectorPro Software. The following parameters were used: z-step was set to 2-4 µm, laser width and numerical aperture were kept to the maximum, and for mosaic acquisitions a 10% overlap between tiles was configured.

For confocal observation, an inverted laser scanning Axio observer microscope (LSM 710, Zeiss) with a 63x/1.4 numerical aperture oil-immersion objective (Zeiss) was used (Bioimaging Center of Lille, France). Images were acquired with the Zen software.

Image processing and 3D analysis

Tiff sequences resulting from light-sheet acquisitions were converted to the Imaris file format using Imaris FileConverter, and tiles were stitched using the Imaris Stitcher.

Finally, Imaris 9.1-9.5 (Bitplane) was used for visualization and 3D processing of the datasets. When necessary, manual segmentation of the signal was performed to highlight the structures of interest. Figures were prepared in Photoshop (Adobe) and GIMP (https://www.gimp.org) and videos were edited with Shotcut (https://shotcut.org/).

Antibodies, reagents and chemicals

Antibody	**Reference**	**Dilution**
Rat anti-GnRH	Gift from Erik Hrabovszky	1:10000
Rabbit anti-Peripherin	AB1530 (Millipore)	1:1000
Chicken anti-Peripherin	ab106276 (Abcam)	1:500
Rabbit anti-GFP	A6455 (Thermofisher)	1:5000 – 1:10000
Chicken anti-GFP	GFP-1020 (Aves)	1:1000 – 1:5000
Triton X100	X100-500ml	Sigma
Sodium Azide	S2002	Sigma
Gelatin	24350	VWR
Methanol	20847	VWR
Dichloromethane	270997	Sigma
Dibenzyl Ether	108014	Sigma
Hydrogen Peroxide 30%	216763	Sigma
EDTA	E5134	Sigma

III. Results

Whole-mount immunostaining and tissue clearing allow visualization of the developing GnRH system in mice

The GnRH neurons are a peculiar neuronal population as, unlike the majority of neuronal cell types, these cells originate in the nasal region before they migrate towards the brain during embryonic development (Wray et al. 1989, Schwanzel-Fukuda et al. 1989). Here, we used an adaptation of the iDISCO+ protocol (Renier et al. 2016) to clear and image mouse embryos at several stages of development (Figure IV-1). Consistent with the literature, GnRH immunoreactivity is first detected in the region of the olfactory placodes (OP), on each side of the medial septum at the 11th embryonic day (E11.5) (Figure IV-1, B). No GnRH neurons are observed at this stage in the upper part of the nasal compartment, at the nose/forebrain junction, or in the brain. As previously reported, staining for peripherin, a marker of the peripheral nervous system (Escurat et al. 1990), also labels the vomeronasal/olfactory axonal scaffold used by GnRH neurons during their migratory process (Fueshko and Wray 1994), extending from the vomeronasal and olfactory epithelia to the presumptive olfactory bulb (OB) area. Twenty-four hours later, at E12.5, the migrating GnRH-immunoreactive population is far more dispersed and forms a continuum throughout the nose, with some cells already reaching the nose/forebrain junction and crossing the cribriform plate (Figure IV-1, C). At this stage, the peripherin-positive olfactory scaffold appears more ramified, reflecting the progressive development of the system, and a higher density of fibres reveals the territory of the OB. Invasion of the brain by GnRH neurons is evident at E14.5, and as reported before (Wray et al. 1989, Schwanzel-Fukuda et al. 1989), roughly half of the population appears to have crossed the nose/forebrain junction at this stage (Figure IV-1, D). Interestingly and in contrast to the nasal compartment, fewer GnRH neurons clusters are seen in the brain as they are starting to scatter. Finally, at E16.5, GnRH neurons of the brain are already adopting their classically reported distribution in the septal and hypothalamic areas, and immunoreactivity is detected as a pseudo-continuum reaching from the olfactory bulbs to the posterior hypothalamus (Figure IV-1, E). Notably, enough GnRH

immunoreactivity is detected in the median eminence to allow visualization of the circumventricular organ at this age (Figure IV-1, E). In the nose, a large portion of the GnRH-immunoreactive population is still associated to the migratory scaffold, while fewer neurons are observed at the nose/forebrain junction. Of note, and in addition to the developing olfactory system, peripherin staining also allowed visualization of the trigeminal ganglion (TGG) and the progressive innervation of their target territories by the branches of the trigeminal nerves. Peripherin staining densifies gradually over time, with little immunoreactivity detected at E11.5, to become highly ramified with immunoreactivity detected in all superficial areas of the skull, as well as a strong staining for the nerves of the nose and in the spinal cord at E16.5 (Figure IV-1).

Figure IV-1. iDISCO-based immunostaining and clearing of mouse embryos at different stages allows whole-mount imaging and 3D visualization of the developing GnRH network. ***A***. *Mouse embryos underwent iDISCO+ treatment consisting in depigmentation, delipidation, immunostaining and solvent-based tissue clearing. Light-sheet microscopy (LSM) enables rapid imaging of the entire cleared samples.* ***B-E***. *Whole-mount immunostainings for GnRH (green) and Peripherin (white) show both the ontology and migration of the GnRH cells, and the progressive innervation of the head in mouse during the embryonic development. GnRH neurons are restricted to the olfactory placodes at E11.5 (B), and seen crossing the cribriform plate at E12.5 (C). At E14.5, GnRH neurons are seen engaging in the brain, ventrally towards the hypothalamus (D). Frontal reprojections show the GnRH neurons traveling along the peripherin-positive nerves of the vomeronasal/olfactory system in the medial nasal region. At E16.5, GnRH neurons have progressed into the brain, and projections to the median eminence are already evident (E). Scale bars: 100µm (B), 200µm (C, D), 500µm (E); Fb: forebrain; IHC: immunohistochemistry; on: olfactory nerve; op: olfactory placode; tn: terminal nerve; vnn: vomeronasal nerve; TGG: trigeminal ganglion; v1/v2/v3: branches of the trigeminal nerve*

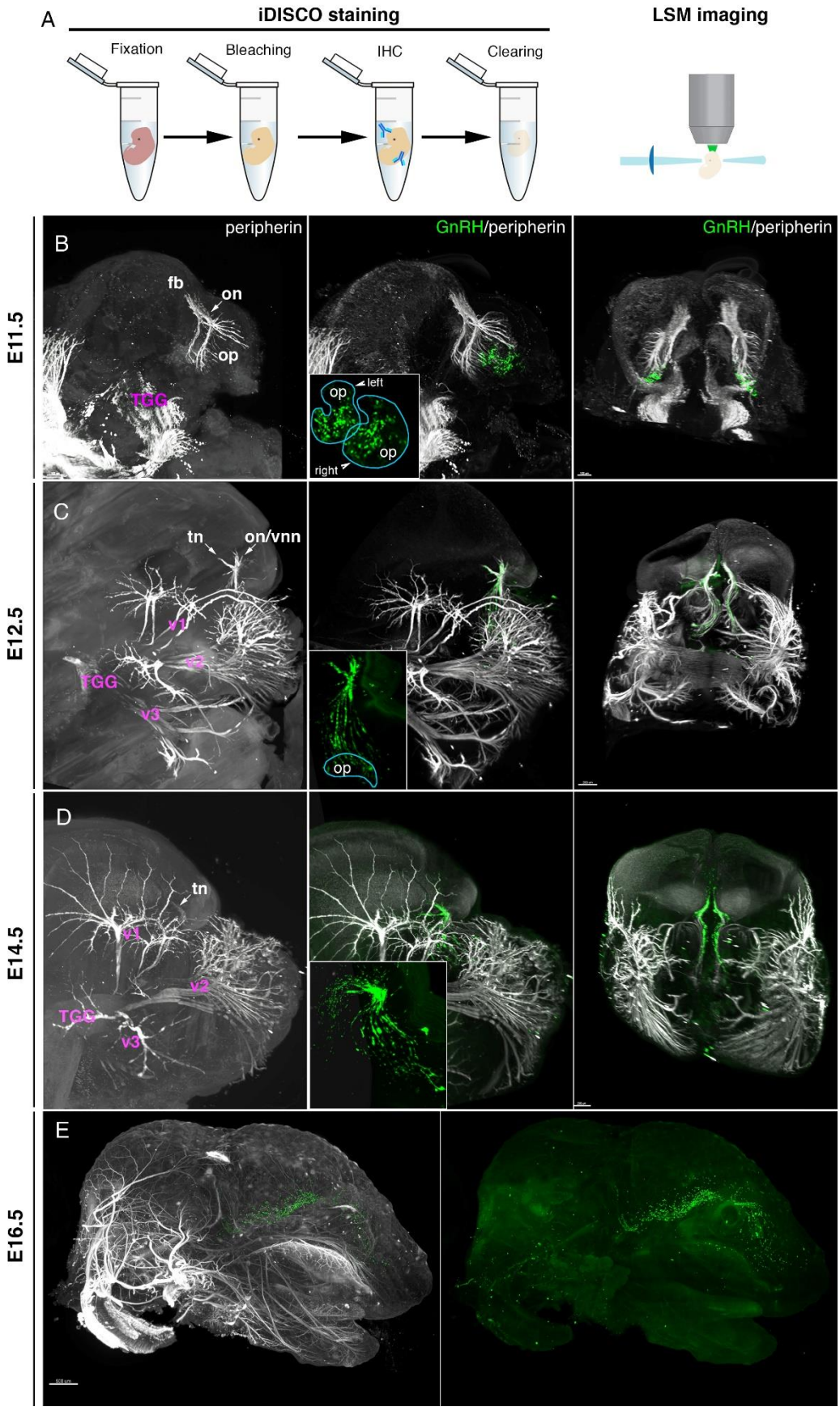
A
iDISCO staining
LSM imaging
Fixation
Bleaching
IHC
Clearing
E11.5
E12.5
E14.5
E16.5
B
peripherin
GnRH/peripherin
GnRH/peripherin
fb
on
op
TGG
left
op
op
right
C
tn
on/vnn
v1
v2
TGG
v3
op
D
tn
v1
v2
TGG
v3
E

3D-rendering and segmentation provide novel ways to study the GnRH neuron migration

Defasciculation of ON/VNN/TN, abnormal innervation of the accessory olfactory bulb (AOB), and decreased or absent migration of GnRH neurons in the brain are among the common features found in hypogonadotropic hypogonadism (HH) and Kallmann Syndrome (KS) but their severity can vary (Matsumoto et al. 2006, Cariboni et al. 2010, Messina et al. 2011, Parkash et al. 2012, Hanchate et al. 2012, Messina and Giacobini 2013, Forni and Wray 2015, Messina et al. 2020). Moreover, given the intermingled relationship of olfactory, vomeronasal, terminal nerve axons within the developing nose, and the lack of exclusive markers for each of these components, it has been near impossible so far to assess with precision the nature of the axonal scaffold used by GnRH neurons during their migratory process. In order to overcome these limitations, we took advantage of an image segmentation approach, which is the process of partitioning a digital image into multiple segments, and applied this technique to the entire stack of images obtained at the light-sheet microscope after whole-head peripherin/GnRH immunolabeling and tissue-clearing. Figure IV-2, C shows a frontal view of an E14.5 head immunostained for peripherin (white) and the results of the segmentation process which, from a single marker (peripherin) allows to precisely distinguish the vomeronasal/terminal axons (red), the trigeminal nerve (light blue) and the olfactory axons (white).

The current dogma of GnRH neuronal migration is that it involves both the olfactory and the vomeronasal axons, which form a mixed scaffold. However, our data now clearly show that GnRH neurons are only associated with VNN/TN, and not olfactory axons, on their journey towards and within the brain (Figure IV-2, C).

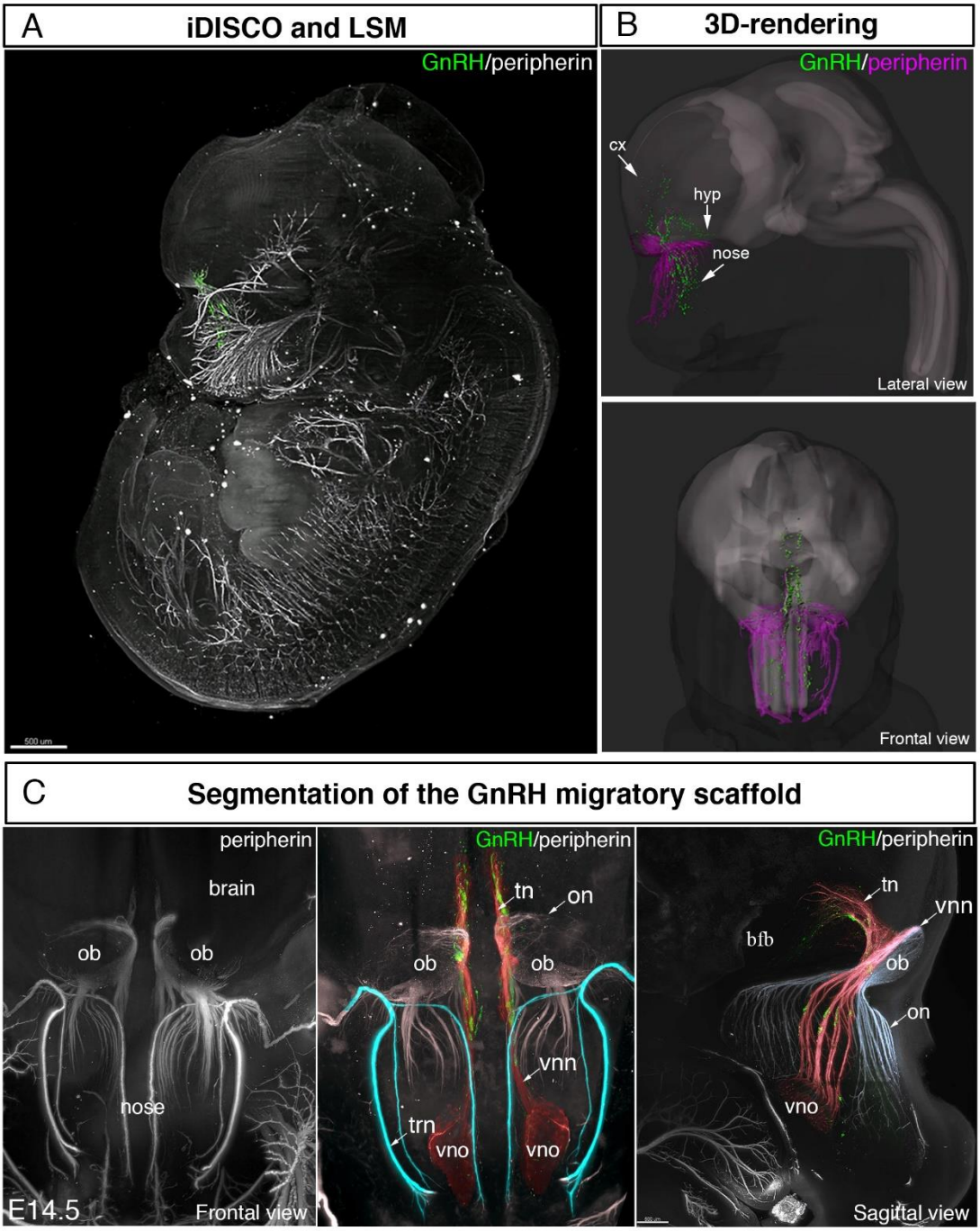

Figure IV–2. Tissue-clearing and light-sheet imaging open new analysis modalities. A*. Light-sheet imaging of an intact E12 embryo stained for peripherin (white) and GnRH (green) reveals the peripheral innervation and the migratory GnRH neurons.* ***B****. Automatic 3D reconstruction of the GnRH neurons (green) and the olfactive/vomeronasal system (purple) from the GnRH and peripherin fluorecent signal respectively.* ***C****. Manual segmentation of the peripherin signal (white) was used to pseudo-color the peripherin-positive nerves of the nasal region, and distinguish between the olfactory (light blue) and*

vomeronasal/terminal nerves (red). Scale bars: 500µm; bfb: basal forebrain; cx: cortex; hyp: hypothalamus; ob: olfactory bulb; on: olfactory nerve; tn: terminal nerve; vnn: vomeronasal nerve; vno: vomeronasal organ

Investigating the early postnatal GnRH population in mice

Previous investigations have shown that the GnRH migratory process ends before birth and proposed that, by the end of fetal development, GnRH neurons are dispersed in their final cerebral locations (Wray et al. 1989). Many other studies that followed during the last 30 years, replicated this concept. However, when it comes to the postnatal development of GnRH neurons, most investigators focused their attentions only to the central compartment, being the main region of action of GnRH neurons. Moreover, due to the presence of thick bones protecting the olfactory structures of mammals, classical histological analysis of these regions has been quite challenging.

In this study, we challenged the concept of a GnRH migration restricted to the fetal age. We combined head decalcification with iDISCO+, followed by 3D-imaging during early postnatal development (Figure 3) and at adulthood (Figure 4). Surprisingly, our results reveal a previously overlooked population of GnRH neurons located in the nose of postnatal animals. Even more intriguingly, these neurons appear to form a continuum of projections and cell bodies reaching from the territory of the VNO to the OB at birth (postnatal day 0, PN0, Figure IV-3, A-F), relayed then by the aforementioned brain population scattered all the way to the hypothalamus. In the VNO, both projections and cell bodies immunoreactive for GnRH were detected, and this was verified also 3 days later at PN3 (Figure IV-3, G-H). Of particular interest is the density of innervation of the VNO by GnRH fibres in this period, as observed at higher magnification (Figure IV-3, F, H). Counting both in 3D and on 2D reslices for validation estimated 193±30 neurons in the nose of animals at PN3 (n=3). In addition, and as previously described (Casoni et al. 2016), a ring-like distribution of GnRH neurons and fibres at the caudal part of the OB could be observed (Figure IV-3, C).

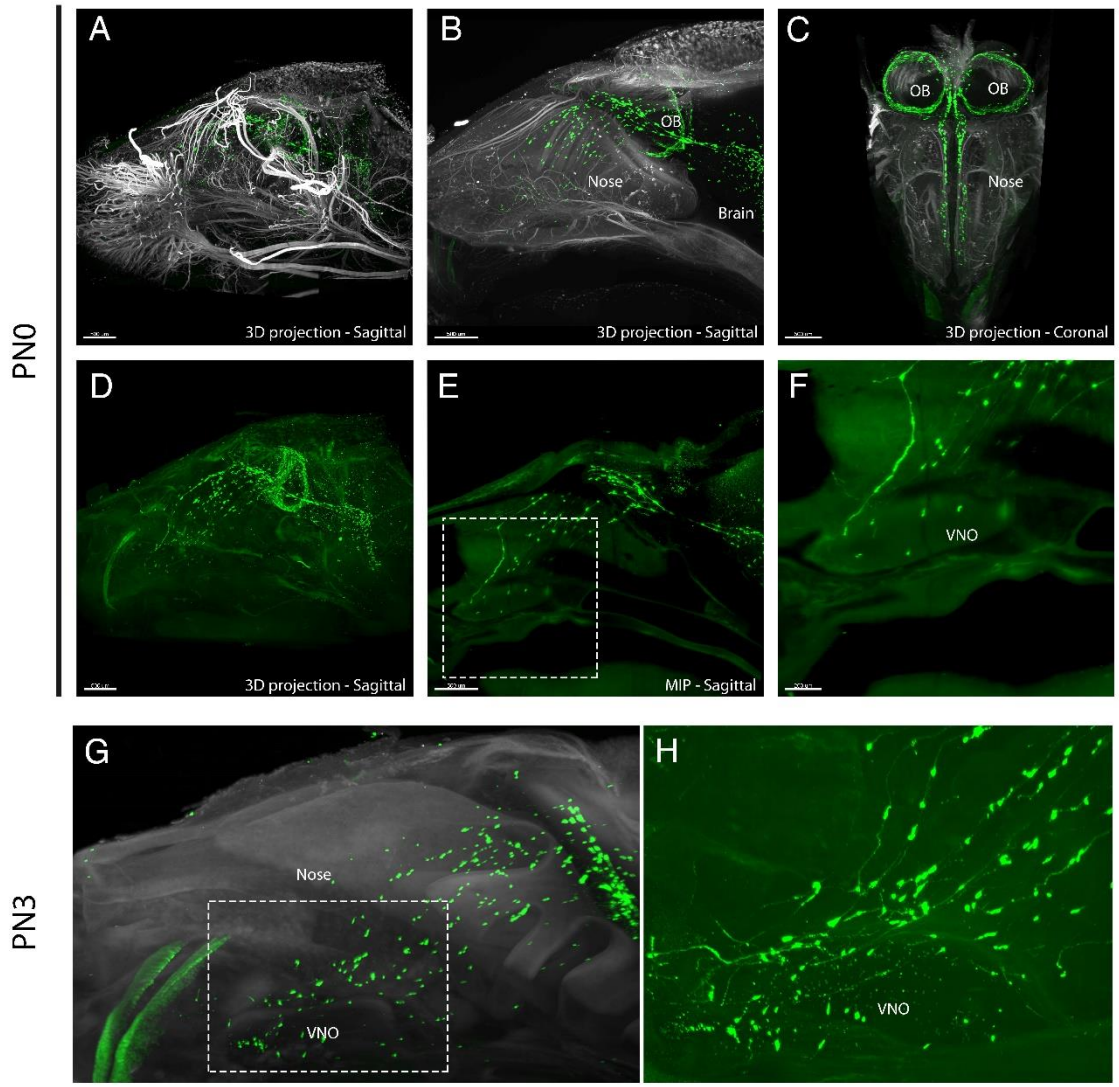

Figure IV-3. Decalcification-enabled iDISCO+ on early postnatal mouse heads. ***A****. A decalcified head from a postantal day 0 mouse (PN0) was processed with iDISCO+ and stained for GnRH (green) and peripherin (white).* ***B****. 3D-projection of a medial part of the head shown in (A) allows visualization of GnRH neurons along peripherin-positive sensory fibers in the nose.* ***C****. Frontal reprojection of the view presented in (B) revels the ring-like distribution of GnRH immunoractivity around the olfactory bulbs.* ***D****. GnRH staining alone from the view presented in (A).* ***E****. Maximum intensity projetion of medial optical sections through the PN0 head shows a continuum of GnRH immunoreactivity throughout the nasal compartement and into the brain.* ***F****. Magnification of the area delimited in (E) reveals immunoreactivity for GnRH in the VNO.* ***G****. Autofluorescence (white) and GnRH immunoreactivity (green) in a decalcified mouse head at PN3. Numerous GnRH neurons are detected in the nose and in the region of the VNO.* ***H****. Magnification of the area delimited in (G) shows the high density of GnRH neuron cell bodies and fibres in the region of the*

VNO. Scale bars: 500µm (A-E); 200µm (F); OB: olfactory bulb; MIP: maximum intensity projection; VNO: vomeronasal organ

GnRH neurons are still present in the nose of adult mice

Intrigued by this population of GnRH neurons in the peripheral olfactory areas, we asked whether it could still be present in the adult mouse and at which extent. Using a similar decalcification procedure, we successfully cleared the whole head of adult animals, with a notably good clearing efficiency in the nasal region (Figure IV-10). We find not only that GnRH neurons are indeed present in the intact nose of adult animals, with tens of cell bodies easily distinguishable in the medial region (Figure IV-4, C), but also that they are not confined to the nose since fibres are seen crossing the nose/brain junction and projecting towards the OB and brain (Figure IV-4, D, E). Additionally, GnRH neurons of the nose still share an apparent connection with the VNO: fibers and cell bodies are detected inside and in close proximity to the vomeronasal epithelium, the territory of which is also marked by a punctuated signal reminiscent of GnRH-immunoreactive terminals (Figure IV-4, E).

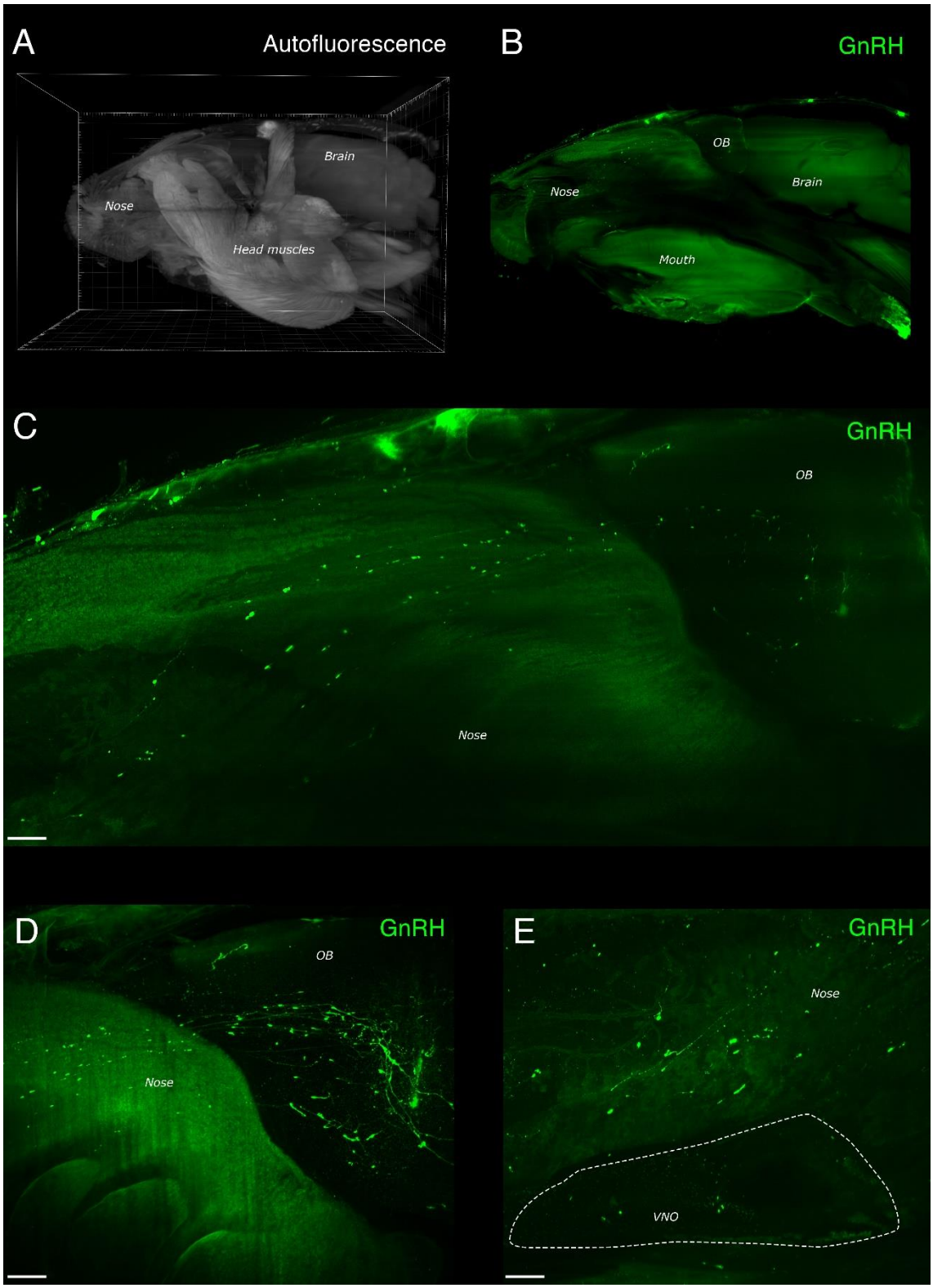

Figure IV-4. Decalcification-enabled iDISCO+ on adult mouse heads. A*. Sagittal projection of a low-magnification (2X) acquisition, showing the autofluorescence in the cleared head of an adult mouse.* ***B****. 250µm-thick sagittal reslice of a low-magnification acquisition in the whole head immunolabled for GnRH.* ***C****. Magnification of (A) centered on the nose/brain junction. GnRH cell bodies are visible and distributed*

rostrocaudally from the nose to the OB. ***D.*** *High-magnification acquisition (4X) reveals a high density of GnRH neurons and fibres at the level of the OB and nose/forebrain junction.* ***E.*** *GnRH neurons and projections are found in close proximity to the VNO, and in the VNO itself. Scale bars: 300µm; OB: olfactory bulb; VNO: vomeronasal organ*

Mapping the central GnRH network in the postnatal mouse

Despite the amount of data gathered over the decades on GnRH cell bodies, projections and interactions in the brain of several species, we are still in need of a definitive and precise picture of their organization. In that regard, tissue clearing and 3D-imaging are well-suited for mapping strategies and studies of networks and long-range projections (Renier et al. 2016, Ueda et al. 2020). We have thus immunolabeled, cleared and imaged intact brains of mice in an effort to map GnRH immunoreactivity in several regions of the juvenile and adult mouse brain. In a juvenile brain (PN7, Figure IV-5), GnRH neurons are rostro-caudally distributed in several regions: rostrally, clusters of cells appear to form a tight continuum on each side of the midline, in-between the two OB and in the nerve layer (Figure IV-5, A), as reported before (Casoni et al. 2016). More laterally, GnRH neurons are found in close apposition to the glomerular layer of the OB, as well as at the level of the accessory olfactory bulb (AOB). Finally, in this region, and while the ring-like distribution observed earlier is less evident at that age, cell bodies are still visible at the caudal part of the OB (Figure IV-5, A). More caudally, the well-known "inverted Y"-shaped distribution of GnRH neurons from the septal regions to the medio-basal hypothalamus is evident (Gross 1976). As expected, GnRH neurons are thus restricted to a narrow area on each side of the midline in the septum, before splitting in the preoptic region in two branches which engage laterally in the hypothalamus (Figure IV-5, A, B). In these two branches, GnRH neurons are more scattered and isolated from each other than in the septum and preoptic region, and that scattering increases following an antero-posterior trajectory. In the posterior hypothalamus, only a handful of cells are found, usually distant of several hundreds of microns as shown in higher-magnification imaging of this region (Figure IV-5, B). Also noticeable at PN7 is the dense staining in the two

circumventricular organs of the hypothalamus, namely the organum vasculosum of lamina terminalis (OVLT) and the ME, illustrative of the high innervation to these structures for blood sensing and GnRH secretion (Figure IV-5, A-D). Finally, the GnRH immunoreactivity in the whole brain is not limited to the olfactory, septal and hypothalamic areas, as single isolated neurons are dispersed throughout other regions (Figure IV-5, A).

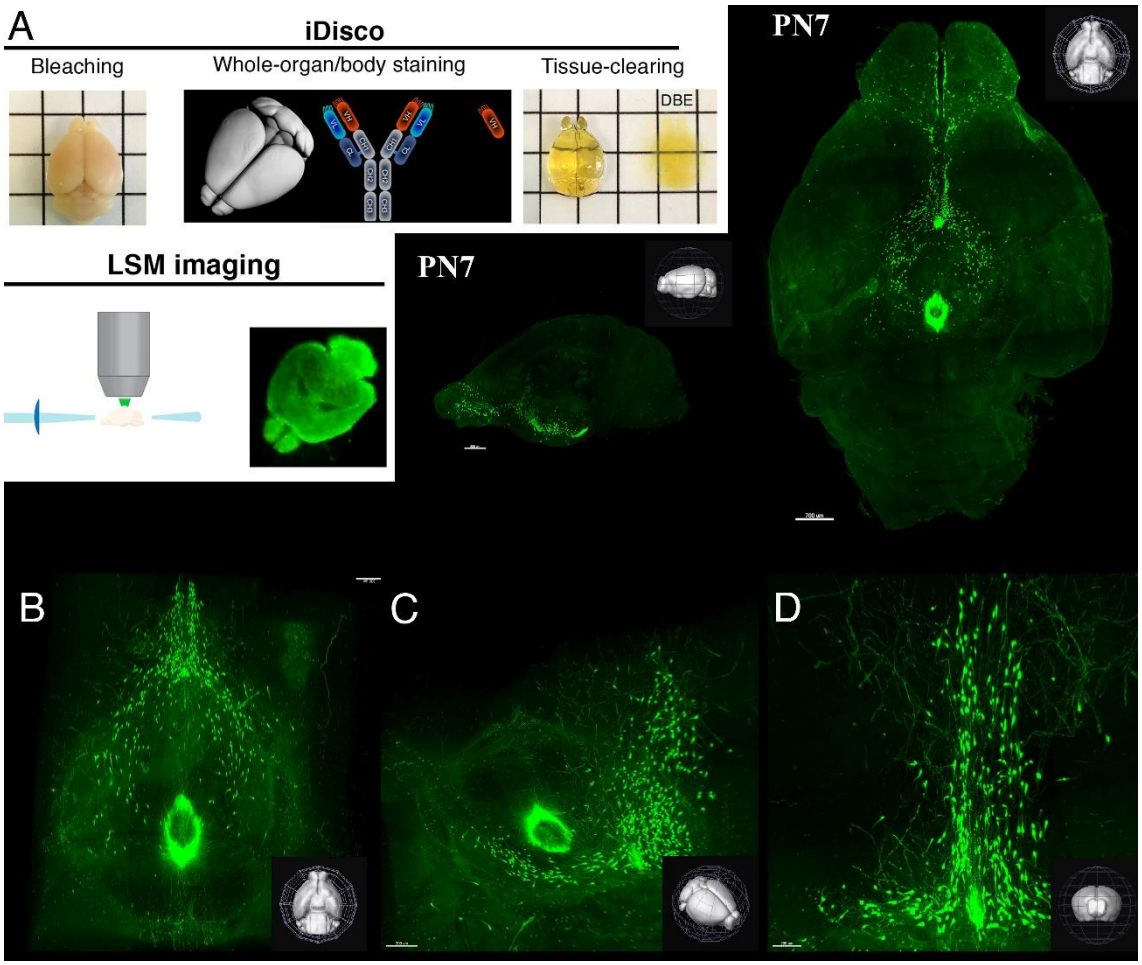

Figure IV-5. iDISCO+ processing of a juvenile mouse brain shows the whole-brain distribution of GnRH. A*. Brains underwent iDISCO+ treatment consisting in pretreatment (depigmentation, delipidation), immunostaining and solvent-based tissue clearing. Light-sheet microscopy (LSM) enables rapid imaging of the entire cleared samples, and subsequent 3D-visualization and reprojection of the rendered sample. Example of whole-brain visualization are given for a postnatal day 7 (PN7) animal.* ***B****. Ventral view of a high-magnification acquisition of the hypothalamus, revealing the typical inverted-Y distribution of the GnRH neurons from the septal region to the preoptic and hypothalamic area. Note the division in two branches that invade laterally the ventral hypothalamus, and the string immunoreactivity*

in fibres innervating the OVLT and ME. ***C****. Anterior perspective view of the hypothalamus shown in (B) showing the high density of GnRH neurons in the preoptic region.* ***D****. Frontal projection of the hypothalamus shown in (B) and (C). Scale bars: 800µm (A), 300µm (C), 200µm (D); ME: median eminence; OVLT: organum vasculosum of lamina terminalis*

In the adult brain (PN90, Figure IV-6), a comparative high-magnification imaging of the hypothalamus brings a stunningly different information. Indeed, numerous GnRH-immunoreactive fibres together contribute to a dense staining in the hypothalamic structures, with projections either following a curved antero-posterior pattern, similar to the branches formed by GnRH cells bodies, or oriented in a straighter manner along the borders of the third ventricle (3V) (Figure IV-6, B). This heavy GnRH-immunolabeling of the fibres is consistent with a more abundant GnRH production and secretion of the peptide occurring in adulthood as compared to juvenile mice (Figure IV-5). In most cases, this innervation seems to go to the OVLT and/or the ME, the latter being notably joined by fibres all along its course. Despite the discontinuous vesicular staining which is characteristic of GnRH immunolabelling (Jennes et al. 1985), tracing of individual fibres is sometimes feasible over long distances and reveals hundreds of micrometre-long projections, while occasional neurons are seen sending two processes in the same direction, in the shape of a U (Figure IV-6, C), as had already been reported (Herde et al. 2013). Finally, segmentation of both hypothalamic and extrahypothalamic signal illustrates the relative proportion of fibres in different regions such as the thalamus and striatum, but also the habenula (Figure IV-6, D, E), all densely innervated. This is, to our knowledge, the first report of such an extent of GnRH distribution in extra-hypothalamic areas of the mouse brain.

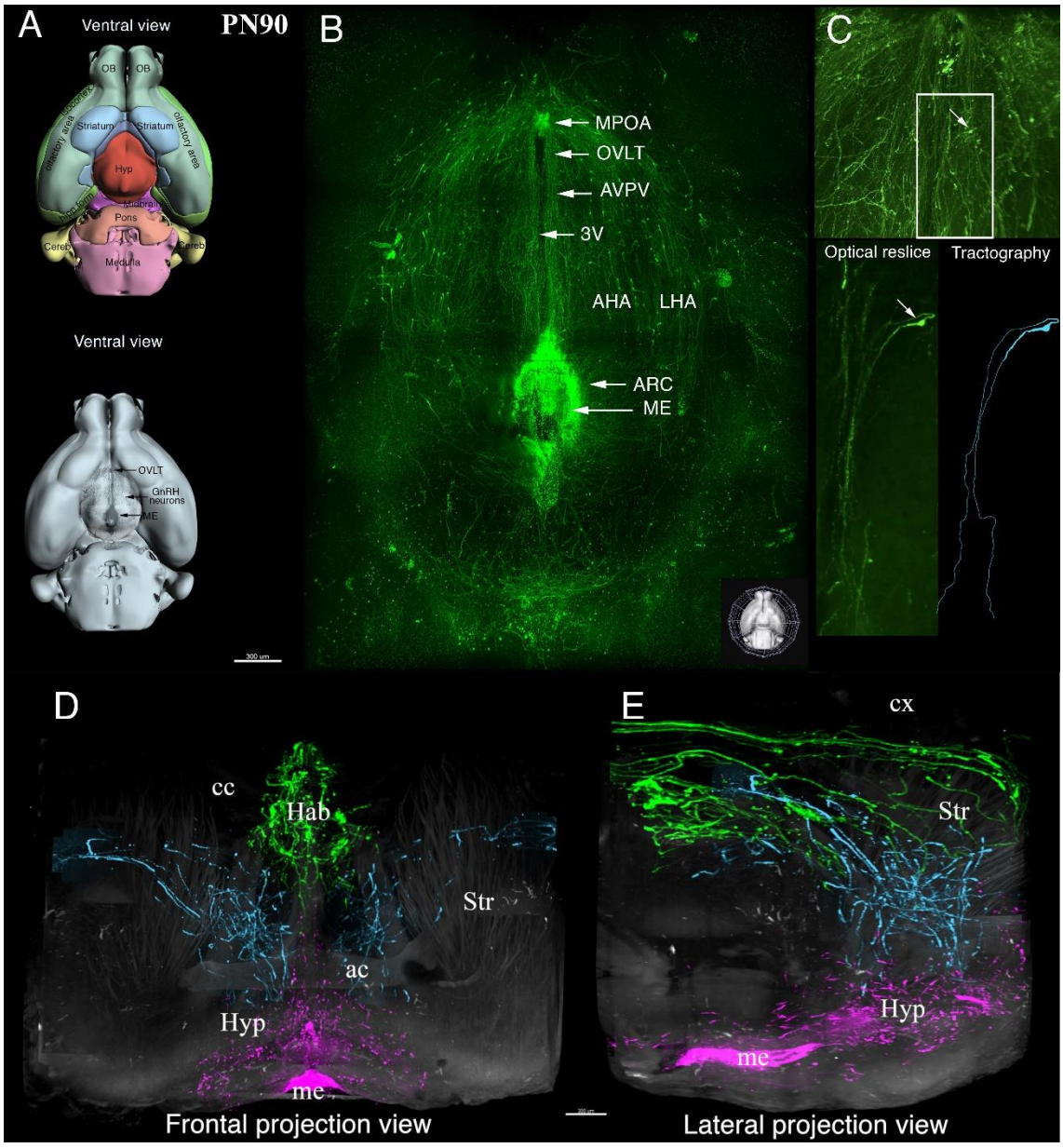

Figure IV-6. iDISCO+ reveals the extent of the adult hypothalamic and extrahypothalamic GnRH immunoreactivity. A*. Ventral redering of the mouse brain from the Allen Brain Atlas.* ***B****. Ventral view of a high magnification acquisition of the intact adult hypothalamus stained for GnRH.* ***C****. Reslicing and segmentation allow tracing of single GnRH-positive projections.* ***D-E****. Automatic signal-based segmentation reveals the extent of GnRH innveration in the hypothalamus (purple) and extrahypothalamic (blue, green) regions, including the cortex, striatum and habenula. Scale bars: 300µm; 3V: third ventricle; ac: anterior comissure; AHA/LHA: anterior/lateral hypothalamic area; ARC: arcuate nucleus; AVPV: anteroventral periventricular nucleus; MPOA: medial preoptic area; OVLT: organum vasculosum of lamina terminalis; cc: corpus callosum; cx: cortex; hab: habenula; hyp: hypothalamus; me: median eminence; str:striatum*

The hypothalamic kisspeptin-GnRH system evolves during the postnatal development

Among the interactors of GnRH neurons, the neuronal population of kisspeptin-immunoreactive cells of the hypothalamus have received increased attention in since the early 2000s, since the fundamental role of kisspeptin signalling in puberty and reproduction has been put forward (de Roux et al. 2003, Seminara et al. 2003), and because the Kisspeptin-NeurokininB-Dynorphin (KNDy) neuronal population of the hypothalamus is thought to drive GnRH/LH pulses (Moore et al. 2018). Reporter lines and trans-synapic tracing have been used before to successfully demonstrate the prenatal development of kisspeptin-GnRH interactions (Kumar et al. 2014, Kumar et al. 2015) as well as postnatal kisspeptin-GnRH functional connections (Kumar et al. 2015). Additionally, tissue clearing-enabled 3D mapping of kisspeptin-expressing cells has been undertaken in recent years by immunolabeling in rats and sheeps (Moore et al. 2018), and through the use of reporter lines and viral tracing in mice (Yeo et al. 2016, Moore et al. 2019). Despite the roles attributed to kisspeptin-GnRH interactions, a detailed description of the relationship between GnRH neurons and kisspeptin neurons over development is, however, still lacking. We set out to perform double-immunostaining over several stages of postnatal development in a KissIC/eR26-τGFP reporter mouse model, in which a Kiss1-expression-dependant Cre-mediated recombination brings τGFP expression in kisspeptin-expressing cells (Mayer et al. 2010, Wen et al. 2011).

Over the postnatal development, immunolabeling for GnRH reveals the inverted Y-shaped distribution of GNRH neurons in the hypothalamus, as well as strong immunoreactivity in the OVLT and ME, but not all along the course of the GnRH neuron processes at PN4, PN10 and PN21 (Figure IV-7, A-D). After puberty and in the adult mouse (PN60), however, strong immunoreactivity for GnRH is also detected in the fibres, as noted before (Figure IV-6 and Figure IV-7, D). Interestingly, at PN4, staining for GFP only reveals the population of kisspeptin-expressing cells of the arcuate nucleus (ARC), but not that of the anteroventral periventricular nucleus (AVPV), suggesting that the latter has not yet matured and expressed kisspeptin (Figure IV-7, A, E, I). Strikingly at PN10, while GFP-immunoreactivity has extended to cover more cells

in the ARC, the AVPV population becomes apparent, hinting that kisspeptin expression is first triggered between PN4 and PN10 (Figure IV-7, B, F, J). In addition, numerous GFP-positive projections can be observed both in sagittal and coronal optical reslices, reflective of strong kisspeptin innervation in the hypothalamus (Figure IV-7, E-L). Of note, fibres seem to emanate from the arcuate population towards the AVPV (Figure IV-7, F-H). Even more cells and projections are GFP-positive at PN21, as puberty is getting closer, and in the adult mouse a high density of GFP-immunoreactive fibres can be observed in both the ARC and the preoptic region and AVPV. Reslices show an increase in the number of cell bodies in these two regions, compared to earlier postnatal and prepubertal stages, but also in other hypothalamic regions (Figure IV-7, F-H). Overall, both the GnRH and kisspeptin populations undergo maturation during the postnatal development. First limited to some cells and projections of the ARC, GFP-immunoreactivity then extends to the AVPV while fibre density in the hypothalamus progressively increases as the animal advances towards puberty. In the adult, the two typical populations of kisspeptin neurons are visible and distinct, although from sagittal reslices it appears that the two regions are connected *via* GFP-positive projections.

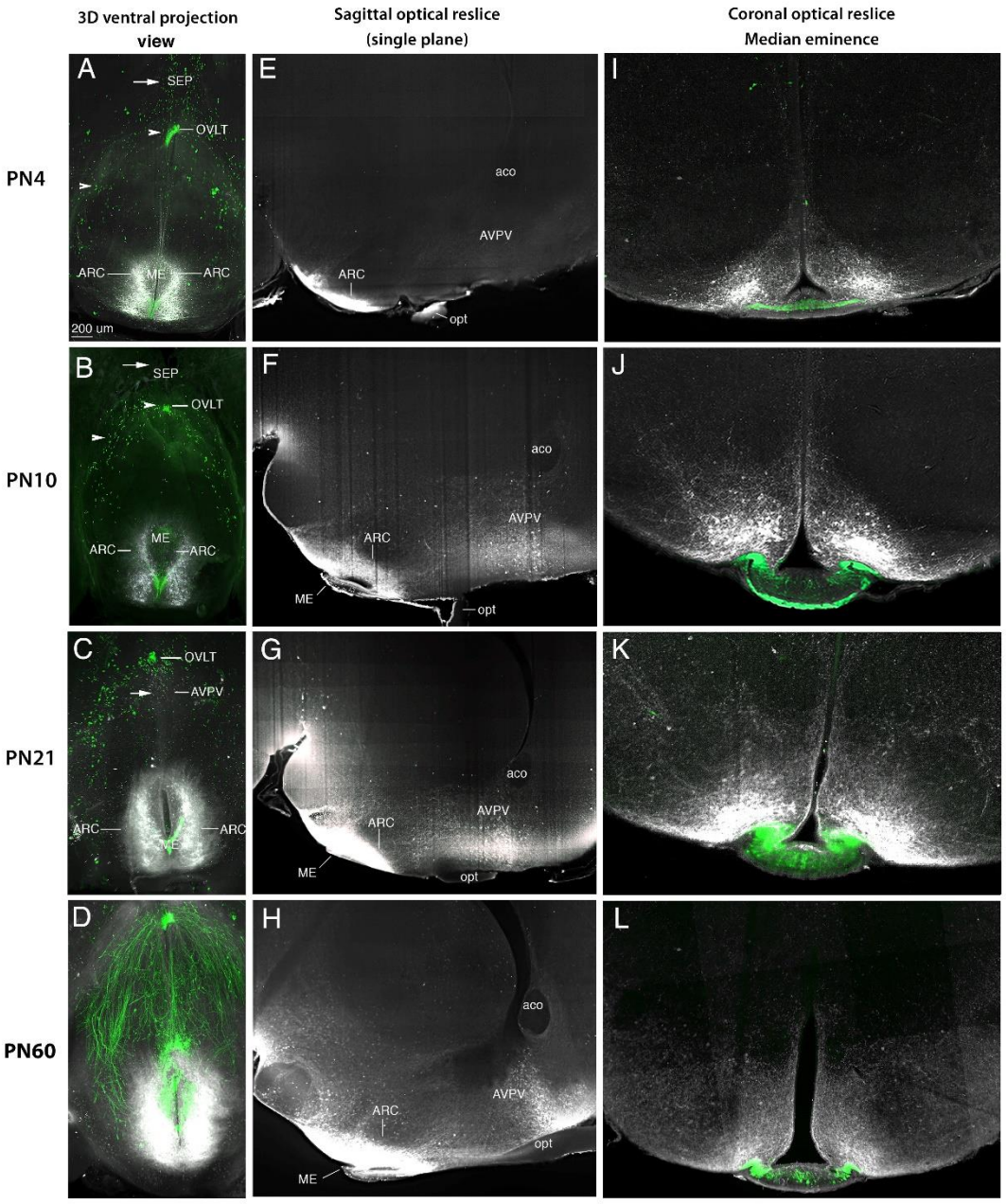

Figure IV-7. iDISCO+ Visualization of the of GFP-expressing kisspeptin neurons of the hypothalamus. ***A-D.*** *Ventral hypothalamic views at PN4, PN10, PN21 and PN90 show GnRH immunoreactivity (green) limited to cell bodies in prepubertal animals, and extended to fibres in the adult. GFP-immunoreactivity (white) is first observable in the arcuate nucleus alone (ARC) in early stages, before the preoptic population is visible at later stages (C-D).* ***E-H.*** *Sagittal optical reslices from 3D-imaged brains show first GFP expression limited to the arcuate nucleus at PN4 (E), before it expands with an increase in positive cell bodies and projections (F-H). Absent at PN4 (E), GFP expression increases gradually over time in the AVPV (F-H) with cell bodies and projections becoming visible.* ***I-L.*** *Coronal reslices through the arcuate*

nucleus shows the gradual increase in GFP expression, reflective of the maturation of the kisspeptin-expressing population of the ARC. Aco: anterior commissure; ARC: arcuate nucleus; AVPV: anteroventral periventricular nucleus; ME: median meinence; OVLT: organum vasculosum of lamina terminalis; SEP: septal region

Extra-hypothalamic GnRH neurons and interactors suggest potential new roles for the GnRH system

GnRH cell bodies and innervation are not confined to the hypothalamus, but are also found in several brain regions (Figure IV-6). In addition, kisspeptin-expressing cells show an important innervation of both hypothalamic and extrahypothalamic regions (Figure IV-7), thus prompting the idea that well-described kisspeptin-GnRH interactions could also take place elsewhere in the brain. The KissIC/eR26-τGFP proved to be a valuable tool to detect kisspeptin populations, even in the case of low protein expression (Kumar et al. 2014). We thus explored the brain distribution of GFP in the previously described KissIC/eR26-τGFP line, as well as the GPIC/eR26-τGFP in which a GPR54-expression-dependant Cre-mediated recombination brings τGFP expression in kisspeptin-receptor expressing cells.

To our surprise, cells and processes immunoreactive for GFP were found throughout the brain for both lines in extra-hypothalamic regions. Notably, we observed positive cells and projections in the cortical regions, along and inside the hippocampal formation, and in the amygdala, in these reporter lines (Figure IV-8). Of note, GFP immunoreactivity was low at early stages, and increased over the postnatal development in these regions, suggesting that it does not derive from ectopic Cre expression during embryogenesis (Figure IV-11). GnRH neurons and innervation were also spotted in extrahypothalamic regions (Figure IV-5, Figure IV-6). Together, this raises the intriguing possibility that kisspeptin signalling through GPR54 could take place in GnRH cells and projections outside the currently defined hypothalamic circuitry, which will require future confirmation. Additionally, whether these interactions participate to the control of reproduction, or to so far undescribed other brain functions will need to be addressed.

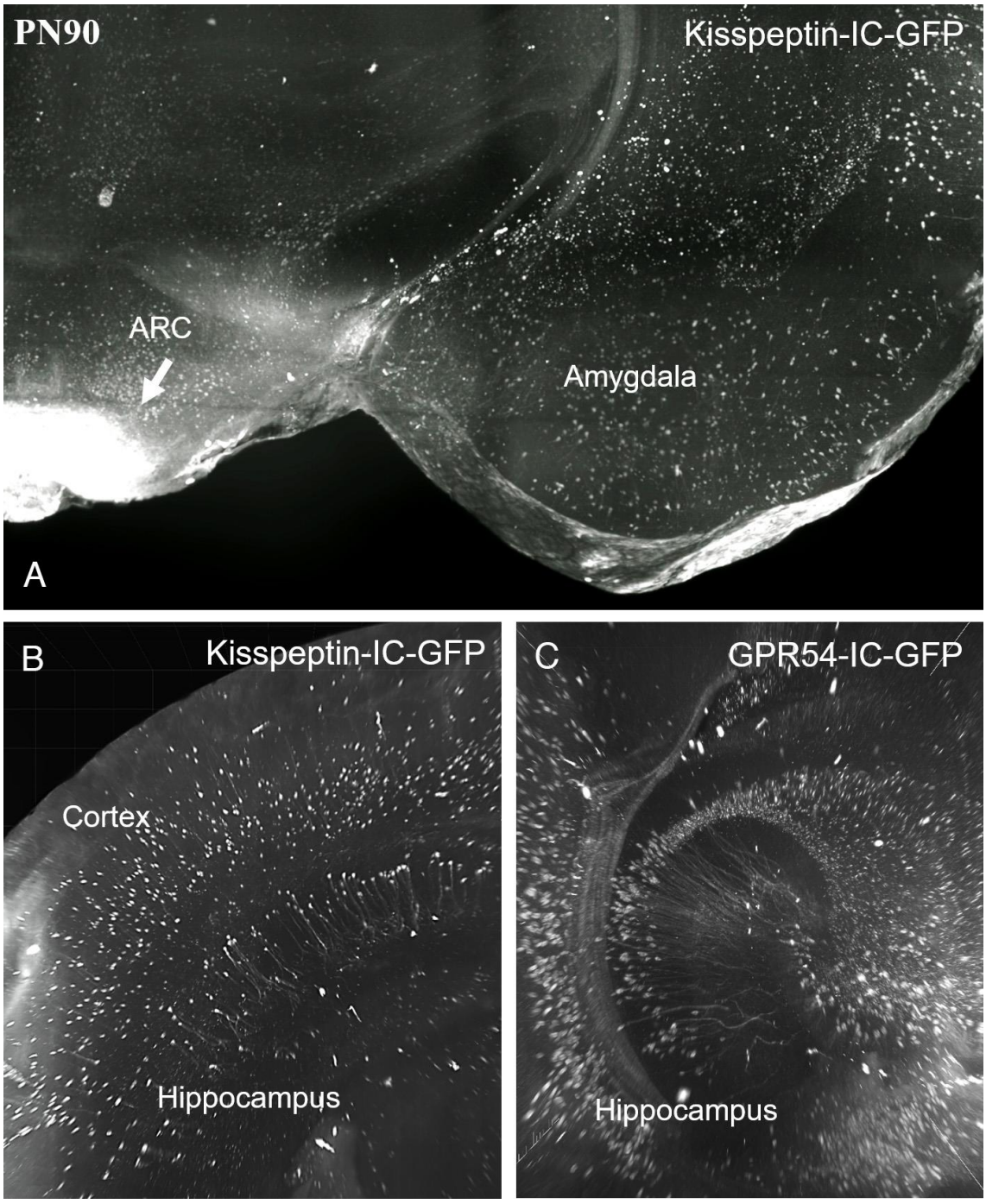

Figure IV-8. Extrahypothalamic kisspeptin and kisspeptin receptor expressing neurons revealed by 3D-imaging. A*. Coronal projection showing GFP immunoreactivity in the arcuate nucleus, and in the amygdala of an adult KISS-IC-GFP mouse brain.* ***B****. Numerous GFP-positive cells are also found in the hippocampus and in the cortex of adult KISS-IC-GFP animals.* ***C****. GFP-immunoreactive cells and projections in the hippocampus of an adult GPR54-IC-GFP brain. ARC: arcuate nucleus*

Multi-scale analysis of GnRH neuronal interactions in the olfactory bulbs

Trying to probe further the extrahypothalamic GnRH neuronal interactions, and given the abundant olfactory GnRH population detected in both young and adult animals (Figure IV-3, Figure IV-4, Casoni et al. 2016), we used a transgenic TH-GFP mouse line (Matsushita et al. 2002) to verify the extent of GnRH interaction with the dopaminergic interneurons located in the glomerular layer of the olfactory bulb which play an essential role in olfactory discrimination. Light-sheet microscopy performs excellently for network-scale or organ-scale imaging and for macroscopic visualization of cellular networks. However, it lacks sufficient resolution to obtain subcellular information and/or detect fine cell-cell interactions (Ueda et al. 2020). This is further aggravated by the dehydration-induced tissue shrinkage of samples in solvent-based tissue clearing techniques (Molbay et al. 2021). In this last part of the study, we aimed at developing new methods to combine volume imaging with high-resolution confocal imaging, in order to overcome the limitations described above. We have shown that iDISCO+ tissue clearing is reversible since following a hydrating procedure, tissues can be returned to their previous hydrated and non-transparent state (Figure 9A). We have also proved that this is suitable for further processing, including freezing, cryosectioning and confocal imaging (Figure 9A). Using iDISCO+ and light-sheet microscopy, we were able to observe the entire GnRH population (immunolabeled in red) throughout the brain (Figure 9B) and then navigate through the olfactory bulbs to visualize some scattered cell bodies and fibres in the caudal part of the OB (Figure 9C, D). After rehydration, freezing and cryosectioning, we could image the OB sections on a confocal microscope, without performing additional rounds of immunostaining (Figure 9E-H). Our data showed indeed that the fluorescence from the former whole-mount immunostaining was preserved, even after light-sheet imaging and tissue reprocessing. After having assessed that, we took advantage of the scattered distribution and small size of the GnRH population in the OB to identify a GnRH cell body in our light-sheet optical sections (Figure 9D), relocate this neuron in a thin OB section and re-image it at high-power and high-resolution using confocal microscopy (Figure 9 E-H). Moreover, we were able to observe close proximity between the GnRH-

immunoreactive neurons surrounding the caudal part of the OB and TH-expressing cells (Figure 9 E-G). Finally, we could visualize very fine (< 1µm) cell-cell interactions (Figure 9H), otherwise impossible to detect using light-sheet microscopy. Interestingly, we observed GnRH terminals in close proximity to dendritic spines of TH neurons (Figure 9H), strongly suggesting communication between these populations. Overall, these data showed that combining light-sheet with confocal imaging makes possible the visualization of single neurons in high resolution, and their assembly into circuits in the intact central nervous system. Our results also open new avenues in the investigation of extra-hypothalamic GnRH populations.

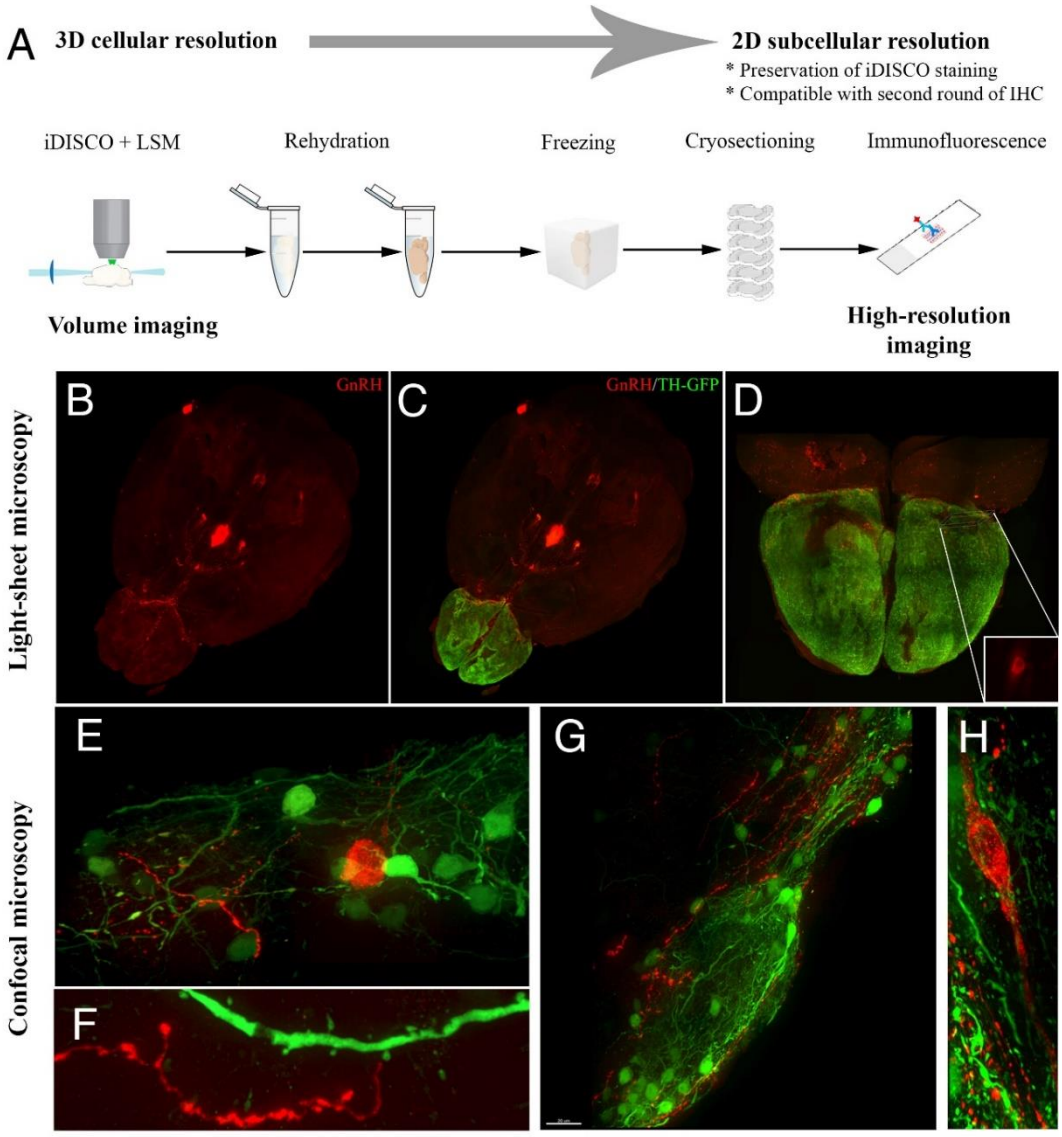

Figure IV-9. Combination of iDISCO+, light-sheet imaging and tissue reprocessing opens new multidimensional imaging possibilities. A*. iDISCO+ processed samples can be rehydrated, frozen and*

cryosection for further reprocessing and high-resolution imaging. ***B-D****. iDISCO+ allows visualization of GnRH (red) and GFP (green) staining at the network and organ scale in a TH-GFP mouse line.* ***E-H****. After sample rehydration and reprocessing, confocal imaging reveals close contacts and probable cell-cell interactions between GnRH and TH cells (E, G, H) and their processes (F).*

IV. Discussion

The GnRH network is the central circuitry controlling reproduction in mammals, and its failures are associated with a number of reproductive disorders. Thus, a precise characterization of the development and maturation of this network is needed to fully comprehend the mechanisms involved and the deleterious consequences of their defects. So far, immunohistochemical studies of GnRH neurons and their interactors, both in physiology and pathology, have greatly relied on sectioning techniques. These techniques come at the cost of a damaging loss of information, and are poorly suited to study migratory, scattered populations and complex networks. In contrast, only very recently have investigators started using modern three-dimensional approaches to further explore the central regulators of reproduction (Casoni et al. 2016, Moore et al. 2018, Malone et al. 2019). Notably, Casoni and colleagues have applied tissue-clearing and 3D imaging to human fetuses, mouse embryos and adult brains to provide new insights on the migration and distribution of GnRH (Casoni et al. 2016).

In the present work, we go further in the characterization of the GnRH network throughout the mouse embryonic and postnatal development. We first observe GnRH neurons in the olfactory placode, in agreement with previous data from the literature (Wray et al. 1989, Schwanzel-Fukuda and Pfaff 1989), and in contrast to human observations that detected first GnRH immunoreactivity outside of the VNO / olfactory epithelium even at early stages (Casoni et al. 2016). We observed, strating from E11.5, the subsequent migration of GnRH-immunoreactive cells through the nose and towards the brain. On this part, our results contrast with earlier works regarding the timing of migration: while previous investigators concluded that the migration was achieved by E16 and that GnRH neurons had assumed their adult distribution at that stage (Wray et al. 1989,

Schwanzel-Fukuda and Pfaff 1989), we found that a substantial part of the total embryonic GnRH population was still present in the nose at E16.5, on the same sensory tracts that delineate their migratory pathway (Wray et al. 1994) (Figure IV-1).

The sensory projections of the olfactory system were also visualized in our samples by immunostaining for peripherin, a marker of peripheral nerves (Escurat et al. 1990) which has been used before to label the developing olfactory system in mice and humans (Gorham et al. 1991, Wray et al. 1994, Casoni et al. 2016). We observed that the migrating GnRH neurons, either in clusters or individualized, are indeed systematically found along these peripherin-positive projections in the nasal region as they project towards the nose/forebrain junction (Wray et al. 1994). While the olfactory and vomeronasal nerves innervate the main and accessory olfactory bulbs, branches of the terminal nerve were seen engaging in the forebrain and were detected at E12, E14 and E16.5. The fact that the putative branches of the terminal nerve are still found in the forebrain at E16.5 is in accordance with the continued migration of GnRH neurons, and the fate of this branches later in development remains to be explored.

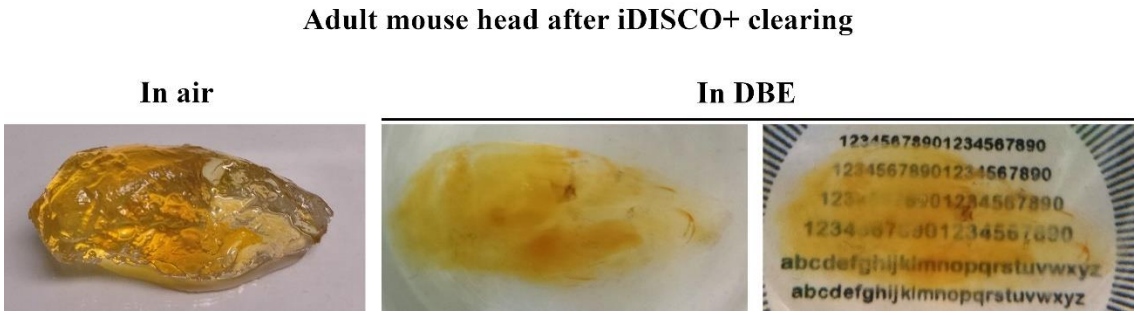

Figure IV-10. iDISCO+ processing of an intact adult mouse head*. EDTA-decalcified heads can be cleared through the iDISCO+ protocol. The figure illustrates a cleared head outside (top) and inside (middle, bottom) the clearing solution. Note the clearing efficiency throughout the head.*

The exact nature of the sensory projections guiding GnRH neuron migration in the nose has long been uncertain, being described as olfactory, vomeronasal, terminal, or a mix of the three based on earlier work (Wray et al. 1994, Yoshida et al. 1995, Yoshida et al. 1999, Forni and Wray 2015) and the co-segregation of reproductive disorders with anosmia/hyposmia such as Kallmann

syndrome in animal models and humans (Forni and Wray 2015, Boehm et al. 2015). Our segmentation results bring the definitive confirmation that GnRH neurons are only found associated with intermingled fibres of the vomeronasal/terminal nerves, but not with olfactory sensory projections on their way to the brain (Figure IV-2). Of note, if we could not discriminate further between vomeronasal and terminal projections, it was recently suggested that only the terminal nerve is required for proper GnRH neuron migration, although this does not preclude their association also with fibres of the vomeronasal nerves (Taroc et al. 2017). Identification of specific markers for the different populations of olfactory/vomeronasal/terminal neurons, would help in getting a definitive answer to this decades-old question.

A secondary observation came from our 3D-imaging of mouse embryos. Indeed, peripherin staining revealed that, mid-development (E11.5), and in addition to a subset of the developing olfactory system, only the trigeminal ganglion and some projections towards the mandibular process were observable in the head. By contrast, the territory of trigeminal innervation extends dramatically over the following days, resulting in the three branches of the trigeminal nerve being discernible by E12.5, and their ramifications subsequently invading their respective territories as described before (Durham and Garrett 2010). This is, to our knowledge, the first report of these events using a three-dimensional approach, and another demonstration of how such methods can benefit to the study of embryonic development (Vieites-Prado and Renier, 2021) (Figure IV-1).

One of the most surprising finding of this work lies in the hundreds of GnRH neurons residing in the nasal regions of postnatal and adult animals (Figure IV-3, Figure IV-4). Whether these GnRH neurons are mature neurons integrated in functional circuits, or migrating GnRH neurons at the adult stage will need to be addressed, for example by staining for markers of immature or migratory neurons such as doublecortin (Gleeson et al. 1999) and by using BrDU/EdU pulse labelling at several embryonic and postnatal stages to time their birth (Jasoni et al. 2009). Although GnRH immunoreactivity has been described before in the nose of the golden hamster (Jennes and Stumpf 1980) and mouse (Jennes 1986), it was then overlooked and its extent was unknown until today. We provide not only a counting of the neurons in this olfactory GnRH

system after birth, but also a demonstration of their connections with both the vomeronasal organ and the brain even in the adult mouse. Their exact role remains, however, elusive and will require further investigation, as will potential contacts with fenestrated vessels in the nose (Jennes 1986). GnRH neurons are indeed known to project outside the blood-brain barrier in the brain (Prevot 2011) and could also act as dual sensors in the nose, integrating circulating cues *via* the blood, and olfactory / pheromonal cues *via* their connection with the olfactory system.

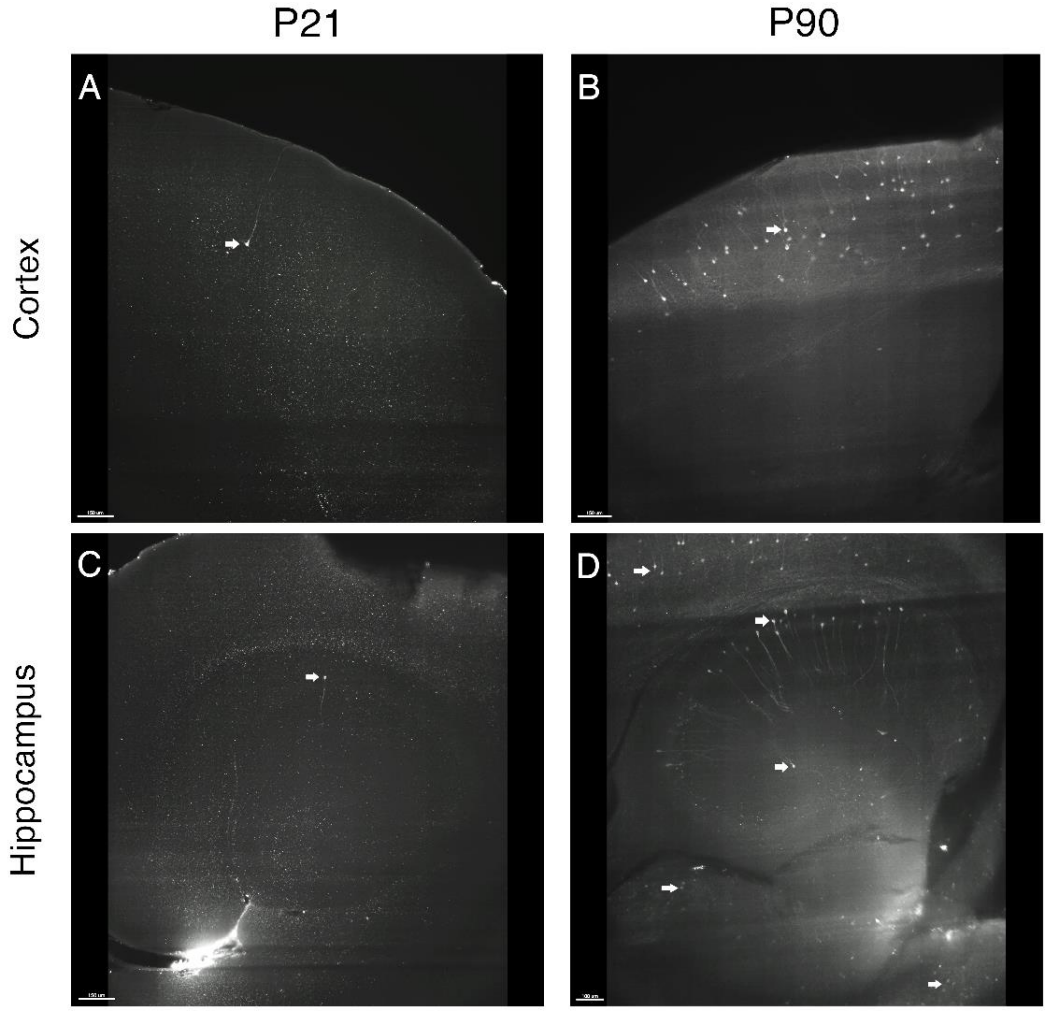

Figure IV-11. GFP immunoreactivity in extrahypothalamic regions of KISS-IC-GFP mouse brains over the postnatal development*. Few GFP-positive neurons can be detected at prepubertal stages throughout the brain of KISS-IC-GFP mouse (A, C). In contrast, a high density of cell bodies and projections are immunoreactive for GFP after puberty and in the adult in these animals (B, D). Scale bars: 150 µm.*

Related also to olfaction is the population of GnRH neurons in the main and accessory olfactory bulbs, and the ring-like distribution of GnRH cells and innervation at the caudal part of the OB

which were recently described through the use of tissue clearing and light-sheet imaging (Casoni et al. 2016). Consistently, we have found GnRH neurons and fibers distributed in the olfactory bulbs at both early postnatal stages and in adult brains, pursuing the continuum of GnRH cells dispersed rostrocaudally from the septum to the hypothalamus (Figure IV-3, Figure IV-4, Figure IV-5). It is unclear what the roles for this specific set of neurons are, but high-resolution imaging strongly suggests interactions between the dopaminergic TH-positive circuits of the olfactory bulbs, involved in olfaction (Cave and Baker 2009), and the OB GnRH neurons (Figure IV-9).

Furthermore, our approach allowed us to document in a new way the maturation of the kisspeptin-expressing neurons of the brain using transgenic mouse lines. The presence of kisspeptin and kisspeptin receptor expression in extrahypothalamic region is not surprising (Oakley et al. 2009, Liu and Herbison 2016), but the large distribution and density of detected cells is unexpected (Figure IV-8). Because kisspeptin's roles in extrahypothalamic regions appears to involve lower physiological levels of kisspeptin secretion (Liu and Herbison 2016), it is possible that kisspeptin immunostainings failed to reveal the extent of the population, which the present transgenic model circumvents. Additionally, previous work documenting kisspeptin expression through direct immunohistochemistry in 3D were conducted in rats and focused only on the hypothalamus (Moore et al. 2018). Additional experiments validating that kisspeptin (receptor) expression indeed occurs in all detected neurons are required. Regarding the development of the two well-described AVPV and ARC kisspeptin populations, the absence of immunoreactivity for GFP in the AVPV population in early postnatal animals is consistent with previous observations in mouse development (Kumar et al. 2014), and so is the extension of the innervation from the ARC kisspeptin neurons to other regions including the AVPV (Bouret et al. 2004) (Figure IV-7). Further studies on the connections of the kisspeptin populations in the murine brain will help in understanding their hypothalamic and extra-hypothalamic roles, in regard or not to GnRH neurons. In that aim, the Cre-expressing lines, together with the whole-brain visualization provided here, enable targeted stereotaxic delivery of Cre-dependent viruses for

chemogenetic/optogenetic manipulation or trans-synaptic tracing of these populations (Kumar et al. 2014, Kumar et al. 2015).

Overall, we have shown that a combination of iDISCO+, light-sheet imaging and tissue reprocessing is particularly well-suited to the study of the neuroendocrine networks controlling reproduction, as it allowed us to provide new information on the development and interactions of GnRH neurons throughout the murine brain. Even more remains to be gained: the work so far is descriptive, but quantitative data can be gathered as well and new tools have emerged to help analyse the distribution and/or innervation of specific cell populations in the brain in an automated or semi-automated manner and with atlas registration (Renier et al. 2016, Wang et al. 2021), which will greatly benefit to neuroendocrinology. In addition, with the democratization of (and advances in) three-dimensional imaging strategies, and with the constant optimization of tissue-clearing protocols and microscopy setups, these techniques will become more easily applicable to a broader range of species, including primates and humans (Xu et al. 2021). Thus, references and templates will be useful to the scientific community on several levels. Establishment of standardized protocols, precise description of the GnRH network development and organization, and development of new analysis pipelines will help in dissecting physiological (sexual dimorphism, estrous cycle variations) and pathological (animal models of reproductive disorders) aspects of the neuroendocrine control of reproduction. As such, the present work is putting in the cornerstone of future studies on the murine GnRH system.

V. References for chapter four

1.Belle, M. et al. Tridimensional Visualization and Analysis of Early Human Development. Cell 169, 161-173.e12 (2017).

2.Berlanga, M. et al. Three-Dimensional Reconstruction of Serial Mouse Brain Sections: Solution for Flattening High-Resolution Large-Scale Mosaics. Frontiers in Neuroanatomy 5, 17 (2011).

3.Boehm, U. et al. Expert consensus document: European Consensus Statement on congenital hypogonadotropic hypogonadism--pathogenesis, diagnosis and treatment. Nat Rev Endocrinol 11, 547–564 (2015).

4.Bouret, S. G., Draper, S. J. & Simerly, R. B. Formation of Projection Pathways from the Arcuate Nucleus of the Hypothalamus to Hypothalamic Regions Implicated in the Neural Control of Feeding Behavior in Mice. J Neurosci 24, 2797–2805 (2004).

5.Cariboni, A. et al. Defective gonadotropin-releasing hormone neuron migration in mice lacking SEMA3A signalling through NRP1 and NRP2: implications for the aetiology of hypogonadotropic hypogonadism. Hum. Mol. Genet. 20, 336–344 (2011).

6.Casoni, F. et al. Development of the neurons controlling fertility in humans: new insights from 3D imaging and transparent fetal brains. Development 143, 3969–3981 (2016).

7.Cave, J. W. & Baker, H. Dopamine systems in the forebrain. Adv Exp Med Biol 651, 15–35 (2009).

8.de Roux, N. et al. Hypogonadotropic hypogonadism due to loss of function of the KiSS1-derived peptide receptor GPR54. Proc Natl Acad Sci U S A 100, 10972–10976 (2003).

9.DURHAM, P. L. & GARRETT, F. G. Development of functional units within trigeminal ganglia correlates with increased expression of proteins involved in neuron–glia interactions. Neuron Glia Biol 6, 171–181 (2010).

10.Ertürk, A. et al. Three-dimensional imaging of solvent-cleared organs using 3DISCO. Nat Protoc 7, 1983–1995 (2012).

11.Escurat, M., Djabali, K., Gumpel, M., Gros, F. & Portier, M. M. Differential expression of two neuronal intermediate-filament proteins, peripherin and the low-molecular-mass neurofilament protein (NF-L), during the development of the rat. J Neurosci 10, 764–784 (1990).

12.Forni, P. E. & Wray, S. GnRH, anosmia and hypogonadotropic hypogonadism - where are we? Front Neuroendocrinol 36, 165–177 (2015).

13.Fueshko, S. & Wray, S. LHRH cells migrate on peripherin fibers in embryonic olfactory explant cultures: an in vitro model for neurophilic neuronal migration. Dev Biol 166, 331–348 (1994).

14.Gleeson, J. G., Lin, P. T., Flanagan, L. A. & Walsh, C. A. Doublecortin Is a Microtubule-Associated Protein and Is Expressed Widely by Migrating Neurons. Neuron 23, 257–271 (1999).

15.Gorham, J. D., Ziff, E. B. & Baker, H. Differential spatial and temporal expression of two type III intermediate filament proteins in olfactory receptor neurons. Neuron 7, 485–497 (1991).

16.Gross, D. S. Distribution of gonadotropin-releasing hormone in the mouse brain as revealed by immunohistochemistry. Endocrinology 98, 1408–1417 (1976).

17.Hanchate, N. K. et al. SEMA3A, a gene involved in axonal pathfinding, is mutated in patients with Kallmann syndrome. PLoS Genet. 8, e1002896 (2012).

18.Herbison, A. E. Control of puberty onset and fertility by gonadotropin-releasing hormone neurons. Nat Rev Endocrinol 12, 452–466 (2016).

19.Herde, M. K., Iremonger, K. J., Constantin, S. & Herbison, A. E. GnRH Neurons Elaborate a Long-Range Projection with Shared Axonal and Dendritic Functions. J Neurosci 33, 12689–12697 (2013).

20.Jasoni, C. L., Porteous, R. W. & Herbison, A. E. Anatomical location of mature GnRH neurons corresponds with their birthdate in the developing mouse. Developmental Dynamics 238, 524–531 (2009).

21.Jennes, L. & Stumpf, W. E. LHRH-systems in the brain of the golden hamster. Cell Tissue Res 209, 239–256 (1980).

22.Jennes, L. & Stumpf, W. E. Gonadotropin-releasing hormone immunoreactive neurons with access to fenestrated capillaries in mouse brain. Neuroscience 18, 403–416 (1986).

23.Jennes, L., Stumpf, W. E. & Sheedy, M. E. Ultrastructural characterization of gonadotropin-releasing hormone (GnRH)-producing neurons. J Comp Neurol 232, 534–547 (1985).

24.Jennes, L. The olfactory gonadotropin-releasing hormone immunoreactive system in mouse. Brain Research 386, 351–363 (1986).

25.Kumar, D. et al. Specialized Subpopulations of Kisspeptin Neurons Communicate With GnRH Neurons in Female Mice. Endocrinology 156, 32–38 (2015).

26.Kumar, D. et al. Murine arcuate nucleus kisspeptin neurons communicate with GnRH neurons in utero. J. Neurosci. 34, 3756–3766 (2014).

27.Kumar, D., Periasamy, V., Freese, M., Voigt, A. & Boehm, U. In Utero Development of Kisspeptin/GnRH Neural Circuitry in Male Mice. Endocrinology 156, 3084–3090 (2015).

28.Liu, X. & Herbison, A. E. Kisspeptin Regulation of Neuronal Activity throughout the Central Nervous System. Endocrinol Metab (Seoul) 31, 193–205 (2016).

29.Malone, S. A. et al. Defective AMH signaling disrupts GnRH neuron development and function and contributes to hypogonadotropic hypogonadism. Elife 8, e47198 (2019).

30.Matsumoto, S. et al. Abnormal development of the olfactory bulb and reproductive system in mice lacking prokineticin receptor PKR2. PNAS 103, 4140–4145 (2006).

31.Matsushita, N. et al. Dynamics of tyrosine hydroxylase promoter activity during midbrain dopaminergic neuron development. J Neurochem 82, 295–304 (2002).

32.Mayer, C. et al. Timing and completion of puberty in female mice depend on estrogen receptor α-signaling in kisspeptin neurons. Proc Natl Acad Sci U S A 107, 22693–22698 (2010).

33.Mayer, C. & Boehm, U. Female reproductive maturation in the absence of kisspeptin/GPR54 signaling. Nat Neurosci 14, 704–710 (2011).

34.Messina, A. et al. Dysregulation of Semaphorin7A/β1-integrin signaling leads to defective GnRH-1 cell migration, abnormal gonadal development and altered fertility. Hum. Mol. Genet. 20, 4759–4774 (2011).

35.Messina, A. & Giacobini, P. Semaphorin signaling in the development and function of the gonadotropin hormone-releasing hormone system. Front Endocrinol (Lausanne) 4, 133 (2013).

36.Messina, A. et al. Neuron-Derived Neurotrophic Factor Is Mutated in Congenital Hypogonadotropic Hypogonadism. Am J Hum Genet 106, 58–70 (2020).

37.Molbay, M., Kolabas, Z. I., Todorov, M. I., Ohn, T. & Ertürk, A. A guidebook for DISCO tissue clearing. Mol Syst Biol 17, e9807 (2021).

38.Moore, A. M., Coolen, L. M., Porter, D. T., Goodman, R. L. & Lehman, M. N. KNDy Cells Revisited. Endocrinology 159, 3219–3234 (2018).

39.Moore, A. M., Coolen, L. M. & Lehman, M. N. Kisspeptin/Neurokinin B/Dynorphin (KNDy) cells as integrators of diverse internal and external cues: evidence from viral-based monosynaptic tract-tracing in mice. Sci Rep 9, 14768 (2019).

40.Moore, A. M., Lucas, K. A., Goodman, R. L., Coolen, L. M. & Lehman, M. N. Three-dimensional imaging of KNDy neurons in the mammalian brain using optical tissue clearing and multiple-label immunocytochemistry. Sci Rep 8, 2242 (2018).

41.Neckel, P. H., Mattheus, U., Hirt, B., Just, L. & Mack, A. F. Large-scale tissue clearing (PACT): Technical evaluation and new perspectives in immunofluorescence, histology and ultrastructure. Sci Rep 6, 34331 (2016).

42.Oakley, A. E., Clifton, D. K. & Steiner, R. A. Kisspeptin signaling in the brain. Endocr Rev 30, 713–743 (2009).

43.Parkash, J. et al. Suppression of β1-Integrin in Gonadotropin-Releasing Hormone Cells Disrupts Migration and Axonal Extension Resulting in Severe Reproductive Alterations. J. Neurosci. 32, 16992–17002 (2012).

44.Prevot, V. GnRH Neurons Directly Listen to the Periphery. Endocrinology 152, 3589–3591 (2011).

45.Renier, N. et al. Mapping of brain activity by automated volume analysis of immediate early genes. Cell 165, 1789–1802 (2016).

46.Reynaud, E. G., Kržič, U., Greger, K. & Stelzer, E. H. K. Light sheet-based fluorescence microscopy: more dimensions, more photons, and less photodamage. HFSP J 2, 266–275 (2008).

47.Schwanzel-Fukuda, M. & Pfaff, D. W. Origin of luteinizing hormone-releasing hormone neurons. Nature 338, 161–164 (1989).

48.Seminara, S. B. et al. The GPR54 gene as a regulator of puberty. N. Engl. J. Med. 349, 1614–1627 (2003).

49.Taroc, E. Z. M., Prasad, A., Lin, J. M. & Forni, P. E. The terminal nerve plays a prominent role in GnRH-1 neuronal migration independent from proper olfactory and vomeronasal connections to the olfactory bulbs. Biology Open 6, 1552–1568 (2017).

50.Topaloglu, A. K. et al. TAC3 and TACR3 mutations in familial hypogonadotropic hypogonadism reveal a key role for Neurokinin B in the central control of reproduction. Nat Genet 41, 354–358 (2009).

51.Ueda, H. R. et al. Tissue clearing and its applications in neuroscience. Nat Rev Neurosci 21, 61–79 (2020).

52.Vanacker, C. et al. Neuropilin-1 expression in GnRH neurons regulates prepubertal weight gain and sexual attraction. EMBO J 39, e104633 (2020).

53.Vieites-Prado, A. & Renier, N. Tissue clearing and 3D imaging in developmental biology. Development 148, dev199369 (2021).

54.Wang, X. et al. Bi-channel image registration and deep-learning segmentation (BIRDS) for efficient, versatile 3D mapping of mouse brain. eLife 10, e63455 (2021).

55.Wen, S. et al. Genetic identification of GnRH receptor neurons: a new model for studying neural circuits underlying reproductive physiology in the mouse brain. Endocrinology 152, 1515–1526 (2011).

56.Wray, S. Development of gonadotropin-releasing hormone-1 neurons. Frontiers in Neuroendocrinology 23, 292–316 (2002).

57.Wray, S., Grant, P. & Gainer, H. Evidence that cells expressing luteinizing hormone-releasing hormone mRNA in the mouse are derived from progenitor cells in the olfactory placode. Proc. Natl. Acad. Sci. U.S.A. 86, 8132–8136 (1989).

58.Wray, S., Key, S., Qualls, R. & Fueshko, S. M. A subset of peripherin positive olfactory axons delineates the luteinizing hormone releasing hormone neuronal migratory pathway in developing mouse. Dev Biol 166, 349–354 (1994).

59.Xu, F. et al. High-throughput mapping of a whole rhesus monkey brain at micrometer resolution. Nat Biotechnol 1–8 (2021) doi:10.1038/s41587-021-00986-5.

60.Yeo, S.-H. et al. Visualisation of Kiss1 Neurone Distribution Using a Kiss1-CRE Transgenic Mouse. Journal of Neuroendocrinology 28, (2016).

61.Yoshida, K., Rutishauser, U., Crandall, J. E. & Schwarting, G. A. Polysialic acid facilitates migration of luteinizing hormone-releasing hormone neurons on vomeronasal axons. J Neurosci 19, 794–801 (1999).

62.Yoshida, K., Tobet, S. A., Crandall, J. E., Jimenez, T. P. & Schwarting, G. A. The migration of luteinizing hormone-releasing hormone neurons in the developing rat is associated with a transient, caudal projection of the vomeronasal nerve. J. Neurosci. 15, 7769–7777 (1995).

CONCLUDING REMARKS

Throughout the present work, an overview of the development and migration of GnRH neurons and their integration in the GnRH network, the central circuit controlling reproduction in mammals, has been provided. Some of the known physiological mechanisms regulating these processes, as well as the consequences of their defects, were also covered (Chapter One). It was notably emphasized that the current knowledge on both the physiological and pathological aspects of the GnRH network remains largely incomplete, and thus, that further work is required to 1) elucidate the wide range of molecules and interactions shaping the GnRH neuron development and maturation and 2) identify precisely the nature of their failures and how they are causative of reproductive disorders.

In Chapter Two, through a collaborative work which I co- first-authored, we report new variants of *SEMA3F* and *PLXNA3* in the etiology of hypogonadotropic hypogonadism. The variants were identified in 15 individuals from a turkish cohort of patients, and were predicted to affect protein function and interaction. Moreover, I performed immunohistochemistry for SEMA3F and PLEXINA1-A3 along the migratory route of GnRH neurons in the human fetus, and found that their expression was consistent with a role of SEMA3F signalling in the regulation of GnRH neuron migration in humans. To further confirm the hypothesis that the variants could affect protein function, I performed molecular and functional cell assays on the identified mutations, revealing that three out of four *SEMA3F* variants were associated with defective expression or secretion, while the two tested *PLXNA3* variants were associated with unexpected isoforms, and one of them also showed altered cellular localization. Altogether, these results strongly argue in favour of the participation of the identified *SEMA3F* and *PLXNA3* variants to the hypogonadotropic hypogonadism phenotype of the patients.

In light of recent advances, the present work also discussed how new imaging methods can revolutionize our investigations of the GnRH network. Chapter Three indeed recapitulated the limitations of previous studies conducted on the GnRH neurons, and how the sectioning methods which were – and still are – routinely used inherently associate with a dramatic loss of information. An overview of modern and trending tissue-clearing and 3D-imaging techniques was

also provided, together with their established and potential contribution to neurosciences and to the neuroendocrinology of reproduction. Notably, recent publications leveraging on these new methods to study the GnRH network, two of which I co-authored, were discussed.

Taking advantage of these techniques, we and others have investigated the ontogeny, migration, and maturation of the GnRH neurons in the mouse brain, as well as the distribution of their well-known interactors the kisspeptin-expressing neurons, and I detailed the results of this study in Chapter Four. Remarkably, we document for the first time with a three-dimensional approach the migratory route of GnRH neurons from the olfactory placode to the brain at several embryonic stages, and describe in the most reliable way to date the distribution of these neurons in the postnatal mouse. Furthermore, we studied the maturation of kisspeptin-expressing neurons, well-known interactors of GnRH neurons, first in the hypothalamus to reveal the timeline and the scope of kisspeptin expression, then in the whole brain, demonstrating a common pattern of expression of GnRH and kisspeptin in several extra-hypothalamic regions. We also shed light on a number of GnRH neurons in the postnatal nasal region, and reveal the extent of this population and its projections, which were previously overlooked by the scientific community. Finally, we report close interactions between GnRH neurons and TH-expressing neurons in the olfactory bulbs by combining tissue clearing and 3D imaging with reprocessing and high-resolution confocal imaging, providing at the same time new ways to study the GnRH circuitry at both the network and the subcellular scale.

In summary, the present work brings important new insights on the neuroendocrine circuits controlling reproduction, and the mechanisms of central reproductive disorders. New players in the etiology of hypogonadotropic hypogonadism and Kallmann Syndrome were identified through mutation screening and functional cell assays, and new data was provided on the development of the complex GnRH circuitry. I am confident that this work will contribute significantly to the field of neuroendocrinology by 1) helping in the identifications of mutations causative of hypogonadotropic hypogonadism and Kallmann Syndrome in patients for whom the causative genes have not yet been identified, and 2) reporting the precise migration and

distribution of GnRH neurons and their interactors in the rodent, while at the same time emphasizing the benefits of using modern imaging approaches, and providing new tools and templates to investigate their defects.

ANNEX – AN OPTIMIZED PROTOCOL FOR TISSUE-CLEARING APPLIED TO MOUSE SAMPLES

Adapted from Renier et al. 2014, Renier et al. 2016, Belle et al. 2017

0) SAMPLE PREPARATION

Dissect the structure of interest if needed. For embryonic tissues, fix in 4% PFA overnight at 4°C. For postnatal stages, perfuse with 4% PFA, and post-fix in PFA 4% overnight at 4°C. When perfusion is not feasible, fixation by immersion for 24-48h in PFA 4% is recommended.

Store sample at 4°C in PBS 1X with sodium azide (0.01-0.05%) as a preservative.

1) SAMPLE PRETREATMENT – Duration: 3 days

__Day 1__

1. Dehydrate the sample in a gradient of Methanol*/PBS, with rotation at RT:

20% MetOH 1 hour	40% MetOH 1 hour	60% MetOH 1 hour	80% MetOH 1 hour	100% MetOH 1 hour	100% MetOH 1 hour

2. Incubate in the **delipidation solution** (2/3 dichloromethane** + 1/3 methanol*) overnight at 4°C with agitation.

__Day 2__

1. Wash for 2 x 1h in 100% Methanol* at RT, then store the sample at 4^0 C in fresh Methanol.
2. At the end of the day, transfer the sample in the 5% H_2O_2 **bleaching solution** (1/6 H_2O_2 30% + 5/6 methanol) and leave overnight at 4°C in agitation.

__Day 3__

Rehydrate your sample in Methanol/PBS 1X, with rotation at RT:

100% MetOH 1 hour	80% MetOH 1 hour	60% MetOH 1 hour	40% MetOH 1 hour	20% MetOH 1 hour	PBS 1 hour

Optional: Store sample at 4°C in PBS 1X with sodium azide (0.01-0.05%) as a preservative

* Methanol is toxic. Handle with gloves and under a hood.

** Dichloromethane is a highly toxic solvent, corrosive to some plastics. Use with thick gloves, under a hood, preferably in glass vials. 5ml eppendorf and 15/50ml tubes are resistant.

2) IMMUNOLABELING – Duration: 10 days to one month

1. Incubate your sample at RT with rotation, in the **permeabilization and blocking solution** (PBSGT = PBS, 0.2% gelatin, 1% Triton X-100, 0.05% sodium azide) for 2 to 4 days depending on the size.
2. Incubate with **primary antibodies** in PBSGT, with rotation at 37°C to increase penetration.
   - The time of incubation depends on the size of the sample, and usually ranges from 5 days for embryos to 2 weeks for an adult mouse brain.
3. Rinse with PBS at least 6 times for 1 hour. Optimally, rinse once more overnight.
4. Incubate with **secondary antibodies** in PBSGT at 37°C with rotation.
   - The time of incubation usually ranges from 2 days (small embryos) to 1 week (adult mouse brain).
   - To avoid aggregates in the sample, it is recommended to filter the secondary antibodies solution with a 0.20 µm filter.
   - Starting from this step, always keep the samples protected from light.
5. Rinse with PBS at least 6 times for 1 hour. Optimally, rinse once more overnight.

Optional: Store sample at 4°C in PBS 1X with sodium azide (0.01-0.05%) as a preservative.

Protect from light

3) TISSUE CLEARING – Duration: 2 days

__Day 1__

1. Dehydrate the sample in a gradient of Methanol*/PBS, with rotation at RT:

20% MetOH 1 hour	40% MetOH 1 hour	60% MetOH 1 hour	80% MetOH 1 hour	100% MetOH 1 hour	100% MetOH 1 hour

2. Incubate in the **delipidation solution** (2/3 dichloromethane** + 1/3 methanol*) overnight at 4°C with agitation.

__Day 2__

1. To wash out the methanol, incubate in 100% dichloromethane** at RT with agitation until the sample sinks (15 min to 1 hour).
2. Transfer the sample in 100% Benzyl Ether (DBE***) for 2 hours in rotation at RT to achieve transparency. Then, transfer the brain to a new DBE solution for storage.

IMPORTANT:
Store the samples in the clearing solution at room temperature
Protect the samples from light
Always fill tubes to the maximum to prevent oxidization

* Methanol is toxic. Handle with gloves and under a hood.

** Dichloromethane is a highly toxic solvent, corrosive to some plastics. Handle with thick gloves under a hood, preferably in glass vials. 5ml eppendorf and 15/50ml tubes are resistant.

*** Benzyl ether / DBE is a toxic solvent, corrosive to some plastics. Handle with thick gloves under a hood, preferably in glass vials. 5ml eppendorf and 15/50ml tubes are resistant.

ANNEX – NEURON-DERIVED NEUROTROPHIC FACTOR IS MUTATED IN CONGENITAL HYPOGONADOTROPIC HYPOGONADISM

ARTICLE

Neuron-Derived Neurotrophic Factor Is Mutated in Congenital Hypogonadotropic Hypogonadism

Andrea Messina,[1,11] Kristiina Pulli,[2,11] Sara Santini,[1,11] James Acierno,[1,9] Johanna Känsäkoski,[3] Daniele Cassatella,[1,9] Cheng Xu,[1] Filippo Casoni,[4,8,9] Samuel A. Malone,[4] Gaetan Ternier,[4] Daniele Conte,[5] Yisrael Sidis,[1] Johanna Tommiska,[3] Kirsi Vaaralahti,[2] Andrew Dwyer,[1] Yoav Gothilf,[6] Giorgio R. Merlo,[5] Federico Santoni,[1] Nicolas J. Niederländer,[1] Paolo Giacobini,[4,12] Taneli Raivio,[2,7,12] and Nelly Pitteloud[1,10,12,*]

Congenital hypogonadotropic hypogonadism (CHH) is a rare genetic disorder characterized by infertility and the absence of puberty. Defects in GnRH neuron migration or altered GnRH secretion and/or action lead to a severe gonadotropin-releasing hormone (GnRH) deficiency. Given the close developmental association of GnRH neurons with the olfactory primary axons, CHH is often associated with anosmia or hyposmia, in which case it is defined as Kallmann syndrome (KS). The genetics of CHH are heterogeneous, and >40 genes are involved either alone or in combination. Several CHH-related genes controlling GnRH ontogeny encode proteins containing fibronectin-3 (FN3) domains, which are important for brain and neural development. Therefore, we hypothesized that defects in other FN3-superfamily genes would underlie CHH. Next-generation sequencing was performed for 240 CHH unrelated probands and filtered for rare, protein-truncating variants (PTVs) in FN3-superfamily genes. Compared to gnomAD controls the CHH cohort was statistically enriched for PTVs in neuron-derived neurotrophic factor (*NDNF*) ($p = 1.40 \times 10^{-6}$). Three heterozygous PTVs (p.Lys62*, p.Tyr128Thrfs*55, and p.Trp469*, all absent from the gnomAD database) and an additional heterozygous missense mutation (p.Thr201Ser) were found in four KS probands. Notably, NDNF is expressed along the GnRH neuron migratory route in both mouse embryos and human fetuses and enhances GnRH neuron migration. Further, knock down of the zebrafish ortholog of *NDNF* resulted in altered GnRH migration. Finally, mice lacking *Ndnf* showed delayed GnRH neuron migration and altered olfactory axonal projections to the olfactory bulb; both results are consistent with a role of *NDNF* in GnRH neuron development. Altogether, our results highlight *NDNF* as a gene involved in the GnRH neuron migration implicated in KS.

Introduction

Congenital hypogonadotropic hypogonadism (CHH [MIM: 146110, MIM: 147950, MIM: 228300, MIM: 229070, MIM: 244200, MIM: 308700, MIM: 610628, MIM: 612370, MIM: 612702, MIM: 614837, MIM: 614838, MIM: 614839, MIM: 614840, MIM: 614841, MIM: 614842, MIM: 614858, MIM: 614880, MIM: 614897, MIM: 615266, MIM: 615267, MIM: 615269, MIM: 615270, MIM: 615271, and MIM: 616030]) is characterized by infertility and the absence of puberty. It is a rare genetic disorder caused by absent secretion or action of gonadotropin-releasing hormone (GnRH) and is often associated with non-reproductive phenotypes. The most commonly associated phenotype is anosmia, which when combined with CHH is defined as Kallmann syndrome (KS [MIM: 308700, MIM: 614897, and MIM: 613301). However, synkinesia, unilateral renal agenesis, sensorineural deafness, cleft palate, and other phenotypes are also observed.[1,2]

The genetics of CHH are complex, and mutations are described in more than 40[1,2] genes. Variable expressivity both within and between families, as well as incomplete penetrance, is often present.[1,2] Although first described as a Mendelian disorder, both monogenic and oligogenic inheritance (i.e., mutations in more than one gene) occur in CHH.[1–3] However, in approximately 50% of affected individuals, no mutations could be identified in the known CHH genes.[3]

To date, the genes implicated in CHH impact GnRH neuron fate, GnRH neuron migration and/or axon projection, GnRH neuron homeostasis, and/or gonadotrope defects. Notably, a unique feature of GnRH neurons is that they originate in the olfactory placode during embryonic development and migrate along the terminal nerve to reach their final destination in the hypothalamus.[4–6] This complex migratory process is orchestrated by an intricate network of genes controlling cell signaling, adhesion, motility, and neurite and axonal elongation.

[1]Service of Endocrinology, Diabetology, and Metabolism, Lausanne University Hospital, 1011 Lausanne, Switzerland; [2]Stem Cells and Metabolism Research Program, Faculty of Medicine, University of Helsinki, 00014 Helsinki, Finland; [3]Department of Physiology, Faculty of Medicine, University of Helsinki, 00014 Helsinki, Finland; [4]Inserm, Jean-Pierre Aubert Research Center, Development and Plasticity of the Neuroendocrine Brain, Unité 1172 Lille, 59045 Lille, France; [5]Department of Molecular Biotechnology and Health Science, University of Torino, 10126 Torino, Italy; [6]Department of Neurobiology, George S. Wise Faculty of Life Sciences and Sagol School of Neurosciences, University of Tel Aviv, Tel Aviv 69978, Israel; [7]Pediatric Research Center, New Children's Hospital, Helsinki University Hospital, 00290 Helsinki, Finland; [8]Division of Neuroscience, San Raffaele Scientific Institute, Milan 20132, Italy, Milan 20132, Italy; [9]Università Vita-Salute San Raffaele, Via Olgettina 58, 20132, Milan, Italy; [10]Faculty of Biology and Medicine, University of Lausanne, Lausanne 1005, Switzerland
[11]These authors contributed equally to this work
[12]These authors contributed equally to this work
*Correspondence: nelly.pitteloud@chuv.ch
https://doi.org/10.1016/j.ajhg.2019.12.003.

ANNEX – NEUROPILIN-1 EXPRESSION IN GNRH NEURONS REGULATES PREPUBERTAL WEIGHT GAIN AND SEXUAL ATTRACTION

Article

TRANSPARENT PROCESS

THE EMBO JOURNAL

Neuropilin-1 expression in GnRH neurons regulates prepubertal weight gain and sexual attraction

Charlotte Vanacker[1,2], Sara Trova[1,2], Sonal Shruti[1,2], Filippo Casoni[1,2], Andrea Messina[1,2], Sophie Croizier[3], Samuel Malone[1,2], Gaetan Ternier[1,2], Naresh Kumar Hanchate[1,2], S Rasika[1,2], Sebastien G Bouret[1,2], Philippe Ciofi[4,5], Paolo Giacobini[1,2,†] & Vincent Prevot[1,2,*,†]

Abstract

Hypothalamic neurons expressing gonadotropin-releasing hormone (GnRH), the "master molecule" regulating reproduction and fertility, migrate from their birthplace in the nose to their destination using a system of guidance cues, which include the semaphorins and their receptors, the neuropilins and plexins, among others. Here, we show that selectively deleting neuropilin-1 in new GnRH neurons enhances their survival and migration, resulting in excess neurons in the hypothalamus and in their unusual accumulation in the accessory olfactory bulb, as well as an acceleration of mature patterns of activity. In female mice, these alterations result in early prepubertal weight gain, premature attraction to male odors, and precocious puberty. Our findings suggest that rather than being influenced by peripheral energy state, GnRH neurons themselves, through neuropilin–semaphorin signaling, might engineer the timing of puberty by regulating peripheral adiposity and behavioral switches, thus acting as a bridge between the reproductive and metabolic axes.

Keywords chemotropic factors; energy homeostasis; hypothalamus; puberty onset; sexual behavior

Subject Category Neuroscience

DOI 10.15252/embj.2020104633 | Received 6 February 2020 | Revised 1 July 2020 | Accepted 13 July 2020 | Published online 5 August 2020

The EMBO Journal (2020) 39: e104633

Introduction

Two of the major imperatives of living beings are the maintenance of energy homeostasis and the transmission of genetic material, i.e. the production of young in animals with sexual reproduction. In mammals, both processes are controlled at the level of the brain, albeit by different hypothalamic circuits.

Fertility, under the control of the hypothalamic–pituitary–gonadal (HPG) axis, is orchestrated by a small population of neuroendocrine neurons producing gonadotropin-releasing hormone (GnRH). The release of GnRH into the hypothalamic–pituitary portal blood circulation drives gonadotropin secretion by the pituitary. The gonadotropins, luteinizing hormone (LH), and follicle stimulating hormone (FSH), in turn, act on the gonads to regulate sex steroid synthesis, gametogenesis, and the onset of puberty in both sexes (Boehm *et al*, 2015; Prevot, 2015; Howard & Dunkel, 2019).

While puberty consists of the permanent activation of the HPG axis and the commencement of adult reproductive function, the process is controlled by a complex array of genetic and environmental determinants, among which the acceleration of growth during the prepubertal period is thought to be a key permissive factor (Parent *et al*, 2003; Abreu & Kaiser, 2016; Howard & Dunkel, 2019). In patients with hypogonadotropic hypogonadism, a deficit in GnRH neuronal migration and function leads to an absence of puberty onset (Boehm *et al*, 2015). However, at the other end of the pathophysiological spectrum, little is known regarding the cellular and molecular mechanisms underlying precocious puberty.

GnRH-secreting neurons originate from both the nasal placode and the neural crest during embryonic development and migrate to the forebrain and hypothalamus along olfactory/terminal nerves (Schwanzel-Fukuda & Pfaff, 1989; Wray *et al*, 1989; Taroc *et al*, 2017). The complex developmental events leading to correct GnRH neuronal migration and secretion are tightly regulated by the specific spatiotemporal expression patterns of growth factors, adhesion molecules, and diffusible guidance cues that are either attractive or repulsive (Giacobini, 2015). The semaphorins constitute one of the largest families of phylogenetically conserved guidance cues, known to regulate multiple processes crucial for neuronal network formation (Tamagnone & Comoglio, 2004; Van Battum *et al*, 2015). The repulsive guidance cue semaphorin 3A (Sema3A) and its receptor, neuropilin-1 (Nrp1), are expressed in a complementary manner in olfactory sensory neurons and are involved in the spatial encoding of sensory information in the olfactory bulb (Imai *et al*, 2009).

1 Laboratory of Development and Plasticity of the Neuroendocrine Brain, Univ. Lille, Inserm, CHU Lille, Lille Neuroscience & Cognition, UMR-S 1172, Lille, France
2 FHU, 1000 Days for Health, Lille, France
3 Center for Integrative Genomics, University of Lausanne, Lausanne, Switzerland
4 Inserm U1215, Neurocentre Magendie, Bordeaux, France
5 Université de Bordeaux, Bordeaux, France
*Corresponding author. Tel: +33 320 62 20 64; Fax: +33 320 53 85 62; E-mail: vincent.prevot@inserm.fr
†These authors contributed equally to this work